Regulation of Skeletal Muscle Metabolism- Supply and Demand

Carla A. Di Maria, B.Sc. (Hons)

Submitted in fulfillment of the requirements

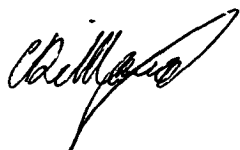of the degree of Doctor of Philosophy.

Division of Biochemistry
University of Tasmania
Jul 2002

Contents

DECLARATION

The work described in this thesis does not contain any material which has been accepted for the award of any other degree or diploma in this or any other university and to the best of my knowledge and belief contains no material previously published by any other person, except where due reference has been acknowledged.

Carla Di Maria

AUTHORITY OF ACCESS

This thesis may be made available for loan and limited copying in accordance with the *Copyright Act* 1968.

Carla Di Maria

ACKNOWLEDGEMENTS

First and foremost, I would like to express my gratitude to my supervisors, Professor Michael G. Clark, and Doctor Stephen Rattigan. Their guidance and expertise was invaluable. The initial stimulus for this research topic was based on the work of Alex Tong, and I commenced this project under his instruction early in 1998. I can only hope the work presented in this thesis is up to the high standard Alex upheld.

The weekly MRG meetings proved a great opportunity to air new ideas, and present data. I would like to thank all members of our group (past and present), Steve Richards, John Newman, Zhang-Lei, Cate Wheatley, Joanne Youd, Michelle Vincent, Ji-Ming Ye, and Cory Griffiths for their guidance, not only for their help on this project, but also as role models as successful and hard working scholars. Thanks also to Nathan Parry, Eloise Bradley and Maree Smith for their friendship and moral support, and to technical staff Geoffrey Appleby, Julie Harris and David Nolan. During the time I worked at Flinders Medical Centre, South Australia, I had the pleasure of working with Doctor Tim Neild in the Smooth Muscle Physiology Lab. I would like to thank Tim and Glenda Neild for their kind hospitality, and also Glenys Crane for help in the laboratory. Also, thanks to Richard Hodgson, John Newman and Michelle Vincent, who kindly gave permission for inclusion of figures in the appendix, and Steve Rattigan for the perfused heart data in Chapter 6.

Special thanks is reserved for my two fellow PhD students, Lucy Clerk, and Michelle Wallis. The three of us started our honours, and PhD projects at the same time. I wish you both the very best of luck for the future. Finally, I would like to thank my parents, my loving partner Roberto Francesconi, and his family for their support throughout.

ABSTRACT

Regulation of Skeletal Muscle Metabolism
– Supply and Demand

This thesis examines the regulation of skeletal muscle metabolism under resting conditions. Previous studies have shown that vasoconstrictors stimulate [type A] or inhibit [type B] metabolism of the constant flow perfused rat hindlimb. There is evidence that this may be due to redistribution of blood flow between the two vascular pathways in skeletal muscle, either increasing [type A] or decreasing [type B] the extent of nutritive perfusion. It is not clear if enhanced nutritive perfusion and therefore enhanced oxygen delivery is enough to account for the observed increase in metabolism with type A vasoconstrictors. It has been proposed that a cellular thermogenic mechanism is activated in addition to redistribution. The identity of this mechanism is not clear. A number of possibilities are explored.

The effects of varied oxygen delivery on hindlimb oxygen uptake were examined. Flow was maintained at a constant level while arterial oxygen content was varied. Three independent methods (1-MX metabolism, microdialysis and laser doppler flowmetry) were utilized to rigorously monitor redistribution. A positive relationship between oxygen delivery and hindlimb oxygen uptake was detected, independent of redistribution. Cellular ATP levels were maintained, though PCr stores were depleted at low oxygen delivery. Lactate efflux increased, but was not considered great enough to fully compensate for diminished ATP production from aerobic sources. In this regard, the perfused rat hindlimb may be considered as an oxygen conforming tissue. Thus oxygen delivery is a key determinant of skeletal muscle metabolic rate, and type A vasoconstrictors may effectively enhance oxygen delivery by improving nutritive perfusion.

Mechanisms accounting for increased oxygen consumption during enhanced delivery were explored. The roles of sodium cycling and accompanying Na^+/K^+-ATPase pump activity were assessed. Comparisons were made between type A vasoconstrictors and the sodium channel labilizer veratridine in both skeletal and cardiac muscle. In perfused skeletal muscle both vasoconstrictor- and veratridine-mediated metabolism were blocked by the sodium pump inhibitor ouabain, however vasoconstrictor-mediated metabolism was resistant to sodium channel inhibition with tetrodotoxin (TTX). The same TTX-resistant vasoconstrictor-thermogenic effect was absent from perfused arrested rat heart, possibly due to differences in vascular anatomy. Intracellular recording techniques failed to detect any change in skeletal fiber membrane potential during type A vasoconstrictor infusion, but did detect changes with veratridine. In summary the data supports the notion that metabolic demand (sodium load with veratridine) can stimulate hindlimb metabolism. However, there was no evidence for type A vasoconstrictor mediated changes in muscle sodium cycling, Na^+/K^+-ATPase activity, or membrane depolarization.

Oxygen consumption of resting skeletal muscle is largely controlled by oxygen delivery, whether this is by changes in bulk flow or flow redistribution. Cellular thermogenic mechanisms may well be activated in response to increased oxygen delivery, though sodium cycling/pumping is no longer a candidate.

TABLE OF CONTENTS

LIST OF FIGURES

LIST OF TABLES

Publications arising directly from this thesis

Na^+ channel and Na^+/K^+-ATPase involvement in norepinephrine- and veratridine-
stimulated metabolism in perfused rat hind limb.

Tong, A.C.Y.; C.A. Di Maria; S. Rattigan; M.G. Clark.

Canadian Journal of Physiology and Pharmacology, 77(5): 350-7, 1998.

Vasoconstrictor stimulation of oxygen uptake present in perfused skeletal muscle but
absent from perfused heart.

Di Maria, C.A.; S. Rattigan; M.G. Clark.

Journal Thermal Biology, 27: 151-158 (2002).

Other Publications

Relationship of MTT reduction to stimulants of muscle metabolism.

Newman, J.M.B.; C.A. Di Maria; S. Rattigan; J.T. Steen; K.A. Miller; T.P.D.
Eldershaw; M.G. Clark.

Chem. Biol. Interact. 128(2): 127-40, 2000.

Changes in nutritive blood flow affects microdialysis outflow/inflow ratio for ^{14}C-
ethanol and ^3H_2O in perfused rat hindlimb.

Newman, J.M.B.; C.A. Di Maria; S. Rattigan; M.G. Clark.

American Journal of Physiology (Heart Circ Physiol), 281(6): H2731-H2737, 2001

Conference Abstracts

Thermogenesis of resting muscle: Key roles for sodium channels and Na^+/K^+-ATPase
in catecholamine effects.

Di Maria C.A.; A.C.Y. Tong; S. Rattigan; M.G. Clark.

ASBMB Combined Conference. Adelaide, SA. Sept.1998.

Thermogenesis in resting skeletal muscle: a role for sodium channels?

Di Maria C.A.; A.C.Y. Tong; S. Rattigan; M.G. Clark.

ASBMB Combined Conference. Gold Coast, QLD. Sept. 1999.

Ca^{2+} and Na^+ cycling during resting skeletal muscle thermogenesis:
Studies in perfused muscle.

Di Maria, C.A.; S. Rattigan; M.G. Clark.

Gordon Research Conference June 2000, Muscle: Excitation Contraction Coupling.

Colby-Sawyer College, New Hampshire, USA.

ABBREVIATIONS

AII	angiotensin II
ADP	adenosine-5'-diphosphate
AMP	adenosine-5'-monophosphate
ANOVA	analysis of variance
ATP	adenosine-5'-triphosphate
A-V	arterio-venous difference
BAT	brown adipose tissue
BSA	bovine serum albumin
$Ca^{2+}ATPase$	calcium adenosine-5'-triphosphatase
Cr	creatine
DGTX	digitoxin
Dig	digoxin
EC	energy charge [calculated by ATP/(ATP+ADP+AMP)]
E_M	plasma membrane potential
HPLC	high performance liquid chromatography
IMP	inosine monophosphate
INO	inosine
LE	lactate efflux
E_M	resting membrane potential
Na^+/K^+-ATPase	sodium, potassium adenosine-5'-triphosphatase
NE	norepinephrine
NST	non-shivering thermogenesis
O/I	microdialysis out to in ratio
Oua	ouabain
PCA	perchloric acid
PCr	phosphocreatine
P_i	inorganic Phosphate
PHE	phenylephrine
PP	perfusion pressure
SNP	sodium nitroprusside
TTX	tetrodotoxin
UCP	uncoupling protein
Vera	veratridine
$\dot{V}O_2$	rate of oxygen consumption
1-MU	1-methylurate
1-MX	1-methylxanthine
^3H_2O	tritiated water
5-HT	5-hydroxytryptamine (serotonin)
^{14}C-ethanol	radioactive ethanol

CHAPTER 1

INTRODUCTION

1.1 Overview

The contribution of skeletal muscle to non-shivering thermogenesis has been debated for many years (171). While many researchers favour brown adipose tissue as the primary source of non-shivering heat in small mammals (42; 43; 217), a considerable body of evidence also implicates skeletal muscle as an important source of non-shivering thermogenesis (NST) in species with and without brown adipose tissue (171). Typically, NST stimulated by catecholamines, cold and diet, is ascribed to thermogenic mechanisms in brown adipocytes. However, evidence of NST induced by catecholamines, cold and diet has also been demonstrated in skeletal muscle, though the biochemical mechanisms responsible are less clear.

The stimulatory effects of type A vasoconstrictors (including catecholamines) on perfused hindlimb metabolism (59), in species with and without brown adipose tissue, is considered firm evidence in favour of non shivering thermogenesis of muscular origin (131; 183; 208). Blood flow is thought to play a significant role in vasoconstrictor-stimulated metabolism, though it is not clear if changes in oxygen delivery are the primary stimulus for increased metabolism, or if additional thermogenic mechanisms are activated in response to enhanced blood flow. The thermogenic mechanisms available in skeletal muscle are discussed herein, with particular reference to those that may be recruited during vasoconstrictor-mediated metabolism.

1.2 Non shivering thermogenesis

1.2.1 Brown adipose tissue versus skeletal muscle

Non-shivering thermogenesis (NST) is defined as the heat produced in response to cold that is not dependent on muscular shivering. This was first noted in cold exposed (5°C) rats treated with curare to prevent muscular contraction (shivering),

where animals survived exposure, while maintaining normal body temperatures (84). In rats and mice, long term cold exposure results in a gradual shift from shivering to non-shivering thermogenesis as the primary heat producing mechanism (123; 147; 170; 170). The finding that norepinephrine induced metabolism is enhanced by cold acclimation, led to the hypothesis that norepinephrine (NE) is the hormonal mediator of NST (163). Heat is produced as a consequence of increased metabolic rate, however the source tissue, and biochemical mechanism of non-shivering thermogenesis is controversial.

Microsphere studies in rodents demonstrate significantly elevated blood flow in brown adipose tissue (BAT) during cold exposure and norepinephrine infusion (117; 118). BAT thermogenesis in rats is also elevated in response to overeating at thermoneutrality (257), and during cold exposure (148). BAT mass increases significantly during cold exposure (119; 173), while bilateral removal of BAT attenuates the cold induced metabolic response (275). Furthermore, the oxidative capacity of BAT was shown to increase with cold acclimation (173). Thus, active BAT metabolism contributes to thermoregulation and dissipation of excess caloric energy, an effect that may be artificially stimulated by the application of catecholamines.

However, several lines of evidence argue that BAT alone, may only be able to account for a portion of total NST induced by cold, diet or catecholamines. Measurements of cytochrome oxidase activity in BAT from cold adapted rats suggest that BAT may account for an absolute maximum of 76% of the additional heat produced (173). The remaining portion of NST must be attributed to tissues other than BAT. Comparisons of cytochrome oxidase activity in cold acclimated gerbil and mouse tissues (liver, BAT and skeletal muscle) were carried out after 4 and 8 weeks of cold acclimation (4°C) (34). After 4 weeks of cold acclimation BAT mass was increased, but muscle mass was decreased by comparison with controls. Cold acclimation led to an increase in the resting metabolic rate, and enhanced the response to injected NE. Combined, these results indicate reduced reliance in shivering, in favour of non-shivering thermogenic mechanisms. Cytochrome oxidase activity of all tissues was elevated following cold acclimation, however BAT alone could not

account for the total increase in metabolic rate. It was calculated that the oxidative capacity of cold adapted muscle exceeded shivering thermogenesis, therefore an energy-consuming pathway other than shivering had been activated in muscle (34). This data supports the idea that muscle non-shivering thermogenic mechanisms may also be up-regulated in response to cold-adaptation.

In the partly isolated curarized leg muscles of the cold acclimated rat, skeletal muscle metabolic rate (A-V oxygen extraction) was shown to increase to a similar extent in response to cold and norepinephrine infusion (172). These changes in leg oxygen consumption after cold and norepinephrine infusion (132% & 134%) almost equaled the whole body oxygen response (126% & 126%). It was suggested that skeletal muscle might account for a large fraction of the total increase in metabolic response to cold. Measurements of cytochrome oxidase activity in skeletal muscle combined with blood flow figures led Janský (168) to the conclusion that skeletal muscle may account for up to 57% of NST in cold acclimated rats. It is however stressed that the metabolic capacity of skeletal muscle is not large enough to account for all heat production by both shivering and non-shivering thermogenic mechanisms. Thus, NST is probably the combined result of increased metabolism is several tissues.

In the absence of BAT, skeletal muscle may assume a more significant role in non-shivering heat production. A comparison of the oxidative capacity of tissues from species with and without BAT (rat versus duckling) appears to support this. In cold acclimated rats, gastrocnemius muscle showed a decrease of 22%, while BAT showed an increase of 544% in oxidative capacity. In contrast, muscles from the cold acclimated duckling, gastrocnemius & pectoralis showed remarkable increases in their oxidative capacities (33% & 195% respectively) (19). Furthermore, evidence for cold, and norepinephrine induced NST has been obtained in the Australian marsupial *Bettongia gaimaridii*, a species devoid of brown adipose tissue. Cold acclimation (4-5°C for 2 weeks) increased resting oxygen consumption by 15%, while the response to norepinephrine was enhanced by cold adaptation (255).

Catecholamine induced NST has also been demonstrated in humans, where BAT is thought to be restricted to small, scattered deposits. In a study by Astrup, Bülow, et al. (12) the thermogenic effects of ephedrine were examined in humans. A minor increase in peri-renal BAT blood flow and temperature was noted in response to ephedrine, however these effects were trivial when compared with the 60% increase in leg oxygen extraction. Extrapolation led to the conclusion that whole body skeletal muscle may account for up to 50% of the ephedrine induced oxygen uptake in humans, while the contribution of BAT was negligible (12). Similarly, Simonsen, Stallknecht, et al. (279) estimate that in humans 40% of the thermogenic epinephrine response is localized to skeletal muscle, while another 5% is attributed to white adipose tissue. Some evidence of cold-adaptation has also been found in humans, since the epinephrine response appears to be potentiated in cold-acclimated subjects [polar swimmers] (188). There is also some evidence to suggest that skeletal muscle may also participate in carbohydrate induced thermogenesis in humans (10; 11).

NST is probably the combined result of increased metabolism in a variety of tissues, with BAT and skeletal muscle as the primary contributors. However, skeletal muscle may assume a more significant role in the absence of BAT. By virtue of its large mass [up to 38% of the total human body mass (174), and 48% of rat body mass (172)] muscle has great potential as a source of non-shivering heat in species with and without brown adipose tissue. While the biochemical mechanism of NST in BAT is relatively well known, it is not clear if the same mechanism operates in skeletal muscle.

1.2.2 Mechanisms of non-shivering thermogenesis

The biochemical mechanism of NST in BAT is well documented (43; 190; 222), and is addressed only briefly here. Mitochondria of BAT are specialized to allow uncoupled respiration, whereby substrate oxidation occurs independently of ATP production. Respiration is uncoupled when the potential energy found in the proton gradient across the inner mitochondrial membrane is dissipated ("wasted") in the form of heat. Protons leak across the inner membrane back into the mitochondrial matrix, by-passing the F_1F_O ATP-synthase (222). Proton leak leads to a dramatic

increase in cellular respiration rate, most likely fuelled by the large multilocular lipid deposits found in BAT. BAT thermogenesis is under tight sympathetic control, and may be pharmacologically activated by the application of β3-adrenergic agonists and norepinephrine (222).

The discovery in the 1970s of an uncoupling protein in mitochondria of brown adipocytes [later named UCP-1, reviewed in (223)] enabled researchers to examine more closely the role of brown adipose tissue in energy expenditure and heat production. The protein was shown to be located exclusively on mitochondria of brown adipocytes. Uncoupling activity of the protein was stimulated by norepinephrine and free fatty acids (205), while purine nucleotides [especially GDP] inhibited UCP-1 activity (212). The uncoupling capacity of UCP-1 is widely acknowledged, but the precise mechanism of ion transport is unknown, though several theories exist [for reviews see (41; 186; 218)]. Consistent with previous suggestion, mouse brown adipose UCP-1 mRNA levels were shown to increase during cold exposure and overeating, while fasting and obesity were associated with decreased UCP-1 expression (216). The advent of transgenic technology allowed the creation of mice over-expressing UCP-1, and as expected UCP-1 over-expression led to reduced adiposity despite hyperphagia in both genetic (185) and dietary (184) models of obesity. Based upon these findings, it was predicted that UCP-1 knockout mice would be cold sensitive, obese and diabetic at an early age.

UCP-1 ablated mice displayed a number of characteristics confirming successful removal of UCP-1 from the genotype. Firstly, no UCP-1 could be detected in the brown adipocytes with polyclonal antibodies (107). Secondly, mitochondria of UCP-1 ablated mice did not possess GDP binding sites (206), nor did GDP have any effect on UCP-1 deficient cells (212). Interestingly, the resting metabolic rate was identical in knockout and wild type brown adipocytes, as were the rates of norepinephrine-induced cAMP accumulation and lipolysis, though the metabolic response to norepinephrine was greatly reduced [only 3% of control (205)]. The response to the β3-adrenergic agonist CL 316,243 was also abnormally low (107). Knockout cells were shown to be in a more "energized" state, indicating greater metabolic efficiency brought about by enhanced coupling efficiency (206).

Alterations in UCP-2 and UCP-3 [UCP-1 homologues] expression were detected in BAT, though no inherent uncoupling was associated with either of these proteins (218). Curiously, mitochondria from UCP-1 ablated were equally as sensitive to the uncoupling effect of free fatty acids as wild type mitochondria, leading the authors the conclusion that free fatty acid stimulated uncoupling was not entirely UCP-1 dependent (206). It was speculated that the residual GDP-insensitive, free fatty acid stimulated proton leak was an intrinsic property of lipids in the mitochondrial membrane. This basal proton leak has since been described in a variety of other cell types that do not express UCP-1 (286).

Creation of the UCP-1 knockout mouse had been a success, but it was quite unexpected that knockout mice maintained a lean phenotype on both standard and high fat diets (107). The importance of UCP-1 in energy expenditure had apparently been overestimated, and it was hypothesized that "other" compensatory thermogenic mechanisms had been activated. These compensatory mechanisms did not however, protect animals during cold exposure, as UCP-1 ablated mice presented with a cold-sensitive phenotype (107).

Generally it is accepted that UCP-1 deficient mice are cold sensitive, however exceptions have been noted. Comparative studies of UCP-1 deficient mice from different genetic backgrounds [F1 hybrids and congenic C57BL/6J and 129/SvImJ mice] highlight an important issue. Hofmann, Loiselle, et al. (154) found that only the congenic animals were cold sensitive, while the hybrids were cold resistant. It was proposed that the hybrids were able to tolerate cold due some compensatory mechanism enabled by heterosis. Thus, the absence of UCP-1 alone does not necessarily dictate a cold sensitive phenotype, and the genetic background of the animals must be stated specifically in these types of studies.

A study by Golozoubova et al. (123), demonstrates that following acclimation [3 weeks at 18°C] UCP-1 deficient mice could withstand cold exposure. Upon exposure to 4°C, the pre-acclimated UCP-1 knockout mice maintained the same basal body temperatures as wild-type controls, while producing heat at four times the resting rate. Measurements of muscular shivering intensity indicate that wild-type

controls gradually replaced shivering with non-shivering thermogenic mechanisms according to conventional understanding, however the UCP-1 ablated animals were still heavily dependent on shivering thermogenesis even after several weeks at 4°C. Curiously, the response to injected norepinephrine and epinephrine was greatly diminished in knockout mice when compared to wild-type controls. It was concluded by the authors that no form of non-shivering thermogenesis other than UCP-1 dependent mechanisms (including adrenergically induced thermogenesis) were recruitable in UCP-1 knockout mice (41; 123). These findings do not however rule out entirely a potential role for skeletal muscle in thermoregulatory NST in UCP-1 ablated mice. It may have been useful to examine the effects of curare in these UCP-1 ablated mice, since it is still possible that shivering and non-shivering thermogenesis may occur simultaneously in skeletal muscle upon cold exposure. The possibility must also be considered that the physical act of shivering increases tissue blood flow, stimulating additional mechanisms of non-shivering thermogenesis in muscle which are effectively masked by shivering. The effects of blood flow on tissue metabolic rate will be discussed further.

Based upon the findings of Enerbäck et al. (107) that UCP-1 deficient mice were cold sensitive but not obese, it was hypothesized that adaptive thermogenesis in other tissues might compensate for the loss of UCP-1. Skeletal muscle has long been considered a candidate, owing to the large mass as a proportion of total body weight. Though unlikely that skeletal muscle alone can compensate fully for the loss of UCP-1 during cold exposure, non-shivering thermogenesis in skeletal muscle may still contribute to energy balance and maintenance of body weight at thermoneutrality. In a study by Monemdjou, Hofmann, et al. (211), basal proton leak was compared in muscles from control and UCP-1 deficient mice. Indeed, the residual rate of GDP-insensitive proton leak was shown to be greater in muscles of UCP-1 deficient animals than in wild type controls. Thus, in the absence of UCP-1, other thermogenic mechanisms in skeletal muscle may be activated, perhaps assuming a more important role in whole body metabolic regulation.

1.2.3 Skeletal Muscle NST is not UCP-1 dependent

Uncoupled respiration via UCP-1 expression is an effective means of increasing heat production and dissipation of excess calories in BAT, however UCP-1 expression is restricted to brown adipose tissue (205). How then does skeletal muscle produce heat? Cold induced NST has been noted previously in bettongs, though UCP-1 expression was not detected before or after cold acclimation (256). The source and mechanism of vasoconstrictor-mediated thermogenesis in the perfused bettong hindlimb was the subject of investigation by Ye, Edwards et al. (311). Vasoconstrictors, norepinephrine and vasopressin induced significantly elevated rates of oxygen consumption ($\dot{V}O_2$), lactate and glycerol efflux, concomitant with elevated perfusion pressures. These metabolic effects were rapidly reversed by the addition of the vasodilator nitroprusside. Since the bulk of the hindlimb mass is skeletal muscle and the development of pressure was critical to the thermogenic effect, it was proposed that skeletal muscle thermogenesis may be under vascular control (312). Similarly, vasoconstrictor-mediated thermogenesis was observed in the perfused hindquarter of the rat (59; 79), a region predominantly composed of skeletal muscle. Thus, vasoconstrictor mediated thermogenesis is observed in skeletal muscle of species with and without BAT.

Measurement of electrical activity in the pectoral muscles of cold exposed pigeons [1°C for several weeks] suggests that birds depend largely on shivering thermogenesis for thermoregulation (157). However, there is evidence that birds may also utilize non-shivering thermogenesis of muscular origin (21). Histological studies of avian tissue failed to detect BAT (21), or UCP-1 (260) despite the presence of mutilocular adipocytes resembling brown adipose deposits (21; 259). More recent studies describe the discovery of an UCP homolog in hummingbird muscle [HmUCP], however uncoupling activity of novel protein has so far only been demonstrated in yeast (297). Barré et al. (21) were able to demonstrate NST in muscovy ducklings [cold acclimated for 5 weeks], where heat production was increased without muscular shivering. The effects of cold acclimation were mimicked by twice daily glucagon injections at thermoneutrality (20), while increasing rates of oxygen consumption (99). The conclusion of these experiments was that NST did

occur in birds, and may be triggered by cold exposure or artificially stimulated by hormones at thermoneutrality.

By monitoring changes in blood flow during cold acclimation and glucagon treatment, Duchamp & Barré (98) determined that a major proportion of avian NST occurred in skeletal muscle. Though the cellular mechanism of avian NST is likely to differ from mammalian NST [catecholamines do not have the same stimulatory effect in birds as in mammals (22; 150)], the effect of increased blood flow on skeletal muscle thermogenesis aroused interest. It was later demonstrated in the perfused chicken hindlimb, that vasoconstrictors norepinephrine and epinephrine also stimulated resting muscle thermogenesis (106), and that these effects were abolished by the vasodilator nitroprusside. It was concluded that vasoconstrictor-stimulated metabolism existed in birds as in marsupials and mammals, and that vascular control of skeletal muscle thermogenesis may be a widespread biological phenomenon.

Skeletal muscle is known to be metabolically responsive to a number of treatments. Skeletal muscle metabolic rate is acutely stimulated by adrenergic agonist infusion [in rats(172), dogs (263) and humans (13; 199; 279)], membrane labilizers veratridine (291), and monensin (unpublished observations from this lab), and hyper-osmotic media (49; 85). Exogenously applied thyroid hormone has also been shown to stimulate skeletal muscle metabolism (26; 88; 278; 294). It is not known if one single biochemical mechanism accounts for increased metabolism by all of these treatments, however it is clear that skeletal muscle thermogenesis is not dependent on UCP-1 expression. Alternative mechanisms are discussed, with particular reference to the regulatory influence of vasoconstrictors on perfused rat hindlimb metabolism.

1.3 Modulation of perfused muscle metabolism by vasoconstrictors
1.3.1 Type A vasoconstrictors stimulate skeletal muscle thermogenesis

Previous reports from this laboratory (79), and others (83; 132; 207; 248) have detailed the stimulatory effects of catecholamines and other vasoconstrictors on perfused rat hindlimb metabolism. The stimulatory (Type A) vasoconstrictors include low dose norepinephrine (<1µM), epinephrine, norephedrine, phenylephrine, methoxamine, amidephrine, angiotensin II, vasopressin, vanilloids (low dose

capsaicin, gingerol, shogoal), and low frequency electrical stimulation of the sympathetic trunk (0.5-4.0 Hz) [reviewed in (59)].

Treatment of the perfused hindlimb with type A vasoconstrictors, leads to increased perfusion pressure (PP), and an increase in the rate of oxygen extraction ($\dot{V}O_2$) (79). Total flow to the hindlimb is constant, but oxygen extraction remains elevated for the duration of treatment. Concomitant with increased oxygen extraction, efflux rates of lactate (144), glycerol (58), uracil, and uric acid (63; 241) are all significantly elevated above basal. Comparison of high-energy phosphate content of freeze-clamped muscles collected in vivo, and after prolonged (3 hour) hindlimb perfusion with vasopressin, revealed no differences in cellular energy status (78). Therefore stimulation of perfused hindlimb metabolism by type A vasoconstrictors does not compromise muscle energy status, in fact there is some evidence to suggest that type A vasoconstrictors (angiotensin II) may improve cellular PCr/ATP ratios [shown in Figure 1 Appendix, data from (300)]. In addition to the observed metabolic effects, type A vasoconstriction was shown to markedly enhance aerobic muscle contractility in the blood-perfused hindlimb. Angiotensin II caused an 80% improvement in aerobic tetanic tension development, and enhanced contraction-induced oxygen uptake during sciatic nerve stimulation of the calf muscle group (gastrocnemius-soleus-plantaris). Curiously, angiotensin II had no effect on tension development during anaerobic contraction (237). Findings from these experiments led to the combined conclusion that type A vasoconstrictors had a potent regulatory effect on aerobic muscle metabolism, and contractility.

1.3.2 Type B vasoconstrictors inhibit skeletal muscle metabolism

In the early 90s, routine testing of different vasoconstrictors in the perfused hindlimb led to the surprise finding that serotonin caused a decrease in metabolic rate (94). High doses of norepinephrine ($\geq 1\mu M$), capsaicin ($>1\mu M$), and high frequency electrical stimulation of the sympathetic trunk (5-10 Hz) were found to have similar effects [reviewed in (59)]. Ascribed the title type B, the metabolic properties of type B vasoconstrictors were outlined as follows. $\dot{V}O_2$ was suppressed below the basal level (94), along with efflux rates of glycerol, uracil, uric acid (59) and lactate efflux (311). Interestingly, insulin-mediated glucose uptake, and 2-deoxyglucose uptake by

the perfused rat hindlimb were both significantly blunted by serotonin infusion (235). In addition to the inhibitory metabolic effects, serotonin was also shown to decrease aerobic (tetanic) contraction-induced tension and oxygen uptake in sciatic nerve stimulated perfused muscle (95). While vasoconstriction is a feature common to both type A and B vasoconstrictors, the metabolic effects are virtual opposites.

1.3.3 Vascular delivery is essential for the effects of type A and B vasoconstrictors

The inclusion of vasodilators nitroprusside, nifedipine, or isoprenaline completely abolished the pressor effects of type A vasoconstrictors in the perfused hindlimb, along with the changes in VO_2 (78; 79), and lactate efflux (145). Furthermore, the inhibitory effects of serotonin on hindlimb $\dot{V}O_2$, and insulin-mediated glucose uptake were partially reversed by the inclusion the vasodilator carbachol (235). Thus development of pressure is essential for the effects of both type A and B vasoconstrictors. In addition to this, type A vasoconstrictors do not have the same thermogenic effects when applied to isolated incubated muscle preparations (69; 104; 139; 145). Similarly, the inhibitory effects of serotonin on insulin mediated glucose uptake (235), and muscle contractility (95) observed during perfusion, were notably absent in isolated incubated rat soleus, and extensor digitorum longus muscles.

Dubois-Ferriére & Chinet (97) made a direct comparison between the thermogenic effects of norepinephrine (NE, $10^{-6}M$) in perifused mouse soleii (from cold adapted animals with varied thyroid status), and in the perfused rat hindlimb. Perifused muscles showed only a transitory stimulation of thermogenesis with NE, not exceeding more than 5% of the basal rate. In contrast, the effects of NE in perfused muscle were far more pronounced. It was concluded that NE did not have any direct thermogenic effects upon the muscle, but the indirect haemodynamic effects (only apparent during perfusion) may be important in regulating metabolic rate. It was suggested that NE may participate in the removal of hypoxic or acidotic restriction on metabolism (97). Thus delivery of the vasoconstrictor via the vascular route, and the development of perfusion pressure is essential to the respective metabolic effects of type A and B vasoconstrictors.

1.3.3.1 Hot pipes- an unlikely theory

The interdependence between vasoconstriction and oxygen consumption led to the development of the "hot pipes" theory, where the stimulated rate of oxygen consumption was attributed to work performed by vascular smooth muscle as it constricted (57; 77). However, this was difficult to reconcile with the serotonin effect, where vasoconstriction was associated with inhibition of hindlimb metabolism. Dora et al. (96) highlight key differences between type A and B vasoconstrictors. The effects of oxygen availability on vasoconstriction were investigated by perfusing under conditions of hypoxia, or in the presence of cyanide or azide. While type B vasoconstriction (serotonin) was unaffected by these treatments, type A vasoconstriction (low dose NE) was completely abolished by hypoxia, cyanide, and azide addition. Type B vasoconstriction induced by high dose NE responded similarly to serotonin, showing no signs of oxygen dependence. It was concluded that vasoconstriction induced by type A was biochemically distinguishable from type B vasoconstriction, and most likely reflected different sites of vasoconstriction on the vascular tree.

Further evidence against the hot-pipes theory comes from later findings in the dual perfused hindlimb of the small rat, where high membrane stabilizing doses (100μM) of the β-adrenergic blocker propranolol blocked the oxygen uptake effect without interfering with vasoconstriction (292). Although vascular delivery and vasoconstriction appear to be essential pre-cursors, increased oxygen uptake with type-A vasoconstrictors could not be wholly attributed to work performed by vascular smooth muscle during constriction (59). The idea once touted by this laboratory that vasoconstrictor mediated thermogenesis derived from vascular tissue is now considered unlikely.

1.3.4 Skeletal muscle has two vascular pathways

Investigation of $\dot{V}O_2$ in the perfused dog hindlimb led Pappenheimer (229) to the observation that alterations in muscle blood flow (caused by either epinephrine, or stimulation of the vasoconstrictor nerves) resulted in distinct changes in arterio-venous oxygen extraction. While epinephrine applied in small doses increased the rate of oxygen extraction, stimulation of the vasoconstrictor nerve decreased $\dot{V}O_2$. It was suggested that nerve stimulation caused diversion of blood flow away from the capillary beds, through regions of low metabolic activity. This theory was supported by the observation that the arterio-venous loss of heat was greater following epinephrine application than nerve stimulation, implying that during nerve stimulation blood flow was shunted through a faster transit route, with a smaller surface area, and less heat loss. Similar results were noted by Grieb et al. (129), with the use of isotopic oxygen and chromium in the perfused dog hindlimb. Both fast and slow blood flow channels were identified. It was noted that the fast channel (so called "shunt") had a short transit time, with minimal nutrient exchange. The slow channel ("sink") had a much longer transit time (thought to be due to the trapping of red blood cells in the capillaries), with a much greater rate of nutrient extraction. These results imply the existence of two vascular pathways through skeletal muscle, with different transit times, and differential rates of nutrient exchange.

Injection of $^{24}Na^+$ into various sites on the cat sartorius muscle, allowed Barlow et al. (15) to characterize differential clearance rates, dependent upon the site of injection. The fastest clearing regions were closely associated with muscle fibers (the regions of high nutritive exchange), while the slowest clearing regions were localized to the intermuscular septa, and tendons. The metabolic activity of this region was quite low, with little nutrient exchange (15). Clearance experiments with radioactive ions ^{131}I (16), and $^{42}K^+$ (239), and other diffusible substances antipyrine, urea and sucrose (239; 240) confirmed these findings.

In a study of the rabbit tenuissimus muscle, Lindbom & Arfors (191) noted that the main feed arterioles (transverse arterioles) supplied two distinct vascular areas in parallel, the muscle capillaries (terminal arterioles), and the adjacent connective tissues. Application of various adrenergic agonists affected the fractional distribution

of microvascular flow between the muscle proper, and the connective tissue (30). Characterization of these two distinct vascular areas provides an explanation for the previously observed differences in muscle oxygen extraction, transit times, and clearance rates. The terms "nutritive and non-nutritive" blood flow were coined to describe these two vascular pathways (59).

1.3.5 Type A and B vasoconstrictors redistribute between the two vascular pathways

The effects of type A and B vasoconstrictors may also be explained in terms of nutritive and non-nutritive flow. Sites of type A and B vasoconstriction are biochemically distinguishable (96), with the serotonin vasoconstrictor sites located on large vessels (158; 187), and adrenergic vasoconstrictor sites restricted to smaller vessels (149). It has been proposed that type A vasoconstrictors enable capillary recruitment (and thus greater nutrient exchange) by constricting at particular sites on the vasculature. A paper from Lindbom & Arfors (192) suggests that the presence of yield shear stress within the capillaries must be overcome by perfusion pressure, before flow can occur. Therefore the number of capillaries perfused is a function of the pressure gradient over the capillary bed (192). Type A vasoconstrictors appear to provide the necessary pressure gradient. Conversely, Type B vasoconstrictors appear to cause shunting of blood flow via the non-nutritive pathway, thereby restricting access of oxygen and nutrients to the muscle fibers. It is therefore conceivable that site-specific vasoconstriction is responsible for flow redistribution, exerting control over perfusate delivery, muscle metabolism and tension development.

Physical evidence has been obtained in support of the view that type A and B vasoconstrictors affect distribution of flow between the two vascular pathways. Perfusion with cell free media enabled detection of trapped red cell washout post equilibration. Red cell efflux with type B vasoconstriction (serotonin) was not different from vehicle, but infusion of a type A vasoconstrictor (low dose NE) led to a marked increase in red cell efflux (219). Similarly, experiments with fluorescein-labeled dextran demonstrate that low dose NE recruited a new vascular space, that was re-accessed only by a second exposure to the same vasoconstrictor. Furthermore, vascular corrosion-casting with a 30μm microsphere acrylate preparation provided a 3D model of the arterial vasculature during control, type A, and type B

vasoconstriction (219). Low dose NE did not change cast weight when compared with control, but did increase the total number of small vessels filled. In contrast, type B (serotonin and high dose NE) decreased the number of vessels filled along with cast weight, apparently restricting flow to fewer vessels of the muscle bed. In separate experiments, the inclusion of fluorescent dextran in the perfusion medium allowed visualization of tendon vessels thought to carry the flow diverted from the muscle bed during type B vasoconstriction. Positioning of a surface fluorimetry probe over the exposed tibial tendon of the perfused limb confirmed an increased fluorescence signal during serotonin infusion (220). Conversely, low dose NE decreased the tendon signal. The tendon vessels are thought to provide the physical basis for at least part of the "functional shunt". However, microsphere embolism studies demonstrate that only some of the non-nutritive (shunt) vessels are found in the tendon regions, while the remainder are homogeneously distributed throughout the muscle (301).

The enzyme xanthine oxidase (located on capillary endothelial cells) converts the substrate 1-methylxanthine (1-MX) to 1-methylurate (1-MU) (175; 230). Inclusion of 1-MX in perfusion media and measurement of 1-MU production enables the extent of capillary endothelial exposure to be monitored. Serotonin was shown to decrease 1-MX metabolism below basal (234). Since no changes were detected in xanthine oxidase activity or flow to individual muscles (61), it was concluded that serotonin had decreased access to capillary xanthine oxidase by shunting flow through the non-nutritive vessels, effectively reducing the available capillary surface area. The next logical prediction, was that type A vasoconstrictors would enhance 1-MX metabolism via capillary recruitment. However, this was not the case, as type A did not substantially increase the rate of 1-MX conversion above basal. It was later speculated that release of endogenous metabolites (xanthine and hypoxanthine) during type A vasoconstriction may competitively inhibit 1-MX metabolism by the enzyme. Exercise-induced capillary recruitment (during sciatic nerve stimulation of the blood perfused constant flow rat hindlimb) did however successfully demonstrate a positive correlation between capillary surface area, and 1-MX metabolism (317).

Further evidence for this compartmentalized model comes from laser Doppler (LDF) monitoring of red cell flux in the blood perfused hindlimb with the use of

implantable microprobes (55). Randomly impaled micro-probes (260μM diameter impaled ~ 90 times across four muscles of the perfused limb) identified heterogeneous sites of microvascular perfusion, with varied responses to infused vasoconstrictors. In the majority of sites (56.7%), LDF signal was increased by NE, and decreased by serotonin (identified as nutritive sites). However, some of the sites (16.5%) gave a decreased LDF signal with NE infusion, and a greater signal with serotonin (non-nutritive sites). The remaining sites (24.7%) showed no net response to either vasoconstrictor (mixed site). This data provides direct evidence for the existence of discrete regions of nutritive and non-nutritive flow within the perfused muscle, and redistribution of flow between these two regions under the influence of type A and B vasoconstrictors. More recently, the effects of type A and B vasoconstrictors on nutritive and non-nutritive flow were demonstrated by monitoring the microdialysis out to in ratios for ^{14}C-ethanol and ^{3}H$_2$O during varied flow rate (221). The out to in ratio was decreased as a function of flow rate, however type A (NE) further decreased this ratio, while type B (serotonin) impeded the decrease at each flow rate (Appendix, Figure 2). Thus, type A vasoconstrictors augment capillary access, while type B vasoconstrictors decrease the extent of capillary perfusion.

Taken together, these findings provide evidence for dual circuitry of perfused muscle, and vascular recruitment/derecruitment by type A and B vasoconstrictors respectively (60; 62). Following cannulation and equilibration, the perfused rat hindlimb appears to assume a dynamic position somewhere between nutritive and non-nutritive flow, which is fully dilated, yet regulatable by applied neural input or infused vasoconstrictors.

1.3.6 Blood flow regulation of skeletal muscle metabolism

The relationship between perfusion flow rate and resting muscle $\dot{V}O_2$ has been noted in many different preparations (55; 103; 133; 221; 228; 285; 305; 310). In addition to enhancing muscle $\dot{V}O_2$, increased perfusion flow rate is also noted to improve cellular energy status (209). These observations imply that under resting conditions muscle metabolism is limited. Though total flow is sufficient for the entire mass of perfused muscle, heterogeneous blood flow distribution may restrict blood flow at the microvascular level (48; 97). Data from our own laboratory supports the

view that resting muscle blood flow is heterogeneous (61; 219). Increased flow rates may stimulate muscle $\dot{V}O_2$ simply by removing the physiological hypoxia imposed by heterogeneous flow (167), thereby removing the micro-scale heterogeneity in O_2 and substrate supply (48). Conceivably, type A vasoconstrictors may also participate in the removal of flow heterogeneity via capillary recruitment. Though total flow remains constant, the fractional distribution is altered in favour of the nutritive capillaries, enhancing microvascular perfusion.

The state of the microcirculation therefore has an important role in the regulation of resting muscle metabolic rate. Exercise is known to recruit a large number of capillaries (178) through vasodilation, increased cardiac output and cell to cell signalling (266). However the regulation of capillary density at rest is less clear. In resting muscle, capillary blood flow appears to be regulated by both active and passive factors (160). Interestingly, no pre-capillary sphincters have been reported in striated muscle (193), and control over capillary blood flow appears to be mediated by closure of the terminal arterioles (126). It is likely that vasoconstrictors exert control over capillary perfusion in the same way.

The increase in $\dot{V}O_2$ with type A vasoconstrictors, may be the result of increased tissue perfusion. Measurements of muscle oxygen extraction and blood flow in response to norepinephrine strongly support this idea (172). This point is also elegantly demonstrated in the human forearm (280), where adrenaline infused into the human forearm caused a significant increase in muscle blood flow and oxygen extraction. However, restriction of blood flow on the contra-lateral forearm (by external compression of the brachial artery) severely blunted the response to adrenaline (280). These findings support the hypothesis that the vascular system plays a key role in the thermogenic effects of catecholamines in skeletal muscle. Alterations in blood flow distribution, whether through changes in fractional distribution or bulk flow, therefore have an important role in the regulation of skeletal muscle metabolism.

The effects of type A and B vasoconstrictors are typically described as either stimulatory or inhibitory on metabolism, and this may be the result of simple changes in perfusate delivery. While the metabolic effects are apparent opposites, an

interesting aside is now touched upon. Infusion of type B vasoconstrictors is associated with increased perfusion pressure, and depressed metabolism. However, upon removal of the vasoconstrictor, metabolism returns to basal values. This return has been questioned as a "stimulation" of metabolism, admittedly from a lower plateau. The question is now posed, is the stimulation of metabolism noted upon serotonin removal, due to the same mechanism as type A vasoconstriction? This question will be addressed in more detail later.

1.3.7 Is vasoconstrictor-mediated metabolism the result of enhanced oxygen delivery?

Increased flow rates have the net effect of increasing microvascular perfusion, and oxygen and substrate delivery. It is not clear if metabolism is stimulated in response to flow itself, or enhanced substrate delivery. Perfused liver metabolism is generally unresponsive to catecholamines (perhaps due to a reduced capacity for capillary recruitment), though elevated arterial oxygen and substrate deliveries (β-hydroxybutyrate and acetate) are effective stimulants of liver metabolism (169). Similarly, catecholamine effects were severely reduced in perifused mouse soleii, though an increase in muscle metabolism was noted in response to increased substrate delivery (acetate and octanoate) (97). Thus, increased oxygen/substrate delivery as a consequence of increased flow, or vasoconstrictor-mediated capillary recruitment may well exert a significant effect on muscle metabolic rate.

A considerable body of evidence suggests that muscle oxygen uptake is dictated directly by oxygen delivery. By varying the haematocrit of the perfusing blood (at constant-flow), researchers were able to demonstrate delivery dependent $\dot{V}O_2$ in dog gracilis muscle, but only below the value of 0.45 ml/min per 100g perfused muscle (181). Above critical values, oxygen uptake ($\dot{V}O_2$) is delivery independent (2; 183). $\dot{V}O_{2MAX}$ is thought to be oxygen limited not only under basal conditions (181; 262), but also during exercise (156; 161; 165; 166; 244; 246). The idea that vasoconstrictors might influence skeletal muscle metabolic rate by altering oxygen delivery raises some interesting issues.

Oxygen conformance has been defined as cellular suppression of metabolism in response to decreased PO_2, without loss of cellular viability or activation of anaerobic energy supply pathways (153). In turtles, and brine shrimp the unique ability to withstand prolonged anoxia is attributed to a combination of events leading to stabilization of the plasma membrane, accompanied by metabolic suppression of up to 90% (151). Experimentally, hypoxic bouts have been shown to induce decreased rates of ion flux, decrease membrane permeability, and suppress sodium pump activity (90), in addition to decreasing urea synthesis and gluconeogenesis (38; 38). Membrane potential is maintained near normoxic levels despite these changes (93) and ATP levels are not depleted. By decreasing ion flux, the requirement for ATP-dependent ion pumping is minimized, thus providing the basis for energy conservation during anoxia. The phenomena of anoxic "channel arrest" has been reported by many groups (38; 90; 91; 93; 151; 232).

The only endothermic systems currently known to utilize channel arrest and metabolic arrest for extending hypoxia tolerance are hypo-perfused hypometabolic tissues and organs of diving animals (151). Perfused skeletal muscle may qualify as such a tissue, owing to heterogeneity of blood flow and micro-vascular perfusion under basal conditions. Type B vasoconstrictors decrease resting muscle metabolic rate by reducing the extent of nutritive perfusion, however, even after prolonged periods, muscle energy charge is not different from basal (300). This suggests that during oxygen limitation/ischemia, skeletal muscle also has the capacity to decrease ATP utilizing processes.

Oxygen conformance has been described in a variety of mammalian cell types including cultured mouse C_2C_{12} cells (8), primary cultures of rat hepatocytes (264), chick and neonatal rat cardiomyocytes (39; 44) and canine skeletal muscle (155). The major energy-consuming processes in mammalian cells include ATP dependent ion pumping, protein synthesis, mitochondrial proton leak, and gluconeogenesis, with minor contributions from urea synthesis, RNA/DNA turnover, and substrate cycling (254). It has been suggested that some, or all of these processes may be preferentially down-regulated during low oxygen limited conditions.

Assuming that under basal conditions, perfused skeletal muscle metabolic rate is oxygen limited owing to heterogeneous perfusion, then type A vasoconstrictors may conceivably relieve this limitation by enhancing microvascular perfusion. The resulting increase in $\dot{V}O_2$ may be a reflection of the return from limited to non-limited metabolism. The observation that PCr and ATP content of perfused muscle samples are improved by type A vasoconstrictors (300) would appear to support this line of reasoning. If low oxygen delivery causes membrane stabilization and "channel arrest", then one must consider the possibility that increased oxygen delivery might increase membrane permeability. Hulbert & Else (164) present the view that the relative leakiness of the plasma membrane is a significant determinant of cellular metabolic rate. Thus, increased metabolism observed during type A vasoconstrictor infusion may the combined result of enhanced tissue perfusion, increased oxygen delivery and increased membrane permeability. This might explain the sensitivity of type A vasoconstrictors to membrane stabilizers (292), and low sodium media (291).

1.3.8 Do type A vasoconstrictors activate cellular thermogenesis in addition to redistribution of flow?

The possibility that vasoconstrictors may influence metabolic rate through alterations in oxygen delivery is enticing. However, an alternative possibility must also be considered. Previous publications focus on the theory that cellular thermogenic mechanisms are activated in addition to vasoconstrictor-mediated redistribution of flow (291; 292). This idea is now investigated in more detail, with discussion of potential thermogenic mechanisms available in skeletal muscle that may be recruited during vasoconstrictor-mediated thermogenesis.

1.3.9 Evidence of cellular thermogenesis

In the examination of potential adrenergic-receptor involvement during type A vasoconstrictor-mediated thermogenesis, several different α- and β-antagonists were trialled in the constant-pressure perfused rat hindlimb. A strong α-adrenergic component of type A mediated metabolism was demonstrated (309), though doses of propranolol sufficient to block β1 and β1-adrenergic receptors (10μM), did not have

significant inhibitory effects on type A mediated metabolism (79). Quite by chance, it was noted that higher doses of propranolol (>50μM), had significant inhibitory effects on type A vasoconstrictor mediated metabolism (292). Further investigation revealed that unlike other β-blockers, propranolol at this dose had membrane-stabilizing properties. Norepinephrine stimulated metabolism was blocked by both (+) and (-) propranolol at 50μM, when only the (-) enantiomer is an active β-blocker. Further studies showed that other β-blockers nadolol and atenolol also at very high concentrations were ineffectual. It was concluded that the inhibitory effects of propranolol on type A vasoconstrictor-mediated metabolism were due to the inherent membrane stabilizing properties of the compound at this dose, and not blockade of β-adrenoreceptors. This was confirmed by the finding that another membrane stabilizer quinidine, was also an effective inhibitor of type A vasoconstrictors in the perfused rat hindlimb (292).

The inhibitory effects of propranolol on vasoconstrictor-mediated metabolism were particularly interesting, because perfusion pressure remained elevated while the metabolic effects ($\dot{V}O_2$, lactate efflux and glycerol efflux) were abolished (292). Prior to this, inhibitors of vasoconstrictor-mediated metabolism had also abolished perfusion pressure (78; 310), leading to the assumption that elevated metabolism was entirely dependent on vasoconstriction and the subsequent redistribution of flow. This was the first demonstration that the vasoconstrictor and metabolic effects may be separated. Even though propranolol did not appear to interfere with type A mediated vasoconstriction, it was not clear if redistribution still occurred as per usual. Examination of red cell washout during angiotensin infusion demonstrates no differences in the pattern of red cell washout in the absence or presence of propranolol (292), even though angiotensin mediated metabolism was suppressed in the presence of propranolol. These data were interpreted as evidence of activation of a cellular thermogenic mechanism in addition to redistribution of flow. The identity of the thermogenic mechanism is not immediately apparent, though several candidates are now explored.

1.4. Thermogenic mechanisms in skeletal muscle

1.4.1 Vasoconstrictor-recruitable thermogenesis

The stimulation of oxygen consumption by type A vasoconstrictors is characterized by a number of features. For a putative mechanism to be considered as a likely candidate, it must comply with the known features of type A vasoconstrictors. First, type A-vasoconstrictor mediated thermogenesis is not dependent on muscular contraction, as NE has been shown to elicit thermogenic effect in rat muscles treated with curare (172). No change in force development is detected during type A vasoconstrictor-mediated metabolism in the perfused rat hindlimb, thus the mechanism will not rely on contractility. Second, vasoconstrictor-stimulation occurs rapidly, corresponding with onset of vasoconstriction (59; 79). Further, the mechanism is readily deactivated upon removal of the vasoconstrictor or upon application of vasodilators (78). The mechanism is also sensitive to low oxygen tension and inhibitors of the electron transport chain (96). Finally, the mechanism appears to be inhibited directly by low sodium media and membrane stabilizers (291; 292). Thermogenic mechanisms available in skeletal muscle are now discussed, with particular reference to those that may be recruited during type A vasoconstrictor-mediated metabolism.

1.4.2 β3-Adrenergic receptors and thermogenesis

The thermogenic effects of intravenous norepinephrine infusion in cold acclimated rats are mediated by a combination of α- and β-adrenergic effects (116). Findings in the constant pressure perfused rat hindlimb are partly consistent with this, since α- and β- agonists (phenylephrine and isoproterenol) each induced increased rates of oxygen consumption (309), though the latter was quite small, and only evident under conditions of constant-flow. During type A norepinephrine-mediated metabolism, a significant α-adrenergic (prazosin-inhibitable) component has been demonstrated, consistent with the findings of Grubb & Folk (132), and auto-radiographic studies in rat hindquarter showing the prevalence of the α_1-subtype adrenoreceptors distributed on the small arteries (203). However the identity of β-receptor responsible for the much smaller increase in muscle oxygen consumption in

the absence of vasoconstriction is less clear. The thermogenic effects of the β-agonist isoproterenol were not blocked by the β1-, β2-antagonist propranolol (309), nor did propranolol significantly inhibit the effects of vasopressin or angiotensin in perfusion (79). It has been proposed that a β-adrenergic receptor (other than β1 or β2) may be responsible for the thermogenic effects of β-agonists, and possibly type A vasoconstrictors in perfused muscle (309).

The atypical-β, or β3 receptor has since been described in BAT and skeletal muscle of the rat (276) and in human adipose tissue (108), displaying resistance to the conventional β-blocker propranolol (4; 46; 47; 196; 276). The discovery that the methyl ester BRL-26830A bound specifically with the β3 receptor gave researchers a tool to pharmacologically manipulate this new β-receptor. Indeed it was shown that BRL 35135A [and a variety of similar compounds BRL 26830, CL 316,242 and SB226552] caused a modest increase basal rates of oxygen consumption (309) and glucose uptake in rat muscle (29; 196; 210). In an 8-week human trial, CL 316, 243 was also noted to enhance insulin sensitivity, lipolysis and fat oxidation (304). Thus, BRL 35135A was shown to have potential anti-obesity and anti-diabetic applications (6; 46; 47).

Studies in mature rats suggest that BAT contributes no more than 8% of the thermogenic effect of BRL 26830 treatment (7), therefore the thermogenic effects of β3-agoninsts are due primarily to other tissues, skeletal muscle in particular (4; 5; 290). Catecholamine activation of β3-receptors is thought to increase mobilization of fatty acids from triglyceride stores in brown and white adipose tissue, thereby increasing the rate of β-oxidation of fatty acids. The mechanism of increased heat production with β3-stimulation is currently thought to involve uncoupling, however the existence of functional uncoupling proteins in skeletal muscle remains unresolved (discussed later).

While BRL 35135A was shown to be thermogenic in the perfused rat hindlimb, these effects were small by comparison with type A vasoconstrictors [18% increase in $\dot{V}O_2$ versus 30%], and may only be evident during constant pressure experiments. Secondly, BRL 35135A was not vasoactive. It therefore seems unlikely

that the mechanism of type A mediated metabolism is dependent on β3-adrenoreceptor activation.

1.4.3 Uncoupled Respiration

1.4.3.1 Proton Leakage

Basal proton leakage has been identified in the mitochondria of many cell types including brain, liver, kidney, thymus and skeletal muscle (225; 251). Demonstrated in both isolated mitochondria, and intact cells, proton leak is not an artifact of isolation (225). The proton conductance pathway is unknown, though it is not attributed to UCP-1 (35; 37; 211; 212; 286), nor is it a simple biophysical leak of the mitochondrial membrane (35). Proton leak decreases the mitochondrial membrane potential, thereby forcing electron transport to work harder in order to counter the leak. For this reason, proton leak is thought to make a substantial contribution to basal oxygen consumption. In perfused skeletal muscle, proton leak has been estimated (with the use of oligomycin) to account for half (52%) of resting respiration rate (251). Combined with data from isolated rat hepatocytes, where 26% of basal oxygen consumption is attributed to proton leak (36), the potential contribution of proton leak to standard metabolic rate (SMR) in the rat is considerable [~18-22%, (251)].

These figures have been queried as overestimates, since resting tissue may have lower ATP requirements than in vivo. In the absence of ATP demand, proton leak will increase proportionally with increased proton motive force (251). Thus similar experiments were conducted under working conditions. Collaborative studies with Brand et al. demonstrate that the contribution of proton leak in perfused skeletal muscle during maximal tetanic contraction was in the vicinity of 34% (251). Proton leak in isolated rat hepatocytes supplied with substrates for ureagenesis and gluconeogenesis to increase the workload at was shown to account for 22% of the metabolic rate (252). Even under working conditions, the contribution of proton leak to SMR was still considerable [~15%,(251)].

These reduced values imply that proton leak becomes less significant during work. However, an alternative explanation is also worthy of mention. The perfused

hindlimb preparation may not be ideal for these types of experiments, due to inhomogeneous perfusion under basal conditions. These results hinge upon adequate delivery of oligomycin to all regions of the perfused hindlimb, in order to block the F_1F_0-ATP synthase. Exercise (tetanic contraction) in the perfused rat hindlimb may lead to enhanced tissue perfusion, and better delivery of oligomycin. The apparently lower value for proton leak during exercise may therefore be a more accurate reflection of the true contribution to total hindlimb respiration. Nonetheless, the contribution of proton leak to standard metabolic rate is still considerable.

Proton leak has also been studied under conditions of metabolic suppression. In muscles from the cold submerged frog during normoxia and anoxia, data was obtained to suggest that total proton leak was reduced during metabolic depression (284). However, this decrease was shown to be secondary to decreased flux through the electron transport train. Estivation in snails is another example of metabolic suppression (135). Evidence was obtained to suggest that remodelling of the mitochondrial membrane composition occurred in hepatopancreas on the estivating snail, allowing a co-ordinated, reversible suppression of mitochondrial membrane-associated processes (287), possibly including proton leak. Thus, proton leak appears to become less significant during periods of metabolic stress (exercise, hypoxia, or metabolic suppression).

If proton leakage is dependent on oxygen delivery in mammals as it appears to be in ectotherms, then vasoconstrictor-mediated thermogenesis in perfused skeletal muscle may be explained in the following terms. Micro-scale heterogeneity of blood flow under basal conditions may limit oxygen delivery and thus the rate of oxygen consumption. The coupling efficiency of oxygen consumption and ATP production might be expected to increase under these conditions, while the rate of uncoupled respiration (proton leak) is reduced to a minimum (122). This situation may be exaggerated during type B vasoconstrictor infusion, where muscle energy status begins to show signs of energetic stress [decreased PCr, Appendix Figure 1(300)]. However, during type A mediated vasoconstriction, enhanced tissue blood flow may facilitate oxygen delivery, relieving the limitation on muscle $\dot{V}O_2$. The rate of proton leak may increase proportionally to the change in oxygen delivery, accounting for a

much larger proportion of the total respiration rate. Thus, vasoconstrictors may affect the rate of uncoupled respiration by changing microvascular oxygen delivery.

1.4.3.2 UCP-1 homologues in skeletal muscle

The discovery of novel UCP's in tissues outside BAT raises the interesting possibility that uncoupled respiration in other tissues may contribute significantly to energy expenditure. While structurally similar [UCP-2, and UCP-3 show 55% and 56% amino acid identity with UCP-1 respectively], the actual function of these UCP homologues is unclear. It is thought that UCP's modulate the respiration rate by altering the potential difference across the mitochondrial membrane, perhaps affecting the quantity of ATP produced by respiration (249). UCP-2 is expressed in most tissues (31; 115), while UCP-3 expression is restricted to BAT, and skeletal muscle, with small amounts in heart and white adipose tissue (33; 124; 298). The function of UCP-3 in skeletal muscle is of particular interest owing to the thermogenic potential of this tissue. Skeletal muscle UCP-3 is postulated to be involved in the regulation of energy expenditure (54), body weight (101), and thermoregulation. UCP-3 has also been implicated in regulation of fatty acid metabolism (261), adaptive responses to acute exercise (82) starvation (101; 261), and the prevention of free radical formation (299).

Interestingly, tissue UCP expression levels have been noted to increase in response to β3-agonist treatment. Data have recently been obtained demonstrating increased UCP-3 levels in rat white adipose tissue (124), UCP-1, UCP-2 and UCP-3 in rat BAT (316), and UCP mRNA levels skeletal muscle and adipose tissue of obese mice (214; 215; 315) undergoing β3-agonist treatment. Thus uncoupled respiration has been suggested as the mechanism accounting for the stimulatory effects of β3-agonists.

Over-expression of murine, or human UCP-3 in yeast (124) or C_2C_{12} myoblasts respectively (32), demonstrates reduced mitochondrial membrane potential, thought to reflect the capacity for uncoupling by this protein. However, in a separate study by Harper et al. (142), where human UCP-3 was overexpressed in yeast

mitochondria, uncoupling was not stimulated by palmitate or superoxide, nor was it inhibited by GDP. It was concluded that uncoupled respiration observed in yeast overexpressing UCP-3 was entirely artifactual, and not attributable to UCP-3 expression (142). Overexpression studies have not resolved this issue.

Mitochondria from UCP-3 knockout mice have been shown to be more coupled than controls (125), with greater rates of free radical generation (299). Comparison with control mice, reveals normal body temperature and weight, normal responses to cold, fasting, stress, and thyroid hormone, with no compensatory increase in UCP-2 levels (125). The resting metabolic rate and respiratory ratio were shown to be the same in control and knockout mice, leading the authors to the conclusion that skeletal muscle UCP-3 is not a major determinant of metabolic rate.

In contrast, a paper from Clapham et al. (54), suggests that skeletal muscle UCP-3 does indeed have the potential to influence whole body metabolism. The authors describe the effects of over-expressing human mitochondrial UCP-3 in a transgenic mouse line [66-fold increase in UCP-3 expression in the inner mitochondrial membrane]. The authors report a decreased mitochondrial membrane potential, supporting a role for UCP-3 in mitochondrial uncoupling. The mice were hyperphagic, but remained lean, with less adipose tissue than wild type controls, strongly implying the involvement of UCP-3 in whole body energy expenditure (54). It must be stressed that genetic manipulation may not give a true indication of the physiological function of these proteins *in vivo*. The effects of more physiological (diet, exercise and cold exposure) manipulations on UCP-3 expression are currently being investigated.

Regulation of UCP-2 and UCP-3 expression is tissue specific (32; 33; 124; 316), resulting in tissue specific responses to the same physiological stimuli. Like UCP-1, UCP-3 expression is decreased by starvation. However, starvation has the curious effect of increasing skeletal muscle UCP-2 and UCP-3 mRNA levels (124). It seems paradoxical to increase the level of uncoupling (a somewhat wasteful mechanism), when substrate supply is severely limited.

An alternative explanation is that starvation leads to tissue wasting, and loss of insulation, hence increased skeletal muscle uncoupling is necessary to provide essential heat (124). There are however, several lines of evidence against this theory. Studies in rats have shown that skeletal muscle contributes significantly to energy conservation during starvation, by decreasing total blood flow through the tissue (200). The second, is that during re-feeding, rats showed an accelerated rate of fat deposition, while UCP-2 & UCP-3 levels rapidly return to control values, but energy expenditure remained low (100). The energy conserving mechanism persists independently of the thermoregulatory needs of the rat. Third, the starvation induced increase in UCP-2 and UCP-3 levels occur even at thermoneutrality (40; 261). Finally, neither short term [48hrs at 6°C, (32)], nor longer-term [20 days at 6°C, (33)] cold exposure affected skeletal muscle UCP-3 expression. It therefore seems unlikely that skeletal muscle UCP's participate in thermoregulatory thermogenesis (261).

A more likely explanation, is that skeletal muscle UCP's participate in metabolic fuel partitioning (101). Dulloo et al. (101) suggest that starvation induced UCP expression may reflect a switch from glucose to lipid as the primary fuel source. The starvation-induced change in UCP-3 is more pronounced in fast glycolytic white muscles than slow red muscles, consistent with the capacity of these muscles to readily shift between glucose and lipid as fuel substrates (261). Adding weight to this argument are the findings of Weigle et al. (302), demonstrating induction of skeletal muscle UCP-3 mRNA merely by infusing free fatty acids. Physiologic states associated with enhanced fat metabolism are positively correlated with increased UCP-3 mRNA levels in skeletal muscle (31). Conditions of fuel depletion [acute exercise, and hypoxia], and artificial metabolic stress [induced by AICAR incubation] have also been shown to induce muscle UCP-3 expression (318). Taken together, these results are more consistent with roles for UCP-2 and UCP-3 in the regulation of lipid as fuel substrates than as mediators of thermoregulatory thermogenesis (101; 261; 318) .

The definitive role of UCP-2 and UCP-3 in skeletal is unclear. Current literature tends away from roles in adaptive thermogenesis, in favour of alternative hypotheses, such as regulation of fuel metabolism. The likelihood that type A

vasoconstrictors induce expression of UCP in skeletal muscle is remote. However, the possibility still remains that type A vasoconstrictors may stimulate uncoupled respiration in muscle, through either endogenously expressed UCPs or proton leak.

1.4.4 Ion cycling

1.4.4.1 Calcium cycling

Contribution of the Ca^{2+}-ATPase to resting muscle metabolic rate is estimated in the vicinity of 5-10% of basal energy metabolism (52; 76; 254). Skeletal muscle has a large pool of calcium sequestered in the sarcoplasmic reticulum, an essential requirement for contraction, however raised intracellular Ca^{2+} [subthreshold for contracture] has the capacity to stimulate metabolic rate and heat production independent of contraction. Cycling of calcium between the sarcoplasmic reticulum and the cytosol [via the Ca^{2+} release channel and the Ca^{2+}-ATPase] has been demonstrated as en effective heat producing mechanism in specialized eye-muscles of several different fish species (27; 28). Modified eye muscles contain large numbers of mitochondria with extensive networks of smooth endoplasmic reticulum, but lack contractile elements. A complex countercurrent heat exchanging vascular system enables transfer of heat to the eyes and brain (27), maintaining temperatures above ambient water. The mitochondria are fully coupled with no detectable expression of UCP (27). Examination of key metabolic enzymes reveals a large capacity for oxidative metabolism (293), with ATP being derived from either lipid or carbohydrate metabolism.

In homeotherms also, evidence has been obtained for increased muscle calcium cycling during cold exposure. Muscles from cold acclimated ducklings show elevated rates of sarcoplasmic reticulum Ca^{2+}-ATPase activity, and a 30-50% increase in the fraction of vesicles containing ryanodine sensitive calcium release channels (102). Elevated calcium cycling may also account for elevated metabolism observed in hyperthyroid models (110; 213; 277; 295). Perhaps the most spectacular example of elevated metabolism through increased calcium cycling is during malignant hyperthermia. A genetic defect in the ryanodine receptor (calcium release channel) predisposes susceptible individuals to a life threatening hypermetabolic condition triggered by a combination of anaesthetics and muscle relaxants commonly

administered pre-operatively. The patient presents with a dangerously high fever (5-10°C above normal), increased $\dot{V}O_2$, metabolic acidosis and muscle rigidity (130; 201). The defective ryanodine receptor is hypersensitive, and fails to deactivate. The channel remains open for longer periods, resulting in calcium flooding. Other cellular processes that are sensitive to calcium levels (contraction, glycolysis etc.) are forced into overdrive causing muscle rigidity and massive efflux of lactic acid. Left untreated, tissue damage and death are likely outcomes.

Is calcium cycling a likely mechanism to account for type A-vasoconstrictor mediated thermogenesis? Activation of intracellular calcium cycling by norepinephrine was examined by Cox & Gibbs (85) in small bundles of rat muscle. No evidence was found to suggest direct activation of intracellular calcium cycling or heat production by norepinephrine, however an alternate possibility still exists. Skeletal muscle calcium cycling is triggered in response to a variety of stimuli, including K^+-depolarization (18; 23; 52; 146; 294) and hyperosmolar media (49; 85). Redistribution of blood flow and increased tissue perfusion may increase the extracellular concentrations of K^+ and or the osmolarity of the perfusing media, thereby activating intracellular calcium cycling. Calcium cycling is therefore considered a potential candidate during type A-vasoconstrictor mediated thermogenesis.

1.4.4.2 Sodium cycling

The proposal that the Na^+/K^+-ATPase (sodium pump) plays a role in skeletal muscle NST has been brought forward a number of times (134; 162; 274; 289). The Na^+/K^+-ATPase is an integral membrane protein found primarily on the sarcolemma of all higher eukaryotes (195), and is particularly prevalent in skeletal muscle (66; 68). The pump is an electrogenic (69), P-type ion proton motive ATPase (159). Three Na^+ are transported out of the cell, for every two K^+ pumped in during each ATP-dependent cycle (281). The sodium pump participates in the maintenance and restoration of resting membrane potential, while assisting with osmotic balance, and cell volume (111). It has been suggested that skeletal muscle may derive non-shivering heat through increased Na^+/K^+-ATPase pump activity and ATP turnover.

The contribution of the sodium pump during basal, cold- and norepinephrine-stimulated metabolism is now explored.

Cardiac glycosides ouabain (an alkaloid extracted from the ouabao tree, *Strophanthus gratus)*, digoxin and digitoxin (derived from foxglove, *Digitalis purpurea*) bind specifically with the sodium pump (121), in a stoichiometric ratio of 1 drug molecule per enzyme (140), inhibiting transport activity and ATP turnover (313). Ouabain is also known to cause a rapid depolarization, as demonstrated in mouse skeletal muscle myoballs (189), and in isolated incubated rat soleus muscle (69), reflecting the importance of the sodium pump in the maintenance of resting plasma membrane potential. Inhibition with the specific inhibitor ouabain enables the contribution of the sodium pump to basal metabolism to be assessed. Conservative estimates place the resting energetic cost of active Na^+/K^+ transport between 4-10 % of basal energy consumption (76). Similar figures are noted in human, rat, and mouse muscle preparations (26; 51; 112; 224). Higher values may be found in the literature, though these values should be regarded with caution especially in cut or non-intact muscle preparations, where the ouabain-inhibitable fraction of basal metabolism is artificially enhanced due to sodium leakage into the cytoplasm (51; 76).

Tissue slices from cold exposed rats appear to display increased rates of oxygen consumption when compared with controls, an effect that was abolished in low sodium media (134). These findings support the idea of increased sodium pump activity during cold exposure. In young pigs exposed to cold, an overall upregulation in the number of ouabain binding sites was noted (87; 143), indicating an overall increase in the concentration of sodium pumps. However, the authors concede that this was probably due to increased muscular activity and tissue hypertrophy during shivering, rather than upregulation of muscle NST. Thus, ouabain binding studies alone are inadequate for estimation of cold induced NST in muscle.

Dubois-Ferriére & Chinet (97) estimated the contribution of muscle sodium pumping during cold acclimation, by measuring the ouabain-suppressible fraction of basal heat production in incubated perifused mouse soleii. In cold acclimated soleii, the ouabain-suppressible fraction of basal heat production was shown to be enhanced (approximately 45%) by comparison with warm acclimated muscles. Shiota &

Masumi (274) also examine the effect of cold exposure on perfused rat hindlimb metabolism. Cold exposure (4°C for up to 20 days) did not significantly affect basal metabolic rate. However, responsiveness to NE was markedly enhanced by cold (> 50% increase in $\dot{V}O_2$). The stimulatory effects of NE were diminished by prior addition of ouabain, propranolol, or phentolamine to the perfusate. These data were interpreted as evidence of increased muscle NST during cold exposure, via increased sodium pump activity (274).

Age, physical activity, and hormonal status are significant factors in the regulation of sodium pump number and activity (66; 67). Excitation is the primary stimulus for Na^+/K^+-ATPase activation (68; 76), though pump activity is also modulated by a variety of humoral factors including epinephrine, norepinephrine, insulin, insulin-like growth factor, calcitonin gene related peptide, calcitonin, amylin, glucocorticoids, cytokines, and neurotransmitters (67; 74; 288). The stimulatory effects of catecholamines on muscle Na^+/K^+-ATPase are evident in a variety of species and preparations (65; 69; 233). Direct effect of catecholamines on the Na^+/K^+-ATPase activity have been demonstrated in isolated incubated muscle preparations, with norepinephrine and epinephrine causing hyperpolarization of rat soleus fibers, along with increased rates of Na^+ extraction (83%) and K^+ accumulation (34%) (69). This catecholamine effect was shown to be mediated via β-adrenergic mechanisms, since it was blocked by low dose propranolol, and mimicked by cAMP and theophylline (69).

Despite these observations, catecholamines do not directly stimulate oxygen consumption in isolated incubated muscle preparations (85; 97). The failure of NE to elicit an increase in isolated muscle metabolism, contrasts with the marked stimulatory effects of NE in the perfused rat hindlimb (97; 231). It has been suggested that the *indirect* vascular effects of NE and other type A vasoconstrictors may be more important in the activation of the sodium pump than direct effects. Observations that type A vasoconstrictor-mediated metabolism is reduced by low sodium perfusion media (291), and propranolol (292) tend to support this theory. The involvement of the Na^+/K^+-ATPase during type A vasoconstrictor-mediated metabolism is therefore a subject of great interest.

1.5 Aims

The regulation of perfused resting skeletal muscle metabolic rate by vasoconstrictors is now examined in more detail. Redistribution of flow is an important aspect of vasoconstrictor-mediated thermogenesis, and it is now proposed that vasoconstrictor-mediated changes in skeletal muscle metabolic rate are the direct result of changes in oxygen delivery at the microvascular level. The potential activation of cellular thermogenic mechanisms in addition to redistribution of flow is also examined, with reference to previous publications implicating the involvement of sodium-dependent mechanisms.

CHAPTER 2

METHODS AND MATERIALS

2.1 Introduction

The following sections outline the methods and materials utilized for the experimental procedures, while experimental protocols are outlined in the individual chapters. Contained are details of the perfused rat hindlimb preparation, isolated rat heart preparation, and assay techniques. The perfused rat hindlimb has previously been validated as a viable *in vitro* system for the study of skeletal muscle metabolism, with muscle being responsible for over 95% of the resting respiration rate (258). Previous work from this laboratory has shown that the levels of high energy metabolites (including ATP, creatine phosphate, ADP, AMP, glucose-6-phosphate, glycogen and lactate ratios), do not differ significantly from *in vivo* muscle values after 3 hours of perfusion, at 25°C, with a flow rate of 4 ml/min (78). Under these conditions, lactate-to-pyruvate ratios were normal, ruling out the possibility of tissue hypoxic degeneration (310).

2.2 Perfused rat hindquarter preparation
2.2.1 Animals

Male Hooded Wistar rats of a local strain were housed in a 12hr light/ 12hr dark cycle, at a constant temperature of 22°C. Animals had free access to water and commercial rat chow (Gibson's, Hobart) containing 20.4% protein, 4.6% lipid, 69% carbohydrate and 6% crude fiber with added vitamins and minerals.

Some experiments required the use of 3-4 week old (70-80g) rats. This was necessary for consistency with previous studies by Tong et al. (291; 292), where the reported levels of Na^+/K^+-ATPase were shown to be maximal (72; 177). Owing to the small muscle mass, both hindlimbs were perfused at a total flow rate of 4 ml/min in a non-recirculating fashion (0.47ml/g muscle/min). All other perfusions were conducted as non-recirculating single hindlimb experiments, with large rats weighing 180-200g, in accordance with previous studies from this laboratory (63; 79; 242; 310). Flow was maintained at 4 ml/min per single hindlimb (0.26 ml/g muscle/min).

Animal care and handling was in accordance with recommendations of the Animal Welfare Committee of the National Health and Medical Research Council (in the Australian Code of practice for the care and use of animals for scientific purposes, 6th Edition, 1997). All anaesthetic, surgical and experimental procedures were approved by the committee for Ethical Aspects of Research Involving Animals of the University of Tasmania.

2.2.2 Surgery

The surgical procedure has been described elsewhere (79), essentially a modified version of the technique used by Ruderman *et al.* (258). Animals were anaesthetized with pentobarbital sodium (Nembutal, Rhone Merieux Australia Pty. Ltd) 60 mg/ml. The amount of anaesthetic required per animal was calculated based upon the recommended dose of 5-6mg/ 100g body weight. Anaesthetic was diluted with isotonic (0.9%) saline and injected i.p. Surgery commenced once animals were completely anaesthetized.

Figure 2.1 illustrates ligation and cannulation positions. Strong cord was used to tie firm ligatures around the base of the tail, and the tarsus of the perfused foot/feet. The abdominal cavity was exposed by a midline incision through the skin and the abdominal wall, extending from the pubic to hepatic regions. Major vessels including the inferior-, and superior-epigastrics, skin vessels, as well as iliolumbars, internal spermatics and ureters were ligated to reduce bleeding during surgery. For single hindlimb perfusions, the right common iliac artery was also ligated, restricting flow to the left limb (this step was omitted for dual hindlimb perfusions). Firm ligatures were placed around the testes, the bladder and the seminal vesicles (in mature rats only), followed by the excision of these organs. Ligation of the descending colon and the duodenum allowed the removal of the viscera.

X Points of cannula insertion

Common Iliac Ligature (tied off for single hindlimb perfusions only)

Vena Cava
Aorta
Renal
Kidney
First pair of ligatures
Second pair of ligatures
Iliolumbar vessels
Internal Spermatic
Ureter
Skin Vessel
Bladder
Seminal vesicle
Foot
Tail
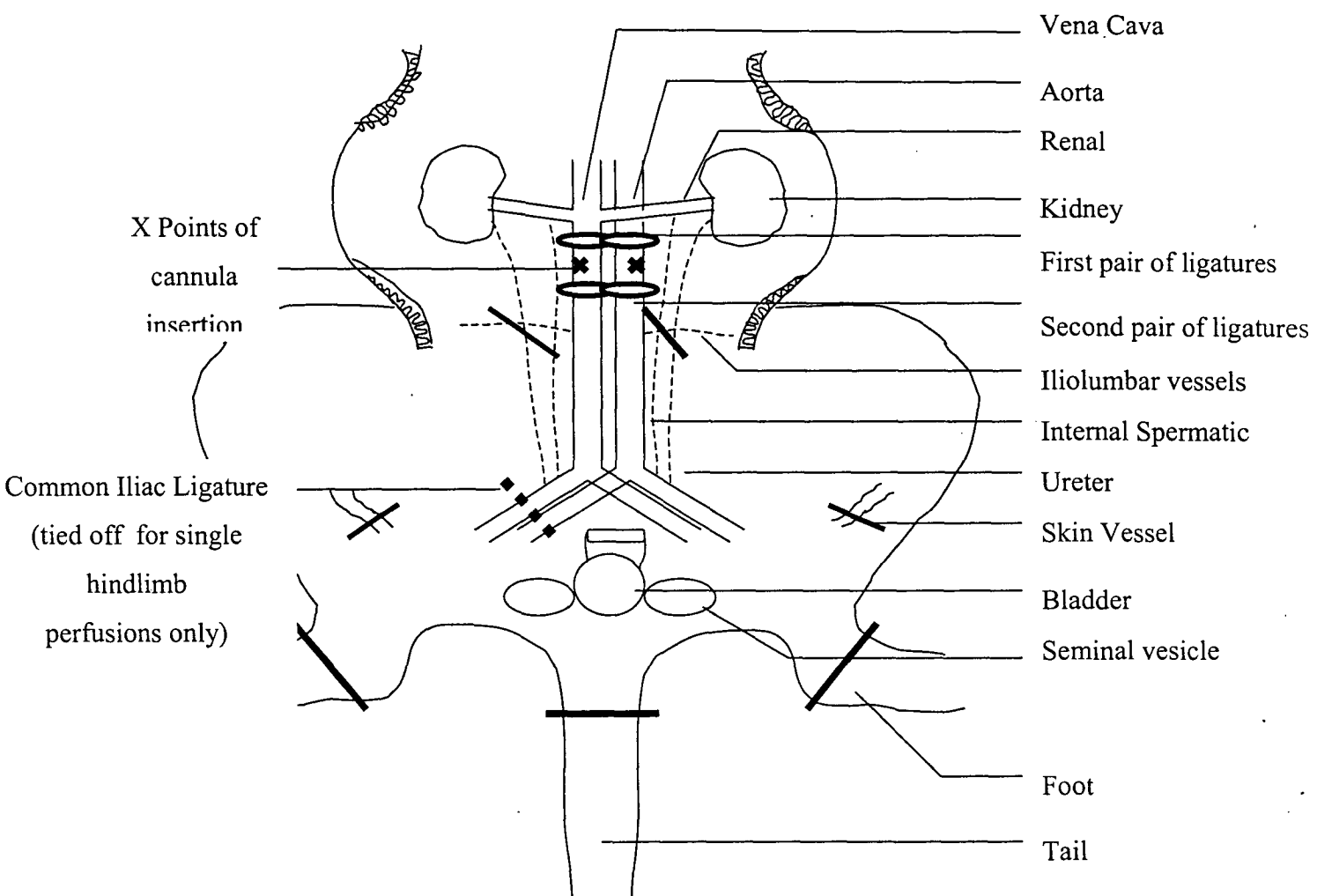
Figure 2.1 Illustration of the ligation and cannulation positions for the surgical preparation of the isolated rat hindlimb.

The perfusion method was modified from Ruderman et al. (1971).

Surgery is the same for single and dual hindlimb perfusions, with the exception of an additional ligature placed around the right common iliac for the single hindlimb perfusion, and the removal of the seminal vesicles in mature rats.

The vena cava and the aorta were delicately separated with a fine pair of forceps, and silk ligatures placed loosely around the vessels. The preparation was heparinized (500μl, 500 IU/ml- David Bull Laboratories Australia), one minute prior to tightening the upper ligature on the vena cava. A Terumo 16G catheter was inserted into the vena cava and secured in position with silk ligatures. Cannulation of the descending aorta was carried out with an 18G Terumo catheter filled with isotonic (0.9%) saline. The saline inside the syringe was slowly expelled to prevent the entry of air bubbles into the preparation, and to aid the washout of red blood cells. The aortic catheter was secured in position with silk ligatures, level with the venous catheter. The tips of the catheters were positions approximately 3mm above the aortic bifurcation.

The entire preparation was then transferred to the perfusion cabinet where the arterial cannula was connected to the inflow line containing oxygenated medium. Care was taken to avoid the entry of air bubbles into the preparation. Approximately 2 minutes elapsed between the time the vena cava was ligated and the flow was re-established. Venous effluent was collected in a waste reservoir. The animal was then killed with a lethal dose of Nembutal administered via an intra-cardiac injection, and a whole body ligature was placed around the level of the L3 and L4 vertebrae to prevent the flow of perfusate to the upper portions of the body. After a few minutes, most of the red blood cells were washed out, and the venous line was connected to the oxygen electrode.

2.2.3 Perfusion apparatus

Figure 2.2 illustrates the hindlimb perfusion apparatus. Perfusions were conducted at 25°C using 2% BSA with 1.27 mM calcium (unless otherwise stated). The buffer reservoir was continuously stirred and gassed with carbogen (95% O_2, 5% CO_2 – BOC Gasses). Buffer was pumped via a peristaltic pump (Masterflex, Cole-Parmer) at a constant flow rate 4 ml/min (for two hindlimb perfusions in small 70-80g. rats, and for single hindlimbs in 180-200g rats). From the reservoir, the buffer was pumped through a heat exchanger coil maintained at 25 ± 1°C by a thermostatically controlled water heater and pump (Julabo EM, John Morris Scientific).
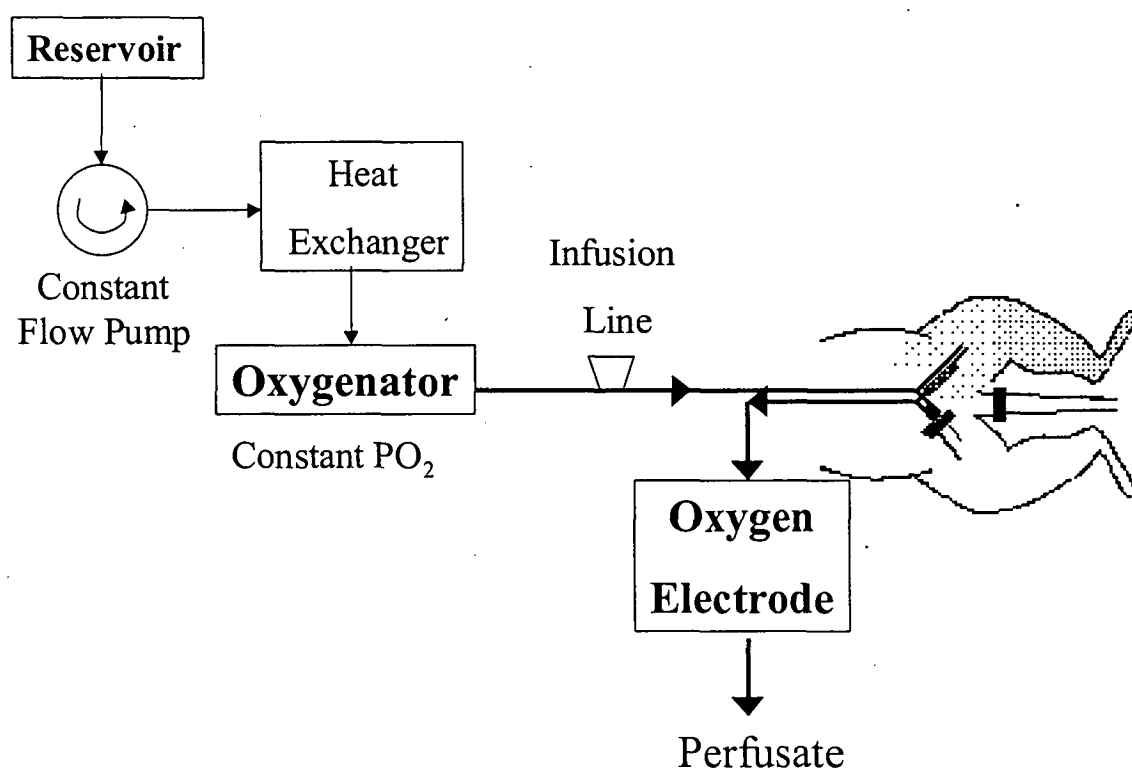
Figure 2.2 Perfusion Apparatus

Following surgical preparation of the isolated hindlimb, the preparation was transferred to the perfusion cabinet and connected to the apparatus. Perfusion media was pumped at constant-flow from a reservoir through a heat exchanger and artificial lung. Warmed, oxygenated media passed through bubble traps before entering the hindlimb. After passing through the hindlimb, perfusion media passed through a Clark type oxygen electrode. Perfusate samples were collected after the electrode.

Perfusate was oxygenated by passage through a sealed silastic artificial lung, continuously gassed with carbogen. Bubbles were prevented from entering the hindlimb by inline bubble traps located proximally to the rat. The entire apparatus was maintained at either 25°C or 37°C.

Arterial pressure development was recorded by means of a pressure transducer (Sphygmomanometer, Malyoung) located proximally to the aorta. Flow was maintained at a constant rate, therefore changes in pressure reflect changes in vascular resistance. This may be seen by applying Poiseuille's Law, for the steady laminar flow of a fluid through a cylindrical tube, where $Q = \pi(P_i - P_o)r^4 / 8\eta L$

where:

Q	= flow rate;
$P_i - P_o$	= pressure difference;
r	= radius of vascular wall;
η	= viscosity of the perfusate;
L	= length of the tubing

Assuming that Q, π, η, and L are all constant, then it may be seen that pressure is proportional to $r^{1/4}$. Therefore, a small decrease in the average radius is reflected by a large increase in pressure. Continuous measurement of oxygen content of venous effluent occurred via a flow-through a water-jacketed Clark-type oxygen electrode (0.5 ml capacity), maintained at $25 \pm 1°C$. Calibrations of the oxygen electrode were made before and after each perfusion with 100% O_2 gas (BOC- Gasses), and air. The oxygen content of gassed arterial perfusate was also determined at the end of each experiment, allowing the extent of electrode drift to be taken into account for calculation of oxygen consumption.

Both PO_2, and perfusion pressure (PP) were recorded continuously on WinDaq Serial Acquisition Version 2.08 (DATAQ Instruments Inc., Microsoft Corp.).

2.2.4 Perfusion media

2.2.4.1 Modified Krebs-Ringer bicarbonate buffer

Perfusion medium consisted of a cell free modified Krebs-Ringer bicarbonate buffer. The constituents of the buffer (mM) were 118 NaCl, 4.7 KCl, 1.19 KH_2PO_4, 1.18 $MgSO_4$, 25 $NaCO_3$, 8.3 D-glucose (monohydrate), with 2% w/v Bovine Serum Albumin (BSA - Fraction V, from CSL Ltd.). Medium was filtered (0.45µm filter paper) before use, and maintained at 4°C, while being gassed with 95%O_2 and 5% CO_2, (carbogen, BOC-Gasses). $CaCl_2$ was added to the perfusion medium to give a final concentration of 1.27 mM, after the perfusate had been gassed.

2.2.4.2 Red blood cell containing medium

For some perfusions, cell free medium was found to be oxygen limiting, therefore a medium containing washed bovine red blood cells was substituted. Fresh bovine erythrocytes were filtered through cheesecloth, and washed three times in filtered saline (0.9% NaCl). Erythrocytes were then washed twice more in Krebs, and stored in gassed (95% oxygen- 5% CO_2) Krebs-Ringer solution at 4°C (317). On the day of use, erythrocytes were washed a further 2 times, until all lysed cells were removed, and filtered once again through 6 layers of pre-washed cheesecloth. Erythrocytes were never more 4 days old when used. The red blood cell containing medium was composed of a modified Krebs-Ringer bicarbonate buffer (the same as described earlier, 2.2.4.1), 4% BSA, 2.54mM $CaCl_2$, 228µl/l heparin, and 1.2mM pyruvate, combined with washed bovine erythrocytes to give a final haematocrit of 33-35%. This perfusion medium resulted in minimal oedema (237). Both the arterial and venous perfusate passed through a continuous Arterio-venous Oxygen Difference Analyser (A-VOX Systems Inc., Texas USA) which measures the spectral difference of arterial versus venous blood at 660nm.

2.2.5 Infusion agents

Agents that were not water-soluble were dissolved first in 100% ethanol, then added to the perfusion medium (final ethanol volume never exceeded 1% final volume). Water-soluble agents were dissolved directly into the perfusion medium. All other agents were prepared freshly on the day of use. NE was prepared in ascorbic acid saline; AII, 5-HT and propranolol in saline; veratridine (free base) was dissolved in dH_2O, and neutralized with concentrated HCl; tetrodotoxin was readily soluble in dH_2O.

2.2.6 Calculation of oxygen consumption ($\dot{V}O_2$)

2.2.6.1 $\dot{V}O_2$ in cell free BSA medium

The rate of the volume of oxygen consumed ($\dot{V}O_2$) by the perfused hindlimb was calculated from the arteriovenous (A-V) difference in oxygen content of the perfusate, with the following formula.

$$O_2 \text{ uptake } = \frac{ap^{25} \text{ x } (PaO_2 - PvO_2) \text{ x flow rate x } 60}{\text{muscle mass}}$$

where ap^{25} = Bunsen solubility coefficient for O_2 in human plasma, at 25°C.

                    = 1.509 mmol/l per mmHg

     PaO_2 = arterial partial pressure of O_2 (mmHg)

     PvO_2 = venous partial pressure of O_2 (mmHg)

     flow rate   = μl /min

     muscle mass   = mass of skeletal muscle perfused in grams,

                    small rats (2-HL) = body weight (g) x 0.141-2.534 (236)

                    large rats (1-HL) = body weight /12 (258)

2.2.6.2 Measurement of $\dot{V}O_2$ in red blood cell containing medium

The AVOX analyser gave an estimate of the arterio-venous oxygen difference based upon the spectral differences of arterial and venous blood at 660nm. Dissolved oxygen content was not measured by the AVOX. The protocol in Chapter 3 requires the arterial oxygen content to be varied, ie. blood was gassed with lessening amounts of

oxygen, hence the arterial blood changed colour as the experiments progressed. The linearity of the AVOX was questionable at these low oxygen tensions, therefore an alternative method for measuring total oxygen content (dissolved and carried) of the blood was sought.

The total oxygen content of perfusate samples was determined using a galvanic cell oxygen analyser (TasCon oxygen content analyser manufactured by the Physiology Department, University of Tasmania). Small blood samples were collected from the arterial line (immediately before the rat), and from the venous line in air tight insulin syringes (1ml B-D Ultra-Fine Insulin Syringe). The rates of oxygen uptake were calculated from arterio-venous oxygen differences, flow rate, expressed per gram of perfused muscle, as previously described (96).

2.3 Perfused rat heart preparation

2.3.1 Animals

Male rats of the local Hooded Wistar strain (180-230g body weight) were used for heart perfusions. Housing conditions, and anesthesia were the same as described in Section 2.2.1.

2.3.2 Isolation and cannulation of the rat heart

Hearts were perfused in a Langendorff manner using a system based on that of Williamson (306). During anesthesia, a cut was made across the upper abdomen; the incision continued laterally through all the layers of the thorax including the ribs, collapsing the lungs, and exposing the beating heart. The aorta was cut at a length 4-5mm from the ventricle, adequate for cannulation. Following removal from the thoracic cavity, the heart with the attached length of aorta was placed into ice cold Krebs. The metal cannula on which the heart was to be mounted in the cabinet, was freely dripping warm oxygenated medium, awaiting cannulation. The aorta was grasped from opposite sides with two pairs of fine curved forceps, gently lifted over the straight metal cannula, and held in position with a metal clip. A ligature was then tied around the aorta, securing the heart on the cannula.

2.3.3 Perfused heart apparatus

The apparatus for heart perfusions was essentially the same setup described in Section 2.2.3. Briefly, perfusion medium (modified Krebs-Henseleit bicarbonate buffer, Section 2.2.4) was pumped at a constant flow through a series of heat exchange coils, and a silastic lung gassed to equilibration with carbogen (95% O_2: 5% CO_2). The perfusion cabinet, and heat exchange system was maintained at 37°C. Hearts were perfused at a constant flow (6.79 ± 0.12 ml.min^{-1}), equivalent to 8.94 ± 0.25 ml.min^{-1}.g wet wt heart $^{-1}$. Oxygen content of the venous perfusate was constantly monitored at 37°C with an in-line Clark-type oxygen electrode, calibrated with O_2 gas and air (as described in Section 2.2.3). Oxygen uptake was calculated according to the method outlined in Section 2.2.6). The cannulated heart was contained within a sealed chamber (volume 10 ml) to prevent exchange of O_2-CO_2 between effluent perfusate and the atmosphere. In this system, drift in measurement was less than 2% hr^{-1} (243). Aortic pressure was continually recorded with a CFP blood pressure monitor (Model 8138).

2.3.4 Heart perfusion medium

Hearts were perfused with a modified Krebs-Henseleit bicarbonate buffer (described in Section 2.2.4.1) containing 0.05mM EDTA, 5mM pyruvate, and 5mM glucose.

2.4 Measurement of membrane potential (E_M) in the perfused rat hindquarter

Measurement of skeletal muscle membrane potential was conducted at Flinders Medical Centre between November 1998, and April 1999. Work was carried out in the Smooth Muscle laboratory under the supervision of Dr. Tim Neild. All experiments were conducted at 25°C, at 4 ml/min flow rate with juvenile (70-100g) rats, with approval of Flinders Medical Centre Animals Ethics Committee. The hindlimb was prepared for a dual hindlimb non-recirculating perfusion (Sections 2.2.1 –2.2.3). Perfusion pressure and oxygen consumption were recorded continuously on a laptop computer with the WinDaq Data Acquisition software installed.

2.4.1 Preparation of the muscle

During the period of equilibration, the hindlimb was prepared for the measurement of membrane potential. A small section of skin covering the tibialis muscle of the animal's left hindlimb was exposed with sharp scissors, taking care not to damage the underlying fascia. The exposed surface was kept moist with perfusion medium, and covered with a piece of laboratory parafilm to prevent drying. Using a felt tip marker, a mark was made on the parafilm, and a small hole pierced through the parafilm with fine scissors. This served as the target area for insertion of the glass electrode.

2.4.2 Apparatus and equipment.

Glass electrodes were made on the day of each experiment, with the use of an electrode pulling machine. Electrodes were filled with 2M KCl solution, and attached to the micromanipulator, with a silver wire electrode in contact with the KCl inside the electrode. This arrangement allowed changes in electrical potential to be detected and quantified. Signals from the electrode were amplified and fed into an oscilloscope. The membrane potential (E_M) data was recorded continuously with MacLab data acquisition software. Figure 2.3 shows the apparatus.

Every effort was made to ensure minimal electrical interference. A thin layer of aluminium foil shielding was used to minimize interference from surrounding light, and electromagnetic equipment. The rat, surrounding equipment, stage and aluminium foil shielding were grounded. The micromanipulator was used to slowly wind the glass electrode downwards, until contact was made with the tissue, and the muscle fascia pierced. At this time, the potential was adjusted to a "zero" reference. Resistance of around $50\text{-}200M\Omega$ was optimal, and those electrodes with resistances outside of this range were discarded.
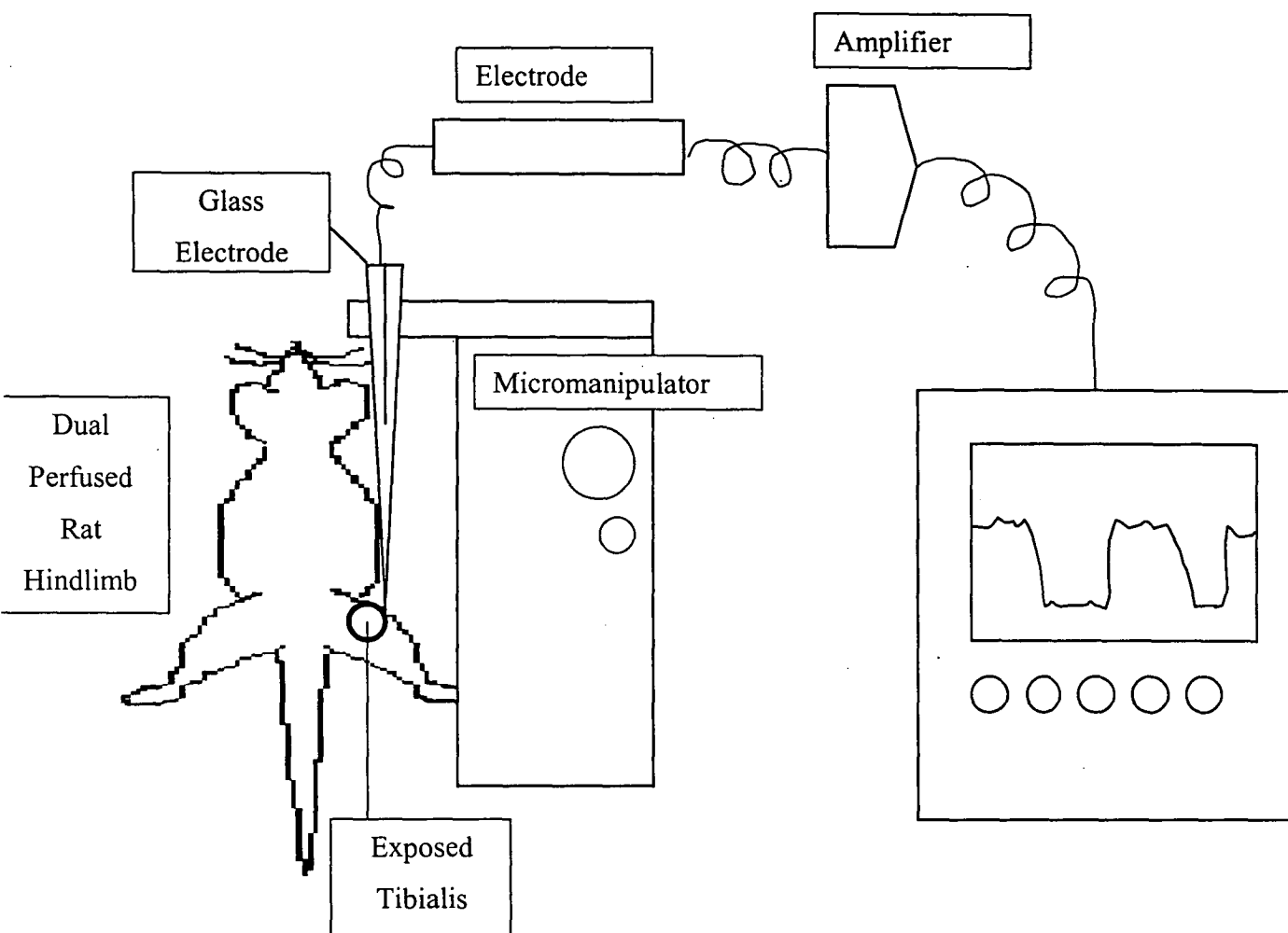
Figure 2.3 Schematic Representation of the equipment setup for the measurement of membrane potential in the perfused rat hindlimb.

The perfused muscle preparation was allowed 50 mins equilibration before commencement of membrane potential measurement. Glass electrodes were used to pierce the muscle in the exposed tibialis region.

With a suitable electrode resistance, and a stable zero position, the micromanipulator was used to wind the electrode down further into the tissue. A successful clean cell entry was indicated by a sudden jump from 0 to $-70mV$, as visualized by the oscilloscope. When the change to $-70mV$ was slow, this typically indicated a poor entry, and was not pursued. Following each impalement, the electrode was wound back upwards to the exterior of the cell to check that there zero reference was still stable, and had not drifted.

2.4.3 Measurement of E_M during agonist infusion

Measurements of membrane potential were made before and during infusion of drugs of interest. During the initial moments of vasoconstrictor infusion, the electrode was withdrawn from the tissue, since vasomotion might damage the fine glass electrode. To ensure that the electrode was not impaling the same damaged fibers repeatedly, the positioning of the electrode was moved slightly with each impalement (in a lateral direction). In each rat, the change in oxygen consumption was allowed to completely recover, before another infusion commenced. The order of experiments was randomized. The glass electrodes used during this study were too large to measure membrane potential in vascular smooth muscle cells, or endothelium, therefore the study was restricted to measurement in skeletal muscle fibers only.

2.4.4 Experimental protocol

Once a stable basal measurement of resting E_M was obtained, the glass electrode was withdrawn from the tissue, and infusion commenced. This was especially important for the infusion of vasoconstrictors, where considerable movement of the tissue was noted. After the change in vascular resistance had plateaued (this often preceded the plateau in $\dot{V}O_2$), the electrode was re-inserted into the tissue for a measurement of E_M during stimulated $\dot{V}O_2$.

2.4.5 Calculation for the estimation of membrane potential in skeletal muscle fibers

The Nernst equation allows calculation of plasma membrane potential based upon intra- and extracellular concentrations, and membrane permeability to individual ions. The Goldman-Hodgman-Katz equation is a modified version of the Nernst equation, given by

$$E_M = \frac{RT}{F} \log_{(10)} \frac{E_K[K]_i + E_{Na}[Na]_i}{E_K[K]_o \quad E_{Na}[Na]_o}$$

Where R   = the thermodynamic gas constant

T   = the absolute temperature

F   = the Faraday constant (96485.309 C/mol)

E_K = potassium permeability constant (1.0 mammalian skeletal muscle)

$[K]_i$ = intracellular potassium concentration (mM)

$[K]_o$ = extracellular potassium concentration (mM), 4.74mM

E_{Na} = sodium permeability constant (0.03 mammalian skeletal muscle)

$[Na]_i$ = intracellular sodium concentration (mM)

$[Na]_o$ = extracellular sodium concentration (mM), 145mM in perfusion medium

NB. At room temperature, the RT/F component of this calculation is approximated at 58mV. Values for intracellular potassium and sodium are estimated at 140, and 10 mM respectively.

2.5 Methods for assessing nutritive and non-nutritive flow in the perfused rat hindlimb

2.5.1 Conversion of 1-MX

Xanthine oxidase, an enzyme located on the capillary endothelium (175), catalyzes the conversion of the exogenous substrate 1-methylxanthine (1-MX) to 1-methylurate (1-MU). Changes in the conversion rate of 1-MX to 1-MU potentially indicate changes in the ratio of nutritive to non-nutritive flow. The conversion rate of 1-MX was shown to increase during exercise in the blood perfused rat hindlimb (317) while the type B vasoconstrictor serotonin decreased 1-MX conversion (234). An increase in the ratio of 1-MU concentration (μM): 1-MX concentration (μM) is

indicative of enhanced nutritive perfusion, while a decrease in 1-MU/1-MX ratio indicates decreased nutritive flow.

20 µM 1-MX was included in perfusion medium. 1-MX (Sigma) was first dissolved in dH$_2$O, with 1M NaOH (100µl) at a final concentration of 20 mM, and 1 ml of this solution was added for every litre of perfusion medium. Arterial + venous samples were collected for later analysis with HPLC (outlined in Section 2.6.2). Samples were centrifuged briefly to remove red blood cells (4°C), and 0.5 ml of the supernatant was added to 0.1 ml of 2M HClO$_4$ and left to precipitate at 0°C. Samples were again centrifuged (8000g for 5 min) to remove precipitate, awaiting HPLC analysis.

2.5.2 Microdialysis sampling of interstitial milieu during perfusion

2.5.2.1 Microdialysis probes

Microdialysis was carried out according to the methods described in Newman et al. (221). Probes were linear in construction, with short length (25mm) of microdialysis tubing (Bioanalytical Systems Inc, Indiana USA, molecular weight cutoff 30 kDa) glued into the blunted end of a snapped off 23G Terumo needle, leaving 20mm tubing free of the needle. The amount of glue was kept to a minimum so that the overall diameter was less than the internal diameter of an 18G syringe needle.

2.5.2.2 Implantation of the microdialysis probe

During surgery (just before heparin injection), a small amount of skin covering the gastrocnemius and tibialis muscles groups was removed. The microdialysis probe was inserted into the muscle via an 18G steel needle, with at least 10mm of dialysis tubing positioned within the muscle bed. During equilibration (shortly after connection of the preparation to the apparatus), the needle end of the microdialysis probe was attached to a syringe pump (WPI, sp101I syringe pump) and flushed with 200µl saline (0.9% NaCl) containing 10mM ^{14}C-ethanol (100nCi/ml) and ^{3}H$_2$O (500nCi/ml) (inflow solution).

2.5.2.3 Microdialysis sampling

For the remainder of the experiment the syringe pump was set at 2μl/min. The hindlimb preparation was allowed to equilibrate for 20 minutes at 4 ml/min of hindlimb perfusate flow before sampling from the probe commenced. During the last 10 minutes of each treatment, 2 microdialysis samples (5 minutes each) were collected into pre-weighed micro-centrifuge tubes (outflow solution). The volume of sample collected was then determined by re-weighing the tubes. The tube along with the sample was then placed into 5 ml counting vials containing 3 ml of scintillant. A known volume of the inflow solution was sampled in the same manner. Vials were then counted for ^{14}C and ^{3}H in a Beckman counter (LS 6500) and the out/in (O/I) ratio for both ^{14}C-ethanol and $^{3}H_2O$ determined.

2.5.3 Laser Doppler Flowmetry

2.5.3.1 Implantation of laser Doppler probes

Impaled laser Doppler flowmetry (LDF) probes were used to measure changes in microvascular perfusion. LDF measurement of nutritive flow is based primarily upon the measurement of non-vectorial cell speed (56). Fiber optic Moor Instruments Lab Server and Lab Satellite fitted with two P10M master probes were used, with two P10s-TCG 260 μm slave probes, each fitted with TCG-fixed fiber. The operational wavelength of the laser light source was 780nm (55). Shortly after connection of the rat to the apparatus, skin covering the calf muscle group was removed, and probes were positioned randomly. The site of implantation was varied, but always within the tibialis, gastrocnemius, or vastus lateralis muscle group. Probes were undisturbed for the remainder of the experiment, while data was recorded continuously using Windaq software.

2.5.3.2 Diagnosis of LDF signal

After implantation, a short (10 min) period was allowed for settling of the probes. Previous studies with LDF probes in perfused muscle show that three different LDF responses are found [nutritive, non-nutritive or mixed, (55)]. To assess the nature

of the site monitored by each probe, a bolus injection of 5-HT (10µl at 0.5µM) was used. 5-HT is known to cause shunting of blood flow through the non-nutritive region. In response to the 5-HT bolus, a nutritive site responded with a downward trend in laser output (signifying decreased flow through the region), while a non-nutritive site was identified by an upward shift in the laser output (increased flow through non-nutritive regions). A site that did not respond satisfactorily as either nutritive or non-nutritive was diagnosed as a mixed site. Data was collected continuously using Windaq software. The approximate proportion of nutritive to non-nutritive sites was 60:40. Data obtained from the laser is expressed as a change from the first measured point in each experiment. That is, the first point is always 1.0. Therefore an increase from 1.0 indicates increased flow through that region.

2.6 Assay of perfusate samples

2.6.1 Lactate assays

Venous samples collected from perfusions were assayed for their lactate content. Samples were centrifuged to remove red blood cells and either assayed immediately or stored at -20°C. Lactate assays were carried out on the YSI Model 2300 STAT Plus Glucose and L-Lactate Analyzer (Yellow Springs Instruments Co. Inc, Yellow Springs, Ohio USA). Values for lactate concentrations were given as mM, which was later converted to $\mu mol.g^{-1}.hr^{-1}$ production or uptake based on flow rate, arterio-venous differences and perfused muscle mass. All samples for one perfusion were assayed in duplicate on the same day.

Lactate efflux ($\mu mol.g^{-1}.hr^{-1}$) was calculated with the use of the following formula.

Lactate Efflux = $\dfrac{\text{(arterial-venous) x flow x 60}}{\text{perfused muscle mass(g)}}$

where   (arterial-venous)   = A-V lactate difference in mM

                   flow rate   = ml/min

                   muscle mass   = see oxygen calculation (Section 2.2.6.1)

2.6.2 Determination of 1-MX and 1-MU, uracil and uric acid content of perfusate samples.

On the day of analysis, precipitated protein was centrifuged out of the sample (3000xg 5 min). Uracil, uric acid, 1-methylurate, and 1-methylxanthine content of the perfusate samples was determined using reverse phase HPLC, essentially as described by Wynants et al. (307), with modifications described by Clark et al. (63), and Rattigan et al. (234). Briefly, these compounds were separated on a LichroCART C8 RP 18e 5µm particle column (Purospher, Merck, Darmstadt Germany), under isocratic conditions at flow rate 1.2 ml/min, with run buffer consisting of 50mM NaH_4PO_4/ 0.3% methanol/ 0.3% acetonitrile/ 0.1% tetrahydrofuran, pH 4.0 with phosphoric acid. 50µl samples were injected, with detection between the wavelengths 259nm to 287nm. Analysis of HPLC profiles was carried out with Star Toolbar Chromatography Workstation v. 5.5.1 (1982-2000) Varian, Inc.

2.7. Determination of high-energy phosphate content of freeze clamped muscle samples

For experiments where determination of intracellular metabolites was required, muscle samples (gastrocnemius, plantaris, soleus group) were collected at the end of the perfusion. The hindlimb was skinned while still perfusing, and then freeze clamped in situ with tongs dipped into liquid nitrogen. The freeze clamped muscle was then cut out, and placed into liquid nitrogen, and stored at -80°C. Muscle samples were ground to a fine powder under liquid nitrogen. 100mg samples of powdered muscle were added to 2 ml of ice cold 0.42M $HClO_4$, vortexed 3 times for 10 sec each (resting on ice in between), and centrifuged at 3000 rpm for 5 mins (IEC centrifuge). 1.0 ml of the supernatant was transferred to a fresh eppendorf tube, and neutralized with 230µl of 1M K_2CO_3, and left for 10 mins on ice. The sample was centrifuged for a further 5 mins at 3000rpm (eppendorf bench-top centrifuge). The supernatant was kept on ice until the time of injection on the HPLC.

Analysis of freeze clamped muscle extracts was essentially the technique of Ye, Clark, et al. (308), with modifications to the solvent system. The HPLC was primed with a run buffer consisting of 20g/l $NH_4H_2PO_4$, 0.5g TBAHS (ion pairing agent), pH to 6.0 with ammonium hydroxide. Samples were separated on a Luna 5µ C8, 250 x 6

mm column (Phenomenex, Australia), under reverse phase ion paired conditions (described elsewhere (272)). A 20µl aliquot of the muscle supernatant was injected, and detection of ATP, ADP, AMP, adenosine, inosine, IMP, NAD, creatine, and creatine phosphate was between the wavelengths 215-254 nm.

2.8 Chemicals

2.8.1 Perfusion medium

NaCl, KCl, $CaCl_2$ were obtained from Ajax Chemicals Australia. KH_2PO_4, $NaHCO_3$, and D-Glucose mono-hydrate were obtained from BDH Chemicals. $MgSO_4$ was from M&B Chemicals -England. Bovine serum albumin was purchased from CSL-Ltd. 1-MX was obtained from CSL, University of Tasmania..

2.8.2 Infusion Agents

NE, AII, 5-HT, veratridine, ryanodine, dantrolene, propranolol, ouabain, digitoxin and digoxin were all obtained from Sigma Chemical Company (St Louis, Mo.), and sodium nitroprusside from Merck (Darmstadt, Germany). Tetrodotoxin was obtained from Alamone Labs (Israel).

2.8.3 HPLC Solvents

All solvents used in HPLC buffers were of analytical grade. Methanol, acetonitrile and tetrahyrafuran were purchased from BDH Chemicals. Phosphoric acid, and NaH_4PO_4 used in the preparation of HPLC buffers were obtained from M&B (Victoria, Australia). Ion pairing agent tertbutyl ammonium hydrogen sulphate (TBAHS) was purchased from Sigma Chemical Company.

CHAPTER 3

EFFECTS OF VARIED OXYGEN DELIVERY ON OXYGEN CONSUMPTION AND FLOW REDISTRIBUTION OF THE PERFUSED RAT HINDLIMB

3.1 Introduction

Oxygen is an essential requirement for energy production and mammalian cell survival. Intricate vascular networks ensure adequate oxygen delivery, and the extent of microvascular perfusion may be varied in accordance with metabolic demand. Hypoxia results in the release of metabolites that regulate local blood flow (202), while muscle contraction is thought to recruit capillaries via cell to cell signalling up the vascular tree (269), facilitating blood flow access and oxygen delivery to the actively respiring tissue. In this scenario, it is the metabolic rate that regulates blood flow and oxygen delivery. However, evidence has also been obtained that blood flow and oxygen delivery may regulate muscle metabolic rate (180; 181; 305; 310).

Type A and B vasoconstrictors are known increase and decrease respectively oxygen consumption of the perfused rat hindlimb (59). Though vasoconstrictors do not alter total flow, the fractional distribution of flow between the nutritive and non-nutritive pathways is altered (220). The possibility is now considered that vasoconstrictor-mediated changes in muscle metabolism are a reflection of varied oxygen delivery. The following experiments attempt to define the effects of altered oxygen delivery on perfused skeletal muscle resting metabolic rate.

3.2 Methods

3.2.1 Animals and perfusion medium

The oxygen carrying capacity of BSA is relatively low, therefore an erythrocyte containing medium was used for the following experiments. All perfusions were conducted in 180-200g animals, as single hindlimb perfusions (Section 2.2.1), at 37°C, with bovine red blood cell containing medium (Hct 33-35%), at 4 ml/min, in a Krebs Henseleit buffer, with 4% BSA, 2.54mM $CaCl_2$, 1.2 mM pyruvate, and 228 IU/l

heparin (Section 2.2.4.2). Flow rate and haematocrit was held constant throughout all experiments.

3.2.2 Varied arterial oxygen mix

The perfusion apparatus was consistent with previous studies (317) with the following modifications. Erythrocyte media was split into two separate flasks, and gassed to equilibration with either Air:CO_2 (95% Air: 5% CO_2) or N_2:CO_2 (95% N_2: 5% CO_2). The following pump configuration was based on a model designed by Peter Arthur (personal communication). Total flow was kept constant at 4 ml/min, as determined by the first pump (Figure 3.1). Pump 1 drew medium from the air-gassed reservoir (henceforth referred to as air). A second pump drew medium from the nitrogen (N_2) gassed reservoir. When only pump 1 was on, the entire 4 ml volume was drawn from the air reservoir. By varying the speed of pump 2, different arterial mixes of air and N_2 blood were achieved, to give varied mixtures of air and N_2 gassed blood.

Pump 1
Constant 4 ml/min

Pump 2
Speed varied
(0-4ml/min)

Air

N_2
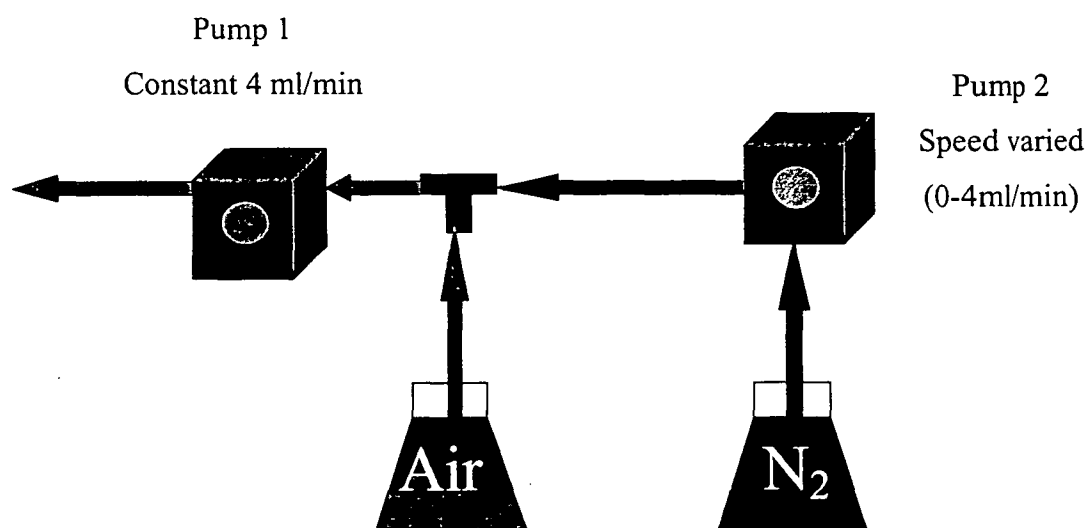
Figure 3.1 Pump configuration

The dual pump configuration allowed control over the mixture of air and N_2 equilibrated blood. Pump 1 was a constant 4ml/min, while the speed of pump 2 was varied (0-4ml/min) to obtain differing mixes.

The following arterial mixes were obtained in this manner (Table 3.1), with 30 mins of perfusion allowed at each mixture. The resulting oxygen concentration of each mixture is shown in Figure 3.2.

Table 3.1 Arterial mixture of Air and N₂ equilibrated blood

Gas Mixture (% air)	Pump 1 setting (ml/min)	Pump 2 setting (ml/min)
100%	4	0
75%	4	1
50%	4	2
25%	4	3
0%	4	4

3.2.3 Determination of arterial and venous oxygen concentrations

The arterial and venous perfusate passed through an arterio-venous oxygen difference analyser (AVOX) (2.2.6.2), comparing the spectral differences in the A-V blood at 660nm. However, these particular experiments presented two problems for the AVOXimeter. Firstly, small leaks in the apparatus were unavoidable (allowing exchange with atmospheric air through tubing and joints etc.). In order to minimize this risk, apparatus tubing was replaced with impermeable polyethylene HPLC grade tubing (1.57mm internal diameter with 0.8mm wall thickness), and tubing lengths between the rat and the AVOX were kept to an absolute minimum. Secondly, the linearity of AVOX measurements at low oxygen tensions was questionable (since the machine is usually calibrated with constant arterial oxygen, and in these experiments arterial oxygen was variable). Therefore an alternative method was sought for the definitive measurement of oxygen content. Samples were drawn in airtight syringes from a port immediately before the rat, and from the venous line, and analysed using a galvanic cell oxygen analyser [TasCon oxygen content analyser manufactured by the Physiology Department, University of Tasmania) (2.2.6.2)]. Total oxygen extraction by the hindlimb was calculated based upon arterio-venous oxygen differences (from both the AVOX and the oximeter), flow rate, and the mass of tissue perfused (2.2.6.2).

3.2.4 Lactate efflux

Small blood samples were collected from the arterial and venous lines, and assayed immediately for their lactate content with a YSI glucose/lactate analyser (Section 2.6.1). Lactate efflux was calculated from A-V differences.

3.2.5 Nutritive and non-nutritive blood flow during varied oxygen delivery

In the current series, flow rate was maintained while oxygen content was varied. Varied oxygen delivery is not expected to alter the distribution of blood flow under resting conditions, however care was taken to rigorously monitor the ratio of nutritive to non-nutritive blood flow. This ensured that oxygen concentration was the only varied parameter, without the added complication of recruitment. Three independent methods were employed to monitor potential changes, these being 1-MX metabolism, microdialysis, and laser doppler flowmetry.

3.2.5.1 1-MX metabolism

$20\mu M$ 1-MX was added to the total blood volume, and allowed sufficient mixing time before splitting into two flasks (air and N_2). Arterial samples were drawn from the infusion port immediately before the rat, while venous samples were taken from the venous line. Red blood cells were removed from the samples by centrifugation, and 0.5 ml of supernatant was added to 0.1 ml 2M $HClO_4$ (Section 2.5.1) for later analysis with HPLC (2.6.2). Samples collected were also analysed for uracil and uric acid contents at the same time as 1-MX.

3.2.5.2 Microdialysis

Microdialysis probe construction, and positioning are outlined in Section 2.5.2. Microdialysate samples (2x5-min) were collected in the last 10-min of each 30-min period of each gas mixture, according to the method of Newman, Di Maria, et al. (221).

3.2.5.3 Laser Doppler Flowmetry

Implantable LDF micro-probes were positioned randomly within the tibialis, gastrocnemius, or vastus lateralis muscle groups (Section 2.5.3). Laser sites were identified as either nutritive, non-nutritive, or mixed at the start of each experiment

with a bolus of 5-HT (10μl at 0.5μM) according to the method of Clark, Youd, et al. (55). Once the laser site was identified, probes were undisturbed for the remainder of the experiment, while data recorded continuously with Windaq software. The first recorded data point was normalized to 1.0. Data from the mixed sites was not retained.

3.2.6 Determination of muscle high energy phosphates and creatine content

The effect of lowered oxygen tension on cellular energy status was assessed. Muscle samples (gastrocnemius, plantaris and soleus) were collected at each steady state oxygen level, by freeze clamping the muscle in situ. Muscles were ground to a fine powder under liquid nitrogen, and analyzed with HPLC for creatine, phosphocreatine, inosine, IMP, AMP, adenosine, ADP, and ATP levels under reverse phase, ion paired conditions (Section 2.7). Cellular Energy charge was calculated by [ATP]/ [ATP] + [ADP] + [AMP], while cellular energy potential was calculated from the formula [PCr] + 2[ATP] + [ADP] (9).

3.2.7 Statistics

All data are presented as means ± SE. Differences were assessed by one-way repeated measures analysis of variance (ANOVA), with pair-wise comparisons by the Student-Newman-Kuels test. All values were compared to control (100% air). Repeated measures ANOVA was not appropriate for the metabolite profiles, since the "end-point" muscle sampling technique only allowed one sample per experiment. Statistical significance was recognized at $P<0.05$. All statistics were carried out using Jandel Scientific SigmaStat software.

3.3 Results
3.3.1 Effects of varied arterial oxygen on hindlimb oxygen extraction

Figure 3.2 illustrates the effects of varied oxygen delivery on arterial ($n=7$) and venous ($n=7$) oxygen content as detected by the oximeter (Panel A). Each consequent change in the gas mixture led to a significant decline in arterial and venous oxygen contents. Mean arterial oxygen content was 7.7 ± 0.4 μmol.ml^{-1} at 100% air mixture, declining to 7.2 ± 0.3 (75%), 6.0 ± 0.3 (50%), 4.7 ± 0.5 (25%), and finally 3.5 ± 0.7 at

0% (*P*<0.001, *n=5*). Though given sufficient time to equilibrate with nitrogen gas prior to the experiment, the 0% gas mixture still contained detectable amounts of oxygen owing to small unavoidable air leaks in the apparatus. Similarly, venous oxygen content also declined with each gas mixture (open symbols, Panel A). The A-V difference in oxygen content was significant at every gas mixture tested (statistics not shown), indicating significant oxygen extraction even at the lowest oxygen delivery. Oxygen consumption calculated from these A-V differences (Panel B) was significantly different from 100% air at 50% and below (*P*<0.05). Panel C shows a positive correlation between arterial oxygen concentration and arterio-venous oxygen delivery.

Figure 3.3 shows the changes in oxygen extraction based upon the spectral differences in arterial and venous blood measured by the AVOXimeter, along with the changes in perfusion pressure, and lactate efflux at each gas mixture. At 100%, air, $\dot{V}O_2$ was 32.19 ± 2.55 $\mu mol.g^{-1}.hr^{-1}$ (*n=32*), with perfusion pressure 35.7 ± 1.1 mmHg (*n=32*), and lactate efflux of 10.9 ± 1.4 $\mu mol.g^{-1}.hr^{-1}$ (*n=9*). As arterial oxygen concentrations declined, $\dot{V}O_2$ also decreased. At 50% gas mixture and below, the rate of oxygen consumption was significantly lower than the 100% air value, (*P*<0.001, at 50%, 25%, and 0%). Return to 100% air at the end of the experiment allowed a complete recovery of $\dot{V}O_2$ to near control levels, 31.5 ± 2.4 $\mu mol.g^{-1}.hr^{-1}$ (*P*= 0.193).

The calculated rates of oxygen consumption from the oximeter and the AVOX compared well, and were not significantly different from each other. The decline in arterial oxygen also caused a gradual increase in perfusion pressure. However, this difference was not significant until 25% air, where pressure was 16.5 mmHg greater than 100% air, (*P*<0.001, *n=9*). Pressure remained elevated (*P*<0.001), even after 100% air was restored. Lactate efflux climbed steadily with each successive change in oxygen delivery, failing to reverse when 100% air was restored at the end of the experiment (Figure 3.3, Panel C).
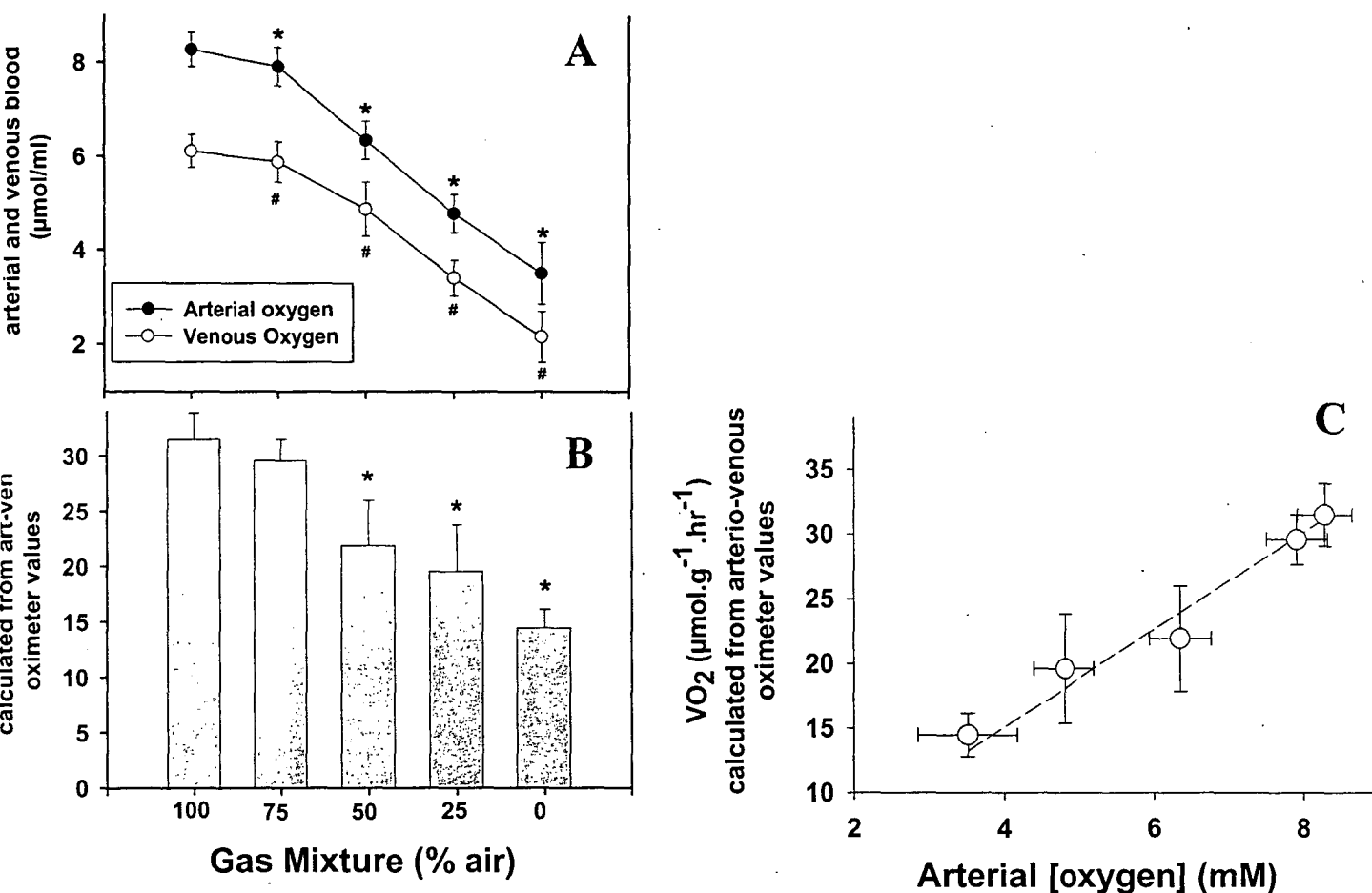
Figure 3.2 Direct Measurement of Arterio-Venous Oxygen Content

*Blood samples were drawn in airtight syringes before and immediately after the perfusing limb, and assayed for their oxygen content with an oximeter. Data shown are means ± SE. Panel A shows changes in arterial (●), and venous (○) oxygen content as gas mixture was varied. * and # denote significant changes from arterial and venous 100% values respectively. Panel B shown oxygen uptake ($\dot{V}O_2$) calculated from arterio-venous oximeter values. * P<0.05, significantly different from 100% air. Panel C is a correlation plot between arterial oxygen and VO2 calculated from oximeter values.*
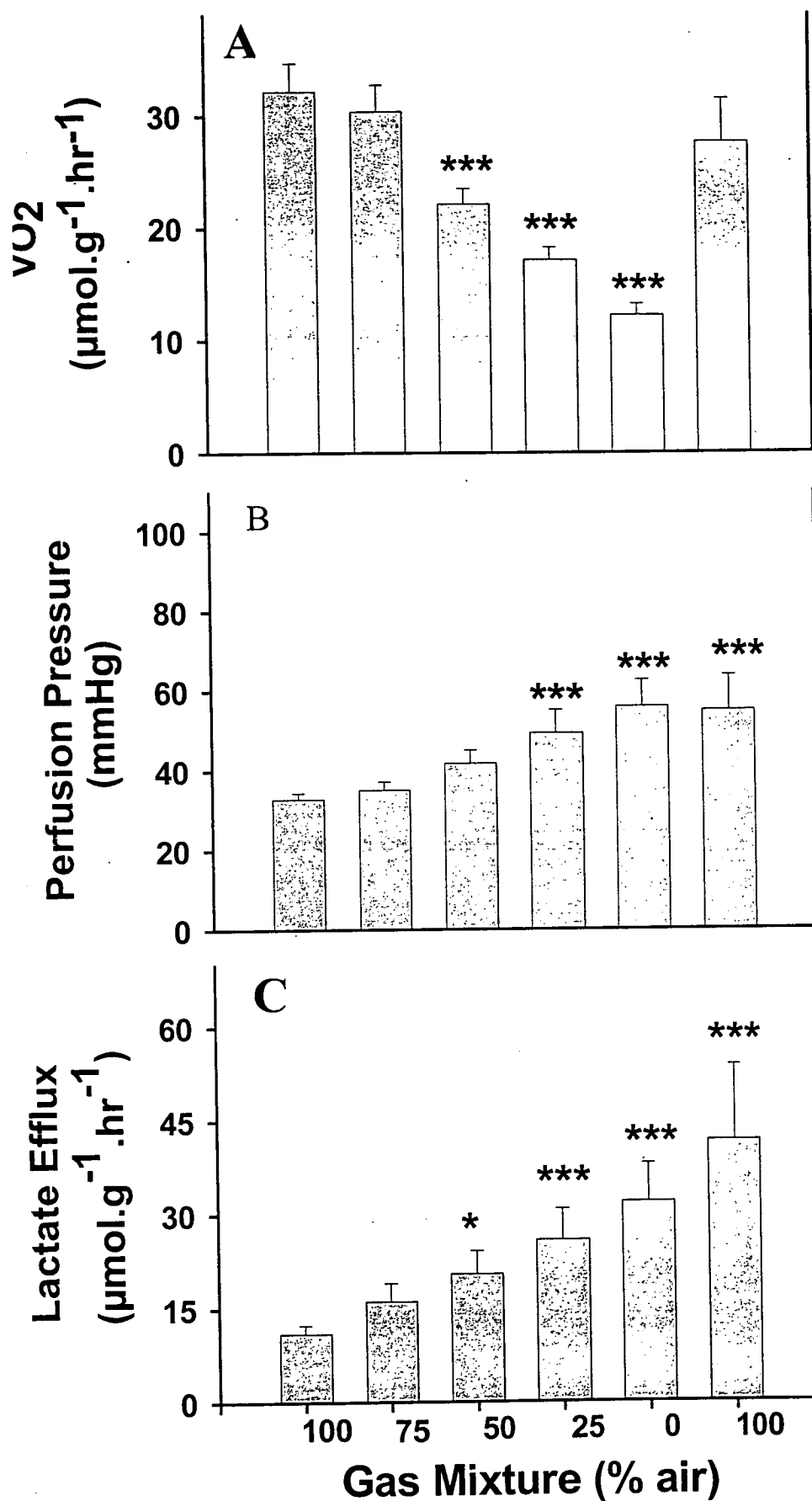
Figure 3.3 Effects of varied arterial oxygen on V̇O₂, PP and LE.

Oxygen consumption (panel A), Perfusion Pressure (panel B), and Lactate efflux (panel C). Values are means ± SE. Statistical differences were assessed by one-way repeated measures ANOVA with pairwise-comparisons by the Student-Newman-Kuels test.

* P<0.05. significantly different from 100% air value.

3.3.2. Monitoring Redistribution of Flow

3.3.2.1 1-MX metabolism, and purine/pyrimidine efflux during varied oxygen delivery

The conversion rate of the exogenously applied substrate 1-MX to 1-MU by the capillary endothelial enzyme xanthine oxidase is regarded as a useful tool in gauging changes in proportion of nutritive flow in the hindlimb. Increased rates of 1-MU production, and 1-MX disappearance are thought to indicate increased capillary blood flow. In the current experiments, no changes in the rate of 1-MU production or 1-MX disappearance were detected at any of the gas mixtures (Figure 3.4, Panels A & B). Similarly, when expressed as a ratio (1-MU production: 1-MX disappearance), no changes were apparent, indicating that no changes occurred the ratio of nutritive to non-nutritive flow during varied oxygen delivery (Panel E). The efflux rates of both uracil and uric acid increased significantly with declining arterial oxygen (Panels C & D)

3.3.2.2 Microdialysis

The out/in ratios for ^3H_2O (Panel A) and ^{14}C-ethanol (Panel B) are shown in Figure 3.5. Data are means $\pm$ SE from 18 separate experiments. A downward shift in the O/I ratio is thought to represent increased clearance from the probe, reflecting enhanced nutritive flow (221). However, in this set of experiments no significant changes were detected in the O/I ratios for either ^3H_2O or ^{14}C-ethanol. These results demonstrate no changes occurred in the exchange rate of diffusible radioactive substances between the microdialysis probe and the perfused tissue, thus the ratio of nutritive to non-nutritive did not change during varied oxygen delivery.

3.3.2.3 Laser Doppler Flowmetry

The response of laser sites diagnosed as nutritive, and non-nutritive to varied oxygen delivery is shown in Figure 3.6 (nutritive Panel A, non-nutritive Panel B). The first recorded signal was converted to 1.0. Varied arterial oxygen caused small fluctuations in LDF signal at both sites, however these changes were not significantly different from the first recorded data point.
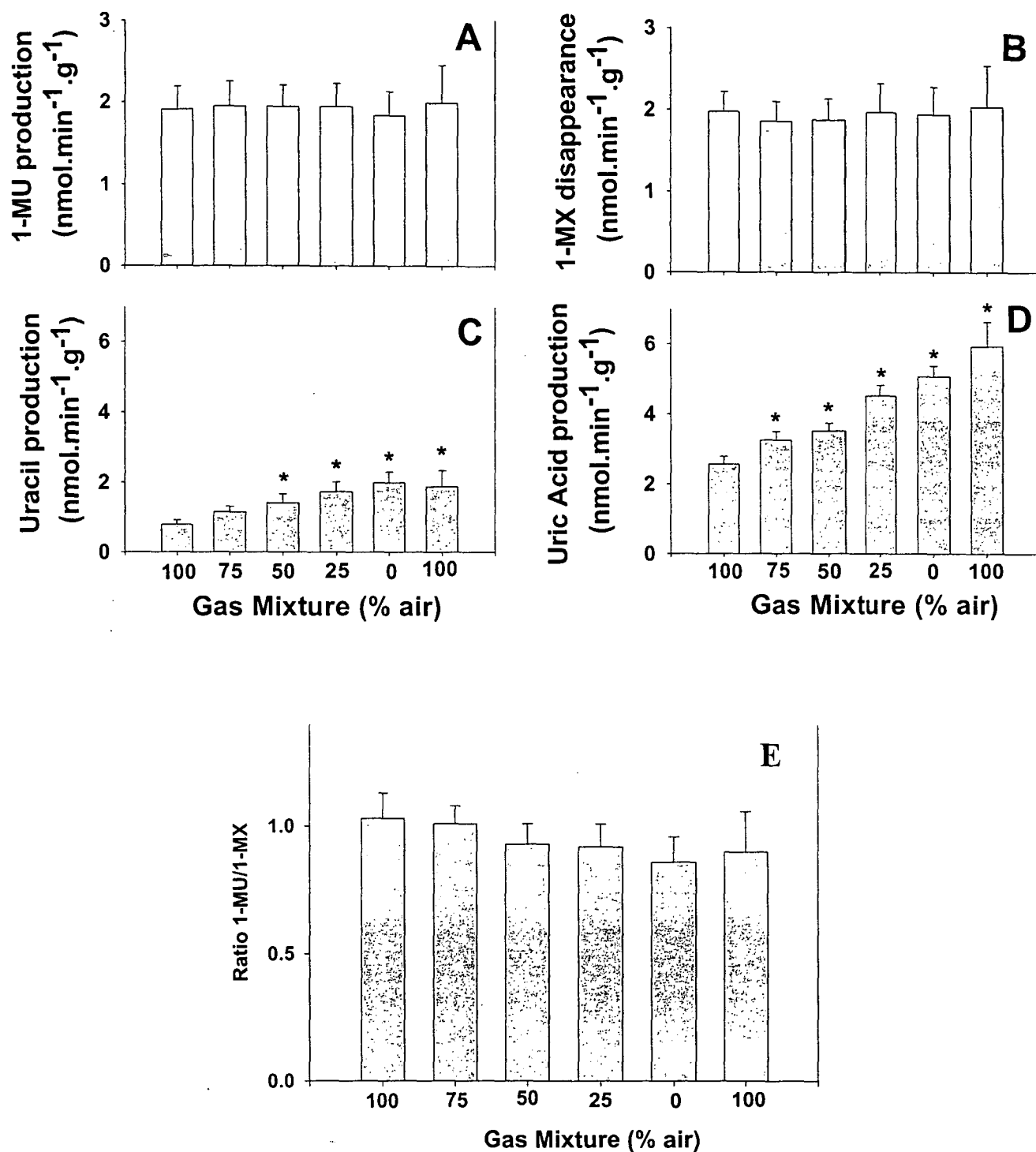
Figure 3.4 1-MU, 1-MX, uracil and uric acid content of perfusate samples

*Venous samples were collected and analyzed by HPLC. The effects of varied oxygen delivery on 1-MU (Panel A), 1-MX (Panel B), uracil (Panel C), and uric acid (Panel D) are shown. The ratio of 1-MU/1-MX is also shown in Panel E. Statistical testing was repeated measures one way ANOVA with pairwise comparisons by the Student-Newman-Kuels method. *P<0.05.*
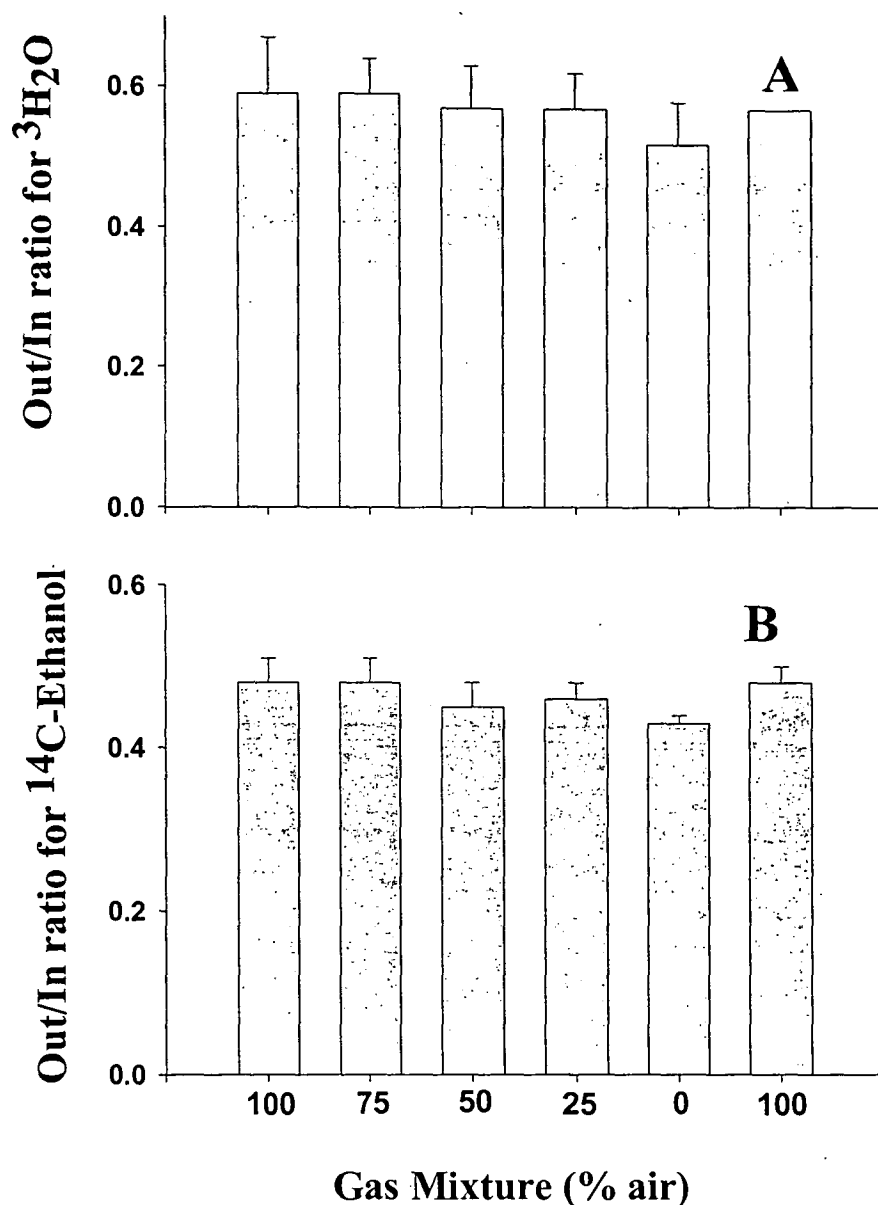
Figure 3.5 Effects of varied arterial oxygen on Microdialysis O/I ratios.

Out/ In ratios for ^3H_2O (Panel A), and ^{14}C-Ethanol (Panel B). Known concentrations of ^3H_2O and ^{14}C-Ethanol were pumped at 2μl/min through microdialysis tubing embedded in the perfused muscle. Outflow samples of dialysate were collected and compared with the inflow solution. No changes were detected in the out/in ratios for either ^3H_2O or ^{14}C-Ethanol. Statistical tests using one-way repeated measures ANOVA with pairwise comparisons using the Student-Newman-Kuels test. P-value was greater than 0.05 for all comparisons.
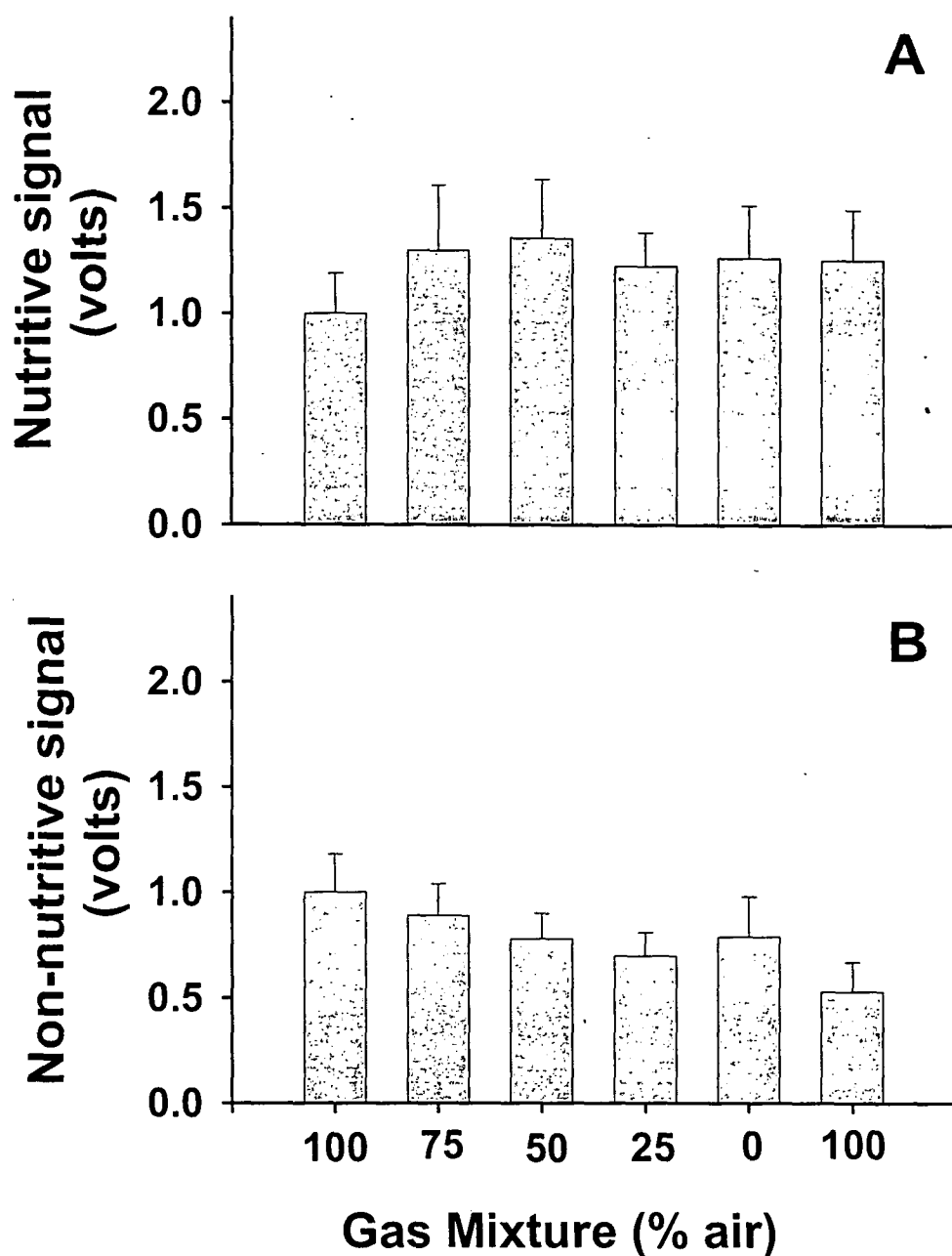
Figure 3.6 Laser Doppler Response during varied Arterial Oxygen

Laser sites were diagnosed as either nutritive or non-nutritive at the beginning of each experiment, as judged by the response to 5-HT bolus (Clark et al. 2001). Data are expressed in relation to the first recorded data point (100% O2 is always 1.0). Panel A shows laser response embedded in nutritive sites, while Panel B illustrates the laser response at non-nutritive sites. Data are means ± SE (n=6 for nutritive and non-nutritive), analysed by one-way repeated measures ANOVA with pairwise comparisons by the Student-Newman-Kuels test.

3.3.3 High energy phosphates content of muscle samples

Shown in Table 3.2 are the results from HPLC analysis of freeze-clamped muscle samples (*n=5* for each gas mixture, total of *n=30* muscles). As the arterial oxygen content declined, phosphocreatine (PCr) levels declined, with a corresponding increase in creatine (Cr). These differences were significant at 25% gas mixture (*P<0.05*) and below. The return to 100% air at the end of the experiment did not allow for full recovery of PCr levels in the 30-min time period. No significant changes were detected in the levels of ATP, ADP or AMP at any gas mixture.

Inosine levels remained fairly constant throughout the oxygen curve, until the lowest oxygen delivery (0% air) was reached, at which time inosine levels showed a large increase from 33.4 ± 9.9 at the start of the experiment, to 170.4 ± 39.2 at 0% (*P<0.001*). Reversal of the gas mixture to normoxia allowed recovery of inosine to pre-hypoxia levels. Adenosine was not detected (detection level 0.01 nmol/g wet wt) in any of the samples.

Data from various metabolite profiles was used to calculate rates of cellular ATP utilization. Based upon [ATP], [ADP] and [AMP] levels, the energy charge (EC) of the muscle remains relatively stable despite the large change in oxygen delivery. There does not appear to be any loss, or degradation of adenine nucleotides from the tissue during the period of hypoxia or recovery. The ratio of PCr/ATP demonstrates a different pattern. While the ATP levels remain relatively constant (Table 3.2), PCr levels are gradually declining. It therefore appears that ATP levels are maintained at the expense of PCr stores. This is also reflected in the calculation for cellular energy potential. The cellular energy potential calculation takes into account both [ATP] and the falling [PCr] when examining cellular energy status. Based upon this calculation, it becomes clear that the total cellular energy potential is under threat by low arterial oxygen tension. Reversal to normoxia at the end of the experiment shows some signs of recovery, though far from complete in the 30-minute recovery period.

Table 3.2. Effects of gas mixture on freeze-clamped Muscle Energy Metabolites.

*Freeze-clamped muscles were ground under liquid nitrogen and extracted with $HClO_4$, then neutralized (Section 2.7) for HPLC analysis under reverse phase-ion paired conditions. Data are means ± SE for n= 5 at each gas mixture (total of n = 30 freeze clamped muscles), and the return to 100% air at the end of the experiments (100#) expressed as units per gram wet weight). Data were analysed statistically with one-way ANOVA with pairwise comparisons by the Student-Newman-Kuels test, * P<0.05. ND = not detectable.*

	Gas Mixture (% air)					
	100	75	50	25	0	100 #
Phosphocreatine (μmol/gww)	20.2 ± 1.8	17.1 ± 2.0	14.1 ± 0.9	10.5 ± 2.2 *	6.0 ± 1.8 *	8.25 ± 2.1 *
Creatine (μmol/gww)	17.4 ± 0.9	19.5 ± 1.5	19.4 ± 1.9	23.6 ± 1.6 *	23.1 ± 0.9	24.6 ± 0.8 *
ATP (μmol/gww)	6.3 ± 0.2	6.8 ± 0.2	5.9 ± 0.4	5.9 ± 0.6	4.8 ± 0.9	5.8 ± 0.5
ADP (μmol/gww)	0.93 ± 0.11	1.04 ± 0.1	0.85 ± 0.06	0.78 ± 0.2	1.11 ± 0.13	1.15 ± 0.14
AMP (nmol/gww)	92.6 ± 22.2	56.0 ± 6.6	67.3 ± 13.1	91.4 ± 26.9	85.1 ± 13.5	109.4 ± 13.5
Inosine (nmol/gww)	33.4 ± 9.9	30.7 ± 3.7	36.8 ± 7.8	19.7 ± 8.1	170.4 ± 39.2 *	61.4 ± 25.8
Adenosine (nmol/gww)	ND	ND	ND	ND	ND	ND
Phosphocreatine / ATP	3.23 ± 0.25	2.53 ± 0.3	2.42 ± 0.19	1.71 ± 0.24 *	1.17 ± 0.24 *	1.53 ± 0.48 *
Energy Charge	0.85 ± 0.02	0.86 ± 0.01	0.87 ± 0.01	0.86 ± 0.04	0.80 ± 0.04	0.82 ± 0.02
Cell Energy potential	33.7 ± 2.2	31.7 ± 2.0	26.8 ± 1.4	23.0 ± 3.2 *	13.4 ± 4.4 *	20.9 ± 1.4 *

3.4 Discussion

The current findings demonstrate a positive relationship between oxygen delivery and resting muscle oxygen consumption (Figure 3.2, Panel C). Failure to detect significant changes in 1-MX metabolism, microdialysis out/in ratios and laser doppler signal during varied oxygen delivery (Figs. 3.4, 3.5 & 3.6) indicates that the decline in $\dot{V}O_2$ occurred independently of redistribution of flow. Thus, varied oxygen delivery did not cause capillary recruitment, de-recruitment or variations in the mass of perfused tissue. With assurance that oxygen concentration was the only variable parameter in these experiments, it is concluded that oxygen delivery has a significant role in the regulation of resting skeletal muscle $\dot{V}O_2$. Limitation of muscle $\dot{V}O_2$ by oxygen delivery has been reported by many other groups in both resting (161; 180; 181), and contracting skeletal muscle preparations (14; 156; 165; 247).

The gradual progression from normal to low oxygen delivery (100-0% air) was accompanied by a noticeable increase in perfusion pressure. The reason for this pressure change is not clear. Pressure development was not causal for redistribution, since no changes were detected in the metabolism of 1-MX, microdialysis exchange or laser doppler signal. Endothelial cells are a likely source of vasoactive substances, and short-term exposure to low oxygen environments is known to induce release of vasoactive substances [reviewed in (114)]. The partial reversibility noted upon return to 100% air (Figure 3.3, Panel B) implies that the constriction was due to the release of local vasoactive substances, production of which ceased once 100% air was restored.

The decline in arterial oxygen concentration was accompanied by a significant increase in lactate efflux (Figure 3.3, Panel C). Lactate efflux increased from 10.9 $\pm$ 1.4 (at 100% air) to 31.9 $\pm$ 6.1 $\mu mol.g^{-1}.hr^{-1}$ (at 0% air) ($P<0.001$). The 30-minute period of normoxia at the end of the experiment did not allow for reversal of LE, instead efflux rates continued to climb, reaching a maximum of 51.7 $\pm$ 12.1 $\mu mol.g^{-1}.hr^{-1}$. Similar patterns were also noted for the efflux rates of uracil, and uric acid (Figure 3.4, Panels A & B). The close association between lactate, uracil and uric acid efflux has been noted previously with the infusion of the type A vasoconstrictor angiotensin II (242).

Traditionally lactate release is regarded as a sign of inadequate oxygen supply. When aerobic ATP production falls, anaerobic metabolism is activated in order to compensate. Assuming a P:O ratio of 2.5 (254), and that 1 mol of ATP is produced for every mol of lactate, the relative contributions of aerobic and anaerobic metabolism to total ATP production may be calculated by simple conversion of $\dot{V}O_2$ and LE values. During normoxia (100% air), total ATP production was calculated at 171 μmol ATP.g^{-1}.hr^{-1}. Between 100 and 0% air, ATP derived from aerobic sources decreased from 160 to 63 μmol ATP.g^{-1}.hr^{-1} (60% decrease). In order to fully compensate for this loss, total LE would need to be in the vicinity of 108 μmol.g^{-1}.hr^{-1}. This is 3 times higher than the actual value (31.9 μmol.g^{-1}.hr^{-1}) observed at 0% air.

Total ATP production calculated from $\dot{V}O_2$ and LE actually decreased from 171 to 95.2 μmol ATP.g^{-1}.hr^{-1} (representing a decrease of 44%) as the arterial gas mixture was changed from 100 to 0% air, indicating that ATP production is also a function of oxygen delivery. However, the proportional contributions of aerobic and anaerobic metabolism were also varied. At 100% air, the percent contributions to ATP production from aerobic and anaerobic metabolism were 93 and 7% respectively. This proportion changed to 66 and 33% at 0% air. Though the proportion of ATP derived from anaerobic sources is elevated, this is still not the dominant source of energy production.

Alternatively, one must consider the possibility that the P/O ratio is substantially less than 2.5, perhaps closer to 1.5 owing to decreased coupling efficiency in the event of basal proton leak (251; 253). Under these conditions, it is estimated that the ATP production changes from 103.9 (100% air) to 68.7 μmol ATP.g^{-1}.hr^{-1} (0% air). Of the initial 100% air value, aerobic respiration is estimated to contribute 89.5% of total ATP production, while LE accounts for the remaining 10%. Under more limited conditions (0% air), it is estimated that LE now contributes a considerably larger proportion of total ATP production (47%). Even under this hypothetical situation, LE is still not the major source of energy production. While LE was significantly elevated in the current data series, this increase is not considered great enough to compensate fully for the loss of ATP production from aerobic sources, confirming that total ATP production declines as a function at oxygen delivery.

If not sufficient to compensate for lost ATP production, why then is lactate release increased during low oxygen delivery? The view that LE is the result of inadequate oxygen delivery has recently been challenged. In a study of human skeletal muscle during graded exercise, lactate release was shown to increase even though intracellular Po_2 remained constant (244). While examining canine gracilis muscle Connett and colleagues (80; 81) noted that intracellular Po_2 levels were unrelated to muscle lactate release, and that lactate release also occurred under fully aerobic conditions. Furthermore, Jobsis & Stainsby (176) demonstrate no difference in the oxidation-state $NADH/NAD^+$ between muscles at rest and while producing lactate. The view now presented, is that muscle LE is attributable to factors other than O_2-limitation of mitochondrial ATP synthesis. Thus, the elevated lactate efflux observed during the course of these experiments is not necessarily the result of inadequate oxygen delivery.

Lactate efflux has also been shown to increase during type A vasoconstrictor mediated metabolism in the perfused rat hindlimb (144; 242). While it is no longer accepted that vasoconstrictor-mediated oxygen $\dot{V}O_2$ is due to work performed by vascular smooth muscle, it is still possible the lactate may originate from vascular tissue as it maintains tone (145). This is in agreement with the current findings, since both perfusion pressure and lactate efflux remain elevated upon return to 100% air (Figure 3.3). Muscle $\dot{V}O_2$ recovered completely upon return to 100% air, despite elevated pressure and lactate, reinforcing our conviction that elevated $\dot{V}O_2$ is not the direct result of vasoconstriction.

An alternative explanation for the appearance of lactate during low oxygen is presented in a paper by Gutierrez and colleagues (136). Comparison of the effects of ischemia and hypoxia in perfused rabbit skeletal muscle led to the following findings. Ischemia caused depletion of muscle PCr levels, but no change in the rate of lactate efflux was noted during or following ischemia. Restoration of normal flow allowed complete recovery of PCr levels. Conversely, hypoxia caused a decrease in PCr that did not recover with re-oxygenation. Lactate efflux began to rise, and continued to climb despite re-oxygenation, consistent with observations in the perfused rat hindlimb. Gutierrez et al. (136) propose that during total ischemia the rate of glycolytic flux is totally dependent on cellular glycogen stores, and this may limit the amount of lactate

produced. However, partially ischemic or hypoxic tissue may suffer damage as a result of unlimited glucose supply, where lactate production continues unchecked, and lactic acidosis may result. No evidence of tissue damage was apparent in these experiments, since $\dot{V}O_2$ recovered completely, and cellular ATP levels were maintained (Fig. 3.3 & Table 3.2). However, a constant glucose supply was maintained, and may have allowed glycolytic pathways to continue unhindered, resulting in a situation where glycolytic intermediates are available in abundance, but oxidative phosphorylation is limited. Thus, elevated lactate efflux observed may be the result of constant glucose supply during low oxygen delivery rather than activation of anaerobic glycolysis.

Examination of muscle high-energy phosphates showed no significant changes in the intracellular concentrations of [ATP], [ADP], [AMP] or [IMP]. However, PCr stores began to decline as soon as arterial oxygen levels were decreased, with a corresponding increase in Cr (Table 3.2), though these changes were not significant until 25% air. Since ATP levels remain constant, it would appear that ATP levels were buffered at the expense of PCr via the creatine kinase reaction. The return to normoxia showed beginnings of very slow PCr recovery, though far from complete in the 30-min recovery period. A very large peak of inosine was detected in samples collected at 0% air. Inosine levels increased over 4 times between 25 and 0% air, however this peak subsided with return to 100% air. Adenosine was not detected in any of the samples. This is not surprising, since adenosine is rapidly broken down in the venous perfusate. However, the sudden appearance of inosine at 0% air, may be a lasting shadow of adenosine release. Similarly, the gradual increase in uric acid (Figure 3.4, Panel D) may also be a breakdown product of adenosine. Though total adenine nucleotide content was not significantly reduced, even a small (nM) loss of adenine from the large (µM) skeletal muscle pool might account for the appearance of nM quantities of inosine and uric acid in the venous samples, perhaps reflecting local adenosine production in response to low oxygen delivery.

Various estimates of cellular energy status are also shown in Table 3.2. No changes were detected in the cellular energy charge. Based on this calculation alone, one might assume no threat upon cellular energy turnover with low oxygen delivery. If no attempt is made to recover loss ATP (via anaerobic sources), and total cellular ATP levels are not declining, then total ATP utilization must be decreasing with oxygen

delivery, and one may speculate on the possibility of oxygen conformance in perfused muscle. However, examination of PCr/ATP ratio reveals that low oxygen delivery does in fact have detrimental effects of on cellular energy turnover. Similar findings were reported by Idström and colleagues (165) in the perfused contracting rat hindlimb with ^{31}P- NMR spectroscopy, where muscle PCr levels were reduced with low oxygen delivery. Calculation of cellular energy potential from the equation ([PCr] + 2[ATP] + [ADP]) also exposes the threat posed to the cell by low oxygen delivery. Thirty minutes after return to 100% air, signs of improvement in cellular energy status are evident, though far from complete. Maintenance of ATP levels is probably not a reflection of decreased ATP utilization, but the result of PCr sacrifice. Presumably prolonged perfusion at the lowest oxygen delivery would exhaust PCr supplies, and ATP levels would also eventually decline.

In order to address the question "is the perfused hindlimb an oxygen conforming tissue?" one must consider a number of issues. In response to progressively decreased arterial oxygen levels, Gutierrez et al. (137) found evidence for both oxygen conformance and oxygen regulation in the blood perfused rabbit hindlimb. The decrease in $\dot{V}O_2$ was always accompanied by increased levels of lactate and Pi, and decreased PCr, consistent with the current data series. Taken together, these findings suggest O_2 supply limitation of metabolism, and activation of anaerobic ATP production. The classical definition of oxygen conformance is a proportional variation in cellular energy requirement in response to changes in oxygen supply (153), without compensatory activation of anaerobic mechanisms. In this regard, the perfused rat hindlimb may not be regarded as a strict oxygen conformer.

On the other hand, skeletal muscle oxygen conformance may only be evident above critical values. The cultured mouse skeletal muscle cell line C_2C_{12} shows evidence of oxygen conformance in the range of 100-10µM (8). $\dot{V}O_2$ was decreased between 25-40%, while cellular ATP and PCr were maintained. Lactate efflux did not increase significantly until oxygen levels fell below 4µM. In the perfused hindlimb, ATP levels were maintained at all oxygen deliveries, and PCr levels did not decline significantly until 25% air (4.7 µmol/ml). At this stage, total oxygen delivery had declined by 38%, and oxygen consumption had been suppressed by more than 45%. Though lactate began to increase at around 50% air (6.0 µmol/ml), this is not

necessarily due to activation of anaerobic ATP production (as discussed earlier). Thus, above 4.7 μmol/ml, oxygen consumption is significantly suppressed without depletion of ATP or PCr stores. It is therefore concluded that the perfused rat hindlimb is capable to a certain extent of oxygen conformance, though this may only be evident above critical values.

Though arterial oxygen concentrations reported here are considerably higher than those for isolated cells (mM versus μM), it must be remembered that tissue mass of the perfused hindlimb is considerably larger (around 15g). The flow rate of 4 ml/min results in tissue perfusion rates of 0.3 ml/g muscle/min, combined with diffusion gradients and heterogeneous perfusion, oxygen delivery at the microvascular level is likely to be in the μM range. This has been demonstrated with the use of oxygen microelectrodes impaled into autoperfused feline muscles, where intramyocellular PO_2 was in the vicinity of 8mmHg (305). Thus comparisons of isolated and perfused muscle preparations are valid.

The strong relationship between O_2 delivery and $\dot{V}O_2$ may be fundamental to the mechanism by which type A vasoconstrictors stimulate resting metabolism in the perfused rat hindlimb. Type A vasoconstrictors do not increase the oxygen content of the blood, nor the total blood flow, but may be effective in increasing the oxygen delivery by enhancing the extent of capillary perfusion. Ergo, the underlying implication of this finding is that even under standard conditions (suitable flow rate and oxygen saturation), muscle metabolic rate is oxygen limited. Previous data obtained in aerobically contracting perfused rat skeletal muscle supports this notion, since the addition of the type A vasoconstrictor angiotensin II was noted to improve tension development by 80%, and contraction-induced oxygen uptake (237). Richardson and colleagues present data along the same lines (244-246), where increased oxygen delivery [through increased oxygen content of inspired air] considerably enhanced $\dot{V}O_2MAX$ in contracting human muscle. It is thus concluded, that type-A mediated redistribution of flow and capillary recruitment is likely to reduce heterogeneity of perfusion, and increase oxygen delivery at the microvascular level, thereby removing physiological restraint on muscle oxygen uptake.

The blood perfused rat hindlimb shows a strong correlation between oxygen delivery and $\dot{V}O_2$ (Figure 3.2). Reduced oxygen delivery did not affect the proportion of nutritive flow, since no significant changes were detected in the rates of 1-MX metabolism, microdialysis O/I ratios for ^3H_2O and ^{14}C-Ethanol, or laser Doppler flowmetry. The elevated rates of lactate efflux, and decreased muscle PCr content suggest secondary activation of anaerobic energy producing pathways during low oxygen delivery. However $\dot{V}O_2$ was significantly depressed before these effects (LE and PCr) were significant. The perfused rat hindlimb may not be a strict oxygen conformer according to the definition of Hochachka & Guppy (153), however, the relationship between oxygen delivery and muscle $\dot{V}O_2$ opens new corridors for the investigation of type-A vasoconstrictor mediated metabolism.

CHAPTER 4

INVOLVEMENT OF Na⁺/K⁺-ATPase AND SODIUM CHANNELS DURING TYPE A- AND VERATRIDINE-STIMULATED METABOLISM.

4.1 Introduction

Stimulation of metabolism by type A vasoconstrictors is known to be sensitive to a variety of treatments, including vasodilators acting via nitric oxide (NO), cAMP, or calcium channel blockade (58), compounds affecting the respiratory chain, and low oxygen tensions (96). The inhibitory effect of propranolol (β-antagonist) on norepinephrine-mediated metabolism in the hindlimb was not entirely unexpected, and has been reported previously by other groups (69; 132; 274). However, the chance finding that high dose ± propranolol (±100μM) blocked the effects of another non-adrenergic type A vasoconstrictor angiotensin II (AII), offered new insight into the potential mechanism of vasoconstrictor-mediated thermogenesis (292).

High dose propranolol selectively blocked the vasoconstrictor-mediated increase in $\dot{V}O_2$, and LE, but did not interfere with the development of pressure, or the redistribution of blood flow (as judged by red cell washout). Inhibition was not attributable to β-antagonism, since other β-antagonists (nadolol and atenolol) were without effect on angiotensin-mediated thermogenesis (292). Comparison with another membrane stabilizer, quinidine (291) led to the conclusion that the inhibitory effects of high dose propranolol and quinidine on angiotensin-mediated metabolism were due to the membrane-stabilizing properties of these agents.

In perfusion, the alkaloid veratridine (sodium channel opener) has also been shown to stimulate $\dot{V}O_2$ and LE, independently of vasoconstriction (292). Veratridine causes persistent activation of sodium channels at resting membrane potentials (45) thus allowing Na^+ influx. Like type A vasoconstrictors, veratridine-mediated metabolism was also blocked by high dose propranolol, and the stimulatory effects of both agents were abolished by low sodium media (291). Combined, these results led to the hypothesis that destabilization of the muscle plasma membrane, and increased rates of ion cycling possibly

involving the Na$^+$/K$^+$-ATPase pump were shared events in the mechanism of stimulated metabolism by both type A vasoconstrictors and the membrane labilizer veratridine (291). The aim of the current chapter is to assess the involvement of Na$^+$/K$^+$-ATPase pump and voltage-gated sodium channels during veratridine- and vasoconstrictor-stimulated metabolism.

4.2 Methods

4.2.1 Animals

For the purpose of this study, experiments were conducted on rats sized between 70-80g. (3-4 weeks old). Ouabain binding studies suggest maximal Na$^+$/K$^+$-ATPase concentrations in this age group (71; 177). Further, it has previously been noted that the maximal NE effect is of a greater magnitude (60% higher) in small rats (70-80g) when compared with larger rats (180-200g) (291).

4.2.2 Dual hindlimb perfusion

The nature of the present study depends upon the integrity of the skeletal muscle plasma membrane being maintained. Many systems employed for the study of muscle metabolism involve the use of cut, isolated, or non-intact muscle preparations. Removal of the muscles, or cutting, will disrupt ion concentration gradients across plasma membranes (51; 76) leading to artificial states of ion distribution. One advantage of the perfused hindlimb model is the intact nature of the preparation, thus maintaining integrity of the skeletal fiber plasma membranes. Owing to the limited muscle mass in small rats, animals were prepared surgically for dual hindlimb non-recirculating perfusion, at a flow of 4 ml/min per 2 hindlimbs (approximately 0.40 - 0.45 ml/min/g muscle), with medium containing 2% BSA, at 25°C. Details of the surgical technique, and perfusion medium/apparatus are outlined in Sections 2.2.2 & 2.2.3.

4.2.3 Perfusion medium and infusion agents

Perfusion media details are given in Section 2.2.4.1. Ouabain and digoxin were dissolved directly into the perfusion medium to give final concentrations of 1mM (dose shown to produce maximal inhibition of active Na$^+$/K$^+$-ATPase transport in rat soleus

muscle (73)), and 30µM respectively. Digitoxin (30µM final) was dissolved in a small quantity of 50% ethanol before being added to the perfusion medium. The final concentration of ethanol in the entire volume never exceeded 0.6%.

Following the 50-min equilibration period with normal medium, the reservoir was changed to one of the designated media (1mM ouabain, 30µM digoxin or 30µM digitoxin). A further 30-mins equilibration was allowed with each new media before vasoconstrictor or veratridine dose curves commenced. Sodium nitroprusside (SNP, 0.5mM) was included in the media for all veratridine experiments to ensure no development of pressure (291), or possible redistribution effects.

4.2.4   NE- and veratridine- dose response curves

Dose response curves were constructed by infusing a concentrated solution of NE to achieve final concentrations of 3, 10, 30, 100 and 300nM, allowing 20-mins at each. Dose response curves were repeated in the presence of 1mM ouabain medium, or 30µM digitoxin. Similarly, veratridine dose response curves were constructed to achieve 3, 10, 30, 100 and 300µM final concentrations, allowing 20 mins at each dose. Veratridine dose response curves were repeated in the presence of 1mM Ouabain, 30µM Digoxin or 30µM Digitoxin (0.5mM SNP included in all veratridine experiments). Venous effluent samples were collected and assayed for their lactate content with a YSI glucose/lactate analyzer (Section 2.6.1).

4.2.5 Effects of tetrodotoxin on NE- and veratridine-mediated changes in metabolism

The involvement of voltage-gated sodium channels was assessed with the use of the sodium channel inhibitor tetrodotoxin (TTX). Following 50-mins equilibration, a constant infusion of either 100nM NE, or 30µM veratridine commenced. Once steady state $\dot{V}O_2$ was attained, the TTX dose response curve commenced. TTX doses ranged from 0.01 to 50µM.

4.3 Results

4.3.1 Basal metabolism

Equilibration of the hindquarter for 50-min in normal 2% BSA led to steady-state values for $\dot{V}O_2$ (11.35 ± 0.33 $\mu mol.g^{-1}.hr^{-1}$) and PP (16.7±1.27 mmHg) before the addition of any agents (*n=30*), data shown in Table 4.1. Lactate efflux was also steady in this time, and remained so for up to 180-min of perfusion (data not shown).

Table 4.1 Effects of sodium nitroprusside, ouabain, digoxin and digoxin on basal metabolism. *Pre-equilibration of the constant flow perfused hindlimb with normal perfusion media allowed measurement of basal metabolism. Following the 50-min pre-equilibration period, perfusion media was changed to either 1 mM ouabain (± 0.5 mM SNP), 30 μM digoxin + SNP, or 30 μM digitoxin + SNP. New steady state values for $\dot{V}O_2$, PP and LE were obtained within 30-40 min. Values are steady state means ± SE (n=5 for all treatments). * significantly different from basal (P<0.05).*

	$\dot{V}O_2$ ($\mu mol.g^{-1}.hr^{-1}$)	PP (mmHg)	LE ($\mu mol.g^{-1}.hr^{-1}$)
Basal	12.8 ± 0.4	21.5 ± 1.3	10.4 ± 1.1
0.5mM SNP	12.6 ± 0.4	19.5 ± 0.9	11.3 ± 1.1
Basal	11.5 ± 0.3	21.5 ± 1.2	7.5 ± 0.2
1mM Ouabain	10.7 ± 0.6	27.5 ± 1.9*	6.8 ± 0.2*
Basal	11.6 ± 0.4	23.5 ± 0.5	9.2 ± 0.1
1mM Ouabain + 0.5mM SNP	11.3 ± 0.2	22.5 ± 0.3	11.2 ± 0.9
Basal	11.3 ± 0.5	22.5 ± 1.2	6.1 ± 0.2
30μM Digoxin + 0.5mM SNP	10.3 ± 0.3	25.5 ± 1.7	6.2 ± 0.3
Basal	9.2 ± 1.5	24.4 ± 2.7	5.0 ± 0.9
30μM Digitoxin + 0.5mM SNP	9.2 ± 1.5	26.6 ± 2.8	4.5 ± 0.2

Substitution of the equilibration medium for one containing 1mM ouabain caused a slight (though insignificant) depression of basal $\dot{V}O_2$. Ouabain also caused small pressure effects (6 mmHg above basal, $P<0.05$, Table 4.1), and a minor suppression of basal lactate efflux (9.3%, $P<0.05$). The inclusion of 0.5mM SNP with ouabain ameliorated these minor effects. Neither 30μM digoxin, nor 30μM digitoxin in the presence of 0.5mM SNP had any significant effects on basal $\dot{V}O_2$, PP or LE within the 30-40 min equilibration period (Table 4.1).

4.3.2 Effects of ouabain on NE dose curve

Figure 4.1 compares the effects of a NE dose response curve ± 1mM ouabain on hindlimb oxygen uptake ($\dot{V}O_2$), perfusion pressure (PP), and lactate efflux (LE). The dose-dependent increase in $\dot{V}O_2$ mediated by NE was almost completely abolished by 1mM ouabain at all doses of NE (3-300nM). The greatest inhibition of $\dot{V}O_2$ by ouabain occurred at the three highest doses of NE (30, 100 and 300nM, where $P<0.01$ for each). Lactate efflux was similarly affected, though significance was found only at 100nM NE. There was some inhibition of PP development by ouabain, however this difference was significant only at the two highest doses of NE (100 and 300 nM, $P<0.05$).

Digitoxin did not significantly affect the NE dose curve, although an inhibitory trend was noted on $\dot{V}O_2$ towards the upper end of the NE curve (data not shown). Unexpectedly, digoxin displayed a slow onset intrinsic pressor effect. Separate control experiments illustrate a time dependent increase in perfusion pressure with 30μM digoxin, commencing after the 50-min equilibration period even in the presence of SNP (data not shown). Thus, it was not possible to test digoxin against NE, since the pressor effect of digoxin may potentiate NE-mediated vasoconstriction, and potentially interfere with redistribution.
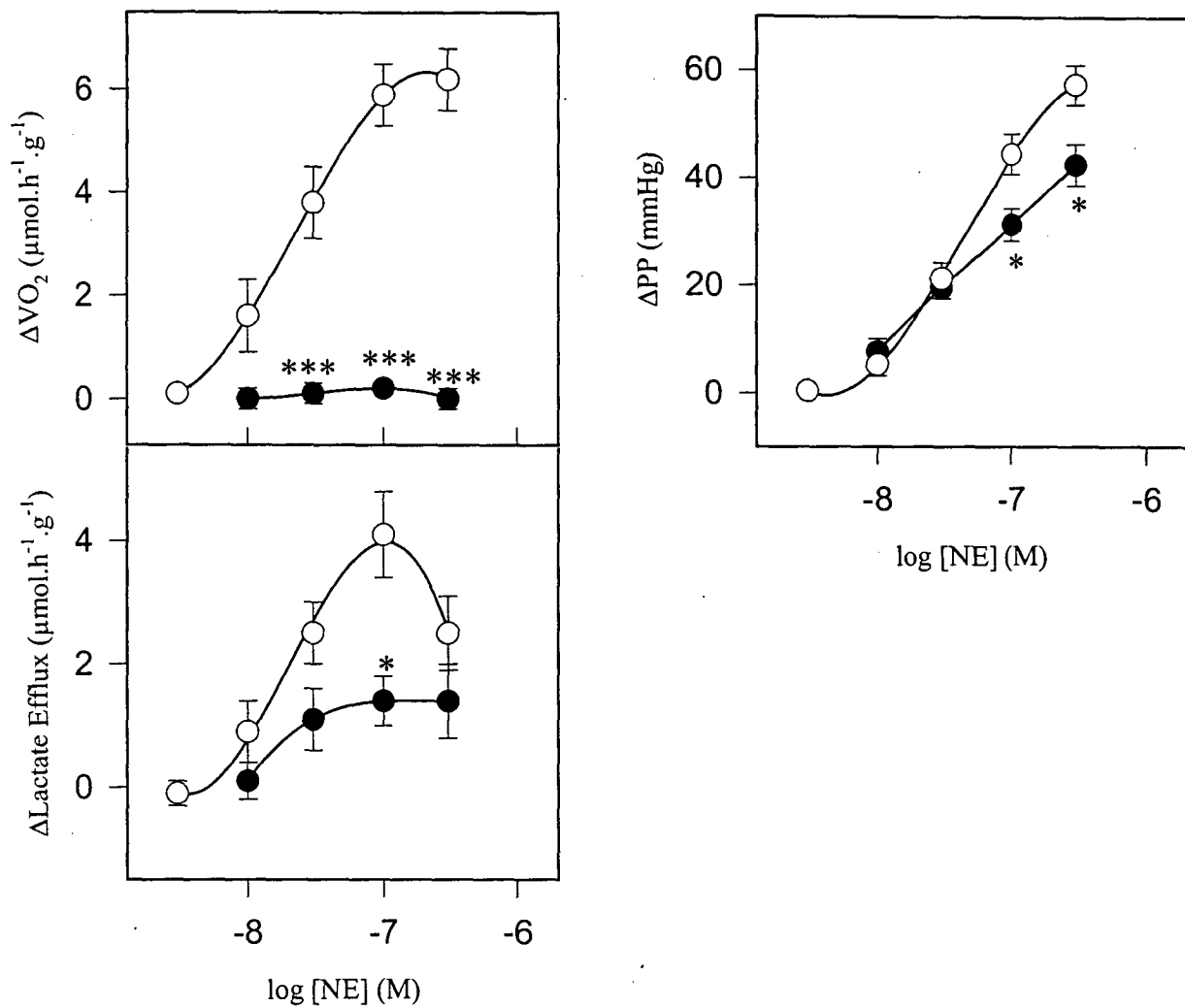
Figure 4.1. Effects of norepinephrine (NE) dose response curve ± 1mM ouabain on oxygen uptake ($\dot{V}O_2$), perfusion pressure (PP), and lactate efflux (LE).

*Both hindlimbs were perfused at a constant flow. Perfusions were either control (O), which has been reported previously (Tong et al. 1998), or in the presence of 1 mM ouabain media (●). Basal and steady-state values are given in Table 4.1. Mean values for changes (from basal or steady state) ± SE are shown (n=5). Significant differences from steady-state stimulation: * P<0.05; ***P<0.001.*

4.3.3 Effects of ouabain, digoxin, and digitoxin on veratridine dose curve.

All three media (ouabain, digoxin and digitoxin) in the presence of 0.5mM SNP significantly inhibited veratridine-mediated stimulation of $\dot{V}O_2$ and LE (Figure 4.2). At doses of veratridine greater than, and equal to 10μM, inhibition of $\dot{V}O_2$ by all agents tested was highly significant ($P<0.001$). The relative percent inhibition of $\dot{V}O_2$ stimulated by 30μM veratridine was 69, 89, and 61% by ouabain, digoxin, and digitoxin respectively.

The inclusion of 0.5mM SNP in control, ouabain and digitoxin media abolished the minor pressure effects due to veratridine. However, the intrinsic pressor effect of digoxin was not attenuated by inclusion of SNP. Since veratridine is not dependent on vasoconstriction to mediate changes in metabolism (as shown by the control veratridine curves in Figure 4.2), the pressor effect of digoxin was not considered problematic. Time control experiments with 30μM digoxin showed the pressure effects to be time dependent. Hence veratridine-mediated changes in metabolism in the presence of digoxin were calculated against a constant moving baseline (data not shown).

Ouabain and its analogues had significant inhibitory effects on veratridine-mediated changes in LE. Maximum inhibition of LE occurred at the maximal stimulatory dose of veratridine (30μM) where all three agents inhibited LE by more than 80% when compared with control (veratridine + SNP), (ouabain $P<0.005$, digoxin $P<0.001$, and digitoxin $P<0.008$).
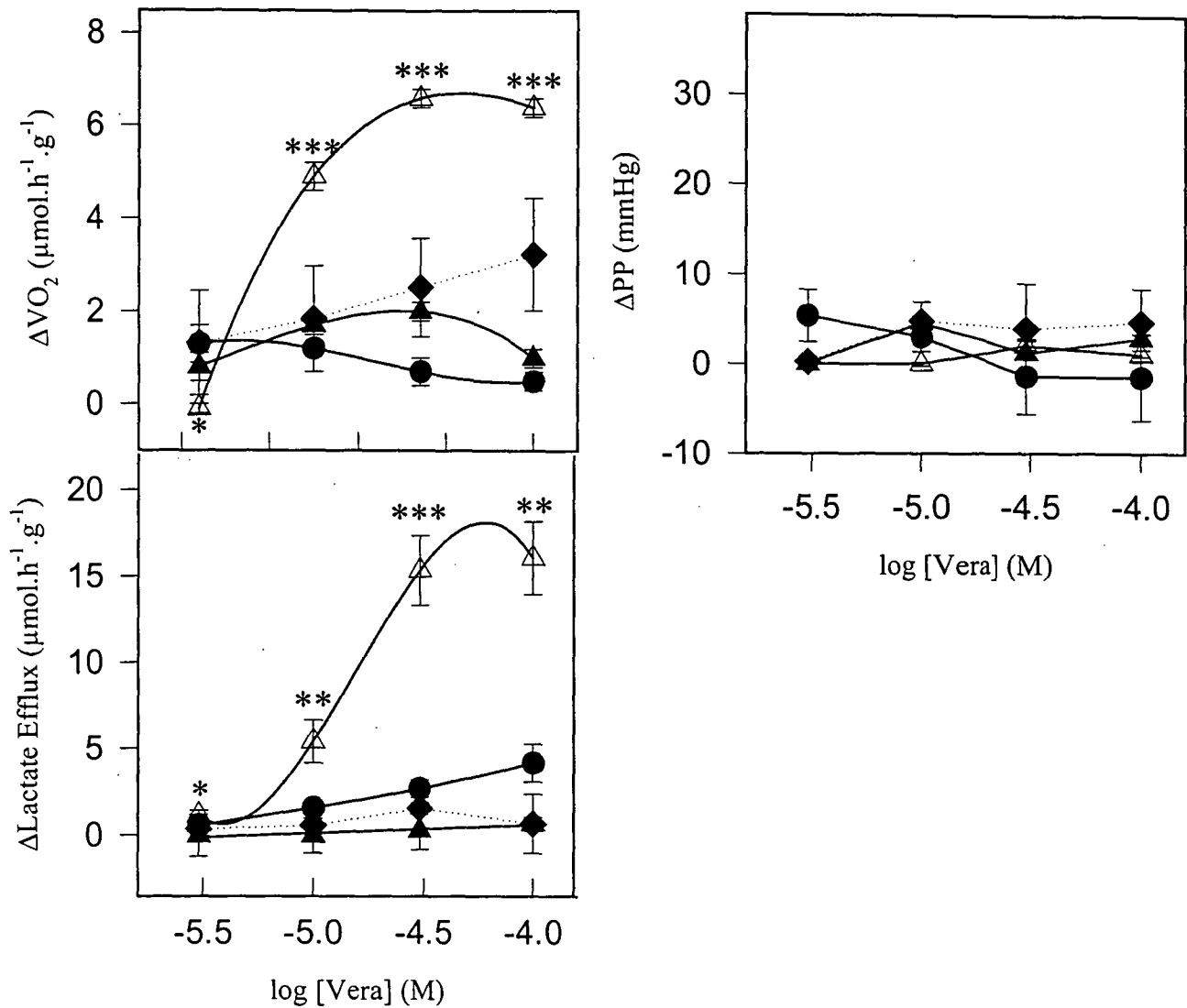
Figure 4.2. Effects of cardiac glycosides against veratridine-mediated changes in oxygen uptake ($\dot{V}O_2$), perfusion pressure (PP, and lactate efflux (LE).

Both hindlimbs were perfused at constant flow. Perfusions were either control + 0.5mM SNP ($\triangle$), reported previously in Tong et al. (1998), or with media containing 1mM ouabain + 0.5mM SNP ($\blacktriangle$), 30μM digoxin + 0.5mM SNP ($\bullet$), or 30μM digitoxin + 0.5mM SNP ($\blacklozenge$). Mean values for changes (from basal or steady state) ±SE are shown (n=5). Basal and steady-state values for $\dot{V}O_2$, PP and LE are shown in Table 4.1. Significant differences from control + SNP are indicated by the following: * P<0.05; ** P<0.01; P<0.001.

4.3.4 Effects of TTX on NE- and veratridine-mediated increases in $\dot{V}O_2$

Figure 4.3 shows the effects of increasing doses of tetrodotoxin against a constant infusion of either 100nM NE, or 30μM veratridine. Control TTX curves (no other agent present) revealed no effect of TTX on basal oxygen consumption ($P>0.05$, data not shown). A pre-infusion of either 100nM NE, or 30μM veratridine was allowed to plateau before TTX infusion commenced. 100nM NE increased $\dot{V}O_2$ 7.21 ± 1.2 μmol.g^{-1}.hr^{-1} above basal ($P<0.05$, $n= 6$), while 30μM veratridine increased $\dot{V}O_2$ by 5.64 ± 0.3μmol.g^{-1}.hr^{-1} ($P<0.05$, $n=5$). NE-mediated changes in $\dot{V}O_2$ were unaffected by doses of TTX in the range 0.1 to 50μM. The veratridine-mediated increase in $\dot{V}O_2$ was highly sensitive to TTX infusion. Above 0.1μM, TTX had almost completely reversed the veratridine effect ($P<0.01$), Figure 4.3).
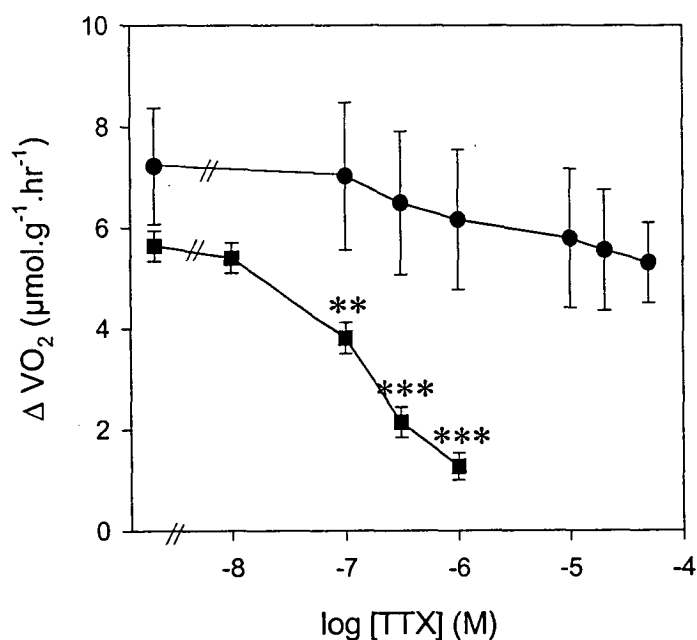
Figure 4.3 Effects of tetrodotoxin (TTX) dose-response curve against steady-state stimulation of oxygen consumption by NE, or veratridine.

*Both hindlimbs were perfused at a constant flow rate. Perfusions were either constant infusion of 100nM NE ± TTX dose-response curve (●), or constant infusion of 30μM veratridine ± TTX dose-response curve (■). Values are mean changes from basal ± SE, (n= 3 for 50 μM TTX, and n =5 for all other treatments). Significant differences from steady-state stimulation (no TTX present): **P<0.01; ***P<0.001.*

4.4 Discussion

The aim of this study was to examine the effects of cardiac glycosides and tetrodotoxin on NE- and veratridine-mediated metabolism, with a view to further explore the mechanism by which type A vasoconstrictors stimulate resting muscle metabolism in the perfused rat hindlimb. Ouabain caused a significant inhibition of both NE- and veratridine-mediated $\dot{V}O_2$, and LE without interfering with the vasoconstrictor properties of NE. While all three cardiac glycosides were effective against veratridine (Figure 4.2), only ouabain was fully effective in antagonizing the effects of NE (Figure 4.1). In addition, the sodium channel blocker tetrodotoxin blocked the effects of veratridine on $\dot{V}O_2$ at relatively low dose (0.01µM), while doses of tetrodotoxin up to 50µM had no effect on norepinephrine-mediated $\dot{V}O_2$. The current data confirm the involvement of the Na^+/K^+-ATPase, but not voltage-gated sodium channels during vasoconstrictor-mediated skeletal muscle metabolism.

In a recent report from this laboratory (291), it was proposed that a common thermogenic mechanism underpinned the stimulatory effects of veratridine and type A-vasoconstrictors in the perfused rat hindlimb. It was proposed that destabilization of the plasma membrane allowed sodium influx, and the observed increase in $\dot{V}O_2$ was most likely a reflection of increased ATP utilization by the Na^+/K^+-ATPase pump (291). The possibility that type A vasoconstrictors act directly upon the Na^+/K^+-ATPase pump is unlikely, given that isolated incubated muscle preparations are not stimulated by vasoconstrictors (50; 69; 85; 97). Activity of the sodium pump does however vary in proportion to intracellular Na^+ (70; 109; 271), as demonstrated in rat and turtle brain synaptosomes with the use of veratridine and tetrodotoxin (105). Thus manipulation of intracellular sodium concentrations has the potential to influence cellular metabolic rate. It is now considered that type A vasoconstrictors may stimulate muscle $\dot{V}O_2$ by increasing myocyte intracellular Na^+ levels, thereby causing a secondary activation of the Na^+/K^+-ATPase.

At rest, basal $\dot{V}O_2$ was not significantly affected by 1mM ouabain (Table 4.1). This denotes minimal contribution of the Na^+/K^+-ATPase during basal metabolism, which is in general agreement with previous reports from this lab (291) and others (76). Neither ouabain nor tetrodotoxin (0.01 to 50µM) significantly affected basal oxygen consumption,

thus sodium pumps and sodium channels do not appear to make a significant contribution to resting muscle oxygen consumption. Microcalorimetric determination in isolated intact resting mammalian skeletal muscle estimates the contribution of the sodium pump to be somewhere between 5-7% of the basal metabolic rate (26; 51; 113). In the rat diaphragm muscle, sodium pump activity may account for as little as 2% of the total energy consumption (86). Higher values have been reported [in mouse soleus and diaphragm, (128)], but these values should be regarded with caution, as discussed by Clausen (76), and others (26). The ouabain-suppressible fraction of muscle heat production is to a large extent determined by the rate of Na^+ influx (76), therefore the greater efficacy of ouabain during agonist-infusion is assumed to be related to increased intracellular sodium levels.

Using literature values, it was interesting to attempt to calculate the potential contribution of active sodium pumping to cellular oxygen consumption. Binding studies with ^{3}H-ouabain estimate the concentration of Na^+/K^+-ATPase pumps in mammalian skeletal muscle to be somewhere between 300- 800 pmol/g wet weight (141). At 37°C, active sodium pumping has been estimated at 16900 nmol Na^+/g/min (75). Using the ratio of 1 ATP for every 3 Na^+ pumped, this corresponds with a maximal rate of ATP turnover of 5600 nmol ATP/g/min (equivalent to 336μmol ATP/g/hr). Assuming 1 mol O_2 is consumed for every 6 mol ATP utilized, this corresponds with a maximal oxygen consumption of 56 μmol O_2/g/hr. Therefore, maximal activation of the sodium pump could easily account for the increase in $\dot{V}O_2$ seen with veratridine, and norepinephrine at 25°C.

The observation that tetrodotoxin blocked veratridine mediated increases in $\dot{V}O_2$ confirms the previous findings of others that veratridine binds to, and acts directly upon voltage-gated sodium channels (198). Only a very small dose (0.01 μM) of TTX was required to almost completely block the veratridine effect (Figure 4.3). However, NE-mediated $\dot{V}O_2$ was not sensitive to tetrodotoxin, even at doses of up to 50 μM (Figure 4.3). It is not clear how NE may activate the sodium pump, if voltage-gated sodium channels are not directly involved. Other potential sodium entry pathways include sodium/calcium exchangers, sodium/hydrogen exchangers, and sodium symports, though it is unlikely that sodium influx via these alternate pathways would be fast enough to account for the rapid onset of type A metabolic effects. There is a slim possibility that NE may be acting upon TTX-resistant (TTX-R) sodium channels. However, this also seems unlikely given that TTX-R sodium channels are usually only found in cardiac muscle (238), immature

myotubes, and denervated skeletal muscle fibers from the adult (45; 120; 250). There are no reports to date of TTX-R sodium channels in normal adult innervated skeletal muscle, but their presence has not been totally discounted. Primary cultures of fetal rat skeletal muscle cells show populations of both TTX-sensitive (high affinity) and TTX-resistant (low affinity) sodium channels co-existing, the two subtypes having different developmental regulation (273). As the myotubes mature, the TTX-R population is gradually replaced with a TTX-S population (120; 138). It is worth considering the age of the rats in this study, at 4-weeks some TTX-R channels may still exist. However, this explanation is also flawed, since type A vasoconstrictors are still effective in mature rats where only TTX-S sodium channels are expected. It is therefore unlikely that type A vasoconstrictors increase intracellular sodium via activation of voltage-gated sodium channels (TTX-R or otherwise).

Skeletal muscle Na^+/K^+-ATPase concentrations also change during the early stages of post natal development. Starting with low Na^+/K^+-ATPase levels at birth, the activity reaches optimal levels at 4 weeks of age (an increase of 5-fold), then declines to a lower plateau in the adult rat (177). It was therefore interesting to note the different effects of NE in 4-week old rats (70-80g), and larger 7-week old rats (180-200g). The same dose of NE (100nM, at 25°C with 2% BSA medium) produced a much larger stimulation of $\dot{V}O_2$ in the smaller rats when compared with larger rats (5.9 ± 0.6 compared with 4.4 ± 0.29μmol.g^{-1}.hr^{-1}), with less pressure development (44.4 ± 3.8 versus 76.4 ± 3.7mmHg) (291). It was speculated at the time that muscle from the smaller rats had a greater concentration of sodium pumps, and therefore a greater capacity for ATP turnover when stimulated by agonists.

Skeletal muscle oxygen metabolic rate is influenced by a variety of ionic interventions, not all of which are dependent on sodium cycling. Metabolic rate is known to be stimulated by high K^+ (20mM) medium in isolated-incubated frog muscle (226), and in perfused rat skeletal muscle (294). Isolated incubated muscle oxygen consumption is also stimulated by ryanodine (24), hyper-osmolar media (49; 85), and caffeine (23). These treatments are all thought to stimulate cellular oxygen consumption by triggering intracellular calcium cycling. Slow intracellular calcium leaks (caused by depolarization in response to elevated extracellular K^+ etc.) trigger the Ca^{2+}-ATPase of the sarcoplasmic reticulum. The demand for ATP stimulates oxidative phosphorylation and thus increases

oxygen consumption. No contraction of the muscle is observed during caffeine exposure, or KCl depolarization, because intracellular calcium levels are sub-threshold for contracture. Calcium cycling as a thermogenic mechanism in skeletal muscle has been proposed previously (28; 89; 201). The potential involvement of skeletal fiber calcium cycling during type A mediated metabolism will be considered further in the next chapter.

The relationship between ion flux, and cellular respiration is well established (38; 105; 152; 164). The energetic cost of ion pumping during normoxia is considerable, but the phenomena of "channel arrest" offers a survival advantage to species regularly exposed to low oxygen environments. During normoxia, the energetic cost of ion pumping in hepatocytes of the western painted turtle was estimated to be in the vicinity of 28% (38). However, conditions of anoxia suppress pump activity by approximately 75%. No changes in plasma membrane potential were detected, and since the activity of the sodium pump was known to be depressed, it was concluded that ion flux was also depressed (38). Thus anoxia has the potential to reduce ion cycling, and the energetic cost of maintaining ionic homeostasis. If the same phenomena of "channel arrest" occurs in mammalian skeletal muscle, it is conceivable that redistribution of flow with type A vasoconstriction might participate in the removal of regional hypoxia imposed by heterogeneous flow during basal conditions. Concomitant with redistribution is enhanced perfusate and oxygen delivery, which may increase membrane permeability and the demand for ATP by the sodium pump as it acts to counter the ionic imbalance. The sensitivity of type A vasoconstrictors to membrane-stabilizers may be a reflection of this phenomena.

In summary, veratridine and type A doses of norepinephrine share ouabain sensitivity. This finding supports the notion of a shared mechanism of action involving activation of Na^+/K^+-ATPase. However, the second major finding, that NE was not blocked by tetrodotoxin is apparently in conflict with this theory. Further studies are required to investigate the role of sodium and calcium cycling during vasoconstrictor-stimulated metabolism in perfused skeletal muscle, and other mechanisms that may potentially activate the Na^+/K^+-ATPase pump.

CHAPTER 5

MEASUREMENT OF MEMBRANE POTENTIAL (E_M) IN SKELETAL MUSCLE FIBERS DURING AGONIST-STIMULATED METABOLISM

5.1 Introduction

In terms of their effects upon perfused skeletal muscle, NE and veratridine share several features in common. The stimulatory effects of both agents on perfused hindlimb oxygen consumption and lactate efflux are abolished by low sodium media (292), membrane stabilizers quinidine and propranolol (291), and the cardiac glycoside ouabain (Chapter 4). Based on these similarities it was proposed destabilization of the plasma membrane, and increased rates of ion cycling might be common events in the stimulation of metabolism by both agents. Type A vasoconstrictors are not blocked by the sodium channel blocker tetrodotoxin (Chapter 4), though this does not exclude the possibility that intracellular sodium levels are elevated via other routes (e.g. tetrodotoxin resistant sodium channels, or sodium exchangers). In order to further investigate this possibility, a study was undertaken to evaluate the effects of type A vasoconstrictors and veratridine on skeletal fiber membrane potential (E_M) during agonist-stimulated metabolism.

Membrane potential (E_M) is the result of the weighted average of the equilibrium potentials for all permeant ions. The weighting factor for each ion is the fraction of the total membrane conductance caused by that ion. That is, the higher the permeability of the membrane to one particular ion, the closer E_M will be to the equilibrium constant for that ion. If stimulated metabolism is dependent upon destabilization of the plasma membrane (e.g. via sodium entry), then depolarization would be expected as E_M moves from resting values (near –70mV) closer to the equilibrium of Na^+ (close to + 60mV).

5.2 Methods

The methods used for this study are described in detail in Section 2.4. The controls and experimental protocols are briefly outlined here. All perfusions were dual hindlimb perfusions conducted in 70-100g animals, at 25°C, 4 ml/min with 2% BSA, and 1.27mM $CaCl_2$. The order of the experiments was randomized. Measurement of E_M during perfusion has not been attempted previously by this group, therefore several controls were required. Time control studies were

conducted to show that there was no deterioration of membrane potential with time, and a positive internal control to check that changes in membrane potential were detectable in the perfused hindlimb preparation

5.2.1 Time controls

Membrane potential (E_M), $\dot{V}_{O2}$ and PP were monitored continuously over a three-hour period of perfusion, with no other intervention. Collection of data commenced after a 50-min equilibration period. Data collected in the 10-min immediately after equilibration were regarded as part of the 1st hour. The average E_M, $\dot{V}O_2$, and PP between hours 1,2 and 3 of perfusion were compared, and analyzed for statistical differences.

5.2.2 Positive internal control – potassium depolarization

A modified version of the Nernst equation (the Goldman-Hodgkin-Katz equation, shown in Section 2.4.5) allows estimation of plasma membrane potential based upon the relative ionic permeability of each species. By substituting known literature values into the Goldman-Hodgkin-Katz equation, it was calculated that an extracellular concentration of 9.4mM potassium chloride (KCl) was required to achieve a 10mV depolarization. Resting E_M was measured in normal (4.74mM KCl buffer), after which the buffer reservoir was changed to one containing 9.4mM KCl. Time was allowed for equilibration with the new medium (20-min), and another measurement of E_M was made. Potassium depolarization of skeletal muscle fibers was fully reversible, therefore two potassium depolarizations were carried out in each preparation, with a recovery period of 40-mins in between.

5.2.3 Agonist-stimulated metabolism

Veratridine was infused at a final concentration of 30 μM, NE at 100 nM, and AII at 5nM. Two different types of vasoconstrictor were used to ensure that any effects observed were a general property of type A vasoconstrictors, and not a particular feature of the adrenergic vasoconstrictor NE alone. Measurements of $\dot{V}O_2$, PP and E_M were made just after equilibration, and compared with measurements obtained once a plateau state of pressure was attained during agonist infusion.

5.2.4 Intracellular metabolites

At the end of each experiment, perfused muscles were skinned and freeze clamped in situ for later analysis of intracellular metabolites (Section 2.7). Muscle samples were collected after 40-mins of basal or 9.4mM KCl perfusion. For experiments where the agonist was infused (veratridine and NE), a 30-min equilibration period was first allowed, followed by 20-mins of agonist infusion.

5.2.5 Statistical analysis

One way analysis of variance (ANOVA) was used to determine any statistically significant differences in $\dot{V}O_2$, PP and E_M between hours 1, 2 and 3 of perfusion for the time control experiments, with pairwise comparisons by the Student-Newman-Kuels method. For KCl, veratridine, NE and AII experiments, data were compared before and after treatment with a students paired t-test. Statistical significance was recognized at $P<0.05$.

5.3 Results

5.3.1 Time controls

Over three hours of time control perfusion, $\dot{V}O_2$ and PP remained stable (Figure 5.1) averaging 13.5 ± 1.0 $\mu mol.g^{-1}.min^{-1}$, and 19.9 ± 0.34 mmHg respectively ($n=5$). The resting membrane potential (E_M) was also stable over this period, averaging -58.6 ± 1.78 mV ($n=5$). There were no statistically significant changes in $\dot{V}O_2$, PP or resting membrane potential between the first, second or third hour of perfusion. $\dot{V}O_2$, PP and E_M are therefore quite stable in time frame utilized for the remaining experiments.

5.3.2 Positive internal control -potassium depolarization

A total of 3 depolarization experiments were completed, with two trials in each animal (3 animals, $n=6$ trials). Average $\dot{V}O_2$, PP and E_M measured during basal perfusion (normal medium) were 11.4 ± 0.01 $\mu mol.g^{-1}.hr^{-1}$, 19.4 ± 0.03 mmHg, and -63.3 ± 0.3 mV respectively (Figure 5.2). The change from normal (4.7mM) KCl buffer to high (9.4mM) KCl buffer did not cause any significant change in $\dot{V}O_2$ or PP, however a depolarization of ~10mV to -54.0 ± 0.4 was observed ($P < 0.003$).
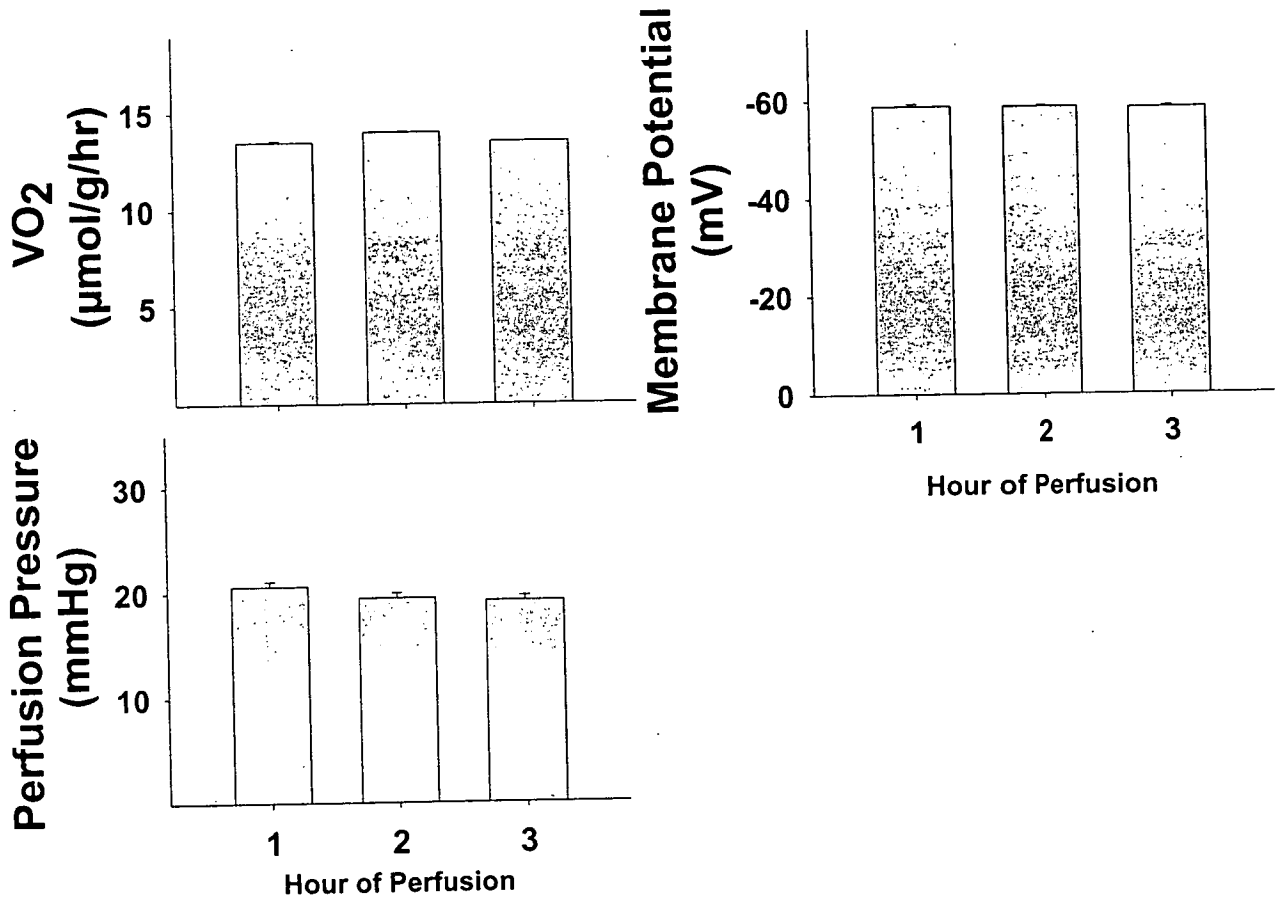
Figure 5.1 Comparison of $\dot{V}O_2$, PP and E_M between first, second and third hour of perfusion

Data were recorded continuously over the three-hour period, then averaged for each hour. No statistically differences were detected in basal $\dot{V}O_2$, PP or E_M over the three hour period.
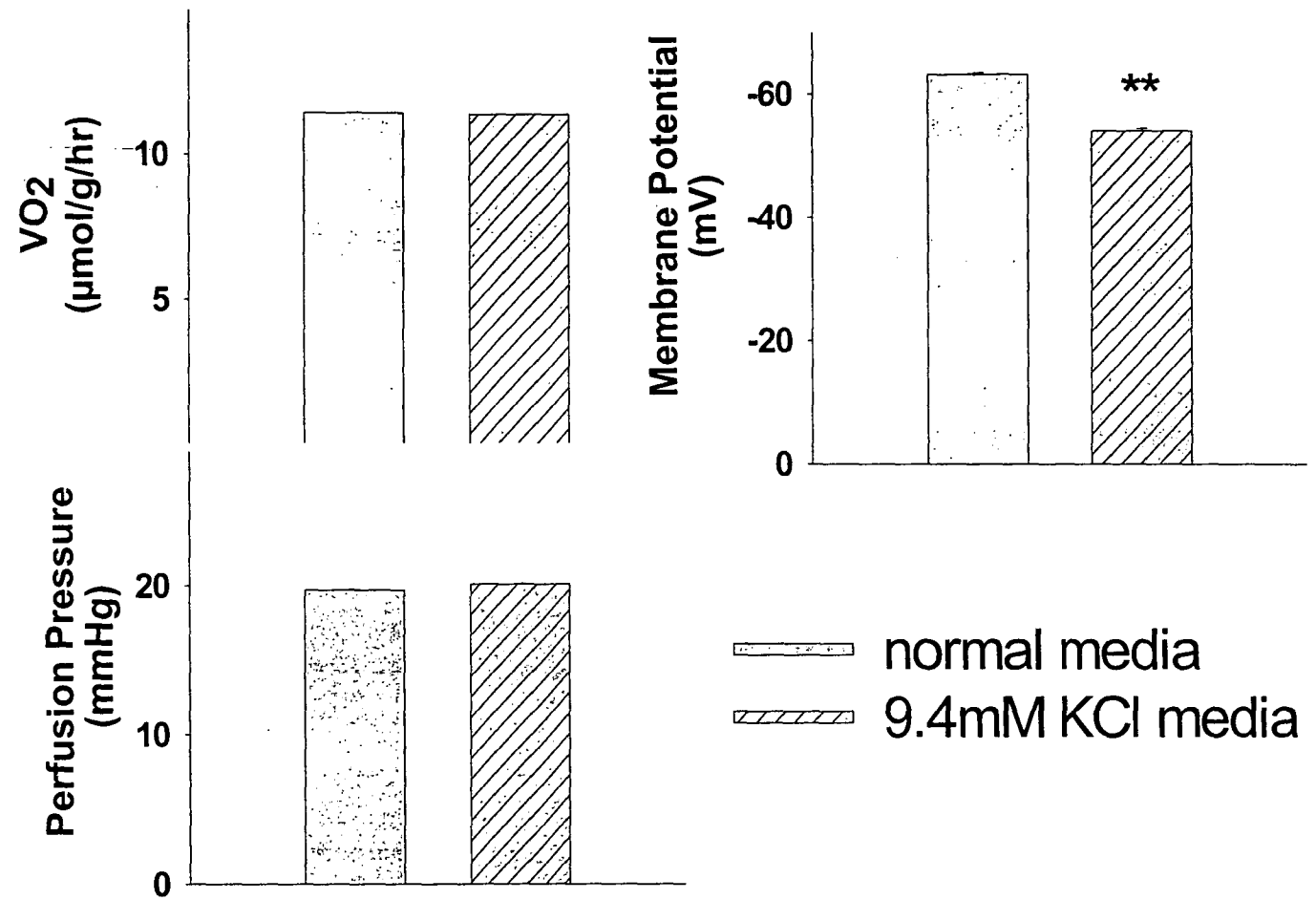
Figure 5.2 Positive Internal Control - Potassium Depolarization

It was calculated that a change in buffer KCl concentration from 4.7mM to 9.4mM should cause a 10mV depolarization. Shown is the effect of normal (4.7mM) and high (9.4mM) KCl media on $\dot{V}O_2$, PP and E_M, for a total of n=6 experiments. **P<0.01.

5.3.3 Agonist-stimulated metabolism

All three agents 30μM Veratridine, 100nM NE and 5nM AII caused significant stimulation of $\dot{V}O_2$ above basal ($P<0.001$, $n=6$, Figure 5.3). Veratridine caused a small, but significant increase in perfusion pressure (about 4mmHg above basal, $P=0.003$). Both NE and AII caused a substantial increase in perfusion pressure above basal, 31.2 mmHg ($P<0.001$), and 39.4 mmHg ($P<0.001$) respectively. Veratridine was the only agent to affect membrane potential, causing depolarization from –62.0 to -41.6 mV, ($P<0.001$). NE and AII infusion did not affect membrane potential.

5.3.5 Intracellular metabolites

The effects of each treatment on muscle metabolites are shown in Table 5.1. Intracellular metabolites did not vary significantly between basal, 9.4mM KCl and NE samples ($P>0.05$). When compared with basal, samples collected during veratridine infusion showed significantly elevated creatine levels (10.8 ± 0.4 to 18.1 ± 1.8 μmol/g wet wt, $P<0.001$), and a depletion of creatine phosphate content (20.3 ± 0.4 to 11.9 ± 2.0 μmol/g wet wt, $P<0.01$). Cellular energy status (calculated from CrP/ATP) was also decreased by veratridine from 3.2 ± 0.1 to 1.9 ± 0.3 ($P<0.01$). ATP levels were not compromised by veratridine infusion ($P>0.05$).

Table 5.1 Muscle Energy Metabolites

Muscle samples were collected after 40-mins of basal perfusion, 40-mins of 9.4mM KCl medium perfusion, or after 20-mins of 100nM NE or 30μM veratridine infusion, n=5 for all values.
**P<0.01, ***P<0.001, assessed by one way ANOVA, with pairwise comparisons to the corresponding basal values by the Student-Newman-Kuels method.

	Treatment			
	Basal	9.4mM KCl	100nM NE	30μM Vera
Creatine (μmol/g wet wt)	10.8 ± 0.4	12.7 ± 0.9	10.5 ± 0.6	18.1 ± 1.8***
Phosphocreatine (μmol/g wet w	20.3 ± 0.4	17.8 ± 1.5	19.4 ± 0.7	11.9 ± 2.0 **
AMP (nmol/g wet wt)	57.2 ± 7.1	56.9 ± 9.0	62.8 ± 7.5	76.3 ± 12.4
ADP (μmol/g wet wt)	0.9 ± 0.02	0.9 ± 0.04	0.8 ± 0.03	0.9 ± 0.06
ATP (μmol/g wet wt)	6.5 ± 0.1	6.3 ± 0.2	6.3 ± 0.2	6.4 ± 0.1
Phosphocreatine/ATP	3.2 ± 0.1	2.8 ± 0.2	3.1 ± 0.1	1.9 ± 0.3**
Energy Charge	0.88 ± 0.003	0.87 ± 0.01	0.88 ± 0.002	0.87 ± 0.01
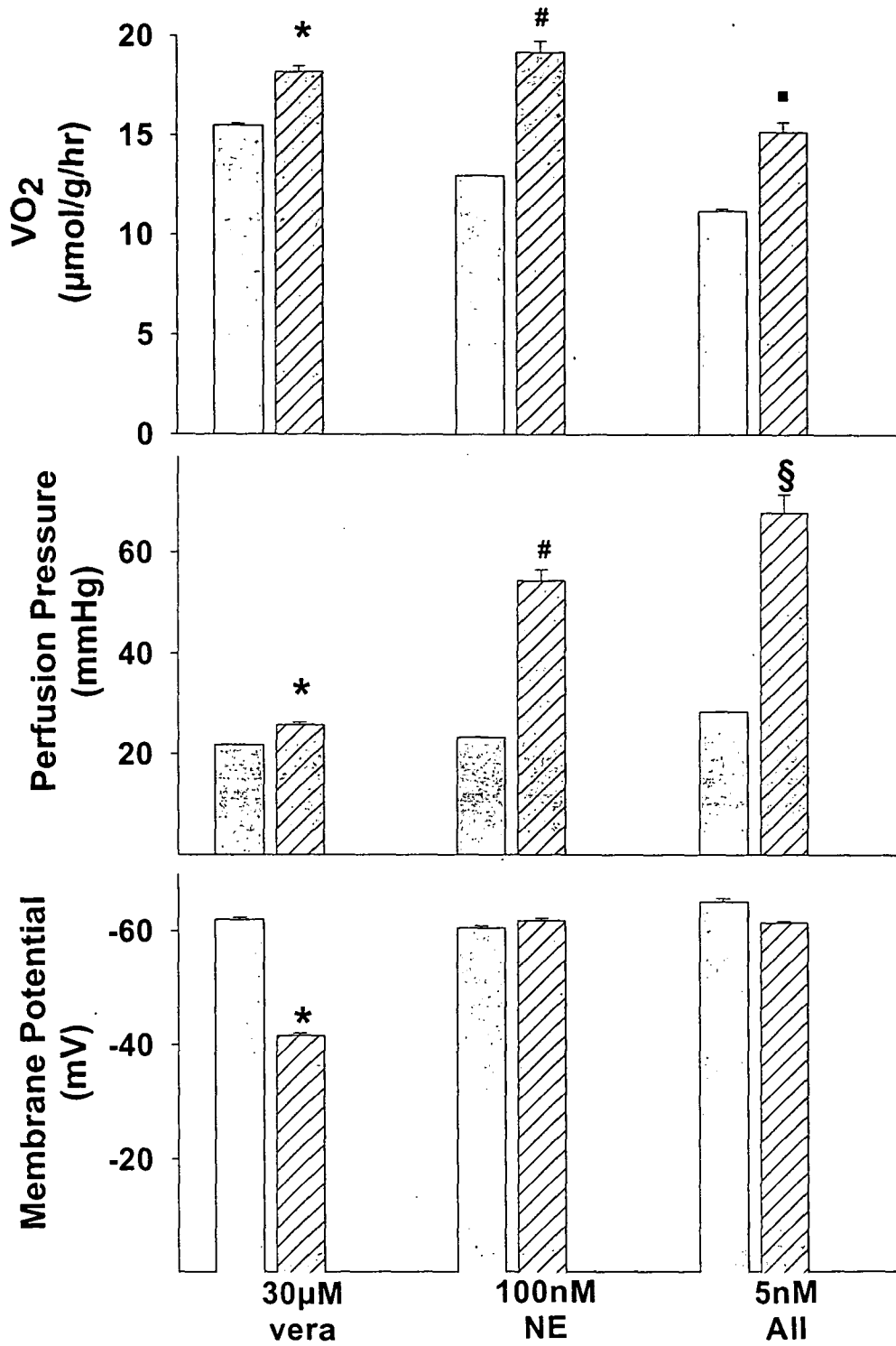
Figure 5.3 Agonist stimulated metabolism

*Effects of 30μM veratridine, 100nM NE, and 5nM AII on $\dot{V}O_2$, PP, and resting membrane potential. Basal values (solid bars) compared with agonist stimulated values (hatched bars). *, #, § = P<0.05, significantly different from basal, for vera, NE and AII respectively.*

5.4 Discussion

The perfused rat hindlimb preparation remained stable over the 3-hour time control period, without deterioration of basal oxygen consumption, perfusion pressure or membrane potential. Raising the extracellular [KCl] of the perfusion medium initiated a small depolarization of the skeletal fibers that was readily detectable. Thus, the current setup provides a viable preparation for monitoring discrete changes in skeletal muscle membrane potential during agonist-stimulated metabolism. All three agents trialled (veratridine, NE and AII) stimulated resting $\dot{V}O_2$. Perfusion pressure was significantly elevated by NE and AII. We have previously demonstrated that veratridine-mediated metabolism is not dependent on vasoconstriction, since the inclusion of nitroprusside abolished the pressure without interfering with the stimulatory oxygen effect (Chapter 4), thus the minor pressure development noted here (~4mmHg) is not considered further. Veratridine was the only agent to cause a measurable change in plasma membrane potential (E_M), consistent with activation of voltage-gated sodium channels. Type A vasoconstrictors NE and AII did not change skeletal muscle E_M, despite significant stimulation of $\dot{V}O_2$. Muscle phosphocreatine stores were depleted by veratridine, but not by NE, further distinguishing these two agents. It therefore seems unlikely, that type A vasoconstrictors stimulate muscle $\dot{V}O_2$ via the same mechanism as veratridine.

Failure to detect depolarization by NE or AII is not entirely unexpected. Only one paper reporting a depolarizing effect of NE on skeletal muscle fibers was found in the literature (289), however no other reports have been made. The possibility that type A-mediated metabolism is due to direct activation of the Na^+/K^+-ATPase pump itself is unlikely, given that type A vasoconstrictors have no effect on $\dot{V}O_2$ in isolated incubated muscle preparations (50; 69; 97; 145), and direct activation of the pump would have been expected to cause hyperpolarization (67). It is possible that type A vasoconstrictors caused a transient depolarization that was not detected by the glass electrode, or missed in the interim of sampling. The sampling technique required that the electrode be lifted clear of the tissue at the onset of vasoconstriction, in order to avoid damage the electrode tip. Again, this seems unlikely given that elevated $\dot{V}O_2$ was sustained for the duration of agonist infusion. If stimulation of $\dot{V}O_2$ was dependent on sodium influx, then depolarization should have been sustained for the same duration as agonist infusion, as noted during veratridine-mediated metabolism. Coupled with finding that type A metabolism is not sensitive to sodium channel blockade, it is concluded that the mechanism of type A-mediated skeletal muscle oxygen uptake is

not dependent on voltage-gated sodium channels or elevated intracellular sodium concentrations, and is thus distinct from veratridine-mediated metabolism.

The question remains, why should type A mediated metabolism be sensitive to low-sodium media, membrane stabilizers and cardiac glycosides? Attention is now drawn to the possibility that vasoconstriction in the vascular smooth muscle participates in the generation of an electrical or diffusible (paracrine) "signal", which has the potential to regulate skeletal muscle metabolism. If generation or transduction of the signal is dependent on changes in smooth muscle membrane potential, the presence of treatments affecting ion permeability would be expected to interfere. The intact nature of the vascular connections may be critical for generation or conduction of the signal, possibly explaining the failure of type A vasoconstrictors to elicit an effect in isolated incubated muscle preparations (97). Unfortunately this hypothesis is difficult to test in the perfused hindlimb, since the glass electrodes used were far too big to successfully penetrate vascular smooth muscle, and it would be virtually impossible to repeatedly locate and successfully penetrate vascular smooth muscle cells in the intact perfused hindlimb without dissection or disruption of flow delivery.

Experiments on vascular smooth muscle in arterioles of the hamster cheek pouch confirm depolarization in association with vasoconstriction when norepinephrine and phenylephrine were applied (303). Depolarization and vasoconstriction were recorded at the site of release and along the length of the arteriole, indicating that both the electrical and vasomotor responses were conducted, most likely via gap junctions. It has been suggested by Segal & Neild (270), that conduction of membrane potential changes between arteriolar smooth muscle and endothelial cells participates in the regulation of blood flow, by coordinating activity of the many branches of the arteriolar network. Conduction of signals via the vascular tree may have a profound effect on skeletal muscle blood flow, and a potentially greater effect on skeletal muscle metabolism. The phenomena of redistribution observed with type A vasoconstrictors may in fact be a concerted conduction of electrical signals along the arterioles, enabling enhanced perfusate access and oxygen delivery. Anatomically, feed arterioles are positioned to control blood flow into skeletal muscle, thus integration of dilator and constrictor stimuli in these vessels may be a key determinant of muscle blood flow during exercise (266), and in our opinion also during type A mediated vasoconstriction. This argument is strengthened by the observation that vascular smooth muscle cells possess tetrodotoxin-resistant sodium channels (296; 314). In addition, experiments in rat mesenteric veins and arterioles of the hamster cheek pouch demonstrate that TTX does not directly affect resting tone, or norepinephrine-induced constriction of vascular smooth muscle (197). Thus transduction of

electrical (sodium dependent) signals along the vascular smooth muscle will be not be blocked by TTX.

Even if the effects of type A vasoconstrictors were due to a paracrine signal of vascular origin, the biochemical mechanism responsible for skeletal muscle thermogenesis is still unknown. Whatever the mechanism, it appears to occur without any detectable change in skeletal fiber plasma membrane potential. The alkaloid ryanodine is known to stimulate skeletal muscle $\dot{V}O_2$ without depolarization (24), therefore intracellular calcium cycling is an attractive explanation, albeit one that is difficult to address experimentally. Exclusion of extracellular calcium from the medium would prevent vasoconstriction (96), thereby wiping out the potential type A effect. Skeletal muscle contains a large pool of intracellular calcium in the sarcoplasmic reticulum, hence skeletal muscle calcium cycling may proceed even in the absence of extracellular calcium. Studies with the Ca^{2+}-ATPase blocker dantrolene may be able to address this issue in perfusion, providing dantrolene achieves suitable access to Ca^{2+}-ATPase sites (located intracellularly). Despite this, stimulation of perfused muscle metabolism by increased intracellular calcium is a slow onset effect (taking up to 10 minutes to substantially increase $\dot{V}O_2$, unpublished observations from this laboratory). Type A vasoconstrictors stimulate $\dot{V}O_2$ rapidly, a response that more closely resembles changes in microvascular oxygen delivery that activation of intracellular ion cycling.

Analysis of muscle high-energy phosphates further distinguishes between NE and veratridine. Veratridine samples showed a marked depletion of phosphocreatine (Table 5.1), but no changes in [ATP]. It seems that the short-term demand for ATP by sodium pump is catered for, at the expense of phosphocreatine. More extreme sodium loads (induced by the sodium ionophore monensin in the isolated guinea pig aorta) have been shown to deplete cellular ATP levels, but only in the absence of glucose (227). Thus raised intracellular sodium places a strain on the cell that ultimately overcomes the metabolic capacity, and compromises cellular energy status. Elevated metabolism with veratridine is probably not a "stimulation" as such, but more of a "rescue attempt". This view is supported by the observation that in isolated incubated contracting rat soleus muscles, veratridine markedly decreased the force of contraction (Tong et al. unpublished observations). In the presence of veratridine, the combined metabolic demand of contraction and increased sodium load was simply too much, and contraction was unsustainable. In contrast, type A vasoconstrictors are not deleterious to the energy status of the cell, since muscle samples collected after 20-mins of NE infusion did not differ from basal in terms of high energy-phosphate content (Table 5.1). Similarly, after three hours of perfusion in the presence of a type A vasoconstrictor (vasopressin),

Colquhoun, Hettiarachchi, et al. (78) found no differences in the high energy-phosphate content of perfused and in vivo muscle samples. There is also some evidence that type A vasoconstrictors may actually enhance cellular energy status [Appendix Figure 1, from (300)]. Herein lies a fundamental difference between veratridine and type A vasoconstrictors.

Despite the apparent similarities, it is now clear that type A vasoconstrictors and veratridine do not stimulate perfused hindlimb metabolism by the same mechanism. Veratridine-mediated metabolism is accompanied by plasma membrane depolarization, and depletion of cellular energy reserves. In conjunction with susceptibility to tetrodotoxin (291), these data are consistent with direct activation of voltage-gated ion channels on the skeletal fibers. In contrast, type A mediated metabolism does not affect plasma membrane potential, or cellular energy status of skeletal fibers. Thus, type A mediated thermogenesis is not attributable to destabilization of skeletal muscle plasma membranes.

CHAPTER 6

COMPARISON OF VASOCONSTRICTOR-MEDIATED THERMOGENESIS IN PERFUSED SKELETAL AND CARDIAC MUSCLE

6.1 Introduction

It is not known if the phenomena of vasoconstrictor-mediated thermogenesis occurs in cardiac muscle as it does in skeletal muscle. The current chapter aims to ascertain if the same tetrodotoxin-resistant vasoconstrictor-mediated thermogenic mechanism demonstrated in the perfused rat hindlimb (Chapter 4), also occurs in perfused arrested rat heart. Evidence from this (59) and other laboratories (17; 127; 229) favour the existence of dual vascular pathways in skeletal muscle. However the existence of dual vascular pathways or significant heterogeneity of blood flow is less likely in heart, due to the comparatively smaller mass and consistently higher rate of contraction.

The main aim of this study was to make a direct comparison between perfused heart and skeletal muscle, and the response to type A vasoconstrictors. If type A vasoconstrictors fail to stimulate arrested heart thermogenesis, this would indicate a heavy reliance on redistribution for the thermogenic effects. However, if type A vasoconstrictors successfully stimulate thermogenesis in the arrested heart, then the thermogenic effects would be attributable to direct activation of a cellular mechanism, since there is less capacity for capillary recruitment in heart than in skeletal muscle.

6.2 Methods

6.2.1 Animals

All experiments were conducted with male Hooded-Wistar rats between the weights of 180-230g.

6.2.2 Perfusions

6.2.2.1 Hindlimb perfusions

The surgical method and apparatus were previously outlined (Section 2.2.2; 2.2.3). Single hindlimb perfusions were conducted at 37°C, with cell free medium, 4% BSA, and 2.54mM $CaCl_2$. Flow rate was maintained at a constant rate of 14 ml/min (0.87 ml/min'g), along with a higher BSA concentration to compensate for the higher rate of oxygen extraction at this temperature.

6.2.2.2 Heart perfusions

Heart perfusions were carried out in accordance with the method outlined in Richards et al. (243). Detailed descriptions of surgery, and apparatus are found in Section 2.3. Perfusion medium was a Krebs-Henseleit bicarbonate buffer, containing 0.05mM EDTA, 5mM pyruvate, and 5mM glucose, equilibrated with carbogen (95% O_2: 5% CO_2). Following removal and cannulation, hearts were perfused at a constant flow rate (6.79 ± 0.12 ml/min), equivalent to 8.94 ± 0.25 ml/min/g wet wt heart (mean ± SE, *n = 18*), at 37°C.

After cannulation a 20-30 min equilibration period was allowed, until oxygen uptake and perfusion pressure reached steady states. Preliminary experiments were conducted to determine an adequate dose of the α-adrenergic combination of phenylephrine plus 0.3mM atenolol that would reproducibly increase both oxygen uptake and perfusion pressure at constant flow. The preliminary results showed that the heart was considerably less sensitive to phenylephrine that the perfused hindlimb, and thus a higher dose of phenylephrine (50μM) was considered optimal.

6.2.3 Experimental protocols

6.2.3.1 Perfused hindlimb preparation

For the hindlimb perfusions where phenylephrine was used, 0.3mM atenolol was also included in the perfusion medium, in order to prevent activation of β-adrenoreceptors (ensuring an α-adrenergic effect only). At this dose, atenolol has no effects on basal or agonist stimulated oxygen uptake (292). Phenylephrine was infused

at a final concentration of 1μM. Putative sodium channel involvement during phenylephrine-stimulated metabolism was tested with the sodium channel inhibitor tetrodotoxin (TTX, 10μM). For the veratridine perfusions (10μM), sodium nitroprusside (SNP 0.5mM) was included in the perfusion medium to prevent any possible vasoconstrictor effects on smooth muscle.

6.2.3.2 Perfused heart preparation

The α-adrenergic combination of 0.3mM atenolol and 50μM phenylephrine was tested in the heart during conditions of normal contraction, and in hearts arrested by infusion of TTX (10μM). For the veratridine experiments, KCl was used in place of TTX to arrest the heart, since TTX is a known inhibitor of veratridine mediated oxygen uptake in perfused hindlimb (Chapter 4), and is likely to be so in heart. When present, veratridine was infused at a final concentration of 10μM.

6.2.4 Statistical analysis

Statistics were carried out using SigmaStat statistical program (Jandel Software Corp.). Each data set was analysed for significant differences by one-way repeated measures analysis of variance, with pair-wise comparisons by the Student-Newman-Kuels test. Statistical significance was recognized at $P<0.05$ level.

6.3 Results

6.3.1 Effects of phenylephrine in perfused hindlimb

Figure 6.1 shows a typical trace of the oxygen uptake and perfusion pressure obtained during 1μM phenylephrine infusion ± 10μM tetrodotoxin (TTX) (0.3mM atenolol included in all phenylephrine experiments). Figure 6.2 illustrates mean values ± SE (*n=5*). Mean basal values in the perfused hindlimb (before phenylephrine) were $31.5 \pm 1.0 \mu mol.g^{-1}.hr^{-1}$ and $40 \pm 5mmHg$ for oxygen consumption and perfusion pressure respectively (*n=5*). One-way repeated measures analysis of variance with pair-wise comparisons using the Student-Newman-Kuels test demonstrates that phenylephrine caused a significant increases ($P<0.05$) in oxygen uptake, under basal conditions (24.1%) and during infusion of TTX (28%). Perfusion pressure was

significantly ($P<0.05$) elevated by phenylephrine during basal (32.2%) and TTX infusion (30.6%). Thus 10μM TTX did not interfere with phenylephrine stimulated oxygen uptake or pressure development in the perfused rat hindlimb.
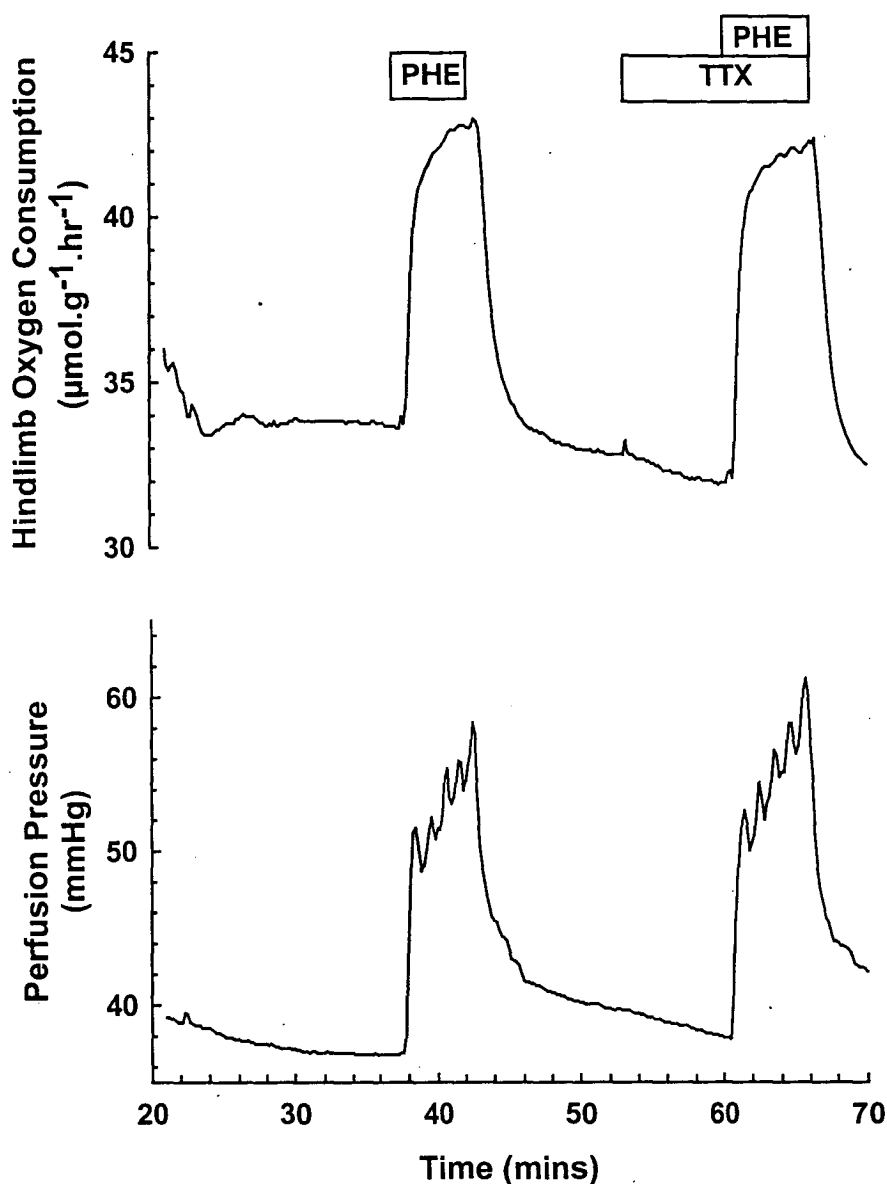
Figure 6.1. Time course for the effects of PHE ± TTX on perfused hindlimb V̇O₂ and PP

Hindlimbs were perfused at a constant flow of 14ml/min. Infusion of 1μM phenylephrine (PHE) commenced after 30-mins equilibration. V̇O₂ and PP recovered after PHE infusion to near basal values, and tetrodotoxin (TTX, 10μM) infusion commenced thereafter. The effects of 1μM PHE in the presence of 10μM TTX were then examined. Shown is a representative trace for one experiment.

Figure 6.2 Effects of phenylephrine ± tetrodotoxin on perfused hindlimb$\dot{V}O_2$ and PP

*Phenylephrine (PHE) was infused at a final concentration of 1μM, while tetrodotoxin (TTX) was infused at 10μM. Values are means ± SE for n=5; *P<0.05, significantly different from basal; # P<0.05, significantly different from TTX treatment tested by repeated measures one-way analysis of variance and pair-wise comparisons using the Student-Newman-Kuels test.*

6.3.2 Effects of veratridine in perfused hindlimb

Figure 6.3 shows the effects of 10μM veratridine in the perfused rat hindlimb in the presence of 0.5mM sodium nitroprusside (SNP). Veratridine (10μM) significantly increased (45%) basal oxygen uptake from 26.1 ± 0.4 to 38 ± 0.9 $\mu mol.g^{-1}.hr^{-1}$ ($P<0.05$, $n=5$). Perfusion pressure was only marginally increased by veratridine from 41.3 ± 1.7 to 43.3 ± 2.3 mmHg, however this change was not significant ($P>0.05$).
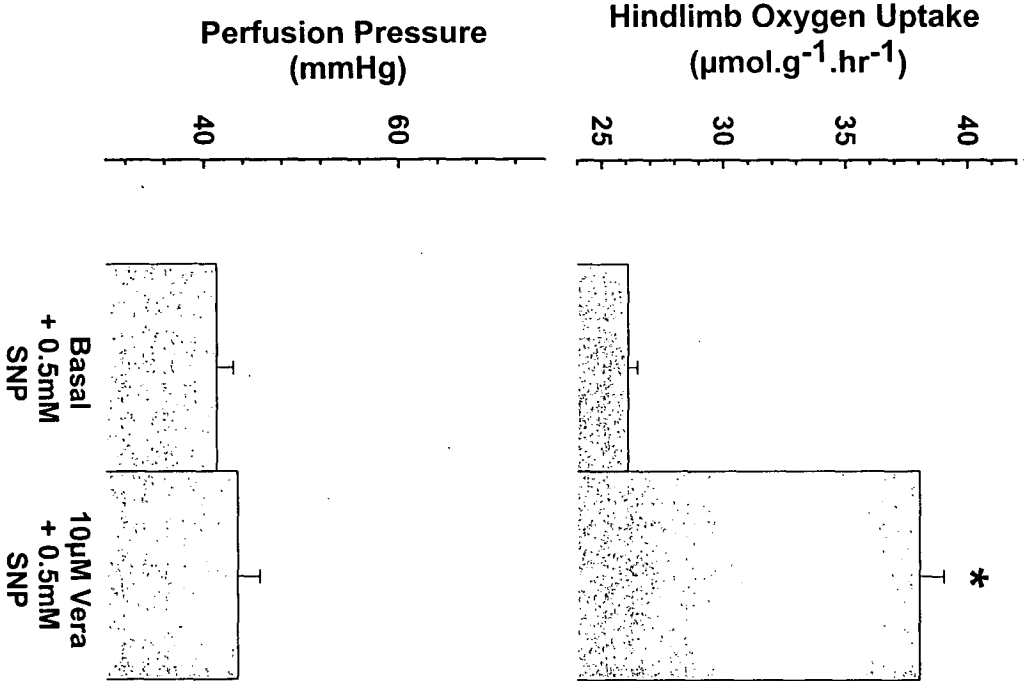
Figure 6.3 Effects of veratridine on perfused hindlimb $\dot{V}O_2$ and PP

0.5mM sodium nitroprusside (SNP) was included in all veratridine experiments in the perfused hindlimb.
Veratridine was infused at a final concentration of 10μM. Values are means ± SE for n=5;

*P<0.05, significantly different from basal.

6.3.3 Effects of phenylephrine in the perfused arrested heart

Shown in Figure 6.4 is a typical trace of the effects of a 7-10-min infusion of 50μM phenylephrine (with 0.3mM atenolol in buffer) while the heart was contracting. 15-20 mins after cessation of phenylephrine infusion, when oxygen and pressure had returned to pre-infusion levels, infusion of 10μM TTX commenced. Contraction rapidly declined within 2-mins of TTX infusion, and no further contraction was observed for the remainder of the experiment (data not shown). When oxygen uptake and pressure had again stabilized, infusion of phenylephrine re-commenced at the same rate used prior to arrest.
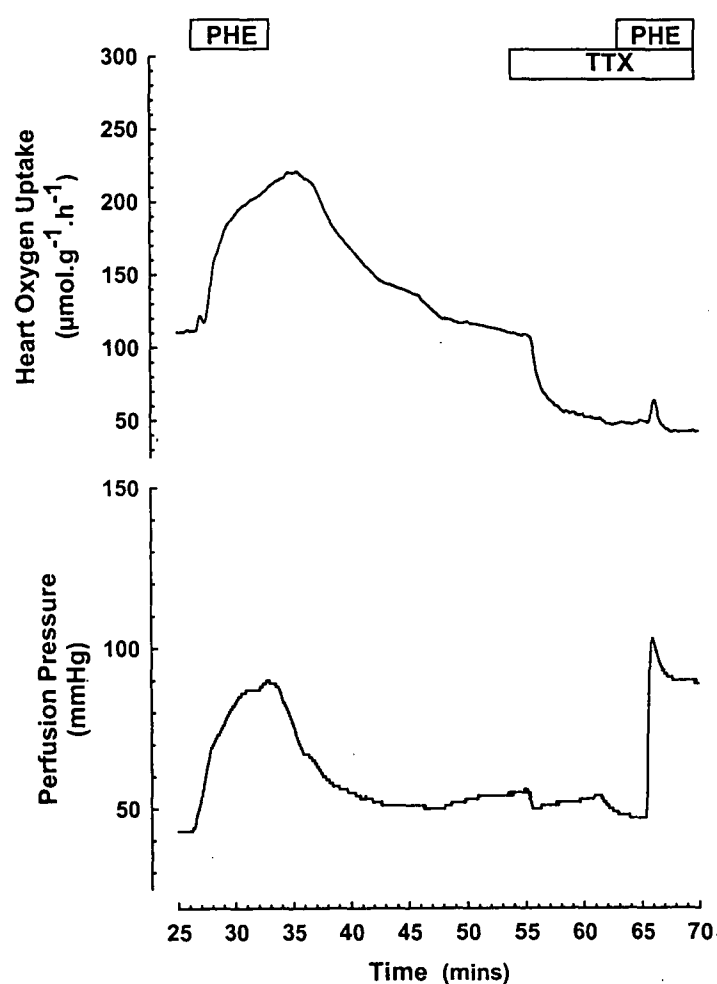
Figure 6.4 Time course for the effects of phenylephrine ± TTX on V̇O₂ and PP of the perfused rat heart.

The perfusion buffer contained 0.3mM atenolol, and perfusions were conducted at constant flow. Phenylephrine (PHE) was infused at a final concentration of 50μM, while tetrodotoxin (TTX) was infused at 10μM. A representative trace for one experiment is shown.

For some hearts, there was a transient stimulation of oxygen uptake coinciding with the commencement of phenylephrine infusion, however, this effect was short lived and soon subsided (Figure 6.4), despite a marked increase in perfusion pressure (Figure 6.5). Figure 6.5 illustrates mean values ± SE ($n=10$) for the effects of 50μM phenylephrine on cardiac $\dot{V}O_2$ and PP, before and after cardiac arrest with 10μM TTX. Phenylephrine caused a significant ($P<0.05$) increase in oxygen uptake (70.4%) when infused into contracting heart, but not in TTX arrested hearts. Perfusion pressure was significantly ($P<0.05$) increased by phenylephrine in both contracting (32.7%) and TTX-arrested (51.4%) hearts. TTX-arrest of contracting hearts caused a significant ($P<0.05$) decrease in basal $\dot{V}O_2$ (52.5%) but no significant change in perfusion pressure. 0.3mM Atenolol did not affect basal oxygen uptake or perfusion pressure (compare Figures 6.5 and 6.7).
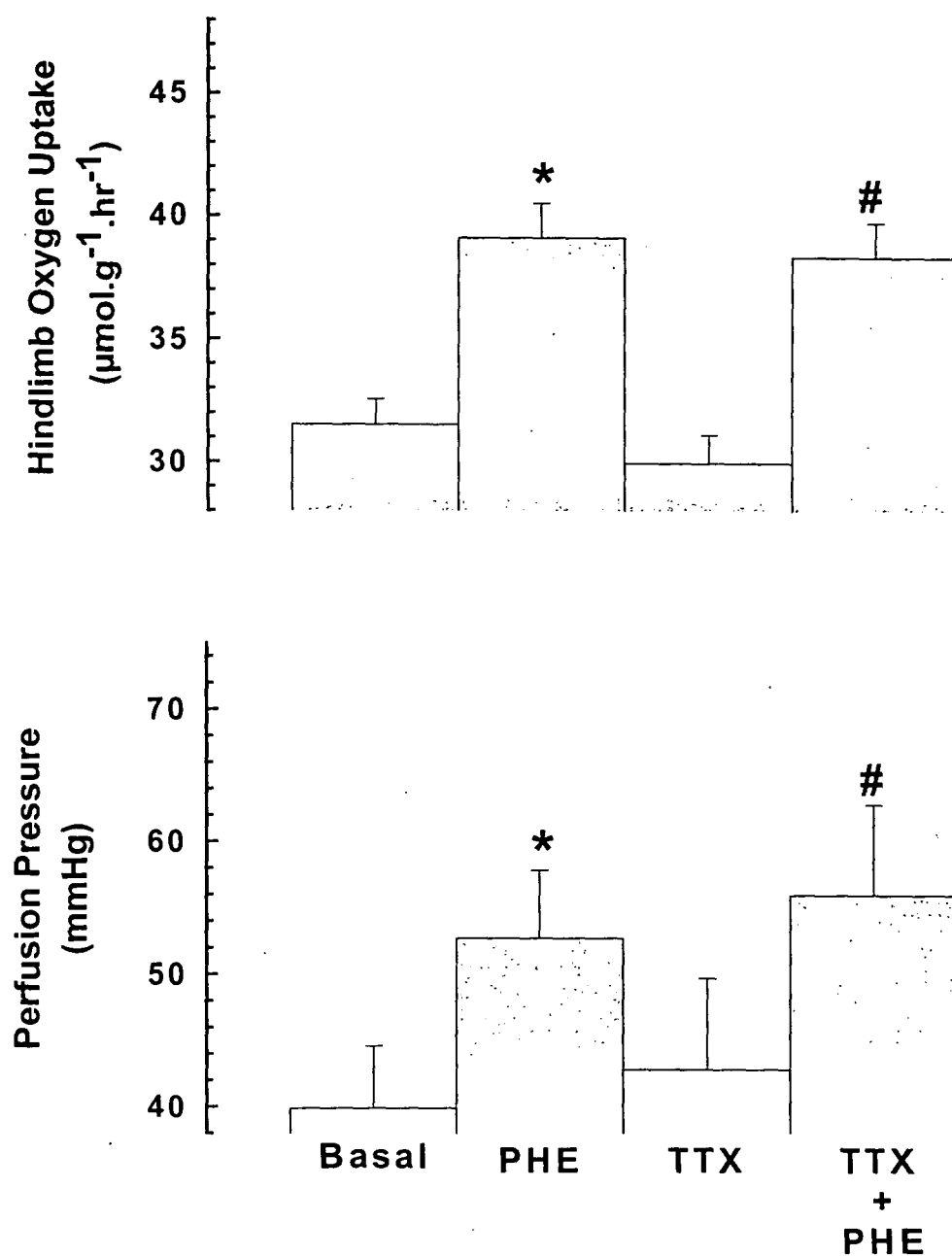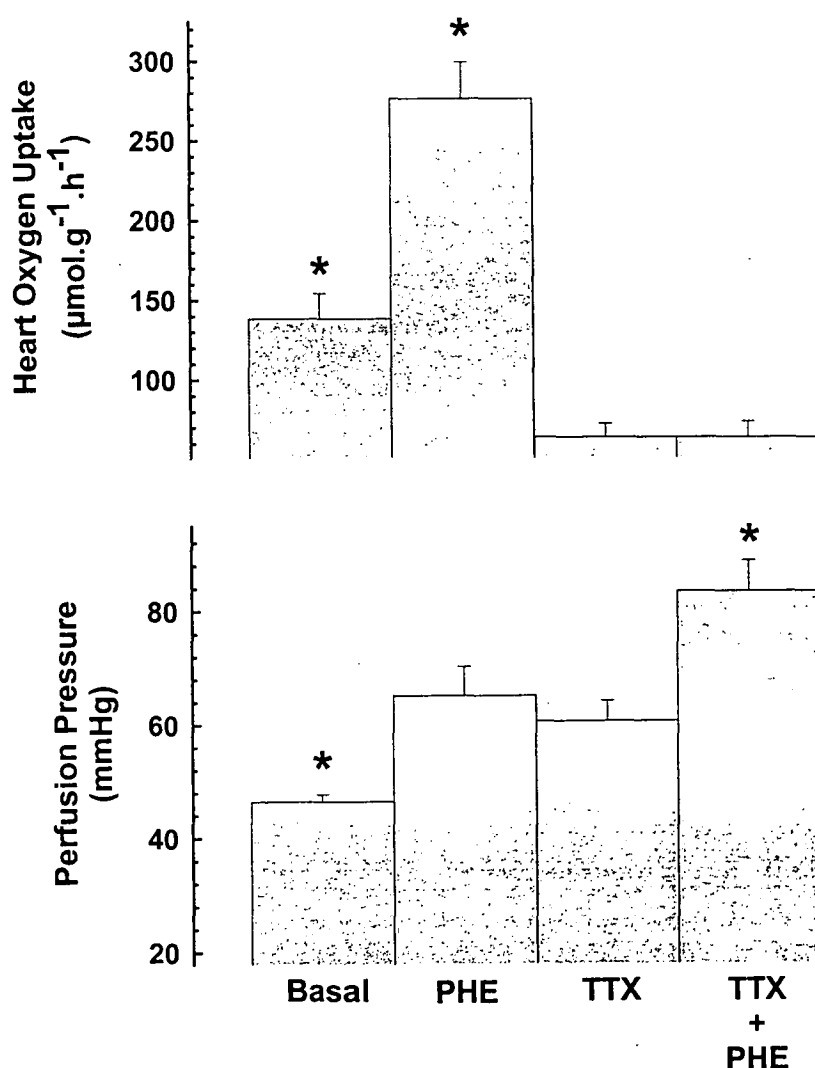

Figure 6.5. Effects of phenylephrine ± TTX on perfused heart $\dot{V}O_2$ and PP.

*Phenylephrine (PHE) was infused at a final concentration of 50μM, while tetrodotoxin (TTX) was infused at 10μM. Values are means ±SE, for n=8 experiments; *P<0.05, significantly different to TTX treatment.*

6.3.4 Effects of veratridine in perfused arrested heart

Shown in Figure 6.6 is a typical trace of oxygen uptake and perfusion pressure obtained during veratridine infusion. Infusion of 40mM KCl caused cardiac-arrest. Contraction ceased within 2-mins of KCl infusion, and no contractions were observed for the remainder of the experiment (data not shown). After 15-mins of KCl infusion, oxygen uptake and perfusion pressure had stabilized, at this time veratridine infusion (10μM) commenced. Oxygen uptake was stimulated by veratridine after a short (approximately 3 min) delay, similar to the delay observed in perfused hindlimb (Tong et al. 1998).
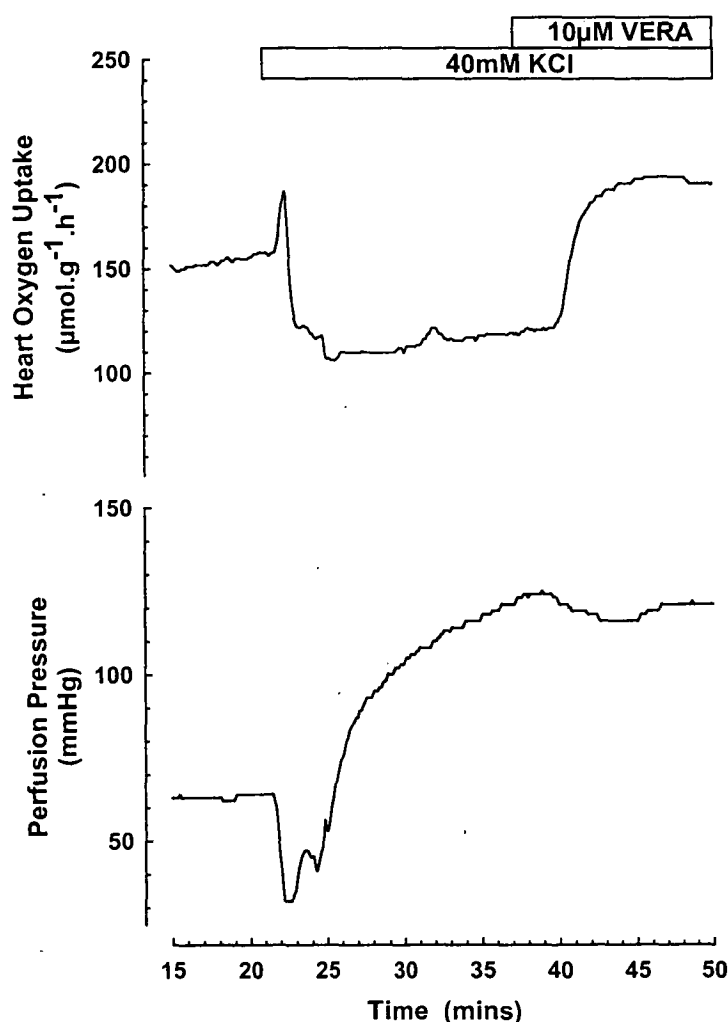
Figure 6.6 Time course for the effect of veratridine on $\dot{V}O_2$ and PP in the KCl-arrested perfused rat heart.

Beating hearts were arrested by infusion of 40mM KCl. Once steady state $\dot{V}O_2$ and PP were attained, 10μM veratridine (Vera) infusion commenced. A representative trace for one experiment is shown.

Figure 6.7 shows the mean ± SE values (*n=8*) for oxygen uptake and perfusion pressure determined before KCl infusion (basal), during KCl infusion (arrest), and after 10mins of KCl and veratridine. KCl arrest caused a significant (*P<0.05*) decrease (32.7%) in oxygen uptake, and an increase (165%) in perfusion pressure. Veratridine infusion resulted in significant (*P<0.05*) increase (55.6%) in arrested-heart oxygen consumption and a further small rise (12.8%) in perfusion pressure.
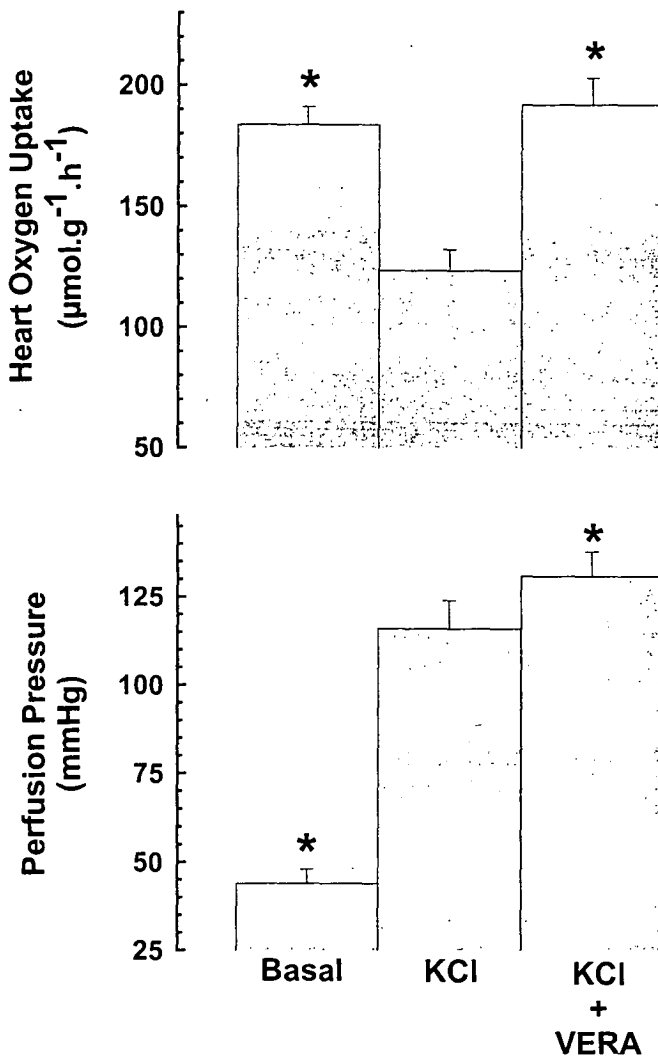
Figure 6.7 Effects of KCl and veratridine on $\dot{V}O_2$ and PP of the perfused rat heart.
Beating hearts were arrested with high KCl infusion (40mM). Following arrest, the effects of 10μM veratridine (Vera) were examined. Values are means ± SE for n=8 experiments.
*P<0.05, significantly different from KCl treatment.

6.4 Discussion

The current experiments were designed to compare the effects of type A vasoconstrictors in perfused heart and skeletal muscle at rest, in order to determine if type A effects were dependent primarily on redistribution of flow, or direct activation of a cellular mechanism. Heart is the ideal candidate tissue in which to examine this issue, since there is less potential for capillary recruitment, and in the non-contractile state cardiac muscle is a comparable resting model. Skeletal muscle $\dot{V}O_2$ was enhanced by the α-adrenergic combination of phenylephrine and atenolol, even in the presence of the sodium channel inhibitor tetrodotoxin (Figs. 6.1 & 6.2), consistent with the findings in Chapter 4. During contraction, the α-adrenergic combination of phenylephrine and atenolol also stimulated cardiac oxygen uptake and perfusion pressure (Fig. 6.5). This was attributed to the well-established α-adrenergic inotropic effect of phenylephrine and other catecholamines (1). However, in the TTX-arrested heart, phenylephrine failed to stimulate oxygen uptake despite development of similar perfusion pressures (Figs. 6.4 & 6.5). Thus, tetrodotoxin-insensitive type A vasoconstrictor-mediated thermogenesis found in perfused skeletal muscle at rest is absent from the perfused arrested rat heart.

The difference between perfused heart and skeletal muscle in terms of vasoconstrictor mediated thermogenesis may be due differences in vascular anatomy. By comparison capillary perfusion is more homogenous in heart, therefore the capacity for capillary recruitment is less than in skeletal muscle. Evidence in favour of this theory comes from microdialysis experiments. In the perfused rat hindlimb at rest, increased flow rate causes a monotonous decrease in out/in ratios of ^{14}C-ethanol and ^{3}H$_2$O (Appendix, Figure 2), however the inclusion of type A and B vasoconstrictors cause a significant change in these ratios. The type A vasoconstrictor norepinephrine (70nM), accelerates the decline in radioactive out/in ratios with increasing flow rate, while type B (300nM serotonin) impedes the decline in flow induced out/in ratios (221). These effects are attributed to recruitment and de-recruitment respectively, either enhancing or impeding the removal radioactive tracer from the microdialysis tubing by affecting local distribution of flow (221). In contrast, similar experiments in the anesthetized autoperfused contracting sheep heart, do not support the existence of

significant heterogeneity of blood flow, or redistribution of flow in cardiac tissue. Microdialysis out/in ratios for ^3H_2O also decreased with increasing flow rate (Appendix, Figure 3), however, the addition of the vasoconstrictor norepinephrine, or vasodilators adenosine or sodium nitroprusside did not influence the flow induced microdialysis out/in ratios (Richard Hodgson honours thesis 2001). Thus, other than changes in total flow, redistribution of flow is not a significant occurrence in the contracting heart. Without the potential for redistribution of blood flow, type A vasoconstrictors may simply be ineffectual in stimulating metabolism. Alternatively it must be considered that the tetrodotoxin-insensitive mechanism triggered by vasoconstrictors in skeletal muscle simply does not exist in perfused arrested heart. It has been suggested that vasoconstrictor-mediated redistribution of blood flow causes production of a paracrine signal of vascular origin, which then triggers thermogenesis in the skeletal fibers (59). Heart may lack this signalling system, therefore even if some redistribution of flow did occur no change in oxygen consumption would be observed.

Cessation of cardiac contraction (by TTX or KCl) significantly decreased cardiac oxygen consumption (Figs. 6.5 and 6.7), indicating that most of oxygen consumed by the beating heart is dedicated to supporting cardiac contractility. Interestingly, cessation of cardiac contractility was also associated with an increase in perfusion pressure when compared with basal (Fig. 6.7). Cardiac contractility may enable production of vasodilatory substances, or prevent the production of vasoconstrictors.

In skeletal muscle (Fig. 6.3) the combination of veratridine and sodium nitroprusside caused a significant increase in $\dot{V}O_2$ that was not dependent on pressure development or redistribution. Resting cardiac oxygen consumption was also enhanced by the addition of veratridine (Fig. 6.7). Increased ionic permeability is thus capable of directly stimulating a thermogenic mechanism in both skeletal and cardiac muscle at rest. The absence of a type A effect in perfused arrested heart, leads us to the conclusion that type A vasoconstrictor-mediated metabolism does not directly activate a cellular thermogenic mechanism. It follows, that the stimulatory effects of type A vasoconstrictors in the perfused hindlimb are likely to be more dependent on redistribution than activation of a cellular mechanism. Thus, increased rates of oxygen

consumption with type A vasoconstriction may be related to changes in perfusate delivery, rather than activation of cellular mechanisms.

In summary, type A vasoconstrictors do not have the same effects in perfused skeletal and cardiac muscle. The TTX-insensitive type A thermogenic effect observed in perfused skeletal muscle is absent from perfused arrested heart. This confirms that the stimulatory effects of type A vasoconstrictors are not due to activation of a cellular mechanism directly. In contrast, the stimulatory effects of veratridine were apparent in both skeletal and cardiac muscle at rest. Thus, direct sodium channel activation can evoke thermogenesis in both tissues, but this is an apparently separate phenomenon from type A mediated thermogenesis. It is therefore concluded that type A mediated thermogenesis in the perfused hindlimb is dependent (at least in the first instance) on redistribution, and enhanced oxygen delivery.

CHAPTER 7

DISCUSSION AND CONCLUSIONS

7.1 Supply and Demand

One of the main findings to emerge from this study is that skeletal muscle metabolic rate may be manipulated by changing substrate supply or by changing the metabolic demand [in agreement with the findings of other groups (48; 254)]. In attempting to define the mechanism of vasoconstrictor-mediated metabolism in the perfused rat hindlimb both substrate supply and metabolic demand were considered. Evidence in favour of either mechanism has been presented in the past [(59; 97) & (292)](291) and this issue is now re-evaluated in light of the current findings.

7.2 Muscle metabolism and supply
7.2.1 Oxygen conformance in perfused skeletal muscle

In order to assess the potential regulation of hindlimb metabolism by vasoconstrictor-mediated changes in oxygen delivery, it was first necessary to establish if the perfused hindlimb preparation was responsive to changes in oxygen delivery alone. Results in Chapter 3 demonstrate clearly that perfused skeletal muscle is indeed responsive to changes in O_2 delivery, without the complication of redistribution or changes in cellular energy status. Lactate levels were elevated, however these changes were not sufficient to compensate fully for the loss of aerobic energy production. After careful consideration of this data, it is concluded that the perfused rat hindlimb preparation is capable of oxygen conformance, at least to a limited extent. Oxygen conformance in perfused muscle may not be strict as in isolated muscle preparations (8; 38; 44; 152), owing to heterogeneous perfusion, however a general relationship between $\dot{V}O_2$ and oxygen delivery was apparent.

7.2.2 Vasoconstrictors affect $\dot{V}O_2$ by changing oxygen delivery

Following the demonstration of oxygen conformance in perfused muscle, the role of vasoconstrictors on oxygen delivery may now be examined in more detail. It

has been suggested that micro-scale heterogeneity in blood flow and oxygen delivery may take part in normal control of muscle respiration (48). The following calculations demonstrate an enormous range over which oxygen consumption is regulated simply by changing total flow or the redistribution of flow. In the blood perfused rat hindlimb, changing the total flow from 1.0 to 9.0 ml/min increases resting oxygen consumption by a factor of almost 3 fold [from 15.7 to 46.9 $\mu mol.g^{-1}.hr^{-1}$(221)]. The addition of NE or 5-HT to the constant-flow blood perfused hindlimb (70 or 300nM respectively at 4 ml/min), results in development of similar perfusion pressures, though NE enhanced basal $\dot{V}O_2$ by 63%, while 5-HT depressed basal oxygen consumption by 10.5%. The mere redistribution of blood flow at constant flow rate therefore has the capacity to influence the resting rate of skeletal muscle oxygen consumption by a factor of almost 2 fold. The combination of varied flow rate and redistribution further augments these effects. At 1.0 ml/min in the presence of 300nM 5-HT, basal $\dot{V}O_2$ was 15.0 $\mu mol.g^{-1}.hr^{-1}$, while 70nM NE at 9 ml/min increased resting $\dot{V}O_2$ to 72.6 $\mu mol.g^{-1}.hr^{-1}$. Therefore, the combination of varied flow rate and vasoconstrictor-mediated redistribution of flow has an enormous capacity (almost 5 fold) to regulate resting skeletal muscle $\dot{V}O_2$.

While muscle $\dot{V}O_2$ is enhanced by increased flow rate (53; 103; 209; 285), muscle $\dot{V}O_2$ is also responsive to increased oxygen carrying capacity of the perfusate (181). Furthermore, muscle perfused with high O_2 affinity blood had a low $\dot{V}O_2$, despite increased flow rates (182). Thus, muscle oxygen uptake is determined to a greater extent by oxygen delivery than by flow rate. The net effect of increased flow is enhanced microvascular perfusion and improvements in oxygen delivery. Though total flow remains constant during type A vasoconstriction, changes in blood flow distribution may have the same net effect as increased flow, namely improvements in microvascular perfusion. Since, the perfused rat hindlimb is now known to respond to changes in oxygen delivery, it is likely that regulatory influence of vasoconstrictors on perfused rat hindlimb metabolism is the result of variations in oxygen delivery at the microvascular level, via redistribution of blood flow.

If muscle $\dot{V}O_2$ is increased by improvements in oxygen delivery, then it must also be assumed that prior to this, oxygen delivery was limiting on muscle metabolic

rate. Muscle oxygen consumption has been shown to be delivery dependent below critical values of oxygen delivery [estimated at $16\mu l$ O_2/min/g in perfused rat gracilis muscle (183)]. Since perfused hindlimb $\dot{V}O2$ was delivery dependent at all gas mixtures trialled, it follows that oxygen delivery was below these critical values. This is intriguing, since flow rate and oxygen content of the perfusion media should have been more than sufficient to adequately supply the entire mass of perfused muscle. Gassing the blood with an air:CO_2 mixture, gives a final blood content of 7.9 μmol O_2/ml. Combined with a flow rate 4.0 ml/min per 15g perfused muscle mass, this should deliver $2.1\mu mol$ O_2/min/g perfused muscle [equivalent to 53.4 μl/min/g, a value far in excess of the $16\mu l$/min/g reported by Janský et al. in perfused rat gracilis (183)]. Why then should muscle $\dot{V}O_2$ be oxygen limited? This discrepancy is most likely due to heterogeneous perfusion under basal conditions, where only a small portion of the total blood flow reaches the nutritive capillary beds. Type B vasoconstrictors apparently exacerbate this situation by restricting nutritive access, further limiting oxygen delivery. However, type A vasoconstrictors are likely to relieve the restriction on perfusate access, restoring a non-restricted state of respiration. The observations that type A vasoconstrictors (300), high flow rates (209), and hyperoxic medium (308) all improve resting muscle ATP and PCr levels, appear to support this view.

Some important questions raised in the introduction are now addressed. Time course graphs show that following the removal of a type B vasoconstrictor, metabolism returns from a depressed level back towards pre-infusion values (94). The questions were posed, can this increase be considered as a stimulation of metabolism, and if so, is this due to the same mechanism as type A vasoconstriction? Assuming oxygen delivery and heterogeneity of flow are the key determinants of hindlimb metabolism, then yes, type B removal is a stimulation of metabolism, and the mechanism is akin to application of a type A vasoconstrictor. Type B vasoconstrictors (serotonin) increase perfusion pressure and cause shunting of blood flow through non-nutritive vessels (219), thereby restricting oxygen delivery and basal metabolic rate. The removal of a type B vasoconstrictor alleviates the situation, allowing pressure to return to pre-infusion levels and restoring flow to a greater number of nutritive vessels. This is essentially the same sequence of events leading to stimulation of metabolism during type A vasoconstriction.

7.2.4 Heterogeneous perfusion leads to metabolic suppression

An interesting sideline also emerges from these results. If perfused hindlimb metabolism is oxygen limited under basal conditions, one might expect to see metabolic indications of hypoxia. When aerobic ATP production fails, anaerobic mechanisms are turned on resulting in lactate efflux. If anaerobic metabolism is insufficient to meet energetic requirements, then PCr levels begin to decline, and eventually ATP levels will also fall (258; 308). However, muscle samples collected *in vivo,* and after 50 and 180 mins of basal perfusion show no changes in cellular ATP, PCr content or lactate efflux (78). Thus, the usual indices of hypoxia do not indicate under-perfusion during basal conditions.

A more extreme example of oxygen limiting conditions might be expected during type B vasoconstriction, where regional hypoxia may result from perfusate shunting (220). Curiously, type B vasoconstriction (serotonin) was shown to inhibit lactate efflux below the basal level in the perfused Bettong hindlimb (311). Freeze clamped muscle samples collected during serotonin infusion into the perfused rat hindlimb show some evidence of PCr decline (300), though it is acknowledged that PCr is a more sensitive indicator of early ischemia (308). Despite this, muscle energy charge and ATP levels were not depleted by serotonin [Appendix Figure 1]. Thus regions of hypo-perfused skeletal muscle appear to be able to tolerate hypoxic conditions without suffering significant damage. In order to maintain cellular viability during hypoxia, one of two responses must occur, either anaerobic ATP producing pathways are activated, or ATP utilization is decreased to match decreased rates of production. Since lactate is not elevated and cellular ATP is not decreased by type B vasoconstrictors, it follows that skeletal muscle viability is maintained during regional hypoxia by decreasing ATP utilization. It is now proposed that the regions of the hindlimb that are less than maximally perfused assume a state of depressed metabolism or hibernation.

7.2.5 Mechanisms of metabolic suppression

The phenomenon of metabolic hibernation has been noted in isolated non-contracting neonatal rat cardiomyocytes (44). When exposed to oxygen concentrations of 5-6 μmol/l, isolated cardiomyocytes decreased their basal rates of oxygen uptake by 36%, though intracellular ATP and PCr concentrations were maintained, with no evidence of anaerobic ATP production. It was concluded that non-contracting isolated cardiomyocytes were able to down-regulate energy utilizing processes during oxygen limiting conditions. However, under more severe conditions (2-3 μmol/l oxygen), isolated cardiomyocytes decreased basal oxygen uptake by 91%, while intracellular ATP was maintained but PCr was decreased by 40%, with a significant switch to anaerobic metabolism (44). Thus, cellular ATP utilization is decreased during both moderate and severe hypoxia, but under more severe conditions cells show signs of energetic stress. These findings are consistent with the present observations in the perfused rat hindlimb.

Metabolic suppression appears to be a widespread protective mechanism employed during hypoxia in ectotherm (91; 93; 135; 152; 283) and endotherm species (44). By decreasing ATP utilization during oxygen limited conditions, substrate reserves are spared and there is no accumulation of toxic end products (283), though exactly which ATP consuming reactions are down-regulated remains unresolved. The major contributors to standard metabolic rate are ion pumping, synthetic pathways, pump/leak cycles and substrate cycling (254). In hypoxia tolerant species (frogs & turtles) evidence has been presented that energy conservation is achieved through a combination of down-regulation of synthetic pathways (38), and reduced membrane permeability through channel arrest (92; 93; 151; 152). It must be noted that these cells are specifically adapted to cope with low oxygen environments, with specific modifications geared towards lowering ATP turnover. By comparison, decreased ATP turnover in mammalian cells is expected to be more modest, occurring over a narrower range of oxygen concentrations than in hypoxia tolerant species. It is not clear if the phenomenon of channel arrest occurs in mammalian tissue as it does in reptilian tissue, though some data has been presented to suggest that membrane-permeability may have a role in regulating metabolic rate in mammalian tissues (164).

Other ATP consuming reactions in mammalian skeletal muscle that may be considered include protein synthesis, urea synthesis, RNA/DNA turnover and substrate cycling (254). Examination of oxygen conformance in the murine skeletal C_2C_{12} cell line shows no decline in the rate of protein synthesis between the oxygen concentrations of 100 and 10μM, despite a significant reduction in basal oxygen consumption (30-40%) (8). However, under more severe conditions (<0.5μm oxygen), cells displayed signs of energetic stress (36% decrease in PCr), and protein synthesis was reduced by 43% (8). Thus, in mammalian tissue, ATP consuming reactions may only be down-regulated during energetic stress. Based on these observations, one may speculate on the order of down-regulation of oxygen consuming reactions during oxygen conformance. While muscle $\dot{V}O_2$ is decreased during moderate hypoxia, protein synthesis was not changed and muscle intracellular ATP levels were maintained (8). This suggests that whichever oxygen consuming mechanism is down-regulated in order to accommodate the decrease in muscle $\dot{V}O_2$, is not linked to ATP production. In skeletal muscle, $\dot{V}O_2$ not linked to ATP production is likely to be the result of mitochondrial proton leak (252). Declining arterial oxygen may first limit the rate of uncoupled respiration (mitochondrial proton leak), while ATP utilization continues normally, until oxygen supply also becomes limiting on ATP production, at which time ATP utilization will also be down-regulated.

7.2.6 Oxygen delivery and mitochondrial proton leak

While the phenomenon of channel arrest has been demonstrated in hypoxia tolerant species (38; 152), the possibility of "proton conductance arrest" has also been suggested as a mechanism enabling energy conservation during hypoxic conditions (282). The high rates mitochondrial proton leak occurring during normoxia [estimated to account for up to 50% of standard metabolic rate in perfused skeletal muscle (251)] may be reduced to barely detectable levels during oxygen limitation. It has been demonstrated in isolated mitochondria from rat liver by Gnaiger et al. (122) that under hypoxic conditions, proton leak and uncoupled respiration are depressed, while the coupling efficiency of oxidative phosphorylation and ATP production is improved. It was speculated that this may have been the result of decreased permeability of the mitochondrial inner membrane during hypoxia (122). A study by

Andersson et al (3) appears to support this, since proton conductance of the mitochondrial membrane was shown to be reduced during 30 mins of hypoxia in rat hepatocytes. This may be also be the case in perfused skeletal muscle [Chapter 3]. At higher rates of oxygen delivery [100% air] coupling efficiency may have been low, leading to P/O ratios close to 1.5, though under more limiting conditions [0% air] coupling efficiency may have been improved, allowing P/O ratios closer to the predicted value of 2.5. However, studies in mitochondria from cold submerged/anoxic frog skeletal muscle suggest that the kinetics of proton conductance are not different between anoxia and normoxia, but proton leak may be reduced as a secondary consequence of reduced electron transport activity (284). The so called "proton conductance arrest" may be more the result of decreased electron transport flux (due to oxygen limitation) than decreased mitochondrial membrane permeability. Nonetheless, proton leak does appear to be reduced during hypoxia. Taking into account previous estimates [50% skeletal muscle oxygen consumption is due to proton leak (251)], decreased proton leak in perfused skeletal muscle mitochondria may offer a significant energy saving during hypoxia.

With this in mind, one questions the mechanism by which vasoconstrictors may affect the rate of mitochondrial proton leak in perfused skeletal muscle. While increased oxygen delivery with type A vasoconstrictors is likely to increase the rate of coupled and uncoupled respiration, it is not immediately clear how type B vasoconstriction, and low oxygen delivery may decrease proton leak. It has been suggested that mitochondrial proton leak may be reduced in four different ways (284). First is to alter the kinetics of proton leak, though this does not appear to occur even after several months of hypoxic submersion in frog skeletal muscle (284). The second is to alter mitochondrial membrane potential by changing electron transport efficiency or cellular ATP turnover. In perfused skeletal muscle, this is probably the most likely explanation, since alterations in oxygen delivery at the microvascular level will affect flux through the electron transport chain, and may also affect cellular ATP turnaround at more severe hypoxia. Finally, proton leak may be influenced by changing the volume density of mitochondria in relation to the cell, or the mitochondrial cristae surface area. During long term metabolic depression, such as that seen in estivating snails (135), remodelling of the phospholipid and protein content of the mitochondrial inner membrane of snail hepatopancreas appears to suppress membrane associated

processes, possibly including proton leak (287). However, type A and B vasoconstrictors affect oxygen delivery in the short term, and are not expected to affect mitochondrial inner membrane structure or composition.

It is therefore concluded that vasoconstrictor mediated metabolism is likely to be the result of varied oxygen delivery, and the subsequent regulation of flux through the electron transport chain. Improved oxygen delivery with type A vasoconstriction, will increase electron transport, and rates of coupled and uncoupled respiration proceed unhindered. One may speculate that the higher the rate of oxygen delivery, the greater the rate of mitochondrial proton leak. Once the immediate cellular requirements for ATP are met, oxygen consumption in excess of this requirement will drive proton motive force and the rate of proton leak. Alternatively, during low oxygen delivery (regional ischemia/hypoxia with type B vasoconstriction) uncoupled respiration will be the first component of oxygen consumption to be down-regulated, until oxygen delivery becomes so low that ATP production is also compromised. At this time, skeletal muscle fibers may assume a state of metabolic hibernation, preventing hypoxic damage.

7.3 Metabolic demand

7.3.1 Muscle $\dot{V}O_2$ stimulated by metabolic demand

Metabolic demand is usually the result of metabolic "stress". Stress may take the form of ionic or osmotic disequilibrium, or increased energy demand induced by cold exposure or muscular contraction. Homeostatic mechanisms are activated in response to these stresses, most of which require ATP. In order to match the increased demand, glycolytic and aerobic ATP production rates are elevated above basal. In the case of the sodium channel opener veratridine, muscle resting $\dot{V}O_2$ is elevated (291), while the sodium ionophore monensin increases basal glucose uptake (25), both in response to the increased demand for ATP-dependent sodium pumping. Similarly, raised intracellular calcium (resulting from KCl depolarization, caffeine, ryanodine, thapsigargin etc.) increases $\dot{V}O_2$ through increased ATP-dependent calcium pumping (52). Elevated rates of oxygen uptake observed during perfusion with hyper-tonic media (mannitol, glucose, or NaCl) (64; 179) may be the result of a similar phenomenon. Stimulation of cellular oxygen uptake in response to stress, is

the direct result of increased ATP demand. Observations in the perfused rat hindlimb, that the effects of type A vasoconstrictors were blocked by agents interfering with sodium permeability (291; 292), led the development of the hypothesis that type A vasoconstrictors may increase skeletal muscle $\dot{V}O_2$ by increasing the rate of ATP-dependent sodium pumping. Comparisons were made between type A vasoconstrictors, and veratridine.

Veratridine-stimulated metabolism displayed all of the characteristic changes in skeletal muscle metabolism one would predict when sodium cycling is directly involved. There were significant increases in resting oxygen uptake, and lactate efflux. These effects were abolished by low sodium medium, and by membrane stabilizers (291; 292). Veratridine-mediated metabolism was also abolished by addition of sodium channel inhibitors, and inhibitors of the Na^+/K^+-ATPase pump (Chapter 4), reflecting a direct relationship between ion cycling and cellular energy turnover. Furthermore, veratridine-stimulated metabolism resulted in a detectable plasma membrane depolarization of perfused skeletal fibers, which was accompanied by a significant decrease in freeze-clamped muscle PCr content (Chapter 5), consistent with increased ATP utilization. The stimulatory effects of increased sodium load on cellular metabolic rate were apparent in both perfused resting skeletal and cardiac muscle (Chapter 6). These findings support the idea that stimulated metabolism during veratridine infusion is the direct result of increased ATP demand by the Na^+/K^+-ATPase pump.

7.3.2 Vasoconstrictors do not increase metabolic demand

In contrast, the results obtained during type A vasoconstrictor-mediated metabolism are not entirely consistent with increased rates of ATP-dependent ion pumping. While low sodium medium, propranolol (291; 292) and ouabain (Chapter 4) were effective inhibitors of the type A vasoconstrictors in perfusion, this was not conclusive evidence that increased $\dot{V}O_2$ was the result of ATP-dependent sodium pumping. Data presented in Chapters 4, 5 & 6 offers firm evidence against this idea. First, failure of tetrodotoxin to block the type A effect in perfusion rules out the involvement of voltage gated sodium channels (Chapter 4). Second, no changes in skeletal muscle plasma membrane potential were detected during type A infusion

(Chapter 5). Third, type A vasoconstrictors do not deplete cellular energy stores (Chapter 5), in fact there is some evidence that cellular energy status may be enhanced in the presence of type A vasoconstrictors (300). Clearly, sodium cycling is not stimulated in skeletal muscle fibers under the impetus of type A vasoconstrictors. Finally, the type A vasoconstrictor effect was absent from perfused arrested heart. If the mechanism of type A vasoconstrictor-mediated thermogenesis was directly dependent on increased intracellular sodium, then an effect should have been apparent in perfused arrested heart. This was not the case. In summary, the evidence presented does not support a role for sodium cycling in skeletal muscle fibers during type A vasoconstrictor-mediated metabolism.

7.3.3 Unresolved issues

The inhibitory effects of low sodium medium, propranolol and ouabain on vasoconstrictor-metabolism remains a perplexing issue. Sodium cycling may still be an important aspect of type A mediated metabolism, though clearly not in the skeletal muscle fibers themselves. Conducted depolarization has been proposed by Segal et al. as a mechanism for transmission of vascular signals along the vascular tree during exercise and application of vasoactive substances (265; 267; 268; 270). Similarly, it is possible that redistribution of flow may be facilitated by a sodium dependent transduction mechanism in vascular smooth muscle during vasoconstrictor-mediated capillary recruitment. Agents that interfere with transduction of electrical signals in the vascular smooth muscle will not only stop the spread of the signal, but will also prevent sustained capillary recruitment.

Previously presented data (292) is now reconsidered in light of this revised opinion. In the original publication, the stimulatory effects of norepinephrine on hindlimb $\dot{V}O2$ were significantly inhibited by both (+) and (−) enantiomers of propranolol. The combination of 100μM (±) propranolol inhibited angiotensin II mediated $\dot{V}O2$ by 64%, though perfusion pressure was also inhibited around 30%. Though stated in the paper that propranolol had only "marginal" effects on angiotensin mediated vasoconstriction, these small changes in perfusion pressure may have been enough to impair vasoconstrictor-mediated capillary recruitment, and thus

redistribution of flow. Similarly, low sodium medium and ouabain may also have interfered with vascular cell signalling, thereby preventing transduction of electrical signals and redistribution of flow. However, tetrodotoxin would not be expected to interfere with this vascular transduction/ capillary recruitment process, since smooth muscle cells have been shown to carry tetrodotoxin-resistant sodium channels (296; 314).

A surrogate indicator of vasoconstrictor-mediated capillary recruitment, is the post equilibration red cell washout, where red cells trapped in the nutritive capillary network are swept out of the preparation during type A vasoconstrictor infusion (219). The apparent observation that propranolol did not interfere with angiotensin II mediated post-equilibration red cell washout (292) implies that vasoconstrictor-mediated redistribution occurs normally, even in the presence of a membrane stabilizer. However, closer inspection of this data reveals that angiotensin II mediated red cell washout is incomplete in the presence of propranolol, since a second smaller red cell washout was detected when propranolol infusion ceased. This suggests that propranolol had prevented complete access to the nutritive region, leaving some red cells trapped in the tissue. This region was only fully accessible by angiotensin II when the membrane-stabilizing agent had been removed, and conduction of the vascular signal was uninterrupted. It is concluded that the inhibitory effects of propranolol, ouabain and low sodium medium on vasoconstrictor-mediated metabolism result from impaired vascular recruitment and limitation of perfusate access, and not as previously suggested from inhibition of a cellular thermogenic mechanism.

One final issue that remains to be addressed is the possibility that muscle metabolism is enhanced by changes in local perfusate ion concentration during type A mediated recruitment of flow. That is, regions of the hindlimb that are less than optimally perfused during basal conditions may have reached a stage where ionic exchange rates have reached a relative state of equilibrium. The sudden opening of these capillaries will change not only flow rate and oxygen delivery, but also ionic and osmolar gradients between the vessel lumen and muscle fibers. It has been suggested that increased flow rate may increase the rate of K^+ exchange by perfused muscle (194), while hyperosmolar buffer has been shown to induce changes in vessel

diameter (204). Unpublished observations from this lab have noted the stimulatory effects of hypertonic or hyperosmolar perfusion media on muscle $\dot{V}O_2$, however these effects are generally slow in onset, and are quite small by comparison with type A vasoconstriction. The results from Chapter 3 demonstrate quite clearly that perfused muscle is highly responsive to changes in oxygen delivery under normo-osmotic conditions, since total flow and the ratio of nutritive to non-nutritive flow remained constant. Thus, the stimulatory type A vasoconstrictor effect is more likely to be related to changes in oxygen delivery, than ionic perturbance during capillary recruitment.

7.5 Summary

In summary, the regulatory influence of vasoconstrictors on perfused skeletal muscle metabolism is attributed to changes in microvascular oxygen delivery, and not activation of ATP consuming reactions. Oxygen delivery appears to be a major regulatory factor in the control of perfused rat hindlimb metabolic rate, and the heterogeneity of blood flow and oxygen delivery imposed by dual vascular pathways has profound effects on skeletal muscle metabolic rate. Utilization of this flow heterogeneity enables regulation of skeletal muscle metabolic rate. Setting a conservative ratio of nutritive blood flow in skeletal muscle, may contribute considerably to whole body energy conservation. However, the full thermogenic capacity of skeletal muscle is readily recruitable simply by enhancing the extent of nutritive perfusion. The increase in metabolism observed with type A vasoconstrictor-mediated redistribution of flow is therefore likely, to be the result of enhanced perfusate access ameliorating oxygen limitation. Alternatively, the decrease in perfused muscle metabolism with type B vasoconstriction is likely to be the result of decreased oxygen delivery and metabolic hibernation in the hypo-perfused regions of the perfused rat hindlimb.

APPENDIX

Figure 1

Effect of vasoconstrictors and microspheres on intra-muscular PCr/Cr, PCr/ATP and Energy Charge (EC) ratios as a function of $\dot{V}O_2$ of the constant-flow perfused rat hindlimb.

1.5×10^6 microsphere injection have been used. Treatments were Vehicle (O), Vehicle + MS (●), 1 μM 5-HT (Δ), 1 μM 5-HT + MS (▲), 5 nM AII ($\square$) and 5 nM AII + MS (■).

Reproduced with permission from Michelle Vincent,

[original figure appears in the paper Vincent, Rattigan et al. 1998 (300)]
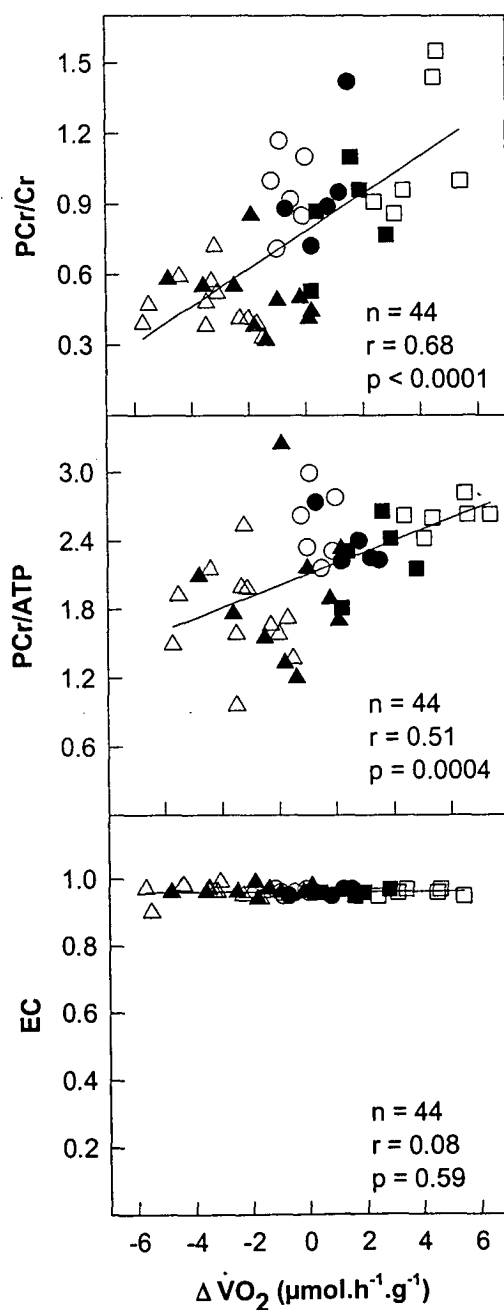
Figure 2

Effects of vehicle (○), NE (■) or 5-HT (▲) on the outflow-to-inflow (O/I) ratio of ^3H_2O in the perfused rat hindlimb at varying flow rates, n=8 for all conditions at all flow rates. Microdialysis flow rate was 2μl/min. Data were compared to 1.0 ml/min within each condition (#P<0.05), or to vehicle (*P<0.05). O/I ratio decreased as a function of increasing flow rate, NE potentiates the decrease, while 5-HT impedes the decrease. Figure reproduced with permission of John Newman, [original findings reported inNewman, Di Maria et al. 2001 (221)]
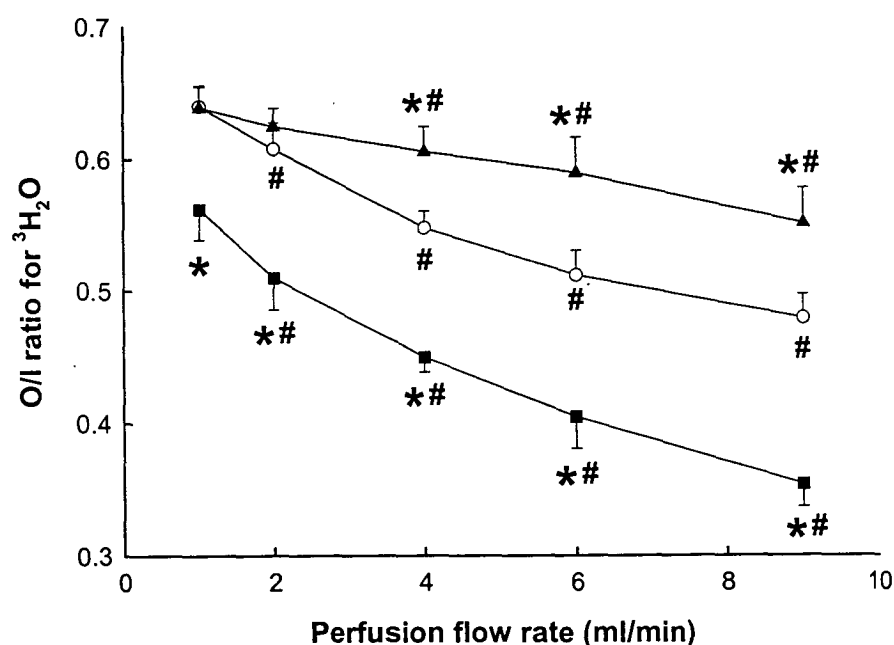
Figure 3

Microdialysis out/in ratios for ^3H_2O in the autoperfused anesthetized sheep heart

The same microdialysis technique used in the perfused rat hindlimb was applied to the beating heart of the anesthetized sheep. Microdialysis probe was 20mm long, and a flow through rate of 10 μl/min was used. Placement of flow probes around the left coronary circumflex artery and pulmonary artery enabled flow rate to be carefully monitored. Additions were either noradrenaline (n=6), sodium nitroprusside (n=3) or adenosine (n=5). The average regression lines for norepinephrine, nitroprusside and adenosine were not significantly different from each other. Graph reproduced with permission of Richard Hodgson, from Honours Thesis 2001.
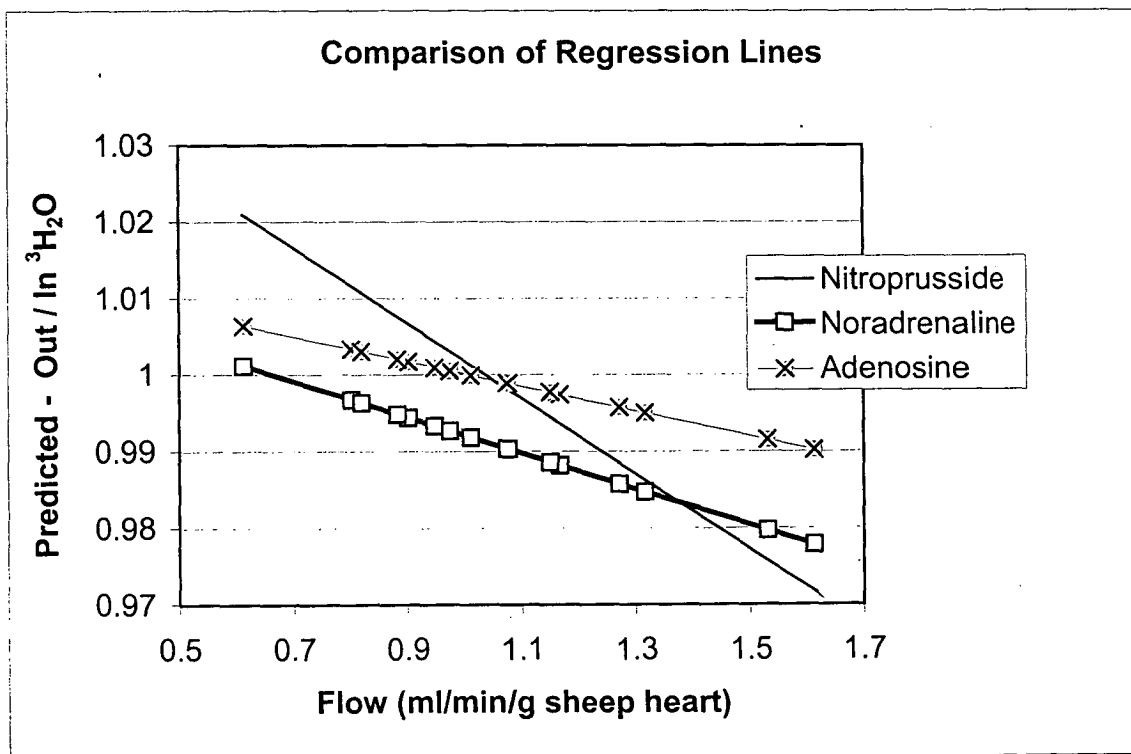
Reference List

1 Aass, H., T. Skomedal, and J. B. Osnes. Demonstration of an alpha adrenoceptor-mediated inotropic effect of norepinephrine in rabbit papillary muscle. *J.Pharmacol.Exp.Ther.* 226: 572-578, 1983.

2 Adams, R. P., L. A. Dieleman, and S. M. Cain. A critical value for O_2 transport in the rat. *J.Appl.Physiol.* 53: 660-664, 1982.

3 Andersson, B. S., T. Y. Aw, and D. P. Jones. Mitochondrial transmembrane potential and pH gradient during anoxia. *Am.J.Physiol.* 252: C349-C355, 1987.

4 Arch, J. R., A. T. Ainsworth, M. A. Cawthorne, V. Piercy, M. V. Sennitt, V. E. Thody, C. Wilson, and S. Wilson. Atypical beta-adrenoceptor on brown adipocytes as target for anti-obesity drugs. *Nature* 309: 163-165, 1984.

5 Arch, J. R., R. J. Bywater, K. A. Coney, R. D. Ellis, P. L. Thurlby, S. A. Smith, and C. Zed. Influences on body composition and mechanism of action of the beta- adrenoceptor agonist BRL26830A. In Lardy, H. and F. Stratman, eds. Hormones, Thermogenesis and Obesity. Elsevier Science Publishing Co. Inc. 1989, 465-476.

6 Arch, J. R., M. A. Cawthorne, K. A. Coney, B. A. Gusterson, V. Piercey, M. V. Sennitt, S. A. Smith, J. Wallace, and S. Wilson. Beta-adrenoceptor-mediated control of thermogenesis, body composition and glucose homeostasis. In Rothwell, N. J. and M. J. Stock, eds. Obesity and Cachexia. John Wiley & Sons Ltd. 1991, 241-268.

7 Arch, J. R. and A. J. Kaumann. Beta3 and atypical beta- adrenoceptors. *Med.Res.Rev.* 13: 663-729, 1993.

8 Arthur, P. G., J. J. Giles, and C. M. Wakeford. Protein Synthesis during oxygen conformance and severe hypoxia in the mouse muscle cell line C2C12. *Biochim.Biophys.Acta* 1475: 83-89, 2000.

9   Arthur, P. G., M. C. Hogan, D. E. Bebout, P. D. Wagner, and P. W. Hochachka. Modeling the effects of hypoxia on ATP turnover in exercising muscle. *J.Appl.Physiol.* 73: 737-742, 1992.

10   Astrup, A., J. Bülow, N. J. Christensen, and J. Madsen. Ephedrine-induced thermogenesis in man: no role for interscapular brown adipose tissue. *Clin.Sci.* 66: 179-186, 1984.

11   Astrup, A., J. Bülow, N. J. Christensen, J. Madsen, and F. Quaade. Facultive thermogenesis induced by carbohydrate: a skeletal muscle component mediated by epinephrine. *Am.J.Physiol.* 250: E226-E229, 1986.

12   Astrup, A., J. Bülow, J. Madsen, and N. J. Christensen. Contribution of BAT and skeletal muscle to thermogenesis induced by ephedrine in man. *Am.J.Physiol.* 248: E507-E515, 1985.

13   Astrup, A., C. Lundsgaard, J. Madsen, and N. J. Christensen. Enhanced thermogenic responsiveness during chronic ephedrine treatment in man. *Am.J.Clin.Nutr.* 42: 83-94, 1985.

14   Barclay, J. K. Hypothesis: local vascular regulation is a key to flow limited muscle function. *Can.J.Sport.Sci.* 15: 9-13, 1990.

15   Barlow, T. E. and A. L. Haigh. Dual circulation in skeletal muscle. *J Physiol (Lond)* 149: 18P-19P, 1959.

16   Barlow, T. E., A. L. Haigh, and D. N. Walder. A search for arteriovenous anastomoses in skeletal muscle. *Proc.Physiol.Soc.* 80P-81P, 1958.

17   Barlow, T. E., A. L. Haigh, and D. N. Walder. Evidence for two vascular pathways in skeletal muscle. *Clin Sci* 20: 367-385, 1961.

18   Barnes, W. S. Depressing effects of calcium antagonists on oxygen consumption in isolated skeletal muscle during potassium depolarization. *Can.J.Physiol.Pharmacol.* 66: 836-840, 1988.

19 Barré, H., L. Bailly, and J. L. Rouanet. Increased oxidative capacity in skeletal muscles from cold-acclimated ducklings : A comparison with rats. *Comp.Biochem.Physiol.* 88B: 519-522, 1987.

20 Barré, H., F. Cohen-Adad, and J. L. Rouanet. Two daily glucagon injections induce non-shivering thermogenesis in Muscovy ducklings. *Am.J.Physiol.* 252: E616-E620, 1987.

21 Barré, H., J. Nedergaard, and B. Cannon. Increased respiration in skeletal muscle mitochondria from cold-acclimated ducklings: Uncoupling effects of free fatty acids. *Comp.Biochem.Physiol.* 85B: 343-348, 1986.

22 Barré, H. and J. Rouanet. Calorigenic effect of glucagon and catecholamines in king penguin chicks. *Am.J.Physiol.* 244: R758-R763, 1983.

23 Bianchi, C. P., S. Narayan, and N. Lakshminarayanaiah. Mobilization of muscle calcium and oxygen uptake in skeletal muscle. pp. 503-15. *In: Carafoli.E., et.al., ed.Calcium transport.in contraction.and.secretion.Amsterdam., North-Holland.,* : 1975.

24 Bianchi, C. Conformation State of the ryanodine receptor and functional effects of ryanodine on skeletal muscle. *Biochem.Pharmacol.* 53: 909-912, 1997.

25 Bihler, I., P. C. Sawh, and P. Charles. Stimulation of glucose transport in skeletal muscle by the sodium ionophore monensin. *Biochim.Biophys.Acta* 8212: 30-36, 1985.

26 Biron, R., A. Burger, A. Chinet, T. Clausen, and R. Dubois-Ferriére. Thyroid hormones and the energetics of active sodium-potassium transport in mammalian skeletal muscles. *J Physiol (Lond)* 297: 47-60, 1979.

27 Block, B. A. Billfish brain and eye heater: A new look at nonshivering heat production. *News Physiol.Sci.* 2: 208-213, 1987.

28 Block, B. A. Thermogenesis in muscle. *Annu.Rev.Physiol.* 56: 535-577, 1994.

29 Board, M., P. Doyle, and M. A. Cawthorne. BRL37344, but not CGP12177, stimulates fuel oxidation by soleus muscle in vitro. *Eur.J.Pharmacol.* 406: 33-40, 2000.

30 Borgström, P., L. Lindbom, K. E. Arfors, and M. Intaglietta. Beta-adrenergic control of resistance in individual vessels in rabbit tenuissimus muscle. *Am.J.Physiol.* 254: H631-H635, 1988.

31 Boss, O., T. Hagan, and B. Lowell. Uncoupling proteins 2 and 3 Potential regulators of mitochondrial energy metabolism. *Diabetes* 49: 143-156, 2000.

32 Boss, O., S. Samec, F. Kuhne, P. Bijlenga, F. Assimacopoulos-Jeannet, J. Seydoux, J. P. Giacobino, and P. Muzzin. Uncoupling protein-3 expression in rodent skeletal muscle is modulated by food intake but not by changes in environmental temperature. *J Biol Chem.* 273: 5-8, 1998.

33 Boss, O., S. Samec, A. Paoloni-Giacobino, C. Rossier, A. Dulloo, J. Seydoux, P. Muzzin, and J. P. Giacobino. Uncoupling protein-3: a new member of the mitochondrial carrier family with tissue-specific expression. *FEBS Lett.* 408: 39-42, 1997.

34 Bourhim, M., H. Barré, S. Oufara, Y. Minaire, J. Chatonnet, F. Cohen-Ada, and J. L. Rouanet. Increase in cytochrome oxidase capacity of BAT and other tissues in cold- acclimated gerbils. *Am.J.Physiol.* 258: R1291-R1298, 1990.

35 Brand, M. D., K. M. Brindle, J. A. Buckingham, J. A. Harper, D. F. Rolfe, and J. A. Stuart. The significance and mechanism of mitochondrial proton conductance. *Int.J.Obes.Relat Metab Disord.* 23 Suppl 6:S4-11: S4-11, 1999.

36 Brand, M. D., L. F. Chien, and P. Diolez. Experimental discrimination between proton leak and redox slip during mithochondrial electron transport. *Biochem.J.* 297: 27-29, 1994.

37 Brand, M. D., L. Chien, E. K. Ainscow, D. F. S. Rolfe, and R. Porter. The causes and functions of mitochondrial proton leak. *Biochim.Biophys.Acta* 1187: 132-139, 1994.

38 Buck, L. T. and P. W. Hochachka. Anoxic suppression of Na(+)-K(+)-ATPase and constant membrane potential in hepatocytes: support for channel arrest. *Am J Physiol* 265: R1020-R1025, 1993.

39 Budinger, G., N. Chandel, Z. Shao, C. Li, A. Melmed, L. Becker, and P. Schumacker. Cellular energy utilization and supply during hypoxia in embryonic cardiac myocytes. *Am.J.Physiol.* 270: L44-L53, 1996.

40 Cadenas, S., J. A. Buckingham, S. Samec, J. Seydoux, N. Din, A. G. Dulloo, and M. D. Brand. UCP2 and UCP3 rise in starved rat skeletal muscle but mitochondrial proton conductance is unchanged. *FEBS Lett.* 462: 257-260, 1999.

41 Cannon, B., V. Golozoubova, A. Matthias, K. Ohlson, A. Jacobsson, and J. Nedergaard. Is there life in the cold without UCP1? Uncoupling proteins and thermoregulatory thermogenesis. In Heldmaier, G. and M. Klingensper, eds. Life in the cold. 2000, 387-400.

42 Cannon, B., J. Houstek, and J. Nedergaard. Brown adipose tissue. More than an effector of thermogenesis? *Ann N Y Acad Sci* 856:171-87: 171-187, 1998.

43 Cannon, B. and J. Nedergaard. Nonshivering thermogenesis and brown adipose tissue. In Blatteis, C. M., ed. Physiology and pathophysiology of temperature regulation. Singapore, World Scientific. 1998, 63-77.

44 Casey, T. and P. G. Arthur. Hibernation in noncontracting mammalian cardiomyocytes. *Circulation* 102: 3124-3129, 2000.

45 Catterall, W. A. Cellular and molecular biology of voltage-gated sodium channels. *Physiol Rev* 72: S15-S48, 1992.

46 Cawthorne, M. A., M. V. Sennitt, J. R. Arch, and S. A. Smith. BRL 35135, a potent and selective atypical beta-adrenoceptor agonist. *Am.J.Clin.Nutr.* 55: 252S-257S, 1992.

47 Challiss, R. A., B. Leighton, S. Wilson, P. L. Thurlby, and J. R. Arch. An investigation of the beta-adrenoceptor that mediates metabolic responses to the novel agonist BRL28410 in rat soleus muscle. *Biochem.Pharmacol.* 37: 947-950, 1988.

48 Chinet, A. Control of respiration in skeletal muscle at rest. *Experientia* 46: 1194-1196, 1990.

49 Chinet, A. Ca(2+)-dependent heat production by rat skeletal muscle in hypertonic media depends on Na(+)-Cl- co-transport stimulation. *J.Physiol.(Lond.)* 461: 689-703, 1993.

50 Chinet, A. and T. Clausen. Energetics of active sodium-potassium transport following stimulation with insulin, adrenaline or salbutamol in rat soleus muscle. *Eur.J.Physiol.* 401: 160-166, 1984.

51 Chinet, A., T. Clausen, and L. Girardier. Microcalorimetric determination of energy expenditure due to active sodium-potassium transport in the soleus muscle and brown adipose tissue of the rat. *J.Physiol.* 265: 43-61, 1977.

52 Chinet, A., A. Decrouy, and P. C. Even. Ca2+-dependent heat production under basal and near-basal conditions in the mouse soleus muscle. *J.Physiol.* 455: 663-678, 1992.

53 Chinet, A. E. and J. Mejsnar. Is resting muscle oxygen uptake controlled by oxygen availability to cells? *J.Appl.Physiol.* 66: 253-260, 1989.

54 Clapham, J. C., J. R. Arch, H. Chapman, A. Haynes, C. Lister, G. B. Moore, V. Piercy, S. A. Carter, I. Lehner, S. A. Smith, L. J. Beeley, R. J. Godden, N. Herrity, M. Skehel, K. K. Changani, P. D. Hockings, D. G. Reid, S. M. Squires, J. Hatcher, B. Trail, J. Latcham, S. Rastan, A. J. Harper, S. Cadenas, J. A.

Buckingham, M. D. Brand, and A. Abuin. Mice overexpressing human uncoupling protein-3 in skeletal muscle are hyperphagic and lean. *Nature* 406: 415-418, 2000.

55   Clark, A. D. H., J. M. Youd, S. Rattigan, E. J. Barrett, and M. G. Clark. Heterogeneity of laser Doppler flowmetry in perfused muscle indicative of nutritive and nonnutritive flow. *Am J Physiol* 280: H1324-H1333, 2001.

56   Clark, M. G., A. D. H. Clark, and S. Rattigan. Failure of laser Doppler signal to correlate with total flow in muscle: Is this a question of vessel architecture? *Microvasc.Res.* 60: 294-301, 2000.

57   Clark, M. G. and E. Q. Colquhoun. Hot pipes. *Today's Life Sci.* 3: 12-22, 1991.

58   Clark, M. G., E. Q. Colquhoun, K. A. Dora, S. Rattigan, T. P. D. Eldershaw, J. L. Hall, A. Matthias, and J. M. Ye. Resting muscle: A source of thermogenesis controlled by vasomodulators. In Milton, A. S., ed. Temperature Regulation: Recent physiological and pharmacological advances. Basel, Birkhauser Verlag. 1994, 355-320.

59   Clark, M. G., E. Q. Colquhoun, S. Rattigan, K. A. Dora, T. P. Eldershaw, J. L. Hall, and J. Ye. Vascular and endocrine control of muscle metabolism. *Am.J.Physiol.* 268: E797-E812, 1995.

60   Clark, M. G., J. M. Newman, and A. D. Clark. Microvascular regulation of muscle metabolism. *Curr.Opin.Clin.Nutr.Metab.Care* 1: 205-210, 1998.

61   Clark, M. G., S. Rattigan, L. H. Clerk, M. A. Vincent, A. D. Clark, J. M. Youd, and J. M. Newman. Nutritive and non-nutritive blood flow: rest and exercise. *Acta Physiol Scand* 168: 519-530, 2000.

62   Clark, M. G., S. Rattigan, K. A. Dora, J. M. B. Newman, J. T. Steen, K. A. Miller, and M. A. Vincent. Vascular and metabolic regulation of muscle. In Kinney, J. M. and H. N. Tucker, eds. Physiology, Stress, and Malnutrition:

Functional Correlates, Nutritional Intervention. New York, Lippincott-Raven. 1997, 325-346.

63 Clark, M. G., S. M. Richards, M. Hettiarachchi, J. Ye, G. J. Appleby, S. Rattigan, and E. Q. Colquhoun. Release of purine and pyrimidine nucleosides and their catabolites from the perfused rat hindlimb in response to noradrenaline, vasopressin, angiotensin II and sciatic-nerve stimulation. *Biochem.J.* 266: 765-770, 1990.

64 Clausen, T. The effect of insulin on glucose transport in muscle cells. *Curr.Top.Memb.Transp.* 6: 169-226, 1975.

65 Clausen, T. Regulation of active Na+-K+ transport in skeletal muscle. *Physiol.Rev.* 66: 542-580, 1986.

66 Clausen, T. Significance of Na+-K+ pump regulation in skeletal muscle. *News Physiol.Sci.* 5: 148-151, 1990.

67 Clausen, T. Long- and short-term regulation of the Na+-K+ pump in skeletal muscle. *News in Physiol.Sci.* 11: 24-30, 1996.

68 Clausen, T. and M. E. Everts. Regulation of the Na,K-pump in skeletal muscle. *Kidney Int.* 35: 1-13, 1989.

69 Clausen, T. and J. A. Flatman. The effect of catecholamines on rat Na-K transport and membrane potential in rat soleus muscle. *J.Physiol.* 270: 383-414, 1977.

70 Clausen, T. and J. A. Flatman. Effects of insulin and epinephrine on Na+-Ka+ and glucose transport in soleus muscle. *Am.J.Physiol.* 252: E492-E499, 1987.

71 Clausen, T. and O. Hansen. The Na+-K+-pump, energy metabolism, and obesity. *Biochem.Biophys.Res.Comm.* 104: 357-362, 1982.

72 Clausen, T., O. Hansen, K. Kjeldsen, and A. Nørgaard. Effect of age, potassium depletion and denervation on specific displaceable [3H]ouabain binding in rat skeletal muscle in vivo. *J.Physiol.(Lond)* 333:367-81: 367-381, 1982.

73 Clausen, T. and P. G. Kohn. The effect of insulin on the transport of sodium and potassium in rat soleus muscle. *J.Physiol.(Lond)* 265: 19-42, 1977.

74 Clausen, T. and O. B. Nielsen. The Na+,K+ pump and muscle contractility. *Acta Physiol.Scand.* 152: 365-373, 1994.

75 Clausen, T., O. B. Nielsen, A. P. Harrison, J. A. Flatman, and K. Overgaard. The Na+,K+ pump and muscle excitability. *Acta Physiol.Scand.* 162: 183-190, 1998.

76 Clausen, T., C. Van Hardeveld, and M. E. Everts. Significance of cation transport in control of energy metabolism and thermogenesis. *Physiol.Rev.* 71: 733-774, 1991.

77 Colquhoun, E. Q. and M. G. Clark. Open question: has thermogenesis in muscle been overlooked and misinterpreted? *News Physiol.Sci.* 6: 256-259, 1991.

78 Colquhoun, E. Q., M. Hettiarachchi, J. M. Ye, S. Rattigan, and M. G. Clark. Inhibition by vasodilators of noradrenaline and vasoconstrictor-mediated, but not skeletal muscle contraction-induced oxygen uptake in the perfused rat hindlimb; implications for non-shivering thermogenesis in muscle tissue. *Gen.Pharmacol.* 21: 141-148, 1990.

79 Colquhoun, E. Q., M. Hettiarachchi, J. M. Ye, E. A. Richter, A. J. Hniat, S. Rattigan, and M. G. Clark. Vasopressin and angiotensin II stimulate oxygen uptake in the perfused rat hindlimb. *Life Sci.* 43: 1747-1754, 1988.

80 Connett, R. J., T. E. Gayeski, and C. R. Honig. Lactate accumulation in fully aerobic, working, dog gracilis muscle. *Am.J.Physiol.* 246: H120-H128, 1984.

81 Connett, R. J., T. E. Gayeski, and C. R. Honig. Lactate efflux is unrelated to intracellular PO2 in a working red muscle in situ. *J.Appl.Physiol.* 61: 402-408, 1986.

82 Cortright, R. N., D. Zheng, J. P. Jones, J. D. Fluckey, S. E. DiCarlo, D. Grujic, B. B. Lowell, and G. L. Dohm. Regulation of skeletal muscle UCP-2 and UCP-3 gene expression by exercise and denervation. *Am J Physiol* 276: E217-E221, 1999.

83 Coté, C., M. C. Thibault, and J. Vallieres. Effect of endurance training and chronic isoproterenol treatment on skeletal muscle sensitivity to norepinephrine. *Life Sci.* 37: 695-701, 1985.

84 Cottle, W. H. and L. D. Carlson. Regulation of heat production in cold-adapted rats. *Proc.Soc.Exp.Biol.Med.* 92: 845-849, 1956.

85 Cox, J. P. and C. L. Gibbs. Skeletal muscle resting metabolism in cold-acclimated rats: effect of age, noradrenaline and hyperosmolarity. *Clin.Exp.Pharmacol.Physiol.* 24: 403-407, 1997.

86 Creese, R. Sodium fluxes in diaphragm muscle and the effects of insulin and serum proteins. *J Physiol (Lond)* 197: 255-278, 1968.

87 Dauncey, M. J. and K. Burton. 3H-ouabain binding sites in porcine skeletal muscle as influenced by environmental temperature and energy intake. *Pflugers Arch.* 414: 317-323, 1989.

88 De Luise, M. and M. Harker. Skeletal muscle metabolism: effect of age, obesity, thyroid and nutritional status. *Horm.Metab.Res.* 21: 410-415, 1989.

89 de Meis, L. ATP synthesis and heat production during Ca(2+) efflux by sarcoplasmic reticulum Ca(2+)-ATPase. *Biochem.Biophys.Res.Commun.* 276: 35-39, 2000.

90 Doll, C. J., P. W. Hochachka, and PB. Reiner. Channel arrest: implications from membrane resistance in turtle neurons. *Am.J.Physiol.* 261: R1321-R1324, 1991.

91 Doll, C. J., P. W. Hochachka, and PB. Reiner. Reduced ionic conductance in turtle brain. *Am.J.Physiol.* 265: R929-R933, 1993.

92 Donohoe, J. A., F. L. Rosenfeldt, C. M. Munsch, and J. F. Williams. The effect of orotic acid treatment on the energy and carbohydrate metabolism of the hypertrophying rat heart. *Int.J.Biochem.* 25: 163-182, 1993.

93 Donohoe, P., T. West, and R. Boutilier. Factors affecting membrane permeability and ionic homeostasis in the cold-submerged frog. *J.Exp.Biol.* 203: 405-414, 2000.

94 Dora, K. A., E. Q. Colquhoun, M. Hettiarachchi, S. Rattigan, and M. G. Clark. The apparent absence of serotonin-mediated vascular thermogenesis in perfused rat hindlimb may result from vascular shunting. *Life Sci.* 48: 1555-1564, 1991.

95 Dora, K. A., S. Rattigan, E. Q. Colquhoun, and M. G. Clark. Aerobic muscle contraction impaired by serotonin-mediated vasoconstriction. *J.Appl.Physiol* 77: 277-284, 1994.

96 Dora, K. A., S. M. Richards, S. Rattigan, E. Q. Colquhoun, and M. G. Clark. Serotonin and norepinephrine vasoconstriction in rat hindlimb have different oxygen requirements. *Am.J.Physiol.* 262: H698-H703, 1992.

97 Dubois-Ferriére, R. and A. E. Chinet. Contribution of skeletal muscle to the regulatory non-shivering thermogenesis in small mammals. *Pflugers Arch.* 390: 224-229, 1981.

98 Duchamp, C. and H. Barré. Skeletal muscle as the major site of nonshivering thermogenesis in cold-acclimated ducklings. *Am.J.Physiol.* 265: R1076-R1083, 1993.

99 Duchamp, C., J. Chatonnet, A. Dittmar, and H. Barré. Increased role of skeletal muscle in the calorigenic response to glucagon of cold-acclimated ducklings. *Am.J.Physiol.* 265: R1084-R1091, 1993.

100 Dulloo, A. G., N. Mensi, J. Seydoux, and L. Girardier. Differential effects of high-fat diets varying in fatty acid composition on the efficiency of lean and fat tissue deposition during weight recovery after low food intake. *Metabolism* 44: 273-279, 1995.

101 Dulloo, A. G. and S. Samec. Uncoupling Proteins : Do They Have a Role in Body Weight Regulation? *News Physiol.Sci.* 15: 313-318, 2000.

102 Dumonteil, E., H. Barré, and G. Meissner. Sarcoplasmic reticulum Ca2+-ATPase and ryanodine receptor in cold-acclimated ducklings and thermogenesis. *Am.J.Physiol.* 265: C507-C513, 1993.

103 Duran, W. N. and E. M. Renkin. Oxygen consumption and blood flow in resting mammalian skeletal muscle. *Am.J.Physiol.* 226: 173-177, 1974.

104 Eaton, R. P. and M. Vaughan. Catecholamine stimulation of oxygen consumption in vitro. *Fed.Proc.* 23: -270, 1964.

105 Edwards, R., P. Lutz, and D. G. Baden. Relationship between energy expenditure and ion channel density in the turtle and rat brain. *Am.J.Physiol.* 257: R1353-R1358, 1989.

106 Eldershaw, T. P., C. Duchamp, J. Ye, M. G. Clark, and E. Q. Colquhoun. Potential for non-shivering thermogenesis in perfused chicken (Gallus domesticus) muscle. *Comp.Biochem.Physiol.A.Physiol.* 117: 545-554, 1997.

107 Enerbäck, S., A. Jacobsson, E. M. Simpson, C. Guerra, H. Yamashita, M. E. Harper, and L. P. Kozak. Mice lacking mitochondrial uncoupling protein are cold-sensitive but not obese. *Nature* 387: 90-94, 1997.

108 Enocksson, S., M. Shimizu, F. Lönnqvist, J. Nordenström, and P. Arner. Demonstration of an in vivo functional β_3-adrenoceptor in man. *J.Clin.Invest.* 95: 2239-2245, 1995.

109 Everts, M. E. and C. Van Hardeveld. Effects of dantrolene on force development in slow- and fast-twitch muscle of euthyroid, hypothyroid, and hyperthyroid rats. *Br.J.Pharmacol.* 92: 47-54, 1987.

110 Everts, M. E., C. Van Hardeveld, H. E. Ter Keurs, and A. A. Kassenaar. Force development and metabolism in skeletal muscle of euthyroid and hypothyroid rats. *Acta Endocrinol.* 97: 221-225, 1981.

111 Ewart, H. S. and A. Klip. Hormonal regulation of the Na+-K+- ATPase: mechanisms underlying rapid and sustained changes in pump activity. *Am.J.Physiol.* 269: C295-C311, 1995.

112 Fagher, B., H. Liedholm, A. Sjögren, and M. Monti. Effects of terbutaline on basal thermogenesis of human skeletal muscle and Na-K pump after 1 week of oral use - a placebo controlled comparison with propranolol. *Br.J.Clin.Pharmac.* 35: 629-635, 1993.

113 Fagher, B., A. Sjögren, and M. Monti. A microcalorimetic study of the sodium-potassium-pump and thermogenesis in human skeletal muscle. *Acta Physiol.Scand.* 131: 355-360, 1987.

114 Faller, D. Endothelial cell responses to hypoxic stress. *Clin.Exp.Pharmacol.Physiol.* 26: 74-84, 1999.

115 Fleury, C., M. Neverova, S. Collins, S. Raimbault, O. Champigny, C. Levi-Meyrueis, F. Bouillaud, M. F. Seldin, R. S. Surwit, D. Ricquier, and C. H. Warden. Uncoupling protein-2: a novel gene linked to obesity and hyperinsulinemia. *Nat.Genet.* 15: 269-272, 1997.

116 Foster, D. O. Auxiliary role of alpha adrenoceptors in brown adipose tissue thermogenesis. In Hales, J. R., ed. Thermal Physiology. Raven Press New York. 1984, 201-204.

117 Foster, D. O. and M. L. Frydman. Comparison of microspheres and 86Rb+ as tracers of the distribution of cardiac output in rats indicates invalidity of 86Rb+-based measurements. *Can.J.Physiol.Pharmacol.* 56: 97-109, 1978.

118 Foster, D. O. and M. L. Frydman. Nonshivering thermogenesis in the rat. II. Measurements of blood flow with microspheres point to brown adipose tissue as the dominant site of the calorigenesis induced by norepinephrine. *Can.J.Physiol.Pharmacol.* 56: 110-122, 1979.

119 Foster, D. O. and M. L. Frydman. Tissue distribution of cold- induced thermogenesis in conscious warm- or cold-acclimated rats reevaluated from changes in tissue blood flow: The dominant role of brown adipose tissue in the replacement of shivering etc. *Can.J.Physiol.Pharmacol.* 57: 257-270, 1979.

120 Frelin, C., P. Vigne, and M. Lazdunski. Na+ channels with high and low affinity tetrodotoxin binding sites in the mammalian skeletal muscle cell. Difference in functional properties and
sequential appearance during rat skeletal myogenesis. *J.Biol.Chem.* 258: 7256-7259, 1983.

121 Glynn, I. M. and J. B. Chappell. A simple method for the preparation of 32P-labelled adenosine triphosphate of high specific activity. *Biochem.J.* 90: 147-149, 1964.

122 Gnaiger, E., G. Méndez, and S. Hand. High phosphorylation efficiency and dpression of uncoupled respiration in mitochondria under hypoxia. *PNAS* 97: 11080-11085, 2000.

123 Golozoubova, V., E. Hohtola, A. Matthias, A. Jacobsson, B. Cannon, and J. Nedergaard. Only UCP-1 can mediate adaptive nonshivering thermogenesis in the cold. *FASEB J.* 15: 2048-2050, 2001.

124 Gong, D. W., Y. He, M. Karas, and M. Reitman. Uncoupling protein-3 is a mediator of thermogenesis regulated by thyroid hormone, beta3-adrenergic agonists, and leptin. *J.Biol.Chem.* 272: 24129-24132, 1997.

125 Gong, D. and S. Monemdjou. Lack of obesity and normal response to fasting and thyroid hormone in mice lacking uncoupling protein-3. *J.Biol.Chem.* 275: 16251-16257, 2000.

126 Granger, H. J., A. H. Goodman, and D. N. Granger. Role of resistance and exchange vessels in local microvascular control of skeletal muscle oxygenation in the dog. *Circ.Res.* 38: 379-385, 1976.

127 Grant, R. T. and H. P. Wright. Anatomical basis for non-nutritive circulation in skeletal muscle exemplified by blood vessels of rat biceps femoris tendon. *J Anat.* 106: 125-133, 1970.

128 Gregg, V. A. and L. P. Milligan. Inhibition by ouabain of the O2 consumption of mouse (Mus musculus) soleus and diaphragm muscles. *Gen.Pharmacol.* 11: 323-325, 1980.

129 Grieb, P., P. Pape, R. Forster, C. Goodwin, S. Nioka, and L. Labbatte. Oxygen exchanges between blood and resting msucle: a shunt-sink hypothesis. *Adv.Exp.Med.Biol.* 191: 309-322, 1983.

130 Gronert, G. A. Malignant hyperthermia. In Miller, R. D., ed. Anesthesia. Churchill Livingstone New York. 1986, 1971-1994.

131 Grubb, B. and G. E. Folk. Effect of cold acclimation on norepinephrine stimulated oxygen consumption in muscle. *J.Comp.Physiol.* 110: 217-226, 1976.

132 Grubb, B. and G. E. Folk. The role of adrenoceptors in norepinephrine-stimulated VO2 in muscle. *Eur.J.Pharmacol.* 43: 217-223, 1977.

133 Grubb, B. and G. E. Folk. Skeletal muscle VO2 in rat and lemming: Effect of blood flow rate. *J.Comp.Physiol.* 128: 185-188, 1978.

134 Guernsey, D. L. and E. D. Stevens. The cell membrane sodium pump as a mechanism for increasing thermogenesis during cold acclimation in rats. *Science* 196: 908-910, 1977.

135 Guppy, M., D. C. Reeves, T. Bishop, P. Withers, J. A. Buckingham, and M. D. Brand. Intrinsic metabolic depression in cells isolated from the hepatopancreas of estivating snails. *FASEB J.* 14: 999-1004, 2000.

136 Gutierrez, G., R. J. Pohil, J. M. Andry, R. Strong, and P. Narayana. Bioenergetics of rabbit skeletal muscle during hypoxemia and ischemia. *J.Appl.Physiol.* 65: 608-616, 1988.

137 Gutierrez, G., R. J. Pohil, and P. Narayana. Skeletal muscle O2 consumption and energy metabolism during hypoxemia. *J.Appl.Physiol.* 66: 2117-2123, 1989.

138 Haimovich, B., J. C. Tanaka, and R. L. Barchi. Developmental appearance of sodium channel subtypes in rat skeletal muscle cultures. *J Neurochem.* 47: 1148-1153, 1986.

139 Hannon, J. P., E. Evonuk, and A. M. Larson. Some physiological and biochemical effects of norepinephrine in the cold-acclimatized rat. *Fed.Proc.* 22: 783-788, 1963.

140 Hansen, O. Interaction of cardiac glycosides with (Na+ + K+)-activated ATPase. A biochemical link to digitalis-induced inotropy. *Pharmacol.Rev.* 36: 143-163, 1984.

141 Hansen, O. and T. Clausen. Quantitative determination of Na+ -K+ -ATPase and other sarcolemmal components in muscle cells. *Am.J.Physiol.* 254: C1-C7, 1988.

142 Harper, J. A., J. A. Stuart, M. Jekabsons, D. Roussel, K. M. Brindle, K. Dickinson, R. Jones, and M. D. Brand. Artifactual uncoupling by uncoupling protein 3 in yeast mitochondria at the concentraions found in mouse and rat skeletal-muscle mitochondria. *Biochem.J.* 361: 45-56, 2002.

143 Harrison, A. P., T. Clausen, C. Duchamp, and M. J. Dauncey. Roles of skeletal muscle morphology and activity in determining Na+-K+-ATPase concentration in young pigs. *Am.J.Physiol.* Regulatory Integrative Comp. Physiol.: R102-R111, 1994.

144 Hettiarachchi, M., E. Q. Colquhoun, J. M. Ye, S. Rattigan, and M. G. Clark. Norephedrine (phenylpropanolamine) stimulates oxygen consumption and lactate production in the perfused rat hindlimb. *Int.J.Obesity* 15: 37-43, 1991.

145 Hettiarachchi, M., K. M. Parsons, S. M. Richards, K. M. Dora, S. Rattigan, E. Q. Colquhoun, and M. G. Clark. Vasoconstrictor-mediated release of lactate from the perfused rat hindlimb. *J.Appl.Physiol.* 73: 2544-2551, 1992.

146 Hill, A. and J. Howarth. The effect of potassium on the resting metabolism of the frog's sartorius. *Proc.R.Soc.Lond.* 147: 21-43, 1957.

147 Himms-Hagen, J. Cellular thermogenesis. *Annual Review of Physiology* Vol 38: 315-351, 1976.

148 Himms-Hagen, J. Thermogenesis in brown adipose tissue as an energy buffer. Implications for obesity. *N.Engl.J Med.* 311: 1549-1558, 1984.

149 Hirst, G. D. and F. R. Edwards. Sympathetic neuroeffector transmission in arteries and arterioles. *Physiol.Rev.* 69: 546-605, 1989.

150 Hissa, R. Controlling mechanisms in avian temperature regulation: a review. *Acta Physiol.Scand.* 132: 1-148, 1988.

151 Hochachka, P. W. Metabolic Arrest. *Intensive Care Med* 12: 127-133, 1986.

152 Hochachka, P. W., L. T. Buck, C. J. Doll, and S. C. Land. Unifying theory of hypoxia tolerance: molecular/metabolic defense and rescue mechanisms for surviving oxygen lack. *Proc Natl.Acad Sci U.S A.* 93: 9493-9498, 1996.

153 Hochachka, P. W. and M. Guppy. The time extension factor. Metabolic Arrest and the Control of Biological Time. Harvard Uni. Press. 1987, 1-9.

154 Hofmann, W., DS. Loiselle, C. Bearden, M. E. Harper, and L. Kozak. Effects of genetic background on thermoregulation and fatty acid-induced uncoupling of mitochondria in UCP-1 deficient mice. *J.Biol.Chem.* 276: 12460-12465, 2001.

155 Hogan, M. C., S. S. Kurdak, and P. G. Arthur. Effect of gradual reduction in O_2 delivery on intracellular homeostasis in contracting skeletal muscle. *J.Appl.Physiol.* 80: 1313-1321, 1996.

156 Hogan, M. C., R. S. Richardson, and S. S. Kurdak. Initial fall in skeletal muscle force development during ischemia is related to oxygen availability. *J.Appl.Physiol* 77: 2380-2384, 1994.

157 Hohtola, E., R. P. Henderson, and M. E. Rashotte. Shivering thermogenesis in the pigeon: a long-term electromyographic study on the effects of activity, diurnal factors, temperature and feeding state. 1996.

158 Hollenberg, N. K. Large and small vessel responses to serotonin in the peripheral circulation. *J.Cardiovasc.Pharmacol.* 7: S89-S91, 1985.

159 Holmgren, M., J. Wagg, F. Bezanilla, R. Rakowski, P. De Weer, and D. Gadsby. Three distinct and sequential steps in the release of sodium ions by the Na+/K+-ATPase. *Nature* 403: 898-901, 2000.

160 Honig, C. R., C. L. Odoroff, and J. L. Frierson. Active and passive capillary control in red muscle at rest and in exercise. *Am.J.Physiol.* 243: H196-H206, 1982.

161 Horstman, D. H., M. Gleser, and J. Delehunt. Effects of altering O2 delivery on VO2 of isolated, working muscle. *Am.J.Physiol* 230: 327-334, 1976.

162 Horwitz, B. A. and M. Eaton. Ouabain-sensitive liver and diaphragm respiration in cold-acclimated hamster. *J.Appl.Physiol.* 42: 150-153, 1977.

163 Hsieh, A. C. and L. D. Carlson. Role of adrenaline and noradrenaline in chemical regulation of heat production. *Am.J.Physiol.* 190: 243-246, 1957.

164 Hulbert, A. J. and P. L. Else. Membranes as possible pacemakers of metabolism. *J Theor.Biol.* 199: 257-274, 1999.

165 Idström, J. P., S. Harihara, B. Chance, T. Schersten, and A. C. Bylund-Fellenius. Oxygen dependence of energy metabolism in contracting and recovering rat skeletal muscle. *Am.J.Physiol.* 248: H40-H48, 1985.

166 Idström, J. P., V. H. Subramanian, B. Chance, T. Schersten, and Bylund-FelleniusAC. Biochemical and 31P-NMR studies of the energy metabolism in relation to oxygen supply in rat skeletal muscle during exercise. *Adv.Exp.Med.Biol.* 169: 489-496, 1984.

167 Idström, J. P., V. H. Subramanian, B. Chance, T. Schersten, and Bylund-FelleniusAC. Energy metabolism in relation to oxygen supply in contracting rat skeletal muscle. *Fed.Proc.* 45: 2937-2941, 1986.

168 Janský, L. Body organ thermogenesis of the rat during exposure to cold and at maximal metabolic rate. *Fed.Proc.* 25: 1297-1305, 1966.

169 Janský, L. Participation of body organs during nonshivering heat production. In Janský, L., ed. Nonshivering Thermogenesis. Swets & Zeitlinger N.V. Amsterdam. 1971, 159-172.

170   Janský, L. Non-shivering thermogenesis and its thermoregulatory significance. *Biol.Rev.* 48: 85-132, 1973.

171   Janský, L. Humoral thermogenesis and its role in maintaining energy balance. *Physiol.Rev.* 75: 237-259, 1995.

172   Janský, L. and J. S. Hart. Participation of skeletal muscle and kidney during nonshivering thermogenesis in cold-acclimated rats. *Can.J.Biochem.Physiol.* 41: 953-964, 1963.

173   Janský, L., Z. Votápková, and E. Feiglová. Total cytochrome oxidase activity of the brown fat and its thermogenic significance. *Physiol.Bohem.* 18: 443-451, 1969.

174   Janssen, I., S. Heymsfield, Z. Wang, and R. Ross. Skeletal muscle and distribution in 486 men and women aged 18-88 yr. *J.Appl.Physiol.* 89: 81-88, 2000.

175   Jarasch, E. D., G. Bruder, and H. W. Heid. Significance of xanthine oxidase in capillary endothelial cells. *Acta Physiol.Scand.* Suppl.548: 39-46, 1986.

176   Jobsis, F. F. and W. Stainsby. Oxidation of NADH during contractions of circulated mammalian skeletal muscle. *Resp.Phyisol.* 4: 292-300, 1968.

177   Kjeldsen, K., A. Nørgaard, and T. Clausen. Age-dependent changes in the number of [3H]ouabain-binding sites in rat soleus muscle. *Biochim.Biophys Acta* 686: 253-256, 1982.

178   Klitzman, B., D. N. Damon, R. J. Gorczynski, and B. R. Duling. Augmented tissue oxygen supply during striated muscle contraction in the hamster. Relative contributions of capillary recruitment, functional dilation, and reduced tissue PO2. *Circ.Res.* 51: 711-721, 1982.

179 Kobayashi, J., T. Osaka, S. Inoue, and S. Kimura. Thermogenesis induced by intravenous infusion of hypertonic solutions in the rat. *J.Physiol.* 535: 601-610, 2001.

180 Kohzuki, H., Y. Enoki, Y. Ohga, S. Sakata, S. Shimizu, T. Morimoto, T. Kishi, and M. Takaki. Effect of blood flow and haematocrit on the relationship between muscle venous PO2 and oxygen uptake in dog maximally contracting gastrocnemius in situ. *Clin.Exp.Pharmacol.Physiol.* 24: 182-187, 1997.

181 Kohzuki, H., Y. Enoki, Y. Ohga, S. Shimizu, and S. Sakata. Oxygen consumption in resting dog gracilis muscle perfused at varying oxygen delivery. *Japan.J.Physiol.* 41: 23-34, 1991.

182 Kohzuki, H., Y. Enoki, S. Sakata, S. Shimizu, and Y. Ohga. High affinity of blood for oxygen reduces oxygen uptake in contracting canine gracilis muscle. *Exp.Physiol.* 79: 71-80, 1994.

183 Kolář, F. and L. Janský. Oxygen consumption in rat skeletal muscle at various rates of oxygen delivery. *Experientia* 40: 353-354, 1984.

184 Kopecký, J., Z. Hodny, M. Rossmeisl, I. Syrovy, and L. P. Kozak. Reduction of dietary obesity in aP2-*Ucp* transgenic mice: Physiology and adipose tissue distribution. *Am.J.Physiol.* 270: E768-E775, 1996.

185 Kopecký, J., G. Clarke, S. Enerbäck, S. Spiegelman, and L. Kozak. Expression of the mitochondrial uncoupling protein gene from the aP2 gene promoter prevents genetic obesity. *J.Clin.Invest.* 96: 2914-2923, 1995.

186 Kozak, L. and M. E. Harper. Mitochondrial Uncoupling Proteins in Energy Expenditure. *Annu.Rev.Nutr.* 20: 339-363, 2000.

187 Lamping, K. G., H. Kanatsuka, C. L. Eastham, W. M. Chilian, and M. L. Marcus. Nonuniform vasomotor responses of the coronary microcirculation of serotonin and vasopressin. *Circ.Res.* 65: 343-351, 1989.

188   Lesna, I., S. Vybíral, L. Janský, and V. Zeman. Human nonshivering thermogenesis. *J.Therm.Biol.* 24: 63-69, 1999.

189   Li, K. and N. Sperelakis. Electrogenic Na-K pump current in rat skeletal myoballs. *J.Cell.Physiol.* 159: 181-186, 1994.

190   Lindberg, O. Brown Adipose Tissue. American Elsevier Publishing Co. New York. 1971.

191   Lindbom, L. and K. E. Arfors. Non-homogeneous blood flow distribution in the rabbit tenuissimus muscle Differential control of total blood flow and capillary perfusion. *Acta Physiol.Scand.* 122: 225-233, 1984.

192   Lindbom, L. and K. E. Arfors. Mechanism and site of control for variation in the number of perfused capillaries in skeletal muscle. *Int.J.Microcirc.Exp.* 4: 19-30, 1985.

193   Lindbom, L., R. F. Tuma, and K. E. Arfors. Influence of oxygen on perfused capillary density and capillary red cell velocity in rabbit skeletal muscle. *Microvasc Res* 19: 197-208, 1980.

194   Lindinger, M. I. and T. Hawke. Increased flow rate and papaverine increase K+ exchange in perfused rat hind-limb skeletal muscle. *Can.J.Physiol.Pharmacol.* 77: 536-543, 1999.

195   Lingrel, J. B. and T. Kuntzweiler. Minireview: Na+, K+-ATPase. *J.Biol.Chem.* 269: 19659-19662, 1994.

196   Liu, Y. L., M. A. Cawthorne, and M. J. Stock. Biphasic effects of the β-adrenoceptor agonist, BRL 37344, on glucose utilization in rat isolated skeletal muscle. *Br.J.Pharmacol.* 117: 1355-1361, 1996.

197   Lombard, J., M. Burke, S. Contney, W. Willems, and W. Stekiel. Effect of tetrodotoxin on membrane potentials and active tone in vascular smooth muscle. *Am.J.Physiol.* 242: H967-H972, 1982.

198 Lombet, A., C. Frelin, J. F. Renaud, and M. Lazdunski. Na+ channels with binding sites of high and low affinity for tetrodotoxin in different excitable and non-excitable cells. *Eur.J.Biochem.* 124: 199-203, 1982.

199 Lundholm, L. and N. Svedymr. Influence of adrenaline on blood flow and metabolism in the human forearm. *Acta Physiol.Scand.* 65: 344-351, 1965.

200 Ma, S. W. and D. O. Foster. Starvation-induced changes in metabolic rate, blood flow, and regional energy expenditure in rats. *Can.J.Physiol.Pharmacol.* 64: 1252-1258, 1986.

201 MacLennan, D. H. and M. S. Phillips. Malignant hyperthermia. *Science* 256: 789-794, 1992.

202 Marshall, J. M. Adenosine and muscle vasodilatation in acute systemic hypoxia. *Acta Physiol Scand.* 168: 561-573, 2000.

203 Martin, W. H., T. K. Tolley, and J. E. Saffitz. Autoradiographic delineation of skeletal muscle alpha1-adrenergic receptor distribution. *Am.J.Physiol.* 259: H1402-H1408, 1990.

204 Massett, M. P., A. Koller, and G. Kaley. Hyperosmolality dilates rat skeletal muscle arterioles: role of endothelial K(ATP) channels and daily exercise. *J.Appl.Physiol* 89: 2227-2234, 2000.

205 Matthias, A., K. Ohlson, M. Freriksson, A. Jacobsson, J. Nedergaard, and B. Cannon. Thermogenic responses in brown fat cells are fully UCP-1 dependent. *J.Biol.Chem.* 275: 25073-25081, 2000.

206 Matthias, A., A. Jacobsson, B. Cannon, and J. Nedergaard. The bioenergetics of brown fat mitochondria from UCP1-ablated mice. Ucp1 is not involved in fatty acid-induced de-energization ("uncoupling"). *J.Biol.Chem.* 274: 28150-28160, 1999.

207 Mejsnar, J. and L. Janský. Means of noradrenalin action during non-shivering thermogenesis in a single muscle. *Int.J.Biometeor.* 15: 321-324, 1971.

208 Mejsnar, J., F. Kolář, and J. Mala. Effects of noradrenaline and the blood perfusion rate on the oxygen consumption of intact and isolated muscles of cold-acclimated rats. *Physiol.Bohemoslovaca* 29: 151-160, 1980.

209 Mejsnar, J. A., M. J. Kushmerick, and D. L. Williams. Phosphocreatine and ATP concentrations increase during flow- stimulated metabolism in a non-contracting muscle. *Experientia* 48: 1125-1127, 1992.

210 Milner, R. E., S. Wilson, J. R. Arch, and P. Trayhurn. Acute effects of a beta-adrenoceptor agonist (BRL 26830A) on rat brown- adipose-tissue mitochondria. *Biochem.J.* 249: 759-763, 1988.

211 Monemdjou, S., W. Hofmann, L. Kozak, and M. E. Harper. Increased mitochondrial proton leak in skeletal muscle mitochondria of UCP1-deficient mice. *Am.J.Physiol.* 279: E941-E946, 2000.

212 Monemdjou, S., L. Kozak, and M. E. Harper. Mitochondrial proton leak in brown adipose tissue mitochondria of UCP1-deficient mice is GDP insensitive. *Am.J.Physiol.* 276: E1073-E1082, 1999.

213 Muller, A., C. Van Hardeveld, W. S. Simonides, and J. van Rijn. The elevation of sarcoplasmic reticulum Ca2+-ATPase levels by thyroid hormone in the L6 muscle cell line is potentiated by insulin-like growth factor-I. *Biochem.J.* 275: 35-40, 1991.

214 Nagase, I., T. Yoshida, K. Kumamoto, T. Umekawa, N. Sakane, H. Nikami, T. Kawada, and M. Saito. Expression of uncoupling protein in skeletal muscle and white fat of obese mice treated with thermogenic β3-adrenergic agonist. *J.Clin.Invest.* 97: 2898-2904, 1996.

215 Nakamura, Y., I. Nagase, A. Asano, N. Sasaki, T. Yoshida, T. Umekawa, N. Sakane, and M. Saito. β3-adrenergic agonist up-regulates uncoupling proteins 2 and 3 in skeletal muscle of the mouse. *J.Vet.Med.Sci.* 63: 309-314, 2001.

216 Nedergaard, J., V. Golozoubova, A. Matthias, A. Asadi, A. Jacobsson, and B. Cannon. UCP1: the only protein able to mediated adaptive non-shivering thermogenesis and metabolic inefficiency. *Biochim.Biophys.Acta* 1504: 82-106, 2001.

217 Nedergaard, J. and O. Lindberg. The brown fat cell. *Int.Rev.Cytol.* 74: 187-285, 1982.

218 Nedergaard, J., A. Matthias, V. Golozoubova, A. Jacobsson, and B. Cannon. UCP1: the original uncoupling protein--and perhaps the only one? New perspectives on UCP1, UCP2, and UCP3 in the light of the bioenergetics of the UCP1-ablated mice. *J.Bioenerg.Biomembr.* 31: 475-491, 1999.

219 Newman, J. M., K. A. Dora, S. Rattigan, S. J. Edwards, E. Q. Colquhoun, and M. G. Clark. Norepinephrine and serotonin vasoconstriction in rat hindlimb control different vascular flow routes. *Am.J.Physiol.* 270: E689-E699, 1996.

220 Newman, J. M., J. T. Steen, and M. G. Clark. Vessels supplying septa and tendons as functional shunts in perfused rat hindlimb. *Microvasc.Res.* 54: 49-57, 1997.

221 Newman, J. M. B., C. A. Di Maria, S. Rattigan, and M. G. Clark. Nutritive blood flow affects microdialysis O/I ratio for ^{14}C-ethanol and ^{3}H$_2$O in perfused rat hindlimb. *Am.J.Physiol.* 281: H2731-H2737, 2001.

222 Nicholls, D. G. and R. M. Locke. Thermogenic mechanisms in brown fat. *Physiol.Rev.* 64: 1-64, 1984.

223 Nicholls, D. and E. Rial. A history of the first uncoupling protein, UCP1. *J.Bioenerg.Biomemb.* 31: 399-406, 1999.

224 Nishimura, M., H. Awano, T. Hasegawa, O. Yagasaki, and K. Ito. Oxygen consumption stimulated by increases in permeability of Na+ of mouse diaphragm muscle in vitro. *Gen.Pharmac.* 22: 539-544, 1991.

225 Nobes, C., G. C. Brown, P. Olive, and M. D. Brand. Non-ohmic proton conductance of the mitochondrial inner membrane in hepatocytes. *J.Biol.Chem.* 265: 12903-12909, 1990.

226 Novotny, I. and F. Vyskocil. Possible role of Ca^{2+} ions in the resting metabolism of frog sartorius muscle during potassium depolarization. *J.Cell.Physiol.* 67: 159-168, 1966.

227 Ozaki, H., T. Kishimoto, S. Chihara, H. Umeno, and N. Urakawa. Action of the Na+ ionophore monensin on vascular smooth muscle of the guinea-pig aorta. *Eur.J.Pharmacol.* 100: 299-307, 1984.

228 Pappenheimer, J. R. Blood flow, arterial oxygen saturation, and oxygen consumption in the isolated perfused hindlimb of the dog. *J.Physiol.* 99: 283-303, 1941.

229 Pappenheimer, J. R. Vasoconstrictor nerves and oxygen consumption in the isolated perfused hindlimb muscles of the dog. *J.Physiol.* 99: 182-200, 1941.

230 Parks, D. A. and D. N. Granger. Xanthine oxidase: biochemistry, distribution and physiology. *Acta Physiol.Scand.* 548: 87-99, 1986.

231 Peng, Z. C., E. Q. Colquhoun, L. J. McLeod, and M. G. Clark. Noradrenaline and vasopressin stimulate oxygen consumption in perfused isolated rat tail and rabbit femoral arteries. *Proc.Aust.Biochem.Soc.* 22: -SP55, 1990.

232 Perez-Pinzon, M., C. Chan, M. Rosenthal, and T. Sick. Membrane and synaptic activity during anoxia in the isolated turtle cerebellum. *Am.J.Physiol.* 263: R1057-R1063, 1992.

233 Pfliegler, G., I. Szabo, and T. Kovacs. The influence of catecholamines on Na, -K transport in slow- and fast-twitch muscles of the rat. *Pflugers Arch.* 398: 236-240, 1983.

234 Rattigan, S., G. J. Appleby, K. A. Miller, J. T. Steen, K. A. Dora, E. Q. Colquhoun, and M. G. Clark. Serotonin inhibition of 1-methylxanthine metabolism parallels its vasoconstrictor activity and inhibition of oxygen uptake in perfused rat hindlimb. *Acta Physiol.Scand.* 161: 161-169, 1997.

235 Rattigan, S., K. A. Dora, E. Q. Colquhoun, and M. G. Clark. Serotonin-mediated acute insulin resistance in the perfused rat hindlimb but not in incubated muscle: a role for the vascular system. *Life Sci* 53: 1545-1555, 1993.

236 Rattigan, S., K. A. Dora, E. Q. Colquhoun, and M. G. Clark. Inhibition of insulin-mediated glucose uptake in rat hindlimb by an alpha-adrenergic vascular effect. *Am.J.Physiol* 268: E305-E311, 1995.

237 Rattigan, S., K. A. Dora, A. C. Y. Tong, and M. G. Clark. Perfused skeletal muscle contraction and metabolism improved by angiotensin II-mediated vasoconstriction. *Am.J.Physiol* 271: E96-103, 1996.

238 Renaud, J. F., T. Kazazoglou, A. Lombet, R. Chicherportiche, E. Jaimovich, G. S. Romey, and M. Lazdunski. The Na+ channel in mammalian cardiac cells. Two kinds of tetrodotoxin receptors in rat heart membranes. *J.Biol.Chem.* 258: 8799-8805, 1983.

239 Renkin, E. M. Exchangability of tissue potassium in skeletal muscle. *Am.J.Physiol.* 197: 1211-1215, 1959.

240 Renkin, E. M. The nutritional-shunt-flow hypothesis in skeletal muscle circulation. *Circ.Res.* 28: I21-I25, 1971.

241 Richards, S. M., M. G. Clark, E. Q. Colquhoun, and S. Rattigan. Re: Precursors of essential hypertension: pulmonary function, heart rate, uric acid, serum cholesterol, and other serum chemistries. *Am.J.Epidemiol.* 133: -753, 1991.

242 Richards, S. M., K. A. Dora, M. Hettiarachchi, S. Rattigan, E. Q. Colquhoun, and M. G. Clark. A close association between vasoconstrictor-mediated uracil and lactate release by the perfused rat hindlimb. *Gen.Pharmac.* 23: 65-69, 1992.

243 Richards, S. M., S. Rattigan, E. Q. Colquhoun, and M. G. Clark. [32P]phosphate autoradiography as an indicator of regional myocardial oxygen consumption? *J Mol Cell Cardiol.* 25: 289-302, 1993.

244 Richardson, R. S. What governs skeletal muscle VO_2 max? New evidence. *Med.Sci.Sports Exerc.* 32: 100-107, 2000.

245 Richardson, R. S., C. Harms, B. Grassi, and R. Hepple. Skeletal muscle:master or slave of the cardiovascular system. *Med.Sci.Sports Exerc.* 32: 89-93, 2000.

246 Richardson, R. S., J. Leigh, P. D. Wagner, and E. Noyszewski. Cellular PO2 as a determinant of maximal mitochondrial O2 consumption in trained human skeletal muscle. *J.Appl.Physiol.* 87: 325-331, 1999.

247 Richardson, R. S., K. Tagore, L. Haseler, M. Jordan, and P. D. Wagner. Increased VO_2max with right shifted Hb-O_2 dissociation curve at a constant O_2 delivery in dog muscle in situ. *J.Appl.Physiol.* 84: 995-1002, 1998.

248 Richter, E. A., L. Turcotte, P. Hespel, and B. Kiens. Metabolic response to exercise. Effect of endurance training and implications for diabetes. *Diabetes Care* 15: 1767-1776, 1992.

249 Ricquier, D. and F. Bouillaud. Mitochondrial uncoupling proteins: from mitochondria to the regulation of energy balance. *J.Physiol.* 529: 3-10, 2000.

250 Rogart, R. and L. Regan. Two subtypes of sodium channel with tetrodotoxin sensitivity and insensitivity detected in denervated mammalian skeletal muscle. *Brain Res.* 329(1-1): 314-318, 1985.

251 Rolfe, D. F. and M. D. Brand. Contribution of mitochondrial proton leak to skeletal muscle respiration and to standard metabolic rate. *Am.J.Physiol* 271: C1380-C1389, 1996.

252 Rolfe, D. F., J. M. Newman, J. A. Buckingham, M. G. Clark, and M. D. Brand. Contribution of mitochondrial proton leak to respiration rate in working skeletal muscle and liver and to SMR. *Am.J.Physiol* 276: C692-C699, 1999.

253 Rolfe, D. F. S. and M. D. Brand. Proton leak and control of oxidative phosphorylation in perfused, resting rat skeletal muscle. *Biochim.Biophys.Acta* 1276: 45-50, 1996.

254 Rolfe, D. F. S. and G. C. Brown. Cellular energy utilization and molecular origin of standard metabolic rate in mammals. *Physiol Rev* 77: 731-758, 1997.

255 Rose, R. W., N. Kuswanti, and E. Q. Colquhoun. Development of endothermy in a Tasmanian marsupial, Bettongia gaimardi and its response to cold and noradrenaline. *J.Comp.Physiol.* 168: 359-363, 1998.

256 Rose, R. W., A. K. West, J. M. Ye, G. McCormick, and E. Q. Colquhoun. Nonshivering thermogenesis in a marsupial (the tasmanian bettong Bettongia gaimardi) is not attributable to brown adipose tissue. *Physiol.Biochem.Soc.* 72: 699-704, 1999.

257 Rothwell, N. J. and M. J. Stock. A role for brown adipose diet-induced thermogenesis. *Nature* 281: 31-35, 1979.

258 Ruderman, N. B., C. R. Houghton, and R. Hems. Evaluation of the isolated perfused rat hindquarter for the study of muscle metabolism. *Biochem.J.* 124: 639-651, 1971.

259 Saarela, S., R. Hissa, A. Pyornila, R. Harjula, M. Ojanen, and M. Orell. Do birds possess brown adipose tissue? *Comp.Biochem.Physiol.* 92A: 219-228, 1989.

260 Saarela, S., J. S. Keith, E. Hohtola, and P. Trayhurn. Is the "mammalian" brown fat-specific mitochondrial uncoupling protein present in adipose tissues of birds? *Comp.Biochem.Physiol.* 100B: 45-49, 1991.

261 Samec, S., J. Seydoux, and A. G. Dulloo. Role of UCP homologues in skeletal muscles and brown adipose tissue: mediators of thermogenesis or regulators of lipids as fuel substrate? *FASEB J.* 12: 715-724, 1998.

262 Schlichtig, R., D. J. Kramer, and M. R. Pinsky. Flow redistribution during progressive hemorrhage is a determinant of critical O2 delivery. *J.Appl.Physiol.* 70: 169-178, 1991.

263 Schmitt, M., P. Meunier, A. Rochas, and J. Chatonnet. Catecholamines and oxygen uptake in dog skeletal muscle in situ. *Pflugers Arch.* 345: 145-158, 1973.

264 Schumacker, P., N. Chandel, and A. G. Agusti. Oxygen conformance of cellular respiration in hepatocytes. *Am.J.Physiol.* 265: L395-L402, 1993.

265 Segal, S. S. Microvascular recruitment in hamster striated muscle: role for conducted vasodilation. *Am.J.Physiol.* 261: H181-H189, 1991.

266 Segal, S. S. Communication among endothelial and smooth muscle cells co ordinates blood flow control during exercise. *NIPS* 7: 152-156, 1992.

267 Segal, S. S., D. N. Damon, and B. R. Duling. Propagation of vasomotor responses coordinates arteriolar resistances. *Am.J.Physiol.* 256: H832-H837, 1989.

268 Segal, S. S. and B. Duling. Communication between feed arteries and microvessels in hamster striated muscle: Segmental vascular responses are functionally co ordinated. *Circ.Res.* 59: 283-290, 1986.

269 Segal, S. S. and D. T. Kurjiaka. Coordination of blood flow control in the resistance vasculature of skeletal muscle. *Med.Sci.Sports Exerc.* 27: 1158-1164, 1995.

270 Segal, S. S. and T. O. Neild. Conducted depolarization in arteriole networks of the guinea-pig small intestine: effect of branching of signal dissipation. *J.Physiol.* 496: 229-244, 1996.

271 Sejersted, O. Maintenance of Na,K-homeostasis by Na,K-pumps in striated muscle. *Prog.Clin.Biol.Res.* 268B: 195-206, 1988.

272 Sellevold, O. F., P. Jynge, and K. Aarstad. High Performance Liquid Chromatography: A rapid isocratic method for determination of creatine compounds and adenine nucleotides in myocardial tissue. *J.Mol.Cell.Cardiol.* 18: 517-527, 1984.

273 Sherman, S. J., J. C. Lawrence, D. J. Messner, Jacoby K, and W. A. Catterall. Tetrodotoxin-sensitive sodium channels in rat muscle cells developing in vitro. *J.Biol.Chem.* 258: 2488-2495, 1983.

274 Shiota, M. and S. Masumi. Effect of norepinephrine on consumption of oxygen in perfused skeletal muscle from cold-exposed rats. *Am.J.Physiol.* 254: E482-E489, 1988.

275 Shum, A., F. Liao, C. Chen, and J. Wang. The role of interscapular brown adipose tissue in cold acclimation in the rat. *Chin.J.Physiol.* 34: 427-437, 1991.

276 Sillence, M. N., N. G. Moore, G. G. Pegg, and D. B. Lindsay. Ligand binding properties of putative beta3-adrenoceptors compared in brown adipose tissue and in skeletal muscle membranes. *Br.J.Pharmacol.* 109: 1157-1163, 1993.

277 Simonides, W. S. and C. Van Hardeveld. Effects of thyroid status on the sarcoplasmic reticulum in slow skeletal muscle of the rat. *Cell Calcium* 7: 147-160, 1986.

278 Simonides, W., M. Thelen, C. van der Linden, A. Muller, and C. Van Hardeveld. Mechanisms of thyroid-hormone regulated expression of the SERCA genes in skeletal muscle: Implications for thermogenesis. *Biosci.Rep.* 21: 139-154, 2001.

279 Simonsen, L., B. Stallknecht, and J. Bülow. Contribution of skeletal muscle and adipose tissue to adrenaline- induced thermogenesis in man. *Int.J.Obesity* 17: S47-S51, 1993.

280 Simonsen, L., B. Štefl, N. J. Christensen, and J. Bülow. Thermogenic response to adrenaline during restricted blood flow in the forearm. *Acta Physiol Scand* 166: 31-38, 1999.

281 Skou, J. C. Effect of ATP on the intermediary steps of the reaction of the (Na+ + K+)- dependent enzyme system. III. Effect on the p-nitrophenylphosphatase activity of the system. *Biochim.Biophys.Acta* 339: 258-273, 1974.

282 St-Pierre, J., M. D. Brand, and R. Boutilier. Mitochondria as ATP consumers: Cellular treason in anoxia. *PNAS* 97: 8670-8674, 2000.

283 St-Pierre, J., G. Tattersall, and R. Boutilier. Metabolic depression and enhanced O2 affinity of mitochondria in hypoxic hypometabolism. *Am.J.Physiol.* 279: R1205-R1214, 2000.

284 St Pierre, J., M. D. Brand, and R. G. Boutilier. The effect of metabolic depression on proton leak rate in mitochondria from hibernating frogs. *J.Exp.Biol.* 203 Pt 9:1469-76: 1469-1476, 2000.

285 Štefl, B., J. A. Mejsnar, and A. Janovska. Energy metabolism of rat skeletal muscle modulated by the rate of perfusion flow. *Exp Physiol* 84: 651-663, 1999.

286 Stuart, J. A., K. M. Brindle, J. A. Harper, and M. D. Brand. Mitochondrial proton leak and the uncoupling proteins. *J.Bioenerg.Biomembr.* 31: 517-525, 1999.

287   Stuart, J. A., T. E. Gilles, and J. S. Ballantyne. Compositional correlates of metabolic depression in the mitochondrial membranes of estivating snails. *Am.J.Physiol.* 275: R1977-R1982, 1998.

288   Sweeney, G. and A. Klip. Mechanisms and consequences of Na+,K+-pump regulation by insulin and leptin. *Cell Mol.Biol.(Noisy.-le-grand)* 47: 363-372, 2001.

289   Teskey, N., B. A. Horwitz, and J. Horwitz. Norepinephrine-induced depolarization of skeletal muscle cells. *Eur.J.Pharmacol.* 30: 352-355, 1975.

290   Thurlby, P. L. and R. D. Ellis. Differences between the effects of noradrenaline and the beta-adrenoceptor agonist BRL 28410 in brown adipose tissue and hindlimb of the anaesthetized rat. *Can.J.Physiol.Pharmacol.* 64: 1111-1114, 1986.

291   Tong, A. C., S. Rattigan, and M. G. Clark. Similarities between vasoconstrictor- and veratridine-stimulated metabolism in perfused rat hind limb. *Can.J.Physiol Pharmacol.* 76: 125-132, 1998.

292   Tong, A. C., S. Rattigan, K. A. Dora, and M. G. Clark. Vasoconstrictor-mediated increase in muscle resting thermogenesis is inhibited by membrane-stabilizing agents. *Can.J.Physiol Pharmacol.* 75: 763-771, 1997.

293   Tullis, A., B. A. Block, and B. D. Sidell. Activities of key metabolic enzymes in the heater organs of scombroid fishes. *J Exp.Biol.* 161:383-403: 383-403, 1991.

294   Van Hardeveld, C. and T. Clausen. Effect of thyroid status on K+-stimulated metabolism and 45Ca exchange in rat skeletal muscle. *Am.J.Physiol.* 247: E421-E430, 1984.

295   Van Hardeveld, C. and A. A. Kassenaar. Influence of experimental hyperthyroidism on skeletal muscle metabolism in the rat. *Acta Endocrinol.(Copenh.)* 85: 71-83, 1977.

296 van Renterghem, C. and M. Lazdunski. A new non-voltage dependent, epithelial-like Na+ channel in vascular smooth muscle cells. *Pflugers Arch.* 419: 401-408, 1991.

297 Vianna, C. R., T. Hagan, C. Y. Zhang, E. Bachman, O. Boss, B. Gereben, A. S. Moriscot, B. B. Lowell, J. Eduardo, P. W. Bicudo, and A. C. Bianco. Cloning and functional characterization of an uncoupling protein homolog in hummingbirds. *Physiol.Genomics* 5: 137-145, 2001.

298 Vidal-Puig, A., G. Solanes, D. Grujic, J. S. Flier, and B. B. Lowell. UCP3: an uncoupling protein homologue expressed preferentially and abundantly in skeletal muscle and brown adipose tissue. *Biochem.Biophys.Res.Commun.* 235: 79-82, 1997.

299 Vidal-Puig, A. J., D. Grujic, C. Y. Zhang, T. Hagen, O. Boss, Y. Ido, A. Szczepanik, J. Wade, V. Mootha, R. Cortright, D. M. Muoio, and B. B. Lowell. Energy metabolism in uncoupling protein·3 gene knockout mice. *J.Biol.Chem.* 275: 16258-16266, 2000.

300 Vincent, M. A., S. Rattigan, and M. G. Clark. Microsphere infusion reverses vasoconstrictor-mediated change in hindlimb oxygen uptake and energy status. *Acta Physiol Scand* 164: 61-69, 1998.

301 Vincent, M. A., S. Rattigan, M. G. Clark, S. Bernard, and R. Glenny. Spatial distribution of nutritive and nonnutritive vascular routes in perfused hindlimb muscle using microspheres. *Microvasc.Res.* 61: 111-121, 2001.

302 Weigle, D. S., L. E. Selfridge, M. W. Schwartz, R. J. Seeley, D. E. Cummings, P. J. Havel, J. L. Kuijper, and H. BeltrandelRio. Elevated free fatty acids induce uncoupling protein 3 expression in muscle: a potential explanation for the effect of fasting. *Diabetes* 47: 298-302, 1998.

303 Welsh, D. and S. S. Segal. Endothelial and smooth muscle cell conduction in arterioles controlling blood flow. *Am.J.Physiol.* 274: H178-H186, 1998.

304 Weyer, C., P. A. Tataranni, S. Snitker, E. J. Danforth, and E. Ravussin. Increase in insulin action and fat oxidation after treatment with CL 316,243, a highly selective beta3-adrenoceptor agonist in humans. *Diabetes* 47: 1555-1561, 1998.

305 Whalen, W. J., D. Buerk, and C. A. Thuning. Blood flow-limited oxygen consumption in resting cat skeletal muscle. *Am.J.Physiol.* 224: 763-768, 1973.

306 Williamson, J. R. Metabolic effects of epinephrine in the isolated, perfused rat heart. 1. Dissociation of the glycogenolytic from the metabolic stimulatory effect. *J.Biol.Chem.* 239: 2721-2729, 1964.

307 Wynants, J., B. Petrov, J. Nijhof, and H. Van Belle. Optimization of a high-performance liquid chromatographic method for the determination of nucleosides and their catabolies. Application to cat and rabbit heart perfusates. *J.Chromatogr.* 386: 297-308, 1987.

308 Ye, J., M. G. Clark, and E. Q. Colquhoun. Creatine phosphate as the preferred early indicator of ischemia in muscular tissues. *J Surg.Res* 61: 227-236, 1996.

309 Ye, J. M., M. G. Clark, and E. Q. Colquhoun. Constant-pressure perfusion of rat hindlimb shows alpha- and beta- adrenergic stimulation of oxygen consumption. *Am J Physiol* 269: E960-E968, 1995.

310 Ye, J. M., E. Q. Colquhoun, M. Hettiarachchi, and M. G. Clark. Flow-induced oxygen uptake by the perfused rat hindlimb is inhibited by vasodilators and augmented by norepinephrine: a possible role for the microvasculature in hindlimb thermogenesis. *Can.J.Physiol.Pharmacol.* 68: 119-125, 1990.

311 Ye, J. M., S. J. Edwards, R. W. Rose, S. Rattigan, M. G. Clark, and E. Q. Colquhoun. Vasoconstrictors alter oxygen, lactate, and glycerol metabolism in the perfused hindlimb of a rat kangaroo. *Am J Physiol* 268: R1217-R1223, 1995.

312 Ye, J. M., S. J. Edwards, R. W. Rose, J. T. Steen, M. G. Clark, and E. Q. Colquhoun. Alpha-adrenergic stimulation of thermogenesis in a rat kangaroo (Marsupialia, Bettongia gaimardi). *Am J Physiol* 271: R586-R592, 1996.

313 Yoda, A. and S. Yoda. Interaction between ouabain and the phosphorylated intermediate Na/K-ATPase. *Mol Pharmacol* 22: 700-705, 1982.

314 Yoshida, S. Tetrodotoxin-resistant sodium channels. *Cell Mol.Neurobiol.* 14: 227-244, 1994.

315 Yoshida, T., T. Umekawa, K. Kumamoto, N. Sakane, A. Kogure, M. Kondo, Y. Wakabayashi, T. Kawada, I. Nagase, and M. Saito. beta 3-Adrenergic agonist induces a functionally active uncoupling protein in fat and slow-twitch muscle fibers. *Am.J.Physiol* 274: E469-E475, 1998.

316 Yoshitomi, H., K. Yamazaki, S. Abe, and I. Tanaka. Differential regulation of mouse uncoupling proteins among brown adipose tissue, white adipose tissue, and skeletal muscle in chronic beta 3 adrenergic receptor agonist treatment. *Biochem.Biophys.Res.Commun.* 253: 85-91, 1998.

317 Youd, J. M., J. M. Newman, M. G. Clark, G. J. Appleby, S. Rattigan, A. C. Tong, and M. A. Vincent. Increased metabolism of infused 1-methylxanthine by working muscle. *Acta Physiol Scand* 166: 301-308, 1999.

318 Zhou, M., B. Lin, S. Coughlin, G. Vallega, and P. Pilch. UCP-3 expression in skeletal muscle: effects of exercise, hypoxia and AMP-activated protein kinase. *Am.J.Physiol.* 279: E622-E629, 2000.

Na⁺ channel and Na⁺-K⁺ ATPase involvement in norepinephrine- and veratridine-stimulated metabolism in perfused rat hind limb

Alex C.Y. Tong, Carla A. Di Maria, Stephen Rattigan, and Michael G. Clark

Abstract: In the constant flow perfused rat hind limb, norepinephrine (NE) evoked increases in oxygen uptake ($\dot{V}o_2$) and lactate efflux (LE) were inhibited by the cardiac glycoside ouabain (1 mM), without interrupting the NE-mediated vasoconstriction. The membrane labilizer veratridine, previously shown to increase $\dot{V}o_2$ and LE, without increasing perfusion pressure, was also shown to be inhibited by the cardiac glycoside ouabain, as well as by the ouabain analogues digitoxin and digoxin. The stimulatory actions of veratridine on $\dot{V}o_2$ were inhibitable by low doses of the specific sodium channel blocker tetrodotoxin (TTX), while NE effects were unaffected, suggesting that NE may be acting via a TTX-insensitive sodium channel. It is concluded that agents such as NE (a vasoconstrictor) or veratridine (a membrane labilizer), which stimulate $\dot{V}o_2$ in the perfused rat hind limb, do so by increasing Na⁺ influx. The observed increases in oxygen consumption and LE are due to Na⁺-K⁺ ATPase activity to pump Na⁺ out of the cell at the expense of ATP turnover. Energy dissipation due to Na⁺ cycling may be a form of facultative thermogenesis attributable to NE that can be stimulated by membrane labilizers such as veratridine in the constant flow perfused rat hind limb.

Key words: membrane labilizer, digitoxin, digoxin, cardiac glycosides, Na⁺-K⁺ ATPase, ouabain.

Résumé : Dans le membre postérieur perfusé à débit constant du rat, les augmentations induites par la norépinéphrine (NE) de la capture d'oxygène ($\dot{V}o_2$) et du flux sortant de lactate (FL) ont été inhibées par le glucoside cardiotonique ouabaïne (1 mM) sans que la vasoconstriction induite par la NE soit interrompue. Le labilisateur membranaire vératridine, connu pour augmenter la $\dot{V}o_2$ et le FL sans augmenter la pression de perfusion, a aussi été inhibé par le glucoside cardiotonique ouabaïne ainsi que par les analogues de l'ouabaïne, digitoxine et digoxine. Les actions stimulatrices de la vératridine sur la $\dot{V}o_2$ ont pu être inhibées par de faibles doses du bloqueur spécifique des canaux sodiques tétrodotoxine (TTX), sans que la NE soit influencée, ce qui porte à penser que la NE peut agir par l'intermédiaire d'un canal sodique sensible à la TTX. On conclut que des agents comme la NE (un vasoconstricteur) ou la vératridine (un labilisateur membranaire) stimulent la $\dot{V}o_2$ dans le membre postérieur perfusé du rat en augmentant le flux entrant de Na⁺. Les augmentations observées de la consommation d'oxygène et du FL résultent de l'activité de la Na⁺-K⁺ ATPase pour extraire le Na⁺ des cellules aux dépens du renouvellement de l'ATP. La dissipation d'énergie induite par le cycle du Na⁺ pourrait être une forme de thermogenèse facultative attribuable à la NE, qui pourrait être stimulée par des labilisateurs membranaires tels que la vératridine dans le membre postérieur perfusé à débit constant du rat.

Mots clés : labilisateur membranaire, digoxine, Na⁺-K⁺ ATPase, digitoxine, glucosides cardiotoniques, ouabaïne.

[Traduit par la Rédaction]

Introduction

Skeletal muscle at rest contributes to whole-body thermogenesis in response to both cold and overeating (Jansky 1995). However, unlike brown adipose tissue, where the mechanism of thermogenesis is defined, the exact mechanism of thermogenesis in resting skeletal muscle remains unclear. Candidate mechanisms include mitochondrial pro-

ton leak (estimated to be responsible for about one-half of the resting muscle thermogenesis (Rolfe and Brand 1996)) and regulated uncoupling of mitochondria involving the recently discovered third member of the uncoupling protein family (UCP-3). However, the exact function of UCP-3 is unknown, even though the involvement of this protein in skeletal muscle thermogenesis has been implied (Gong et al. 1997; Larkin et al. 1997). A third candidate mechanism for resting muscle thermogenesis relates to the observed stimulatory effects of adrenergic vasoconstrictors, particularly in perfused muscle preparations (Jansky and Hart 1963; Grubb and Folk 1977; Richter et al. 1982; Côté et al. 1985), where apart from an accompanying increase in perfusion pressure, little is known about the underlying mechanism. Studies from this laboratory have extended those original findings by showing, in the perfused rat hind limb preparation, that

A.C.Y. Tong,[1] C.A. Di Maria, S. Rattigan, and M.G. Clark.[2] Division of Biochemistry, University of Tasmania, GPO Box 252-58, Hobart 7001, Australia.

[1]Deceased.
[2]Author for correspondence (e-mail: Michael.Clark@utas.edu.au).

thermogenesis is stimulated by other vasoconstrictors including angiotensin II (AII) and vasopressin (Colquhoun et al. 1988; Ye et al. 1990). In addition, increased flow rate leading to elevated perfusion pressures also stimulated oxygen consumption (Ye et al. 1990). The relationship between vasoconstriction and changes in muscle metabolism (Clark et al. 1994) appeared to be obligatory since the addition of vasodilatory agents decreased vasoconstriction and reversed the metabolic effects (Colquhoun et al. 1988, 1990; Ye et al. 1990). Since the stimulatory effects of these vasoconstrictors were demonstrable in perfusion only, and not in isolated incubated muscle preparations (Dubois-Ferriere and Chinet 1981; Hettiarachchi et al. 1992), it was proposed that the increase in oxygen consumption observed under vasoconstriction was due to work performed by the smooth vascular muscle itself as it contracted to hold perfusion pressure (Colquhoun et al. 1988, 1990; Ye et al. 1990; Colquhoun and Clark 1991; Clark et al. 1994).

However, more recent studies where membrane-stabilizing agents were found to inhibit the vasoconstrictor-mediated increase in oxygen uptake ($\dot{V}o_2$) without affecting vasoconstriction (Tong et al. 1997) suggested that the increase in $\dot{V}o_2$ originates from skeletal muscle and was the result of an indirect vascular effect. A key element of the indirect vascular mechanism appears to be the redistribution of flow between two distinct vascular pathways within muscle (Clark et al. 1997). Evidence includes the vasoconstrictor-mediated washout of red blood cells from the perfused tissue, even after a suitable equilibration period (Newman et al. 1996). In addition, fluorescent dextran (M_r 150 000) studies showed that this marker was entrapped in a new vascular space accessed by low-dose norepinephrine (LDNE) (Newman et al. 1996). Furthermore, LDNE vasoconstriction was shown to cause an increase in the number of vessels filled with vascular casting medium and, in other experiments, to decrease the diameter of large tendon vessels in the tibialis region of the biceps femoris as shown by surface fluorimetry (Newman et al. 1996, 1997). On the basis of this evidence, it was proposed that vasoconstrictors cause a redistribution of flow from a non-nutritive route to a nutritive route where vessels are in close proximity to regions with high metabolic activity.

Conversely, other vasoconstrictors that inhibit metabolism are thought to restrict flow to the nutritive pathway and redirect flow through functional vascular shunts or the non-nutritive pathway. For example, serotonin (5HT), which inhibits metabolism including $\dot{V}o_2$, was shown to decrease the total number of vessels perfused with casting medium and to increase the diameter of the large tendon vessels (Newman et al. 1996, 1997). No red blood cell washout was observed, regardless of the magnitude of the increase in perfusion pressure due to 5HT infusion (Newman et al. 1996). More recently, veratridine (a putative Na^+ channel opener) has been found to increase perfused hind limb $\dot{V}o_2$ (Tong et al. 1998) without significant pressure development. Thus it is possible to have a marked stimulation of oxygen consumption without vasoconstriction. The increase in oxygen consumption was dose dependent, accompanied by a large increase in lactate efflux (LE), and was similar in magnitude to the changes caused by norepinephrine (NE) (Tong et al. 1998).

The increase in $\dot{V}o_2$ by resting perfused hind limb due to NE, AII, or veratridine may each involve the same mechanism of destabilization of skeletal muscle plasma membrane Na^+ channels. Such a shared mechanism is suggested by the observation that NE-, AII-, or veratridine-mediated increases in metabolism are each inhibited by low Na^+ medium, or high ("membrane-stabilizing") doses of ($\pm$)-propranolol (a membrane stabilizer makes voltage-sensitive channels less voltage sensitive, and therefore harder to activate) (Tong et al. 1997, 1998). Since previous work by others on a non-muscle tissue indicates that the activation of Na^+ influx is accompanied by activation of the Na^+–K^+ ATPase to maintain membrane potential with corresponding changes in metabolism (Edwards et al. 1989), we have investigated the involvement of the Na^+–K^+ ATPase and Na^+ channels by using cardiac glycosides and tetrodotoxin, respectively, on NE- and veratridine-mediated increases in metabolism in the constant flow perfused rat hind limb.

Materials and methods

Animals

Animals were cared for in accordance with the recommendations of the Animal Welfare Committee of the National Health and Medical Research Council (in *Australian Code of Practice for the Care and Use of Animals for Scientific Purposes*, 1990). The Committee on the Ethical Aspects of Research Involving Animals of the University of Tasmania approved all subsequent experimental procedures used. Male Hooded Wistar rats of a local strain were housed in a 12 h light : 12 h dark cycle at 22°C. Water and commercial rat chow (Gibsons, Hobart) were freely available. Pentobarbital sodium (5–6 mg/100 g body weight intraperitoneally) was administered to the animals prior to surgery.

Hind-limb perfusions

The surgical procedure for dual hind limb perfusion was the same protocol described in previous papers (Tong et al. 1998), an adaptation from Colquhoun et al. (1988).

Young rats (70–80 g, approximately 4 weeks of age) were used in this series of experiments. Previous experimentation has demonstrated the optimal NE response to be approximately 60% higher in smaller (70–80 g) rats than larger (180–200 g) animals (Tong et al. 1997, 1998).

Both hind limbs of young rats were perfused using a constant flow rate of 4.0 ± 0.1 mL·min^{-1} (0.45 mL·min^{-1}·g^{-1} muscle). The perfusion was carried out in a non-recycling mode at 25°C, using medium comprising modified Krebs–Henseleit bicarbonate buffer with 2% (w/v) bovine serum albumin (BSA, fraction V), 8.3 mM glucose, and 1.27 mM $CaCl_2$, and gassed with 95% O_2 – 5% CO_2. An equilibration period of 50 min preceded each investigation. Perfusion pressure was constantly recorded via a pressure transducer fitted to a side arm proximal to the arterial catheter. The constant arterial oxygen content (Pao_2) was determined at the commencement and end of each perfusion. Venous effluent oxygen levels (Pvo_2) were monitored continuously using a flow-through Clark-type oxygen electrode, and samples of the effluent were collected at specified times for lactate analysis. The volume of oxygen consumed ($\dot{V}o_2$) was calculated from the arteriovenous difference as micromoles per gram of hind limb tissue perfused per hour (μmol·g^{-1}·h^{-1}) with the use of the following equation:

$$\dot{V}o_2 = \frac{ap^{25} \times (Pao_2 - Pvo_2) \times \text{flow rate} \times 60}{\text{muscle mass (g)}}$$

Table 1. Steady-state values for oxygen uptake ($\dot{V}o_2$), perfusion pressure (PP), and lactate efflux (LE) with normal medium in the presence or absence of 0.5 mM nitroprusside (NP); 1 mM ouabain medium (with or without 0.5 mM NP); 30 µM digoxin with 0.5 mM NP; and 30 µM digitoxin with 0.5 mM NP in the constant flow perfused rat hind limb.

	$\dot{V}o_2$ (μmol·h^{-1}·g^{-1})	PP (mmHg)	LE (μmol·h^{-1}·g^{-1})
Basal	12.8 ± 0.4	21.5 ± 1.3	10.4 ± 1.1
0.5 mM NP	12.6 ± 0.4	19.5 ± 0.9	11.3 ± 1.1
Basal	11.5 ± 0.3	21.5 ± 1.2	7.5 ± 0.2
1 mM ouabain	10.7 ± 0.6	27.5 ± 1.9*	6.8 ± 0.2*
Basal	11.6 ± 0.4	23.5 ± 0.5	9.2 ± 0.1
1 mM ouabain + 0.5 mM NP	11.3 ± 0.2	22.5 ± 0.3	11.2 ± 0.9
Basal	11.3 ± 0.5	22.5 ± 1.2	6.1 ± 0.2
30 µM digoxin + 0.5 mM NP	10.3 ± 0.3	25.5 ± 1.7	6.2 ± 0.3
Basal	9.2 ± 1.5	24.4 ± 2.7	5.0 ± 0.9
30 µM digitoxin + 0.5 mM NP	9.2 ± 1.5	26.6 ± 2.8	4.5 ± 0.2

Note: Hind limbs were perfused at constant flow and allowed 50 min pre-equilibration with normal perfusion medium, at which time the buffer was changed to 1 mM ouabain or 1 mM ouabain + 0.5 mM NP, 30 µM digoxin + 0.5 mM NP, or 30 µM digitoxin + 0.5 mM NP. Companion basal values are shown for each change to the perfusion buffer. New steady-state values for $\dot{V}o_2$, LE, and PP were reached within 30–40 min. Values are steady-state means ± SE for 5 perfusions. Values for pressure have been corrected for cannula resistance. *Significantly different (Student's paired t-test; $p < 0.05$) from Basal.

where ap^{25} is the bunsen solubility coefficient for O_2 at 25°C in human plasma (1.509 mmol·L^{-1}·mmHg^{-1}), Pao_2 and Pvo_2 are the measured arterial and venous oxygen levels (in mmHg), flow rate is in µL/min, and for small rats the mass (in g) of the perfused muscle is calculated as body weight × 0.141 − 2.534 (Rattigan et al. 1995).

Other media

Trial perfusions were conducted beforehand to ascertain the optimal effects for a given concentration of each agent. Ouabain, from Sigma Chemical Company (St. Louis, Mo.), was dissolved in the perfusion medium to give a final concentration of 1 mM (dose shown by prior testing to give optimal effects). Digoxin (Sigma) and nitroprusside (Merck, Darmstadt, Germany) were dissolved into the perfusion medium to give 30 µM and 0.5 mM, respectively. Digitoxin (Sigma; final concentration 30 µM, optimal dose for ouabain analogues shown by prior testing) was dissolved in a small quantity of 50% ethanol before being added to the 2% BSA with the 0.5 mM sodium nitroprusside. The final concentration of ethanol in the entire buffer volume was less than 0.6%. Each of the following reagents (from Sigma Chemical Company) was freshly prepared as a stock solution and infused at a rate of less than or equal to 1:200 of the flow rate: 10 mM veratridine (free base) dissolved in H_2O, and neutralized with concentrated HCl; 1 mM NE dissolved in 0.1% ascorbic acid − 0.9% NaCl. Tetrodotoxin with citrate (Alomone Labs, Israel) was prepared in distilled water.

Dose curves for NE and veratridine

After a 50-min equilibration period, stepwise increasing doses of the drug were infused, with each dose period lasting 20 min (Tong et al. 1998). Doses of NE tested ranged from 0.003 to 0.3 µM. The NE dose–response value for each data point was the average of four equally spread 5-min time points during the 20-min dose. Doses of veratridine tested ranged from 3 to 300 µM. For veratridine, the dose–response value for each data point was the average of three points taken at 10, 15, and 20 min during the 20-min dose period.

Dose–response curves for NE and veratridine in the presence of cardiac glycosides

For 1 mM ouabain, 30 µM digoxin, and 30 µM digitoxin perfusions, the hind limb was first pre-equilibrated with normal buffer for 50 min, after which time the buffer was changed to the designated medium (ouabain, digoxin, or digitoxin). Two other analogues of ouabain were chosen to show that the inhibitory effect on $\dot{V}o_2$ was a general property of cardiac glycosides, and not a unique property of ouabain alone. A further 30-min equilibration time was allowed with the new medium. The transition from normal buffer to 1 mM ouabain or 30 µM digitoxin containing media resulted in small transient effects on $\dot{V}o_2$ and perfusion pressure (PP), which were ignored. The transition from normal buffer to 30 µM digoxin was accompanied by the onset of a gradual increase in PP (data not shown), which continued for the remainder of the experiment. This pressure increase was not blocked by the presence of sodium nitroprusside, but did not have any significant effects on $\dot{V}o_2$. Therefore, digoxin PP was plotted against a constant moving baseline, to compensate for this increase. The study proper commenced when $\dot{V}o_2$ returned to near basal level (steady state, see Table 1), usually within 30–40 min. The data presented are the changes from the new steady state.
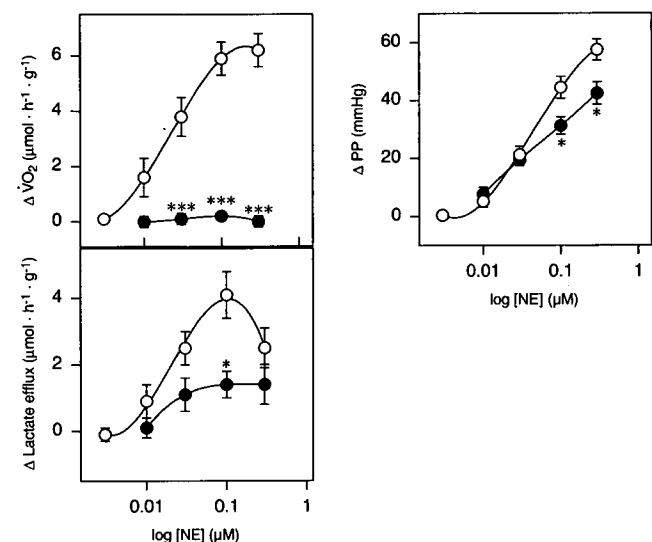
Effects of tetrodotoxin on NE- and veratridine-mediated changes

In a final series of experiments the effects of the sodium channel blocker tetrodotoxin (TTX) on NE- and veratridine-mediated increases in $\dot{V}o_2$, LE, and PP were assessed. After 50 min equilibration with 2% BSA, a constant infusion of either 0.1 µM NE or 30 µM veratridine was commenced. A period of 30 min was allowed for steady-state stimulation of $\dot{V}o_2$ before TTX infusion commenced. TTX dose–response curves against both NE and veratridine were then conducted, with doses of TTX ranging from 0.01 to 50 µM.

Statistical analysis

Repeated measures two-way analysis of variance was used to test the hypothesis that there was no difference in oxygen consumption,

Fig. 1. Dose–response curves for norepinephrine (NE) on oxygen uptake ($\dot{V}o_2$), perfusion pressure (PP), and lactate efflux. Both hind limbs were perfused at constant flow. Perfusions were either control (○), which has been reported previously (Tong et al. 1998), or in 1 mM ouabain medium (●). Basal and steady-state values are given in Table 1. Mean values for changes (from basal or steady state) ± SE are shown, where $n = 5$. Significant differences from steady-state stimulation: $*p < 0.05$; $***p < 0.001$.

Fig. 2. Dose–response curves for veratridine (Vera) on oxygen uptake ($\dot{V}o_2$), perfusion pressure (PP), and lactate efflux. Both hind limbs were perfused at constant flow. Perfusions were either control, i.e., 0.5 mM nitroprusside (△), which has been reported previously (Tong et al. 1998), or with medium containing 1 mM ouabain medium with 0.5 mM nitroprusside (▲), 30 μM digoxin with 0.5 mM nitroprusside (●), or 30 μM digitoxin with 0.5 mM nitroprusside (◆). Mean values for changes (from basal and steady state) ± SE are shown, where $n = 5$. Basal or steady-state values for $\dot{V}o_2$, PP, and lactate efflux are given in Table 1. Significant differences of nitroprusside alone from cardiac glycoside treated groups: $*p < 0.05$; $**p < 0.01$; $***p < 0.001$.

perfusion pressure, or lactate efflux with each treatment, for norepinephrine or veratridine dose–response curves. When a significant difference was detected ($p < 0.05$), pairwise comparisons were made with the use of the Student–Newman–Keuls test, and t-tests to determine the dose of norepinephrine or veratridine at which treatments were significantly different. These tests were performed with the use of the SigmaStat statistical program (Jandel Software).
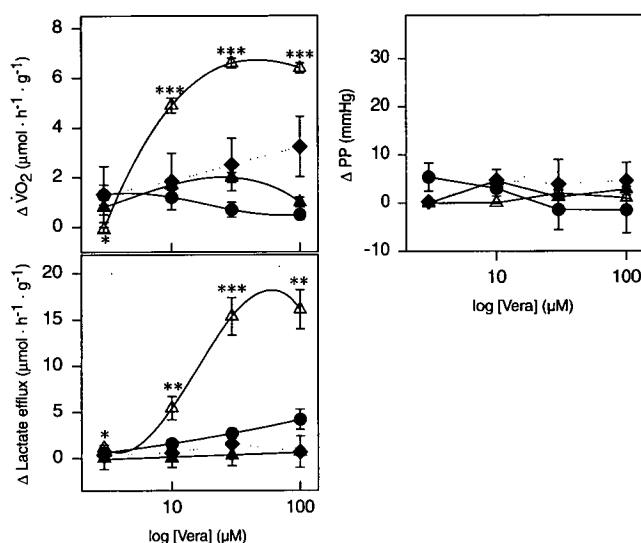
Results

Effects of cardiac glycosides on basal metabolism

Equilibration of the perfused rat hind limb for 50 min led to steady-state values for Pao_2 (647 ± 6.5 mmHg), $\dot{V}o_2$ (11.35 ± 0.33 μmol·g^{-1}·h^{-1}), and PP (16.7 ± 1.27 mmHg) before the addition of any agents ($n = 30$). Lactate efflux was also steady within this time, and remained constant for up to 180 min of perfusion (data not shown). Substitution of the perfusion medium with one containing 1 mM ouabain caused an increase in perfusion pressure (6 mmHg greater than basal values, see Table 1). However, the inclusion of 0.5 mM sodium nitroprusside (a nitrovasodilator) together with ouabain in the perfusion medium abolished this pressure effect. Accordingly, 0.5 mM sodium nitroprusside was included in the perfusion media for all veratridine dose–response curves. The inclusion of nitroprusside in NE experiments was not possible, since NP would affect the vasoconstrictor response to NE (Colquhoun et al. 1990).

Effects of ouabain on NE-mediated response

Figure 1 shows the effects of 1 mM ouabain against a NE dose–response curve. The NE dose-dependent increase in $\dot{V}o_2$ was almost completely inhibited by 1 mM ouabain at all

doses of NE (0.003 to 0.3 μM). The greatest inhibition of oxygen consumption occurred at the three highest doses of NE (0.03, 0.1, and 0.3 μM, where $p < 0.01$ for each).

Lactate efflux was similarly affected, although large variations in the values meant that blockade by ouabain was significant at only one dose of NE (0.1 μM). At this dose lactate efflux was reduced by 1 mM ouabain from 4.0 ± 0.8 to 1.4 ± 0.4 μmol·g^{-1}·h^{-1} ($p < 0.05$). Pressure development was least affected, with a significant inhibition of 26% at the highest NE doses (0.1 and 0.3 μM, $p < 0.05$, Fig. 1). Digitoxin (another ouabain analogue) did not significantly affect the NE dose–response curves, although an inhibitory trend on $\dot{V}o_2$ at the highest doses of NE was evident (data not shown). Because of the intrinsic pressor effect of digoxin, we were unable to test digoxin alone against NE.

Effects of ouabain and digitoxin and digoxin on veratridine-mediated response

Figure 2 shows the effects of 1 mM ouabain + 0.5 mM nitroprusside, 30 μM digitoxin + 0.5 mM nitroprusside, and 30 μM digoxin + 0.5 mM nitroprusside on the dose-dependent effects of veratridine to stimulate $\dot{V}o_2$ and LE. Nitroprusside was included to eliminate any small changes in perfusion pressure attributable to veratridine. From previous studies (Tong et al. 1998), nitroprusside (0.5 mM) was found to have no effect on veratridine-mediated increases in $\dot{V}o_2$ and LE. All three agents (1 mM ouabain, 30 μM digitoxin, and 30 μM digoxin, each in the presence of 0.5 mM nitroprusside) significantly blocked veratridine-

Fig. 3. Dose–response curves of TTX against either 100 nM NE or 30 μM veratridine. Both hind limbs were perfused at a constant flow rate. Perfusions were either constant infusion of NE with TTX dose–response curve (●) or constant infusion of veratridine with TTX dose–response curve (■). Values are the mean changes from basal ± SE, $n = 3$ for 50 μM TTX and $n = 5$ for all other doses. Significant differences from steady-state stimulation (no TTX): **$p < 0.01$; ***$p < 0.001$.
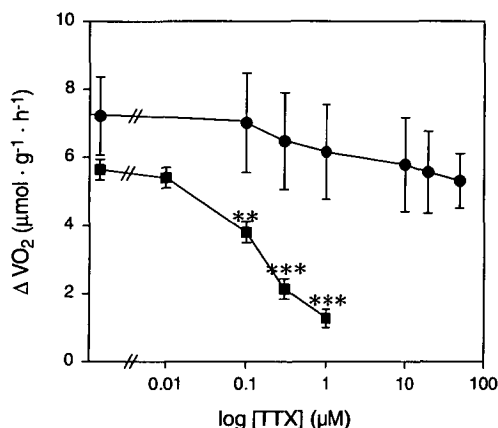
mediated increases in $\dot{V}o_2$ and LE. At doses of veratridine greater than and equal to 10 μM, inhibition of $\dot{V}o_2$ by all agents tested was highly significant ($p < 0.001$, Fig. 2). At 30 μM veratridine (the dose having the maximal stimulatory effects on $\dot{V}o_2$ and LE), the relative percent inhibition of $\dot{V}o_2$ by ouabain, digoxin, and digitoxin was 69, 89, and 61%, respectively.

In the presence of nitroprusside, there was no significant increase in perfusion pressure above basal due to veratridine. In addition, neither ouabain nor digitoxin had any significant effect on perfusion pressure in the presence of nitroprusside (Fig. 2). However, digoxin produced an intrinsic pressor effect, even in the presence of nitroprusside. Thus perfusion pressure continued to increase throughout the time course of the veratridine dose–response curve. Since the increase in pressure was independent of veratridine, controls were run without veratridine and the data were corrected for the increase in pressure (Fig. 2). The time-dependent increase in pressure with digoxin + nitroprusside was without significant effect on either oxygen consumption or LE (Table 1).

Ouabain and its analogues had significant inhibitory effects on veratridine-stimulated LE at all doses of veratridine within the dose range. The inhibitory effects on LE were similar to those observed for $\dot{V}o_2$. Maximum inhibition of LE occurred at the maximum stimulatory dose of veratridine (30 μM), where all three agents inhibited LE by more than 82% when compared with control (veratridine + nitroprusside) (ouabain, $p < 0.0005$; digoxin, $p < 0.001$; and digitoxin, $p < 0.008$).

Effects of TTX on NE- and veratridine-mediated increases in $\dot{V}o_2$

Figure 3 shows the effects of increasing doses of tetrodotoxin against a constant infusion of a single dose of either NE (0.1 μM) or veratridine (30 μM). Infusion of NE alone or veratridine alone increased $\dot{V}o_2$ above basal by 7.21 ± 1.2

($p < 0.05$; $n = 6$) and 5.64 ± 0.3 μmol·g^{-1}·h^{-1} ($p < 0.05$, $n =$ 5), respectively. Stimulation of $\dot{V}o_2$ by 0.1 μM NE was unaffected by doses of tetrodotoxin in the range of 0.1–50 μM ($p > 0.05$).

Veratridine (30 μM) caused increases in $\dot{V}o_2$ similar to those caused by NE, but this increase in $\dot{V}o_2$ was susceptible to tetrodotoxin. Inhibition by tetrodotoxin was most apparent at doses of 0.1 μM and greater, almost completely reversing the stimulation of $\dot{V}o_2$ due to veratridine (0.1 μM, 0.3 μM and 1.0 μM significantly different from veratridine alone $p < 0.01$, $p < 0.001$, $p < 0.001$, respectively, Fig. 3).

Discussion

The objective of this study was to examine the effects of cardiac glycosides and tetrodotoxin on veratridine- and NE-mediated increases in metabolism of the constant flow perfused rat hind limb, with a view to further exploring the mechanism by which NE increases resting muscle metabolism in this preparation. The main findings indicate that ouabain blocks the stimulatory effects of both NE and veratridine on $\dot{V}o_2$, without affecting vasoconstrictor activity (Figs. 1 and 2). The ouabain analogues digoxin and digitoxin also significantly inhibited veratridine-mediated increases in $\dot{V}o_2$ and LE (Fig. 2). Digitoxin was shown to block NE-mediated increases to a small degree (data not shown), but not as effectively as ouabain. The specific sodium channel blocker TTX also blocked the veratridine-mediated increase in $\dot{V}o_2$ but had no effect on NE-induced changes (Fig. 3).

The increased metabolism due to NE over the dose range of 0.003 to 0.3 μM accompanied by vasoconstriction has been regarded by us in the past as having implication for facultative thermogenesis in resting skeletal muscle (Colquhoun et al. 1990; Clark et al. 1995; Newman et al. 1996). In our most recent report, the mechanism to explain the thermogenic action of NE was found to be shared with the membrane labilizer veratridine, and to involve Na$^+$ influx (Tong et al. 1998). The relevant associated energy dissipation process has been suggested to be the result of ATP turnover due to activation of the Na$^+$–K$^+$ ATPase in maintaining the plasma membrane potential by pumping the Na$^+$ out of the cell (Tong et al. 1998). There are precedents for a close association of Na$^+$ inward movement and stimulation of the Na$^+$–K$^+$ ATPase. Edwards et al. (1989) using turtle brain synaptosome preparation demonstrated that oxygen consumption could be increased by increasing Na$^+$ channel activity with veratridine or inhibiting it with tetrodotoxin, respectively. In addition, Cohen and Lechene (1990) using isolated rat hepatocytes found that uptake of alanine was followed by an increase in the rate of Na$^+$ entry, an increase in intracellular Na$^+$ content, and an increase in ouabain-inhibitable rubidium uptake (a measure of Na$^+$–K$^+$ ATPase pump rate). Taken together, these and our own findings from the present study suggest regulation of the Na$^+$–K$^+$ ATPase via intracellular [Na$^+$] and concomitant modulation of cellular oxygen consumption. Should a mechanism involving coupling between Na$^+$ conductance and energy expenditure through the Na$^+$–K$^+$ ATPase operate in muscle, it may well also provide a mechanism for reduced energy consumption

during hypometabolism. In this respect Hochachka et al. (1996) have focused attention on reduced membrane conductance as a mechanism for conserving energy during hypometabolic states.

Na^+–K^+ ATPase is an integral plasma membrane protein that transports $3Na^+$ out and $2K^+$ into the cytoplasm at the expense of ATP turnover. The structure and function of this protein has been intensively explored over the years and plausible mechanisms have been thoroughly reviewed (De Weer et al. 1988; Jorgensen 1992). Activation of this enzyme is thought to be voltage dependent due to precedent Na^+ translocation process (De Weer et al. 1988), and skeletal muscle may have sufficient Na^+–K^+ ATPase activity to match the increases in $\dot{V}o_2$ and LE noted in the present study (Clausen et al. 1998). Its expression at the plasma membrane is subject to regulation by hormones, long-term exercise, and other factors (Clausen 1996a, 1996b). In addition, it has been noted that rats injected with thyroid hormone show increases in oxygen consumption in incubated liver slices and diaphragm, which is attributed to an increase in Na^+–K^+ ATPase concentration in the tissues (Izmail-Beigi and Edelman 1970). It has been demonstrated that thyroid (Lin and Akera 1978) or glucocorticoid (Dorup and Clausen 1997) hormones injected intraperitoneally stimulate increased expression of the enzyme in rat skeletal muscle by 100 and 50%, respectively. In addition, changes in Na^+–K^+ ATPase levels occur during early post-natal development in skeletal muscle. Starting with low Na^+–K^+ ATPase concentration at birth, the activity reaches optimal levels at 4 weeks of age (increase of 5-fold), then declines to a lower plateau in the adult rat (Kjeldsen et al. 1982). Therefore it was interesting to note that in an age comparison between 4 week old (70–80 g) and larger (7 weeks old) rats of 180–200 g, the NE-mediated increases in hind limb $\dot{V}o_2$ under similar perfusion conditions showed a greater increase in $\dot{V}o_2$ in the small rats despite a lower perfusion pressure development (Tong et al. 1998).

In the constant flow perfused rat hind limb system, basal oxygen consumption is not affected by 1 mM ouabain at steady state (Table 1), although a small increase in perfusion pressure was evident. This suggests that Na^+–K^+ ATPase activity is not a significant factor in the basal energy consuming process, which is in general agreement with reports that the basal energy component due to Na^+–K^+ ATPase activity in muscle is very low (Clausen et al. 1991). Indeed this represents approximately 5–7% of basal metabolic rate in isolated intact resting mammalian skeletal muscle when measured by microcalorimetric determination (Chinet et al. 1977; Biron et al. 1979; Fagher et al. 1987) or in a sealed oxygen electrode chamber (Wardlaw 1986). Using the rat diaphragm muscle, it has been shown that as little as 2% of total basal energy consumption can be attributed to Na^+–K^+ ATPase activity (Creese 1968). However, there is one report that claims much higher levels of Na^+–K^+ ATPase involvement in resting skeletal muscle (Gregg and Milligan 1980), but this may not be correct as Clausen (Clausen et al. 1991) and others (Biron et al. 1979) have shown that the activity may be artificially increased due to an effect of using cut or nonintact muscle preparations. The absence of a contribution of the Na^+–K^+ ATPase activity to basal state metabolism is

consistent with the observations that neither high dose (±)-propranolol (membrane-stabilizing action) or low extracellular Na^+ medium (both of which impede sodium cycling activity) also has very little effect on resting metabolic rate in the same system (Tong et al. 1998).

Apart from acting as a potent inhibitor of Na^+–K^+ ATPase activity, as a result of a conformational modulation of the extracellular phase of the channel (Caldwell and Keynes 1959; Hansen 1984; Jorgensen 1992), ouabain and other cardiac glycosides have been reported to directly stimulate calcium release from cardiac sarcoplasmic reticulum through activation of Ca^{2+} release (McGarry and Williams 1993) and to enhance transient inward calcium current of heart (Marban and Tsien 1982). Of these, only the two former mechanisms are possibilities for skeletal muscle. Since resting muscle tension does not appear to have changed with either veratridine or NE (unpublished observations), it seems most likely that effects of the cardiac glycosides on skeletal muscle can be attributed to inhibition of the Na^+–K^+ ATPase. Thus our present study confirms the findings of Shiota and Masumi (1988) that NE-mediated increases in $\dot{V}o_2$ and LE in the constant flow perfused rat hind limb are blocked by ouabain and involve Na^+–K^+ ATPase activity. We also show that veratridine-mediated increases in $\dot{V}o_2$ and LE are blocked by the Na^+–K^+ ATPase inhibitors (Figs. 1 and 2), adding further merit to the notion that some aspects of the mechanism of action of veratridine and NE might be shared (Tong et al. 1998).

The observation that tetrodotoxin blocks veratridine-mediated increases in $\dot{V}o_2$ confirms the previous finding of others that veratridine acts on a tetrodotoxin-sensitive Na^+ channel (Lombet et al. 1982). In the present study, NE was unaffected by tetrodotoxin even at concentrations of up to 50 µM. However, the mechanism by which NE stimulates $\dot{V}o_2$ is clearly dependent on sodium flux through the cell membrane since the actions of NE are negated by low Na^+ medium, the membrane stabilizer propranolol (Tong et al. 1997), and the Na^+–K^+ ATPase blocker ouabain. This implies that NE is acting on a sodium channel that is tetrodotoxin insensitive, even though channels of this kind have only been reported in cardiac muscle (Catterall 1992) and denervated skeletal muscle of the adult rat (Rogart and Regan 1985; Catterall 1992). There are no reports to date of tetrodotoxin-insensitive channels in normal innervated skeletal muscle, but their presence has not been totally discounted. For example, in primary cultures of fetal rat skeletal muscle cells, populations of both tetrodotoxin-sensitive and -insensitive channels have been shown to coexist, with the two subtypes having different developmental regulation (Sherman et al. 1983). A further consideration in this study is the age of the rats. At 4 weeks of age, TTX-insensitive channels may still be present.

It is interesting that in addition to the absence of effect of TTX on the NE-mediated increase in $\dot{V}o_2$, ouabain analogues were also poorly effective against NE. This may suggest that a complex exists between the specific Na^+ channel activated by NE and the Na^+–K^+ ATPase pumps. If so, a different Na^+ channel may influence the Na^+–K^+ ATPase to such an extent that its sensitivity to ouabain analogues is also altered.

In summary, data from the present study lend additional

support to the notion that NE- and veratridine-mediated increases in resting muscle metabolism share a common mechanism, involving Na^+ channel activation, and a ouabain-sensitive step, presumably the Na^+–K^+ ATPase. This may provide a mechanism for the facultative thermogenesis seen in resting skeletal muscle in response to NE demonstrated by us (Colquhoun et al. 1990; Clark et al. 1995) and others (Jansky and Hart 1963; Grubb and Folk 1977; Richter et al. 1982; Côté et al. 1985; Shiota and Masumi 1988) in the constant flow perfused muscle preparation. However, there still remains uncertainty as to the identity of the tetrodotoxin-insensitive sodium channel that NE, angiotensin II, and related vasoconstrictors indirectly activate and the mechanism(s) by which this activation occurs.

Acknowledgements

References

Biron, R., Burger, A., Chinet, A., Clausen, T., and Dubois-Ferriere, R. 1979. Thyroid hormones and the energetics of active sodium–potassium transport in mammalian skeletal muscles. J. Physiol. (London), **297**: 47–60.

Caldwell, P.C., and Keynes, R.D. 1959. The effect of ouabain on the efflux of sodium from a squid giant axon. J. Physiol. (London), **148**: 8P–9P.

Catterall, W.A. 1992. Cellular and molecular biology of voltage-gated sodium channels. Physiol. Rev. **72**: S15–S48.

Chinet, A., Clausen, T., and Girardier, L. 1977. Microcalorimetric determination of energy expenditure due to active sodium–potassium transport in the soleus muscle and brown adipose tissue of the rat. J. Physiol. (London), **265**: 43–61.

Clark, M.G., Colquhoun, E.Q., Dora, K.A., Rattigan, S., Eldershaw, T.P.D., Hall, J.L., Matthias, A., and Ye, J.M. 1994. Resting muscle, a source of thermogenesis controlled by vasomodulators. *In* Temperature regulation, advances in pharmacological sciences. *Edited by* A.S. Milton. Birkhaeuser Verlag, Basel. pp. 315–320.

Clark, M.G., Colquhoun, E.Q., Rattigan, S., Dora, K.A., Eldershaw, T.P., Hall, J.L., and Ye, J. 1995. Vascular and endocrine control of muscle metabolism. Am. J. Physiol. **268**: E797–E812.

Clark, M.G., Rattigan, S., Dora, K.A., Newman, J.M.B., Steen, J.T., Miller, K.A., and Vincent, M.A. 1997. Vascular and metabolic regulation of muscle. *In* Physiology, stress, and malnutrition: functional correlates, nutritional intervention. *Edited by* J.M. Kinney and H.N. Tucker. Lippincott-Raven, New York. pp. 325–346.

Clausen, T. 1996a. Long- and short-term regulation of the Na^+–K^+ pump in skeletal muscle. News Physiol. Sci. **11**: 24–30.

Clausen, T. 1996b. The Na^+,K^+ pump in skeletal muscle: quantification, regulation and functional significance. Acta Physiol. Scand. **156**: 227–235.

Clausen, T., Van Hardeveld, C., and Everts, M.E. 1991. Significance of cation transport in control of energy metabolism and thermogenesis. Physiol. Rev. **71**: 733–774.

Clausen, T., Nielsen, O.B., Harrison, A.P., Flatman, J.A., and Overgaard, K. 1998. The Na^+,K^+ pump and muscle excitability. Acta Physiol. Scand. **162**: 183–190.

Cohen, B.J., and Lechene, C. 1990. Alanine stimulation of passive potassium efflux in hepatocytes is independent of Na^+–K^+ pump activity. Am. J. Physiol. **258**: C24–C29.

Colquhoun, E.Q., and Clark, M.G. 1991. Open question: has thermogenesis in muscle been overlooked and misinterpreted? News Physiol. Sci. **6**: 256–259.

Colquhoun, E.Q., Hettiarachchi, M., Ye, J.M., Richter, E.A., Hniat, A.J., Rattigan, S., and Clark, M.G. 1988. Vasopressin and angiotensin II stimulate oxygen uptake in the perfused rat hindlimb. Life Sci. **43**: 1747–1754.

Colquhoun, E.Q., Hettiarachchi, M., Ye, J.M., Rattigan, S., and Clark, M.G. 1990. Inhibition by vasodilators of noradrenaline and vasoconstrictor-mediated, but not skeletal muscle contraction-induced oxygen uptake in the perfused rat hindlimb; implications for non-shivering thermogenesis in muscle tissue. Gen. Pharmacol. **21**: 141–148.

Côté, C., Thibault, M.C., and Vallières, J. 1985. Effect of endurance training and chronic isoproterenol treatment on skeletal muscle sensitivity to norepinephrine. Life Sci. **37**: 695–701.

Creese, R. 1968. Sodium fluxes in diaphragm muscle and the effects of insulin and serum proteins. J. Physiol. (London), **197**: 255–278.

De Weer, P., Gadsby, D.C., and Rakowski, R.F. 1988. Voltage dependence of the Na–K pump. Annu. Rev. Physiol. **50**: 225–241.

Dorup, I., and Clausen, T. 1997. Effects of adrenal steroids on the concentration of Na^+–K^+ pumps in rat skeletal muscle. J. Endocrinol. **152**: 49–57.

Dubois-Ferrière, R., and Chinet, A.E. 1981. Contribution of skeletal muscle to the regulatory non-shivering thermogenesis in small mammals. Pfluegers Arch. **390**: 224–229.

Edwards, R.A., Lutz, P.L., and Baden, D.G. 1989. Relationship between energy expenditure and ion channel density in the turtle and rat brain. Am. J. Physiol. **257**: R1354–R1358.

Fagher, B., Sjogren, A., and Monti, M. 1987. A microcalorimetric study of the sodium–potassium-pump and thermogenesis in human skeletal muscle. Acta Physiol. Scand. **131**: 355–360.

Gong, D.W., He, Y., Karas, M., and Reitman, M. 1997. Uncoupling protein-3 is a mediator of thermogenesis regulated by thyroid hormone, beta3-adrenergic agonists, and leptin. J. Biol. Chem. **272**: 24 129 – 24 132.

Gregg, V.A., and Milligan, L.P. 1980. Inhibition by ouabain of the O_2 consumption of mouse (*Mus musculus*) soleus and diaphragm muscles. Gen. Pharmacol. **11**: 323–325.

Grubb, B., and Folk, G.E. 1977. The role of adrenoceptors in norepinephrine-stimulated Vo_2 in muscle. Eur. J. Pharmacol. **43**: 217–223.

Hansen, O. 1984. Interaction of cardiac glycosides with (Na^+ + K^+)-activated ATPase. A biochemical link to digitalis-induced inotropy. Pharmacol. Rev. **36**: 143–163.

Hettiarachchi, M., Parsons, K.M., Richards, S.M., Dora, K.M., Rattigan, S., Colquhoun, E.Q., and Clark, M.G. 1992. Vasoconstrictor-mediated release of lactate from the perfused rat hindlimb. J. Appl. Physiol. **73**: 2544–2551.

Hochachka, P.W., Buck, L.T., Doll, C.J., and Land, S.C. 1996. Unifying theory of hypoxia tolerance: molecular/metabolic defense and rescue mechanisms for surviving oxygen lack. Proc. Natl. Acad. Sci. U.S.A. **93**(18): 9493–9498.

Izmail-Beigi, F., and Edelman, I.S. 1970. Mechanism of thyroid calorigenesis: role of active sodium transport. Proc. Natl. Acad. Sci U.S A. **67**: 1071–1078.

Jansky, L. 1995. Humoral thermogenesis and its role in maintaining energy balance. Physiol. Rev. **75**: 237–259.

Jansky, L., and Hart, J.S. 1963. Participation of skeletal muscle and

kidney during nonshivering thermogenesis in cold-acclimated rats. Can. J. Biochem. Physiol. **41**: 953–964.

Jorgensen, P.L. 1992. Na⁺/K⁺-ATPase, structure and transport mechanism. *In* Molecular aspects of transport proteins. *Edited by* J.J.H.H.M. De Pont. Elsevier, Amsterdam. pp. 1–26.

Kjeldsen, K., Nørgaard, A., and Clausen, T. 1982. Age-dependent changes in the number of [³H]ouabain-binding sites in rat soleus muscle. Biochim. Biophys. Acta, **686**: 253–256.

Larkin, S., Mull, E., Miao, W., Pittner, R., Albrandt, K., Moore, C., Young, A., Denaro, M., and Beaumont, K. 1997. Regulation of the third member of the uncoupling protein family, UCP3, by cold and thyroid hormone. Biochem. Biophys. Res. Commun. **240**: 222–227.

Lin, M.H., and Akera, T. 1978. Increased (Na⁺,K⁺)-ATPase concentrations in various tissues of rats caused by thyroid hormone treatment. J. Biol. Chem. **253**: 723–726.

Lombet, A., Frelin, C., Renaud, J.F., and Lazdunski, M. 1982. Na⁺ channels with binding sites of high and low affinity for tetrodotoxin in different excitable and non-excitable cells. Eur. J. Biochem. **124**: 199–203.

Marban, E., and Tsien, R.W. 1982. Enhancement of calcium current during digitalis inotropy in mammalian heart: positive feedback regulation by intracellular calcium? J. Physiol. (London), **329**: 589–614.

McGarry, S.J., and Williams, A.J. 1993. Digoxin activates sarcoplasmic reticulum Ca(2+)-release channels: a possible role in cardiac inotropy. Br. J. Pharmacol. **108**: 1043–1050.

Newman, J.M., Dora, K.A., Rattigan, S., Edwards, S.J., Colquhoun, E.Q., and Clark, M.G. 1996. Norepinephrine and serotonin vasoconstriction in rat hindlimb control different vascular flow routes. Am. J. Physiol. **270**: E689–E699.

Newman, J.M., Steen, J.T., and Clark, M.G. 1997. Vessels supplying septa and tendons as functional shunts in perfused rat hindlimb. Microvasc. Res. **54**: 49–57.

Rattigan, S., Dora, K.A., Colquhoun, E.Q., and Clark, M.G. 1995.

Inhibition of insulin-mediated glucose uptake in rat hindlimb by an α-adrenergic effect. Am. J. Physiol. **268**: E305–E311.

Richter, E.A., Ruderman, N.B., Gavras, H., Belur, E.R., and Galbo, H. 1982. Muscle glycogenolysis during exercise: dual control by epinephrine and contractions. Am. J. Physiol. **242**: E25–E32.

Rogart, R.B., and Regan, L.J. 1985. Two subtypes of sodium channel with tetrodotoxin sensitivity and insensitivity detected in denervated mammalian skeletal muscle. Brain Res. **329**: 314–318.

Rolfe, D.F., and Brand, M.D. 1996. Contribution of mitochondrial proton leak to skeletal muscle respiration and to standard metabolic rate. Am. J. Physiol. **271**: C1380–C1389.

Sherman, S.J., Lawrence, J.C., Messner, D.J., Jacoby, K., and Catterall, W.A. 1983. Tetrodotoxin-sensitive sodium channels in rat muscle cells developing in vitro. J. Biol. Chem. **258**: 2488–2495.

Shiota, M., and Masumi, S. 1988. Effect of norepinephrine on consumption of oxygen in perfused skeletal muscle from cold-exposed rats. Am. J. Physiol. **254**: E482–E489.

Tong, A.C.Y., Rattigan, S., Dora, K.A., and Clark, M.G. 1997. Vasoconstrictor-mediated increase in muscle resting thermogenesis is inhibited by membrane-stabilizing agents. Can. J. Physiol. Pharmacol. **75**: 763–771.

Tong, A.C.Y., Rattigan, S., and Clark, M.G. 1998. Similarities between vasoconstrictor- and veratridine-stimulated metabolism in perfused rat hind limb. Can. J. Physiol. Pharmacol. **76**: 125–132.

Wardlaw, G.M. 1986. The effect of ouabain on basal and thyroid hormone-stimulated muscle oxygen consumption. Int. J. Biochem. **18**: 279–281.

Ye, J.-M., Colquhoun, E.Q., Hettiarachchi, M., and Clark, M.G. 1990. Flow-induced oxygen uptake by the perfused rat hindlimb is inhibited by vasodilators and augmented by norepinephrine: a possible role for the microvasculature in hindlimb thermogenesis. Can. J. Physiol. Pharmacol. **68**: 119–125.

Relationship of MTT reduction to stimulants of muscle metabolism

John M.B. Newman, Carla A. DiMaria, Stephen Rattigan, John T. Steen, Kelly A. Miller, Tristram P.D. Eldershaw, Michael G. Clark *

Division of Biochemistry, Medical School, University of Tasmania, GPO Box 252-58, Hobart Tas., 7001, Australia

Abstract

MTT, a positively charged tetrazolium salt, is widely used as an indicator of cell viability and metabolism and has potential for histochemical identification of tissue regions of hypermetabolism. In the present study, MTT was infused in the constant-flow perfused rat hindlimb to assess the effect of various agents and particularly vasoconstrictors that increase muscle metabolism. Reduction of MTT to the insoluble formazan in muscles assessed at the end of experiments was linear over a 30 min period and production rates were greater in red fibre types than white fibre types. The vasoconstrictors, norepinephrine (100 nM) and angiotensin (10 nM) decreased MTT formazan production in all muscles but increased hindlimb oxygen uptake and lactate efflux. Veratridine, a Na^+ channel opener that increases hindlimb oxygen uptake and lactate efflux without increases in perfusion pressure, also decreased MTT formazan production. Membrane stabilizing doses (100 μM) of (±)-propranolol reversed the inhibitory effects of angiotensin and veratridine on MTT formazan production. Muscle contractions elicited by stimulation of the sciatic nerve, reversed the norepinephrine-mediated inhibitory effects on MTT formazan production, even though oxygen consumption and lactate efflux were further stimulated. Stimulation of hindlimb muscle oxygen uptake by pentachlorophenol, a mitochondrial uncoupler, was not associated with alterations in MTT formazan production. It is concluded that apart from muscle

* Corresponding author. Tel.: + 61-3-62262672; fax: + 61-3-62262703.
E-mail address: michael.clark@utas.edu.au (M.G. Clark).

contractions MTT formazan production does not increase with increased muscle metabolism. Since the vasoconstrictors angiotensin and norepinephrine as well as veratridine activate Na^+ channels and the Na^+/K^+ pump, energy required for Na^+ pumping may be required for MTT reduction. It is unlikely that vasoconstrictors that stimulate oxygen uptake do so by uncoupling respiration. © 2000 Elsevier Science Ireland Ltd. All rights reserved.

Keywords: Skeletal muscle; Membrane potential; Vasoconstrictors; Sodium channel

1. Introduction

Tetrazolium dyes are used widely to assay for growth in cultured cell systems [1], particularly in the area of toxicity testing [2]. The mechanism by which tetrazolium salts are converted to colored complexes appears to involve reduction by the addition of electrons donated by several dehydrogenases, where these may be cytosolic enzymes [3] or mitochondrial enzymes of the respiratory chain [1,4]. Despite the uncertainty regarding the site(s) of MTT reduction within the cell [1,3], it is clear that the MTT reduction rate closely relates to the number of actively respiring cells in cell culture [1,2,5].

The advantages of some tetrazolium salts (particularly MTT, 3-(4,5-dimethylthiazol-2-yl)-2,5-diphenyltetrazolium bromide) in monitoring growth of cell cultures are apparent in the use of microplate assays, particularly microculture tetrazolium assays [1], where ease of use and avoidance of radioisotopes replaces the use of [³H] thymidine incorporation and related approaches. MTT also affords another advantage in that the yellow water soluble MTT is converted upon reduction to a lipid insoluble purple formazan that becomes trapped within the cell, and particularly mitochondria. Having been so successful as an indicator of metabolism in cell culture, a questionarises as to whether it is similarly useful for intact tissue metabolism and could MTT be used to locate the cells or tissues responsible for increases in metabolism.

Muscle metabolism can be stimulated in the perfused rat hindlimb in a number of ways. These include muscle contraction [6], as well as agents such as selected vasoconstrictors [7], Na^+ channel openers like veratridine [8] and mitochondrial uncouplers. Vasoconstrictor effects to stimulate muscle metabolism in the constant-flow perfused rat hindlimb appear to involve redistribution of flow from non-nutritive connective tissue vessels to the nutritive route probably permitting more complete perfusion of muscle capillaries [9]. A histochemical marker of metabolism would thus have the potential to confirm this possibility.

In the present study we have measured MTT formazan production in the calf muscles of the constant-flow perfused rat hindlimb to investigate the relationship between the increases in muscle metabolism induced in a variety of ways and MTT reduction.

2. Methods

2.1. Hindlimb perfusions

Hooded Wistar rats were cared for in accordance with the principles of the Australian Code of Practice for the Care and Use of Animals for Scientific Purposes (1990, Australian Government Printing Service, Canberra). Males (180–200 g) were housed at 22°C and a 12/12 h light/dark cycle with free access to water and food (commercial rat chow, Gibsons, Hobart, Australia, containing 20.4% protein, 4.6% lipid, 69% carbohydrate and 6% crude fibre with added vitamins and minerals). Animals were anaesthetized with an intraperitoneal injection of pentobarbital sodium (6 mg/100 g body wt.). Surgery was essentially as described by others [10] with additional details as given previously [11,12]. Flow was controlled so as to perfuse exclusively the left limb by ligation of the right common iliac artery. Perfusions were performed at 25°C using a modified Krebs-Henseleit buffer containing 2% bovine serum albumin (BSA) or 4% Ficoll®, 8.3 mM glucose and 1.27 mM $CaCl_2$. The buffer reservoir was gassed with 95% O_2-5% CO_2 at 4°C to enable full oxygenation. A constant flow rate of 4.0 ± 0.2 ml/min or 0.27 ± 0.01 ml/min/g muscle was maintained and venous effluent flowed through a 0.5 ml thermostatically controlled chamber containing a Clark-type oxygen electrode to measure oxygen content. Comparison of perfusions at 25°C without red blood cells and at 37°C with red blood cells indicates that there is very little difference in agonist response and energy status of the muscle [7,13]. Perfusion pressure was continuously monitored by a pressure transducer fitted into a branch of the arterial cannula. After passage through the hindlimb and oxygen electrode, the perfusate was then either sampled or discarded. Oxygen uptake was calculated as described previously using the appropriate Bunsen coefficient [14]. The mass of muscle perfused has been previously determined for rats this size [15]. Details for sciatic nerve stimulation were as given previously [6].

2.2. Hindlimb reduction of MTT

Hindlimbs were equilibrated for 30 min prior to infusion of either norepinephrine (NE), angiotensin II (AII), veratridine (Vera), (±)-propranolol (Prop) or vehicle for 50 min. For perfusions involving (±)-propranolol in addition to vasoconstrictor or veratridine, the (±)-propranolol was infused 10 min prior to infusion of other agonists. Commencement of MTT (10 μg/ml, final) infusion began at 10 min after the start of the agonist/vehicle infusion and was maintained for a total of 30 min. This allowed a washout period of 10 min while still maintaining infusion of the agonist. The perfusion was then terminated and the muscle groups excised, freeze-dried and homogenized in 2 ml of isopropanol. After centrifugation at $1000 \times g$ for 20 min, the absorbance of the supernatant was measured at 570 nm to determine the concentration of reduced MTT (formazan).

Effluent perfusate concentrations of unconverted MTT and the reduced product were monitored at intervals throughout the infusion period. This was conducted to

check that the fraction of MTT extracted by the hindlimb remained constant ($\sim 40\%$) and that reduced MTT did not appear ($< 0.1\%$).

The extinction coefficient of formazan was determined using diaphorase and NADH to completely reduce a known amount of MTT to formazan product. Rates of reduction were calculated as mmol formazan formed/h/g dry wt. It was necessary to freeze-dry the muscle samples as the water content of the muscle caused turbidity of the isopropanol extract.

3. Statistical analysis

All data is presented as mean $\pm$ S.E. Differences in data were analysed either by Student's t-test or by analysis of variance (one-way or two-way ANOVA) with pairwise comparison by the Student–Newman–Kuel Test. Statistical significance was assumed at $P < 0.05$.

4. Results

4.1. Time course of MTT reduction

MTT (1–20 µg/ml) when infused during hindlimb perfusion had no vasoconstrictor activity, but at the highest doses (10–20 µg/ml) produced a minor vasodilatory effect against the pre-constricted hindlimb; that is with angiotensin II (AII) or norepinephrine (NE) (data not shown). On this basis a dose of 10 µg/ml was considered a compromise that avoided significant vasoactivity, but permitted sufficient MTT for reduction to be determined within a reasonable time frame.

Fig. 1 shows the amount of MTT converted to its formazan over 10, 20 or 30 min by the soleus, gastrocnemius and plantaris muscle group of the perfused rat hindlimb, respectively. Muscles were combined before analysis to ensure that the amount of MTT formazan produced was well above the detection limit of the assay. This would have been a problem for some of the individual muscles, especially soleus with NE infusion at the 10 and 20 min time intervals. The amounts increased linearly over the 30 min interval for both control (no additions) and NE (100 nM) infused hindlimbs, but the amount with NE was significantly less than that of the control at the 20 and 30 min time intervals, respectively.

4.2. Effects of vasoconstrictors

Fig. 2(a) shows that each of the vasoconstrictors, NE (100 nM) and AII (10 nM) increased perfusion pressure, oxygen uptake and lactate efflux. The metabolic effects of NE corresponded to an increase in oxygen uptake of 40.2% from 7.86 ± 0.26 to 11.02 ± 0.33 µmol/g per h. AII produced a similar stimulatory effect increasing the rate of oxygen uptake by 35.7%. Lactate efflux was increased from 8.81 ± 0.46 by 5.95 ± 0.85 and 7.83 ± 0.96 µmol/g per h, for NE and AII, respec-

tively. MTT formazan production in individual muscles is shown in Fig. 2(b). The relative order of muscle MTT formazan production under basal (no addition) conditions was soleus > gastrocnemius red > extensor digitorum longus > plantaris > tibialis > gastrocnemius white. For all muscles both vasoconstrictors decreased the rate of MTT formazan production when measured at 30 min (Fig. 2(b)). The inhibitory effects of NE were greatest in soleus (49.5%) and gastrocnemius red (53.7%).

Infusion of (±)-propranolol (100 μM) alone caused a slight increase in oxygen uptake and perfusion pressure, but had no effect on lactate efflux, or MTT formazan production in any of the muscles sampled. When added with AII, however, it significantly impaired the increase in oxygen uptake and lactate efflux due to AII without decreasing the perfusion pressure (Fig. 2(a)). The MTT formazan production rate was significantly increased compared to AII alone (Fig. 2(b)). Also, (±)-propranolol blocked the inhibition of MTT formazan production and stimulation of oxygen uptake and lactate efflux by NE (data not shown).

4.3. Effects of exercise

In a separate series of experiments the sciatic nerve in the flank of the perfused hindlimb was continuously stimulated during NE and MTT infusion and formazan production determined in individual muscles after 30 min. Contraction ($n = 3$) increased oxygen uptake beyond that caused by NE. It also reversed the inhibitory
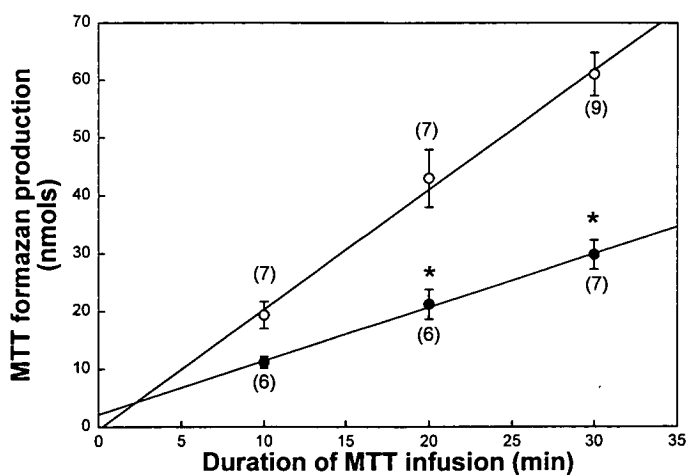

Fig. 1. MTT formazan formation by perfused rat hindlimb muscles. Hindlimbs were perfused at constant flow and vehicle (O) or 100 nM NE (●) infused for 10 min before, during and for 10 min after the infusion of MTT. Muscles of the lower leg comprising the soleus, gastrocnemius and plantaris were excised and treated as described in the text for the measurement of formazan formation. Average values for the combined muscle group were determined and means ± S.E. are shown. *$P < 0.05$ vs. vehicle (two-way ANOVA with pairwise comparison by the Student–Newman–Kuel test); n values are given in parentheses.
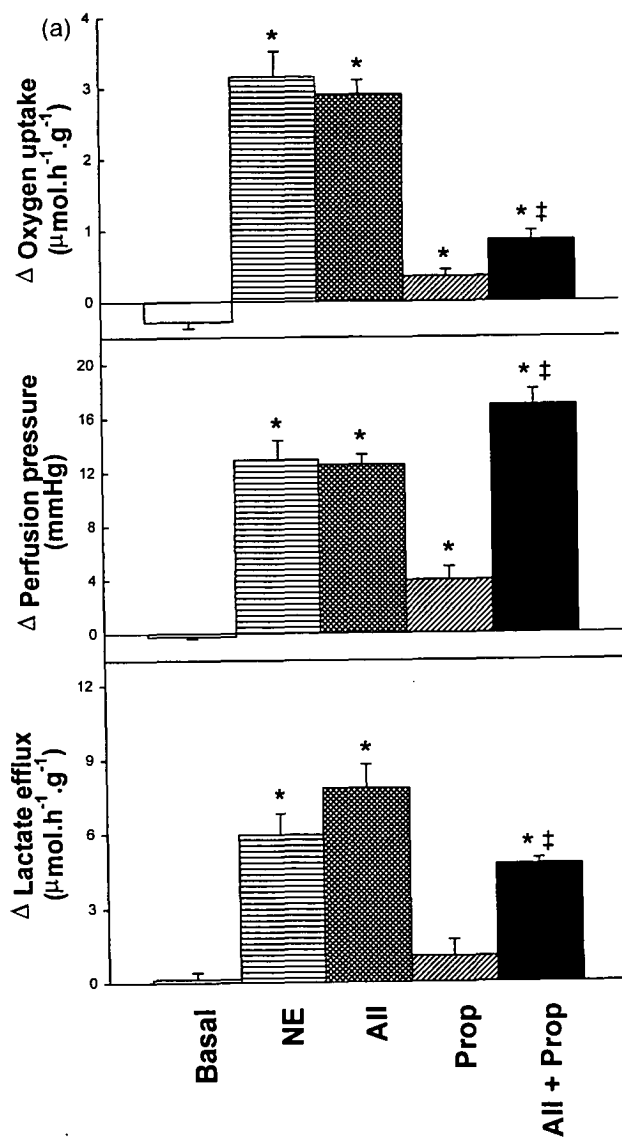
Fig. 2. Effects of the vasoconstrictors, 100 nM norepinephrine (NE), 10 nM angiotensin II (AII) and 100 μM propranolol (Prop) on: (a) oxygen uptake, lactate efflux and perfusion pressure by perfused hindlimb (during the infusion of MTT); and (b) MTT formazan production by individual muscles (at the end of MTT infusion). Experimental details are given in the text. Values are means ± S.E. ($n = 9$, 7, 12, 5 and 8 for basal, NE, AII, Prop and Prop + AII respectively). *$P < 0.05$ compared to control, ‡$P < 0.05$ compared to AII (pairwise comparison by Student–Newman–Kuel method after one-way ANOVA).

effects of NE on MTT formazan production in the five muscles, soleus (from 0.39 ± 0.03 to 0.80 ± 0.06, $P < 0.001$), plantaris (from 0.30 ± 0.02 to 0.66 ± 0.04, $P < 0.001$), gastrocnemius (from 0.24 ± 0.02 to 0.56 ± 0.07, $P < 0.001$), tibialis (from 0.34 ± 0.02 to 0.54 ± 0.06, $P < 0.01$) and extensor digitorum longus (from 0.45 ± 0.03 to 0.75 ± 0.05 μmol/g dry wt./h, $P < 0.001$).

4.4. Effects of veratridine

Veratridine, unlike NE and AII, stimulates oxygen uptake by the hindlimb independent of vasoconstriction activity [8]. Accordingly, experiments were conducted to assess whether the rate of MTT reduction was affected. Fig. 3(a) shows that veratridine increased both oxygen uptake and lactate efflux without change in perfusion pressure. MTT formazan production was significantly inhibited by veratridine in all muscles sampled (Fig. 3(b)). In addition, 100 μM ($\pm$)-propranolol, which at this dose, acts as a membrane stabilizer, reversed the veratridine-mediated changes of metabolism as well as the production of MTT formazan.

4.5. Effects of uncoupling

Pentachlorophenol (PCP) is a mitochondrial uncoupler which stimulates respiration without vasoconstrictor activity. Experiments were conducted to determine the
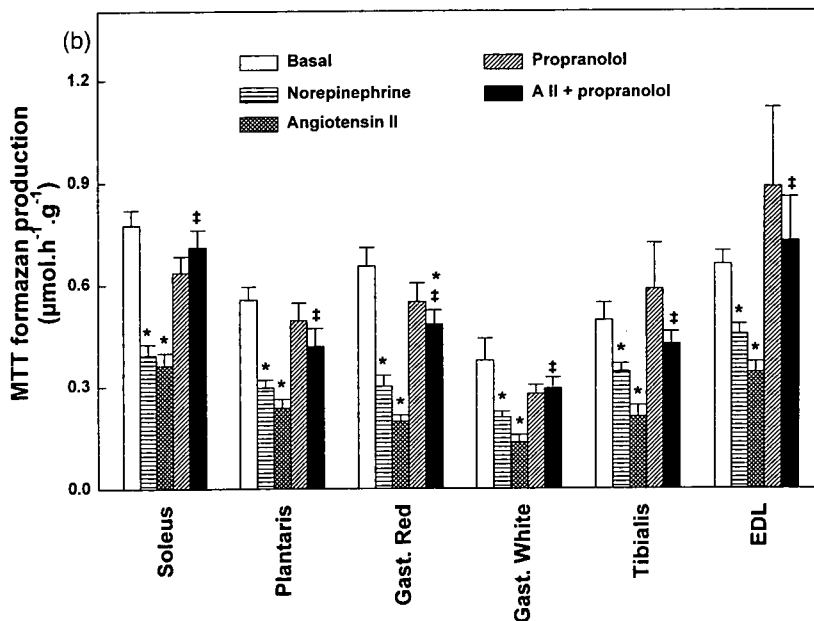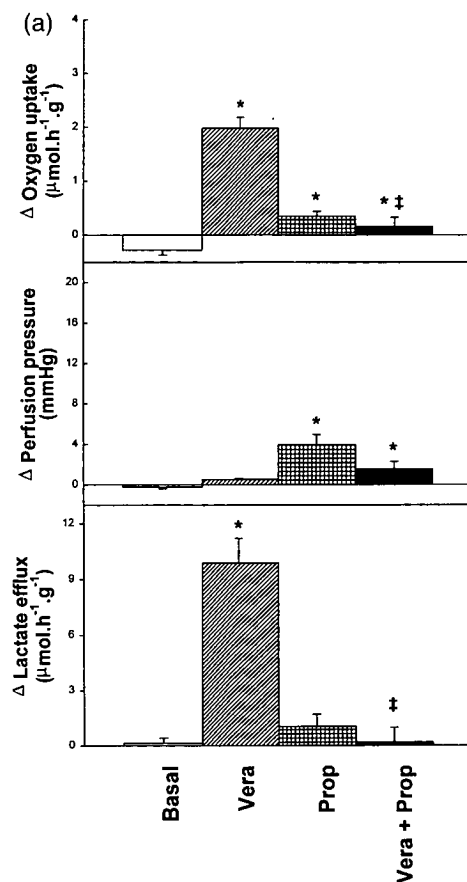

Fig. 2. (*Continued*)

Fig. 3. Effects of 30 μM veratridine (Vera) and 100 μM propranolol (Prop) on: (a) oxygen uptake, lactate efflux and perfusion pressure by perfused hindlimb (during the infusion of MTT); and (b) MTT formazan production by individual muscles (at the end of MTT infusion). Experimental details are given in the text. Values are means ± S.E. ($n = 9$, 7, 5 and 6 for basal, Vera, Prop and Vera + Prop, respectively). *$P < 0.05$ compared to control, ‡$P < 0.05$ compared to veratridine (pairwise comparison by Student–Newman–Kuel method after one-way ANOVA).

effect of 5 μM PCP on MTT formazan production. Ficoll® was used instead of BSA in the perfusion medium for these experiments because PCP is highly lipophilic and binds strongly to BSA but not Ficoll®. Data obtained in the presence of Ficoll® is shown in Table 1. Using Ficoll® instead of BSA gave a slightly higher basal pressure ($P < 0.01$), but did not affect the basal oxygen uptake or MTT formazan production by the muscles. PCP did not affect the MTT formazan production even though there was an increase in oxygen uptake of 40.4%.

5. Discussion

The main finding emerging from this study was that MTT reduction by muscles of the perfused rat hindlimb was not consistently linked to changes in muscle metabolism. Thus, apart from muscle contraction in the presence of NE where MTT reduction increased in parallel to the increase in muscle metabolism, other stimulants of muscle metabolism either inhibited (vasoconstrictors and veratridine), or had no effect (uncoupler) on the rate of MTT reduction. Overall, this would appear to be contrary to several reports where metabolism is closely linked to the rate of MTT reduction [1]. It would also be contrary to the wide spread use of MTT in cell toxicity studies where MTT metabolism has been assumed to reflect the number of viable respiring cells present [2].

For the vasoconstrictors angiotensin and norepinephrine, where metabolism was clearly stimulated MTT reduction was inhibited. Thus the use of MTT as an agent to locate the cellular sites of extra oxygen consumption stimulated by these vasoconstrictors would be inappropriate. Indeed the finding that both veratridine as well as NE and AII vasoconstrictor effects on metabolism and MTT reduction were blocked by membrane stabilizers such as propranolol that inhibit Na^+ channels, suggest that the energy required for MTT reduction is the same as that required for Na^+ pumping out of the cell, but different to that supporting uncoupled respiration induced by pentachlorophenol.
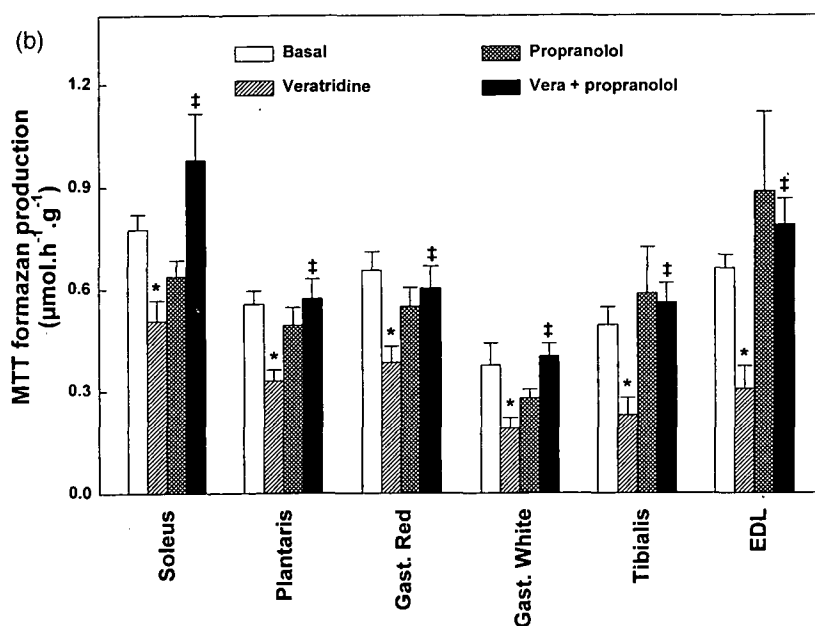

Fig. 3. (*Continued*)

Table 1

Effect of Ficoll[®] and 5 μM pentachlorophenol (PCP) on oxygen uptake, perfusion pressure and MTT formazan production in calf muscles in the perfused rat hindlimb[a]

	Basal (BSA) ($n = 9$)	Basal (Ficoll[®]) ($n = 4$)	PCP (Ficoll[®]) ($n = 4$)
Oxygen uptake (μmol/h/g)	7.81 ± 0.29	8.90 ± 0.74	12.50 ± 0.09[c]
Perfusion pressure (mmHg)	18.1 ± 0.9	23.8 ± 0.5[b]	25.8 ± 1.8
MTT formazan production (μmol/h/g)			
Soleus	0.78 ± 0.04	0.89 ± 0.11	1.12 ± 0.02
Plantaris	0.56 ± 0.04	0.59 ± 0.10	0.62 ± 0.06
Gastrocnemius red	0.66 ± 0.05	0.62 ± 0.10	0.75 ± 0.09
Gastrocnemius white	0.38 ± 0.07	0.41 ± 0.08	0.42 ± 0.05
Tibialis	0.50 ± 0.05	0.51 ± 0.09	0.39 ± 0.09
Extensor digitorum longus	0.66 ± 0.04	0.76 ± 0.12	0.55 ± 0.11

[a] Experimental details are given in the text. Data are mean ± S.E. with n values indicated. Student's t-test was used to determine significant differences.

[b] $P < 0.01$ compared to basal (BSA).

[c] $P < 0.01$ compared to basal (Ficoll[®]).

MTT is a positively charged yellow tetrazolium dye and enters the cell where it is reduced to an insoluble purple formazan by cleavage of the tetrazolium ring by dehydrogenase enzymes of the cytosol and mitochondria [3]. TPMP[+], another positively charged molecule is also taken up by viable cells. The accumulation of TPMP[+] in the mitochondrial matrix is a function of its cytosolic concentration and hence is influenced by potential and pH differences across both plasma and mitochondrial membrane [16]. However, MTT accumulation in the mitochondria may not only be the result of the mitochondrial membrane potential, but also formation of an insoluble end product which is effectively removed from further reaction. This aspect is highlighted by the linear rate of MTT reduction even at 30 min whereas the unmetabolised TPMP[+] reaches steady state accumulation within 8 min albeit in another tissue [16].

The precise site(s) at which MTT is reduced has been systematically studied [3]. They propose that in the bone marrow-derived cell line 32D most of the cellular reduction of MTT occurs extra-mitochondrially and probably involves the pyridine nucleotide cofactors NADH and NADPH. Other researchers have focused on establishing the mitochondrial site at which MTT is reduced and largely ignored the possibility that reduction might be occurring outside the mitochondria. If the bulk of the MTT reduction does indeed occur on the outer surface of the inner mitochondrial membrane [3] then the vasoconstrictor- and veratridine-stimulated metabolic events are competing for access to these dehydrogenases and thus decreasing MTT reduction. We have previously shown that veratridine increases hindlimb oxygen uptake, and this stimulatory effect is opposed by low Na^{+} or propranolol [8] at membrane-stabilizing doses thought to inhibit Na^{+} channels. Similarly, using a turtle brain synaptosome preparation it has been demonstrated

that oxygen consumption could be increased or decreased by increasing Na^+ channel activity with veratridine or closing the Na^+ channel with tetrodotoxin, respectively [17].

Changes in plasma membrane potential may alter mitochondrial membrane potential [16]. However, the effects on the mitochondrial membrane potential were relatively small and a more recent study confirmed this [18]. Using rat liver slices they found that while high K^+ medium decreased the plasma membrane potential (as reflected by increased uptake of $[^{14}C]SCN^-$), it had no significant effect on the uptake of $[^3H]TPMP^+$. This contrasted with addition of the uncoupler CCCP which greatly reduced $TPMP^+$ uptake without affecting uptake of $[^{14}C]SCN^-$. These findings suggest that uptake of cationic dyes such as MTT are likely to be more affected by changes in the mitochondrial membrane potential (such as due to uncoupling) than to changes in plasma membrane potential as might occur with Na^+ channel opening. However, in the present study, the addition of the uncoupler PCP did not affect the reduction of MTT. This could support the idea that MTT is not converted solely within the mitochondria [3]. Obviously this will require further study.

The vasoconstrictors NE and angiotensin II, unlike veratridine, mediate major changes in flow distribution within the hindlimb muscles. There is indirect evidence that the vasoconstrictors act to diminish non-nutritive flow and in so doing increase nutritive flow or muscle capillary surface area in a constant flow preparation. Improved perfusion and greater provision of nutrients to the muscle fibres should not decrease MTT reduction. It would appear that the increase in nutritive flow is not fibre type specific as NE and AII decreased MTT formazan production in all muscles sampled. Also, the alteration of flow distribution per se does not seem to contribute to the overall result since propranolol reversed the inhibitory effects of NE and AII. Previous papers show that propranolol at this concentration (100 μM) does not affect the redistribution of flow caused by NE or AII [8,19].

The involvement of different fibre types during muscle contraction could contribute to the effects seen since it is not known whether the increase in MTT formazan production from that of NE with exercise was derived from stimulated or unstimulated fibres. Reliable conclusions about the relationship between MTT reduction and other metabolic parameters in specific sets of fibres cannot be made from the data for muscle contraction.

It is possible however, that increased competition between oxygen and MTT for reducing equivalents results in less MTT reduced. Each molecule of oxygen reduced by the respiratory chain requires four electrons. One molecule of MTT requires two electrons for reduction. However, the proportion of electrons required for oxygen relative to that for MTT under basal perfusion conditions is 31:1. Thus increased competition could only occur if oxygen supply was the only change resulting from vasoconstrictor action. Analysis of metabolites indicates that vasoconstrictors increase glycerol efflux [9] in amounts to suggest that fatty acid availability has markedly increased to exceed the amount of reducing equivalents required to support the actual increase in oxygen uptake. If so, this would lessen the possibility of a competition for reducing equivalents between oxygen and MTT developing.

However, some support in favor of a generally diminished reducing equivalent availability comes from pyruvate analyses conducted in conjunction with lactate determinations (J-M. Ye, PhD thesis, University of Tasmania). These analyses indicated that the muscle lactate/pyruvate ratio decreased from 9.2 ± 1.1 to 3.1 ± 0.7 as a result of NE infusion into the constant flow perfused rat hindlimb. Using the formula:

$$K = \frac{[\text{Pyruvate}][\text{NADH}][\text{H}^+]}{[\text{Lactate}][\text{NAD}^+]}$$

from [20], the calculated cytosolic 'free NAD^+/free NADH' would then have increased from 988 to 2909 (assuming $K = 1.11 \times 10^{-11}$ M and a pH of 7.0). Thus it is possible that the vasoconstrictors NE and angiotensin II have depleted the reduced pyridine nucleotide pool sufficiently to lower MTT reduction by simply increasing oxygen availability or by other unknown mechanisms.

Tetrazolium dyes have also been extensively used in assays for superoxide and superoxide dismutase (SOD). Nitro blue tetrazolium is most commonly used [20–23] although other tetrazoliums such as XTT [24] and MTT [25] have been employed. In the present study, however, AII, NE or veratridine increased oxygen uptake of the muscle, which would be expected to increase production of superoxide and hence the reduction of MTT. Since AII, NE or veratridine caused a decrease in the reduction of MTT, the involvement of superoxide is unlikely to be a major factor.

Finally, it is worth noting that muscle contraction elicited by sciatic nerve stimulation completely overcame the inhibitory effect of NE on MTT reduction. Because oxygen uptake rate is much higher when contraction and NE are combined than for NE alone, it would seem unlikely that NE-mediated decrease in MTT reduction is the result of competition for reducing equivalents between oxygen and MTT. Moreover, the findings also imply that whatever the process responsible, it is reversed by muscle contraction induced by nerve stimulation. In this respect nerve stimulation would lead to plasma membrane hyperpolarization and the re-establishment of a favorable charge gradient for MTT entry.

In summary, MTT is reduced at a constant rate by perfused rat hindlimb muscles. Although rates generally appear to be greatest in muscles rich in slow oxidative and /or fast oxidative glycolytic fibres and are stimulated by muscle contractions, MTT reduction does not always correlate with muscle metabolism. Uncoupling mitochondria had no effect on MTT reduction whereas vasoconstrictors that increase metabolism decrease MTT reduction.

References

[1] N.J. Marshall, C.J. Goodwin, S.J. Holt, A critical assessment of the use of microculture tetrazolium assays to measure cell growth and function, Growth Regul. 5 (1995) 69–84.

[2] T. Mosmann, Rapid colorimetric assay for cellular growth and survival: application to proliferation and cytotoxicity assays, J. Immunol. Meth. 65 (1983) 55–63.

[3] M.V. Berridge, A.S. Tan, Characterization of the cellular reduction of 3-(4,5-dimethylthiazol-2-yl)-2,5-diphenyltetrazolium bromide (MTT): subcellular localization, substrate dependence, and involvement of mitochondrial electron transport in MTT reduction, Arch. Biochem. Biophys. 303 (1993) 474–482.

[4] T.F. Slater, B. Sawyer, U. Strauli, Studies on succinate-tetrazolium reductase systems. III. Points of coupling of four different tetrazolium salts, Biochim. Biophys. Acta 77 (1963) 383–393.

[5] R. Stowe, D.W. Koenig, S.K. Mishra, et al., Nondestructive and continuous spectrophotometric measurement of cell respiration using a tetrazolium-formazan microemulsion, J. Microbial. Methods 22 (1995) 283–292.

[6] S. Rattigan, K.A. Dora, A.C. Tong, et al., Perfused skeletal muscle contraction and metabolism improved by angiotensin II-mediated vasoconstriction, Am. J. Physiol. 271 (1996) E96–103.

[7] M.G. Clark, E.Q. Colquhoun, S. Rattigan, et al., Vascular and endocrine control of muscle metabolism, Am. J. Physiol. 268 (1995) E797–E812.

[8] A.C. Tong, S. Rattigan, M.G. Clark, Similarities between vasoconstrictor- and veratridine-stimulated metabolism in perfused rat hind limb, Can. J. Physiol. Pharmacol. 76 (1998) 125–132.

[9] M.G. Clark, S. Rattigan, K.A. Dora et al., Vascular and metabolic regulation of muscle, in: J.M. Kinney, H.N. Tucker (Eds.), Physiology, Stress and Malnutrition: Functional Correlates, Nutrition and Intervention, Lippincott-Raven Publishers, Philadelphia, 1997, pp. 325–346.

[10] N.B. Ruderman, C.R. Houghton, R. Hems, Evaluation of the isolated perfused rat hindquarter for the study of muscle metabolism, Biochem. J. 124 (1971) 639–651.

[11] E.Q. Colquhoun, M. Hettiarachchi, J.M. Ye, et al., Vasopressin and angiotensin II stimulate oxygen uptake in the perfused rat hindlimb, Life Sci. 43 (1988) 1747–1754.

[12] J.M. Ye, E.Q. Colquhoun, M. Hettiarachchi, et al., Flow-induced oxygen uptake by the perfused rat hindlimb is inhibited by vasodilators and augmented by norepinephrine: a possible role for the microvasculature in hindlimb thermogenesis, Can. J. Physiol. Pharmacol. 68 (1990) 119–125.

[13] K.A. Dora, S. Rattigan, E.Q. Colquhoun, et al., Aerobic muscle contraction impaired by serotonin-mediated vasoconstriction, J. Appl. Physiol. 77 (1994) 277–284.

[14] K.A. Dora, S.M. Richards, S. Rattigan, et al., Serotonin and norepinephrine vasoconstriction in rat hindlimb have different oxygen requirements, Am. J. Physiol. 262 (1992) H698–H703.

[15] S. Rattigan, K.A. Dora, E.Q. Colquhoun, et al., Inhibition of insulin-mediated glucose uptake in rat hindlimb by an alpha-adrenergic vascular effect, Am. J. Physiol. 268 (1995) E305–E311.

[16] J.B. Hoek, D.G. nicholls, J.R. Williamson, Determination of the mitochondrial protonmotive force in isolated hepatocytes, J. Biol. Chem. 255 (1980) 1458–1464.

[17] R.A. Edwards, P.L. Lutz, D.G. Baden, Relationship between energy expenditure and ion channel density in the turtle and rat brain, Am. J. Physiol. 257 (1989) R1354–R1358.

[18] W.M. Nazareth, J.K. Sethi, A.E. McLean, Effect of paracetamol on mitochondrial membrane function in rat liver slices, Biochem. Pharmacol. 42 (1991) 931–936.

[19] A.C. Tong, S. Rattigan, K.A. Dora, et al., Vasoconstrictor-mediated increase in muscle resting thermogenesis is inhibited by membrane-stabilising agents, Can. J. Physiol. Pharmacol. 75 (1997) 763–771.

[20] D.H. Williamson, P. Lund, H.A. Krebs, The Redox state of free nicotinamide-adenine dinucleotide in the cytoplasm and mitochondria of rat liver, Biochem. J. 103 (1967) 514–527.

[21] W.M. Armstead, W.G. Mayhan, Superoxide generation links protein kinase C activation to impaired ATP-sensitive K^+ channel function after brain injury, Stroke 30 (1999) 153–159.

[22] H.D. Wang, P.J. Pagano, Y. Du, et al., Superoxide anion from the adventitia of the rat thoracic aorta inactivates nitric oxide, Circ. Res. 82 (1998) 810–818.

[23] J.F. Ewing, D.R. Janero, Microplate superoxide dismutase assay employing a nonenzymatic superoxide generator, Anal. Biochem. 232 (1995) 243–248.

[24] H. Ukeda, S. Maeda, T. Ishii, et al., Spectrophotometric assay for superoxide dismutase based on tetrazolium salt 3′-1-(phenylamino)-carbonyl-3, 4-tetrazolium]-bis(4-methoxy-6-nitro)benzenesulfonic acid hydrate reduction by xanthine–xanthine oxidase, Anal. Biochem. 251 (1997) 206–209.

[25] E.O. Gomez, C. Mendoza-Milla, M.J. Ibarra-Sanchez, et al., Ceramide reproduces late appearance of oxidative stress during TNF- mediated cell death in L929 cells, Biochem. Biophys. Res. Commun. 228 (1996) 505–509.

Nutritive blood flow affects microdialysis O/I ratio for [14C]ethanol and ^3H_2O in perfused rat hindlimb

AQ: 1

JOHN M. B. NEWMAN, CARLA A. DI MARIA,
STEPHEN RATTIGAN, AND MICHAEL G. CLARK
Department of Biochemistry, Medical School, University of Tasmania, Hobart 7001, Australia

Newman, John M. B., Carla A. Di Maria, Stephen Rattigan, and Michael G. Clark. Nutritive blood flow affects microdialysis O/I ratio for [14C]ethanol and ^3H_2O in perfused rat hindlimb. *Am J Physiol Heart Circ Physiol* 281: H000–H000, 2001.—Changes in the microdialysis outflow-to-inflow (O/I) ratio for [14C]ethanol and ^3H_2O were determined in the perfused rat hindlimb after increases and decreases in nutritive flow mediated by the vasoconstrictors norepinephrine (NE) and serotonin (5-HT), respectively. Microdialysis probes (containing 10 mM [14C]ethanol and ^3H_2O pumped at 1 or 2 µl/min) were inserted through the calf of the rat. Hindlimb perfusion flow rate was varied from 6 to 56 ml·min^{-1}·100 g^{-1} in the presence of NE, 5-HT, or saline vehicle. The O/I ratios for both tracers were determined at each perfusion flow rate, as was perfusion pressure, oxygen uptake (a surrogate indicator of nutritive flow), and lactate release. Both tracers showed a decreased O/I ratio as hindlimb perfusion flow was increased, with [14C]ethanol being higher than ^3H_2O. NE decreased the O/I ratio compared with vehicle, and 5-HT increased it for both tracers and both microdialysis flow rates. We conclude that the microdialysis O/I ratio, while able to detect changes in total flow, is also sensitive to changes in nutritive and nonnutritive flow, where the latter still extracts tracer, but less than the former.

vasoconstrictors; interstitial fluid; nutritive/nonnutritive blood flow; total blood flow; skeletal muscle; outflow-to-inflow ratio

MICRODIALYSIS IS A TECHNIQUE used to monitor the concentrations of biologically important compounds in the interstitial fluid of various organs including the brain, skin, adipose tissue, and muscle (for reviews, see Refs. 3 and 16). The technique is also used to monitor blood flow in tissues by the addition of ethanol to the microdialysis solution. As it passes through the probe, ethanol diffuses into the tissue and is removed by the blood. The ratio of the outflow concentration to inflow concentration (O/I ratio) of ethanol has been found to vary inversely with the total blood flow in skeletal muscle (19, 36), which has been mathematically modeled (38). The method has been extended to use [14C]ethanol as well as ^3H_2O, both of which have been shown to give similar qualitative results (36), with

^3H_2O having a lower O/I ratio, reflecting its ability to diffuse more readily across the dialysis membrane and through the interstitial fluid.

Work in this laboratory using the constant flow perfused rat hindlimb has followed from a number of studies that concluded that there were two vascular pathways in skeletal muscle (1, 15, 21, 27, 32) and has been recently reviewed (7). It has led to the finding that vasoconstrictors can be characterized into two groups based on their effects on muscle metabolism (6). These vasoconstrictor-mediated changes occur without any changes in bulk flow between individual muscles or other tissues, as indicated by microsphere embolism (7). The first group, type A, to which norepinephrine (NE) belongs, increase oxygen uptake (11), aerobic muscle contraction (31), and release of lactate (17), glycerol (5), uracil, and uric acid (9). Type B vasoconstrictors, to which serotonin (5-HT) belongs, on the other hand, decrease oxygen uptake (12), aerobic muscle contraction (13), insulin-mediated glucose uptake (29), and acute release of lactate (6), glycerol (6), uric acid, and uracil (6). These effects of vasoconstrictors are mediated via the vasculature, because the effects on pressure and metabolism can be reversed by the addition of vasodilators (10, 11, 17, 29). In addition, the stimulatory (or inhibitory) effects of vasoconstrictors on contractility or insulin-mediated glucose uptake seen in perfused muscle are absent when muscles are isolated and incubated (13, 29, 30). Accordingly, we proposed that the two types of vasoconstrictors (A and B) achieve these effects by redistributing flow at the microvascular level, with type A or B increasing or decreasing nutritive flow, respectively (7). To add to this notion, we have shown that type A vasoconstrictors increase blood flow to vessels supplying the muscle cells (7, 25), whereas type B vasoconstrictors redirect flow away from the muscle cells (7, 25) toward vessels of limited exchange capacity probably associated with the interfibrillar septa of muscle and with tendon (26). An inverse relationship between oxygen uptake and tendon vessel flow exists (26), suggesting that, under the conditions of the constant-flow perfused hindlimb, oxygen uptake is a surrogate indicator of nutritive

| tapraid4/h4-ahea/h4-ahea/h41201/h41200d01a | sweigarl | S=6 | 9/5/01 | 13:16 | MS: H0335-1 | Ini: 12e/kmp | Input-DCT-nlk |

H2   NUTRITIVE FLOW AND MICRODIALYSIS

flow. Further evidence that the nonnutritive route is present in the muscle body comes from our most recent studies (4, 37) where both nutritive and nonnutritive routes were found to be distributed homogeneously in muscle.

The redirection of flow within each muscle of the perfused rat hindlimb in the absence of changes in total flow may have important implications for the microdialysis ethanol technique. The addition of a type A vasoconstrictor would be expected to switch flow from nonnutritive to nutritive and thereby improve the removal of ethanol from the probe, leading to a decrease in the O/I ratio. Type B vasoconstrictors would have the opposite effect, switching flow from the nutritive to the nonnutritive, which still extracts tracer, but less than nutritive flow; thus the O/I ratio should increase. In this study, the O/I ratio for [^{14}C]ethanol and ^3H_2O were determined in the perfused rat hindlimb over a range of total blood flow rates with and without the addition of the vasoconstrictors NE or 5-HT to alter the proportion of nutritive to nonnutritive flow.

METHODS

Animals. Male hooded Wistar rats were cared for in accordance with the principles of the Australian Code of Practice for the Care and Use of Animals for Scientific Purposes (Australian Government Printing Service; Canberra, Australia). Experimental procedures were approved by the Committee on the Ethical Aspects of Research Involving Animals of the University of Tasmania. Rats (180–200 g) were housed at 22°C and were given free access to water and a commercial rat chow (Gibsons; Hobart, Australia; containing 20.4% protein, 4.6% lipid, 69% carbohydrate, and 6% crude fiber with added vitamins and minerals). Anesthesia was administered by pentobarbitone sodium (6 mg/100 g body wt ip) before all surgical procedures.

F1   Microdialysis probes were linear in construction (Fig. 1A). The point of a 23-gauge Terumo syringe needle was blunted by filing, and the syringe adapter was removed. A short length (25 mm) of microdialysis tubing (Bioanalytical Systems; molecular-weight cutoff, 30 kDa; outer diameter, 320
AQ: 2 μm) was inserted into the blunt end of the needle to a depth of ~5 mm and glued using Araldite. The amount of glue was kept to a minimum so that the overall diameter was less than the internal diameter of a 16-gauge syringe needle.

Hindlimb perfusions. Perfusions were conducted in a temperature-controlled cabinet set at 37°C. The perfusion medium was a modified Krebs-Henseleit buffer (118 mM NaCl, 4.7 mM KCl, 1.2 mM KH_2PO_4, 1.2 mM $MgSO_4$, 25 mM $NaHCO_3$, and 8.3 mM glucose) containing 2.5 mM $CaCl_2$, 4% bovine serum albumin, and washed bovine erythrocytes (35% hematocrit). Fresh bovine erythrocytes were washed three times in saline (0.9% NaCl) and twice in Krebs-Henseleit buffer and were stored in Krebs-Henseleit buffer at 4°C until use (erythrocytes were never >5 days old when used). Perfusate was gassed via a Silastic tube oxygenator with 95% air-5% CO_2 and brought to 37°C by a heat exchanger coil. Both the arterial and venous perfusate passed through an arteriovenous oxygen difference analyzer (A-VOX Systems), which measures the spectral difference of arterial versus venous blood at 660 nm (35). Arterial pressure and the arteriovenous difference in blood oxygen (in ml O_2/100 ml blood) were recorded continuously by the data acquisition
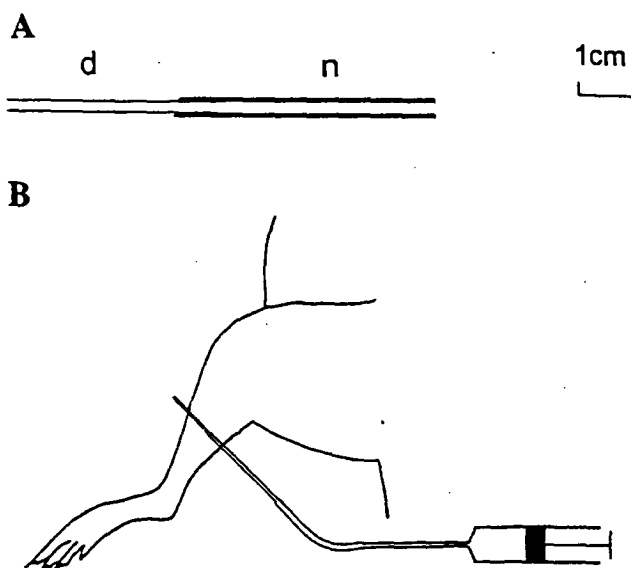

Fig. 1. Microdialysis probe design and positioning in rat hindlimb muscles. *A*: the linear probe comprised 25 mm of dialysis tubing (d), of which ~5 mm was glued inside a 23-gauge syringe needle (n). Scale is indicated by the bar. *B*: positioning in the lower leg muscles required a 18-gauge syringe needle to be carefully inserted through the muscle, right to left. The steel end of the probe was inserted into the emergent end of the 18-gauge needle, which was then slowly withdrawn, leaving only the microdialysis tubing in contact with the muscle. Other details are given in the text.

program Windaq. The arterial and venous perfusate were periodically sampled for the determination of lactate concentration on a Yellow Springs Instrument glucose/lactate analyzer.

Hindlimb surgery was essentially as described in Ref. 34 with modifications as given in Ref. 11. Flow was restricted to the left hindlimb by ligation of the right common iliac artery and vein. Also during the surgery, a small area of skin over the gastrocnemius and tibialis muscles was removed. One or two microdialysis probes were inserted into the muscle with the aid of an 18-gauge syringe needle. This was achieved by initially inserting the 18-gauge steel needle through the muscle at the site where the probe was to be positioned. The steel 23-gauge needle end of the probe was then inserted into the emergent end of the 18-gauge needle, which was then slowly withdrawn. Care was taken to ensure that the probe remained snugly within the 18-gauge needle. Withdrawal was continued until 10 mm of the dialysis tubing was positioned within the muscle (Fig. 1B). The 18-gauge needle was discarded, and the needle end of the microdialysis probe was attached to a syringe pump. During equilibration of the hindlimb preparation, the microdialysis probes were flushed with 200 μl saline (0.9% NaCl) containing 10 mM [^{14}C]ethanol (100 nCi/ml) and ^3H_2O (500 nCi/ml). For the remainder of the experiment, the syringe pumps were set at 1 or 2 μl/min. The hindlimb preparation was allowed to equilibrate for 20 min at 4 ml/min of hindlimb perfusate flow before the addition of either 70 nM NE, 300 nM 5-HT, or saline vehicle into the arterial perfusate. After equilibration, the hindlimb perfusion flow rate was changed at 30-min intervals in a stepwise manner to 1, 2, 4, 6, and 9 ml/min. To minimize evaporative loss, microdialysate samples were collected into narrow preweighed microfuge tubes (diameter, 12 × 4 mm), which were uncapped. Samples were collected in the last 10

min with either one 10-min sample for probes set at 1 μl/min or two 5-min samples for probes set at 2 μl/min. The volume of sample collected was then determined by reweighing the tubes, which were then put into 5-ml vials containing 3 ml of scintillant. Prior testing indicated that the volume of the collected dialysate was as expected from the perfusion rate and time of collection; the consecutive 5-min samples at 2 μl/min were averaged because they were not significantly different. A known volume of the inflow solution was also put into a vial containing 3 ml of scintillant. Vials were then counted for ^{14}C and ^{3}H in a Beckman counter (LS 6500), and the O/I ratios for both [14C]ethanol and [3]H_2O were determined.

A separate set of experiments was conducted to assess the effect of a vasodilator on the O/I ratio of [14C]ethanol and [3]H_2O. Perfusions were equilibrated with a single probe in the calf muscle set at 2 μl/min and the perfusion flow rate at 4 ml/min for 40 min. Subsequently, either saline vehicle, 0.5 mM nitroprusside (NP), 70 nM NE, 70 nM NE + 0.5 mM NP, 300 nM 5-HT, or 300 nM 5-HT + 0.5 mM NP were infused for 40 min. During the last 10 min of the equilibration and treatment periods, two 5-min samples of microdialysate were collected. The O/I ratios for [14C]ethanol and [3]H_2O were determined in the same way as the previous set of experiments.

Statistics. One-way or two-way repeated-measures ANOVA was performed using SigmaStat (SPSS Science; Chicago, IL), with comparisons made between conditions using the Student-Newman-Kuels' post hoc test. Significance was assumed at the level of $P < 0.05$. Data are presented as means ± SE; if error bars are not visible, they are within the symbol.

RESULTS

Figure 2 shows changes in hindlimb perfusion pressure, oxygen uptake, and lactate efflux of the perfused hindlimb in response to increasing total flow. At the doses chosen, NE and 5-HT produced similar increases in pressure, which were significantly above that of the vehicle (Fig. 2A). Figure 2B shows that NE significantly increased oxygen uptake compared with vehicle at all flow rates except 1 ml/min, whereas 5-HT significantly decreased oxygen uptake at the higher three flow rates. Lactate efflux was significantly different to vehicle in the presence of NE at the three higher flow rates but was unaffected by 5-HT (Fig. 2C).

The effect of increasing hindlimb perfusion flow rates on the O/I ratio for [14C]ethanol is shown in Fig. 3. Figure 3A shows data from probes set at 1 μl/min, and Fig. 3B shows data from probes set at 2 μl/min. Increasing the perfusion flow rate decreased the O/I ratio for [14C]ethanol under all three conditions, as indicated by a significant difference compared with values at 1 ml/min. NE significantly decreased the O/I ratio compared with vehicle at perfusion flow rates of 2, 6, and 9 ml/min for probes set at 1 μl/min (Fig. 3A) and at all perfusion flow rates for probes set at 2 μl/min (Fig. 3B). 5-HT, on the other hand, significantly increased the O/I ratio at perfusion flow rates of 4, 6, and 9 ml/min for probes set at 1 μl/min (Fig. 3A) and at 6 and 9 ml/min for probes set at 2 μl/min (Fig. 3B).

The effect of increasing hindlimb perfusion flow rates on the O/I ratio for [3]H_2O is shown in Fig. 4.
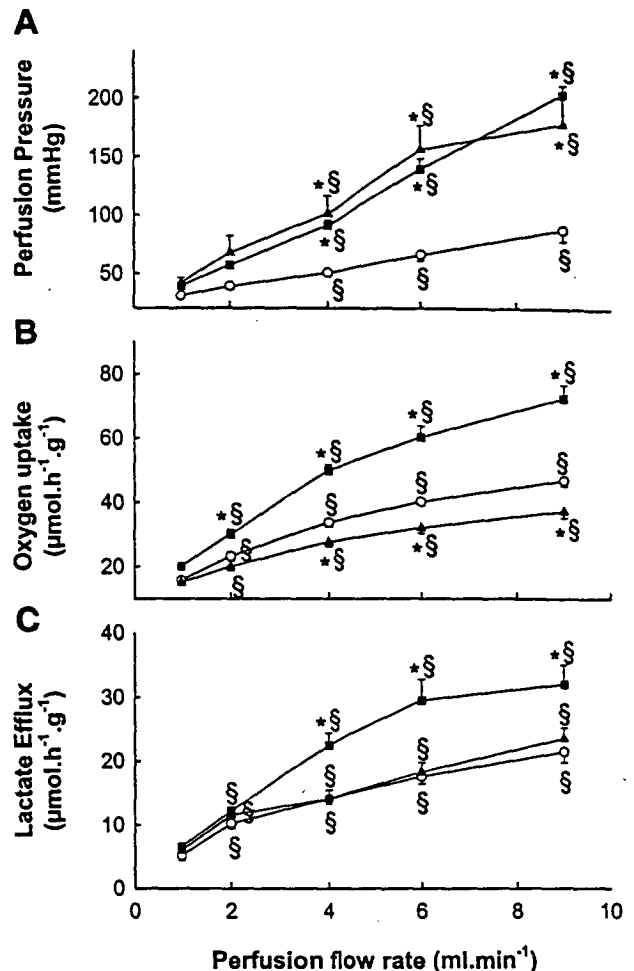

Fig. 2. Effect of vehicle, norepinephrine (NE), or serotonin (5-HT) on perfusion pressure (A), oxygen uptake (B), and lactate efflux (C) in the perfused rat hindlimb at varying total flow rates. The conditions were: ○, vehicle; ■, NE; and ▲, 5-HT; $n = 6$ for all conditions at flow rates of 1 and 2 ml/min and $n = 10$ for the higher flow rates. Statistical significant was assessed by two-way repeated-measures ANOVA, with comparisons using the Student-Newman-Kuels' multiple-comparison procedure. Data were compared with 1 ml/min within each condition (§$P < 0.05$) or to vehicle values at corresponding perfusion flow rates (*$P < 0.05$).

Increasing perfusion flow rate led to decreasing O/I ratios for [3]H_2O under all three conditions (shown by a significant difference compared with values at 1 ml/min). NE significantly decreased the O/I ratio for [3]H_2O at all perfusion flow rates for both probe flow rates compared with vehicle. 5-HT significantly increased the O/I ratio compared with basal at all perfusion flow rates except 1 ml/min for probes set at 1 μl/min (Fig. 4A) and perfusion flow rates of 4–9 ml/min for probes set at 2 μl/min (Fig. 4B).

Figure 5 shows the effect of the vasodilator NP as well as NE and 5-HT on the oxygen uptake, perfusion pressure, and O/I ratios for [14C]ethanol and [3]H_2O. NP blocked all of the increase in pressure due to NE or 5-HT. There was a slight dilation below basal, although this was not significant. The effect of NP on oxygen
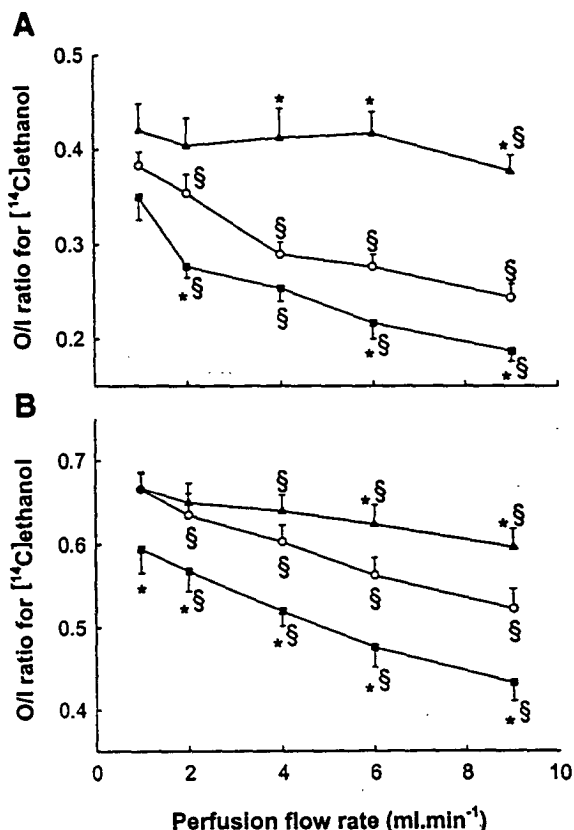
| tapraid4/h4-ahea/h4-ahea/h41201/h41200d01a | sweigari | S=6 | 9/5/01 | 13:16 | MS: H0335-1 | Ini: 12e/kmp | Input-DCT-nik |

H4   NUTRITIVE FLOW AND MICRODIALYSIS

Fig. 3. Effect of vehicle, NE, or 5-HT on the outflow-to-inflow (O/I) ratio of [14C]ethanol in the perfused rat hindlimb. Microdialysis probes were set at 1 μl/min (A) or 2 μl/min (B). Conditions and symbols were the same as in Fig. 2; n = 8 for all conditions at all perfusion flow rates in A and the same as for Fig. 2 in B. Data were compared with 1 ml/min within each condition (§$P < 0.05$) or to vehicle values at corresponding perfusion flow rates (*$P < 0.05$).

by microsphere entrapment being unchanged by NE or 5-HT (5).

Explanations for this must, therefore, concentrate on how NE and 5-HT can affect the removal of [14C]ethanol and ^3H_2O from the microdialysis probe. For the tracers to be removed from the system, they must first diffuse into the interstitial fluid and from there into the capillaries to be carried away by the blood flow. Diffusion into the capillaries can be affected by two things: one is the blood flow rate through capillaries with direct access to the interstitial fluid and the other is the number of capillaries through which the blood flow is passing at any time. The total blood flow, as assessed by 15-μm microsphere distribution, to individual muscles was unaffected by NE or 5-HT (5). It is thus the second component which the vasoconstrictors are likely to have altered. That is, we would envisage that NE and 5-HT have changed the effective tissue blood flow at a level of vessels smaller than 15 μm that are in contact with the interstitial fluid around the probe. Therefore, because NE decreased the O/I ratio, it is
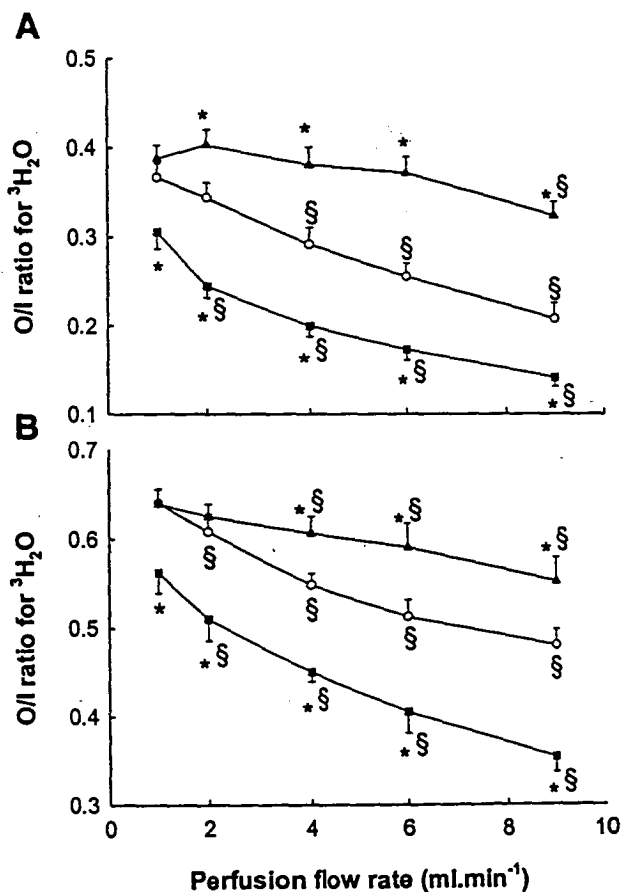
uptake was inhibitory and so did not block the 5-HT-mediated decrease in oxygen uptake. NP, however, was able to block the increase in oxygen uptake due to NE. NP entirely blocked the change in the O/I ratios for both tracers due to NE and 5-HT. A tendency for NP to increase the O/I ratio under basal conditions was not significant.

DISCUSSION

The major finding arising from this study is that, whereas the O/I ratio of [14C]ethanol and ^3H_2O is inversely related to the total flow in the perfused rat hindlimb, the ratio can also be affected by the addition of the vasoconstrictors NE and 5-HT. The inverse relationship between the O/I ratio and total flow supports data by other researchers (19, 36). The important new data are that two vasoconstrictors that have similar effects on pressure, but opposing effects on muscle oxygen uptake and hence nutritive flow, can also have opposing effects on the O/I ratios of [14C]ethanol and ^3H_2O. This is despite the proportion of total flow to individual muscles and muscle as a whole, as indicated

Fig. 4. Effect of vehicle, NE, or 5-HT on the O/I ratio of ^3H_2O in the perfused rat hindlimb. Microdialysis probes were set at 1 μl/min (A) or 2 μl/min (B). Conditions and symbols were the same as in Figs. 2 and 3; n = 8 for all conditions at all perfusion flow rates in A and the same as for Fig. 2 in B. Data were compared with 1 ml/min within each condition (§$P < 0.05$) or to vehicle values at corresponding perfusion flow rates (*$P < 0.05$).
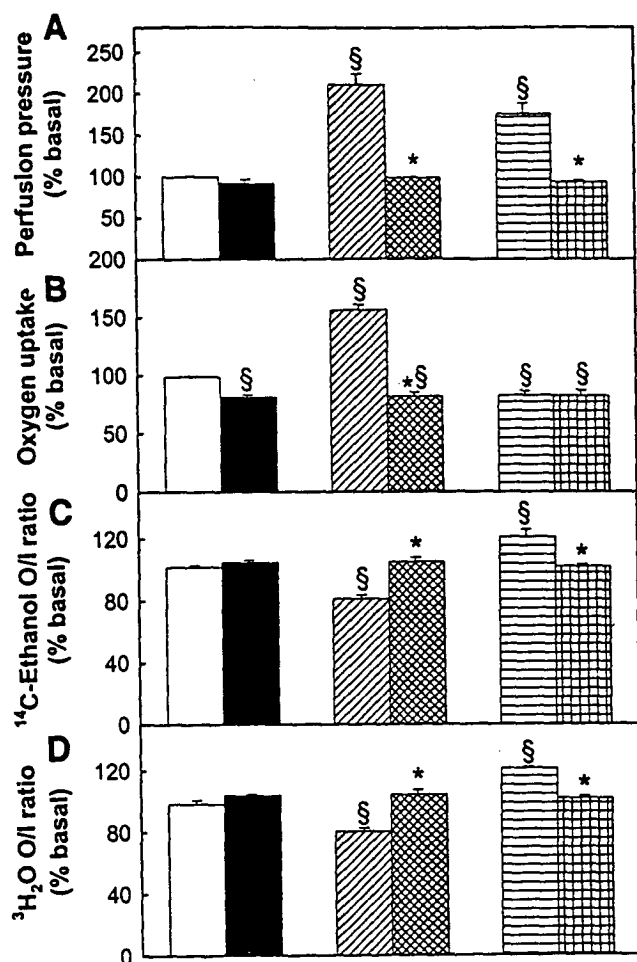
| tapraid4/h4-ahea/h4-ahea/h41201/h41200d01a | sweigart | S=6 | 9/5/01 | 13:16 | MS: H0335-1 | Ini: 12e/kmp | Input-DCT-nlk |

NUTRITIVE FLOW AND MICRODIALYSIS   H5

Fig. 5. Effect of vehicle, nitroprusside (NP), NE, and 5-HT on perfusion pressure (A), oxygen uptake (B), O/I ratio for [^{14}C]ethanol (C), and O/I ratio for ^{3}H$_2$O (D). Perfusion flow rate was 4 ml/min and probe flow rate was 2 µl/min. Data are shown as a percentage of the corresponding basal for each condition: vehicle (open bars; n = 5), 0.5 mM NP (solid bars; n = 4), 70 nM NE (hatched bars; n = 5), 70 nM NE + 0.5 mM NP (crosshatched bars; n = 4), 300 nM 5-HT (horizontally lined bars; n = 4), and 300 nM 5-HT + 0.5 mM NP (horizontally and vertically lined bars; n = 4). Statistical significance was assessed by two-way repeated-measures ANOVA, with comparison using the Student-Newman-Kuels' multiple-comparison test. Data were compared with their corresponding basal values (§P < 0.05) or to corresponding data without NP (*P < 0.05).

likely to have increased the local tissue blood flow adjacent to the probe by increasing the number of capillaries and/or the flow rate through the capillaries near the probe. Because total flow to each muscle remained constant, the increase in flow around the probe must come at the expense of flow to another part of the muscle. The concept of increased number of capillaries being perfused is consistent with previous studies showing that NE accesses a new vascular space in muscle (25) at the expense of flow in the nonnutritive route, which may located nearby in muscle (4) or in connective tissue (26).

5-HT, on the other hand, probably decreased the number of capillaries and/or the flow rate through

capillaries in contact with interstitial fluid around the probe. In a complementary fashion to NE, 5-HT is likely to have increased flow through vessels smaller than 15 µm that are less involved with nutrient exchange but still within the muscle for the total flow to the muscle to remain constant. Again, this is consistent with previous studies, where 5-HT was found to deny access to a vascular space (25), increase nonnutritive flow (4), and increase connective tissue vessel flow (26).

It is important to note that the effects of either NE or 5-HT to change the O/I ratios were blocked by the nitrovasodilator sodium NP in association with blockade of the pressure increases. This confirms that the effects of NE and 5-HT are the result of the vasoconstrictor activity and are not the result of receptor-mediated metabolic effects in the skeletal muscle. Because the perfused rat hindlimb is essentially fully dilated under basal conditions, NP has no significant pressure-lowering effect unless the hindlimb vasculature is preconstricted by either NE or 5-HT. (Fig. 5A). Thus NP prevents flow redistribution by relaxing the sites constricted by either agonist.

At present, there are no methods that allow a quantitative assessment of the proportion of nutritive to nonnutritive flow either under basal conditions (no additions) or after NE or 5-HT addition. Thus the interventions serve simply to alter the proportion of flow, and, at best, only approximations can be made. For example, Fig. 4A shows that 5-HT addition at the total flow rate of 9 ml/min increased the O/I ratio of ^{3}H$_2$O to a value of nutritive flow comparable with that of NE at 1 ml/min. From that, the nutritive flow after 5-HT is approximately one-ninth the total flow, providing NE has fully recruited nutritive flow at 1 ml/min. However, the precise proportion is unknown, and the extent of change induced by each agonist is dependent on dose and bulk perfusion flow rate. While this may account for the similar O/I ratios, such absolute values for relative flow in the two routes must be treated with caution.

The O/I ratio for ethanol has been used in animals to monitor blood flow changes during insulin infusion (14, 20, 22) as well as in humans during hyperinsulinemia (33), glucose ingestion (23), or exercise (18). A recent study (28) on exercising humans showed that exercise, which increased femoral blood flow, decreased the O/I ratio of ethanol but that the O/I ratio was unaffected by the subsequent infusion of adenosine despite further increases in femoral blood flow. The authors concluded AQ: 3 that the O/I ratio of ethanol was due to changes in the probe recovery during exercise rather than the increase in flow to the muscles. This apparent discrepancy between flow and O/I ratio may be explained by the notion of two vascular routes through muscle. The infusion of vasodilators such as adenosine, while increasing total blood flow, would not necessarily increase the flow to capillaries in intimate contact with muscle cells. This has indeed been shown to be the case for isoproterenol, which specifically dilates the transverse arterioles of the rabbit tenuissimus muscle to increase flow to the connective tissue at the expense of

tapraid4/h4-ahea/h4-ahea/h41201/h41200d01a | sweigard | S=6 | 9/5/01 | 13:16 | MS: H0335-1 | Ini: 12e/kmp | Input-DCT-nlk

H6   NUTRITIVE FLOW AND MICRODIALYSIS

flow to muscle (2). Data from this study also suggest that the vasodilator NP does not enhance nutritive flow in that it decreased oxygen uptake and had a tendency to increase the O/I ratio for both [^{14}C]ethanol and ^3H_2O under basal (vehicle only) conditions (Fig. 5).

The use of the microdialysis O/I ratio as a putative indicator of total blood flow in skeletal muscle would seem to be of use only if the proportion of nutritive to nonnutritive flow remains constant. The presence of two vascular pathways in muscle may have also led to discrepancies between total flow and laser Doppler flowmetry (LDF). A study (24) using LDF on rat skeletal muscle during ganglionic blockade found that changes in LDF signal were dissociated with changes in total muscle blood flow, as measured by microspheres during the infusion of vasoactive drugs. In a recent study (4) from our laboratory, the LDF signal from implantable microprobes inserted into muscles of the perfused rat hindlimb was investigated. The data showed there were three characteristic responses to the infusion of NE and 5-HT indicative of discrete regions of nutritive and nonnutritive flow in muscle. Larger surface probes showed only one type of response, that of increasing nutritive flow in response to NE (4).

This study therefore provides further evidence for the existence of two flow pathways within muscle, the nutritive and nonnutritive vessels (7, 8). The nonnutritive vessels, which are probably distributed throughout the muscle in the interfibrillar septa, are readily visible in the tendon region (26). They would probably be of short length and larger diameter, but still be capillary in nature and therefore unable to pass 15-μm microspheres and with a low capacity for nutrient exchange. The model most likely is one where there are both nutritive and nonnutritive routes in the immediate vicinity of the probe, so that the two vasoconstrictors have simply acted by switching flow from the nutritive route, which can pick up the ^3H_2O or [^{14}C]ethanol, to the nonnutritive route, which still extracts tracer but less than nutritive flow. Given that the probe is 320 μm in diameter, the region within the muscle tissue sensed by the probe is likely to be a cylinder of 640–1,120 μm [i.e., 2- to 3.5-fold the diameter of the probe (38)]. If this is so, then the region of sensing would contain both nutritive and nonnutritive routes, as recently detected using a randomly placed 260-μm-diameter LDF microprobe (4) and predicted by the findings of Vincent et al. (37)

The O/I ratio of ethanol in skeletal muscle has been mathematically modeled (38). The model described how the O/I ratio changed as the flow rate through the microdialysis probe and the blood flow rate changed. A further study (19) showed consistency between the model and experimental data. However, there was no contingency for the distribution of flow within muscle. Clearly, this requires a reconsideration of the model (38) particularly in view of our present findings and the presence of two alternative flow routes in muscle.

It is assumed that the vasoconstrictors do not affect the metabolism of ethanol, which would then affect the

O/I ratio. Metabolism of ethanol would seem very unlikely because the O/I ratios of both tracers, [^{14}C]ethanol and ^3H_2O, show very similar patterns (Figs. 3 and 4) and muscle does not appreciably metabolize ethanol because it contains no alcohol dehydrogenase. Metabolic effects of the vasoconstrictors are also unlikely because the addition of the vasodilator NP blocked the effect of NE and 5-HT on the O/I ratios.

There appears to be little advantage between either of the tracers used in this study due to the similarity of the results gained by them. It may be, however, that ^3H_2O is a more useful tracer because it is more freely diffusable. Also, ethanol is more prone to evaporation in the collection tube than water and thus can lead to greater errors in measurement. Indeed, if a proportion of the ethanol evaporated, this would not make an appreciable difference to the volume collected but would mean that the actual concentration of [^{14}C]ethanol was underestimated. In the case of ^3H_2O, any loss by evaporation would be matched by a loss of total volume without a net effect on tracer concentration. This may be reflected in the fact that, whereas the O/I ratio of [^{14}C]ethanol was above that for ^3H_2O, the difference is not as great as has been reported previously (36).

In conclusion, the current study demonstrates that the O/I ratios of [^{14}C]ethanol and ^3H_2O reflect both the total flow to muscle and the distribution of flow in pathways within muscle. Therefore, the distribution of flow within muscle, specifically the proportion of total flow that is nutritive, must be taken into account in the interpretation of data obtained with this method. The findings reinforce the notion that the nonnutritive route carries flow but is unavailable for nutrient as well as [^{14}C]ethanol and ^3H_2O exchange. Finally, providing bulk blood flow to muscle remains constant, microdialysis using the O/I ratio of [^{14}C]ethanol or ^3H_2O has the potential to be a qualitative measure of the proportion of nutritive to nonnutritive flow.

REFERENCES

1. Barlow TE, Haigh AL, and Walder DN. Evidence for two vascular pathways in skeletal muscle. Clin Sci 20: 367–385, 1961.
2. Borgstrom P, Bruttig SP, Lindbom L, Intaglietta M, and Arfors KE. Microvascular responses in rabbit skeletal muscle after fixed volume hemorrhage. Am J Physiol Heart Circ Physiol 259: H190–H196, 1990.
3. Chaurasia CS. In vivo microdialysis sampling: theory and applications. Biomed Chromatogr 13: 317–332, 1999.
4. Clark AD, Youd JM, Rattigan S, Barrett EJ, and Clark MG. Heterogeneity of laser Doppler flowmetry in perfused muscle indicative of nutritive and nonnutritive flow. Am J Physiol Heart Circ Physiol 280: H1324–H1333, 2001.
5. Clark MG, Colquhoun EQ, Dora KA, Rattigan S, Eldershaw TPD, Hall JL, Matthias A, and Ye JM. Resting muscle: a source of thermogenesis controlled by vasomodulators. In: Temperature Regulation: Recent Physiological and Pharmacological Advances, edited by Milton AS. Basel: Birkhauser Verlag, 1994, p. 355–320. AQ:

6. Clark MG, Colquhoun EQ, Rattigan S, Dora KA, Eldershaw TP, Hall JL, and Ye J. Vascular and endocrine control of muscle metabolism. *Am J Physiol Endocrinol Metab* 268: E797–E812, 1995.

7. Clark MG, Rattigan S, Clerk LH, Vincent MA, Clark AD, Youd JM, and Newman JM. Nutritive and non-nutritive blood flow: rest and exercise. *Acta Physiol Scand* 168: 519–530, 2000.

8. Clark MG, Rattigan S, Newman JM, and Eldershaw TP. Vascular control of nutrient delivery by flow redistribution within muscle: implications for exercise and post-exercise muscle metabolism. *Int J Sports Med* 19: 391–400, 1998.

9. Clark MG, Richards SM, Hettiarachchi M, Ye JM, Appleby GJ, Rattigan S, and Colquhoun EQ. Release of purine and pyrimidine nucleosides and their catabolites from the perfused rat hindlimb in response to noradrenaline, vasopressin, angiotensin II and sciatic-nerve stimulation. *Biochem J* 266: 765–770, 1990.

10. Colquhoun EQ, Hettiarachchi M, Ye JM, Rattigan S, and Clark MG. Inhibition by vasodilators of noradrenaline and vasoconstrictor-mediated, but not skeletal muscle contraction-induced, oxygen uptake in the perfused rat hindlimb–implications for non-shivering thermogenesis in muscle tissue. *Gen Pharmacol* 21: 141–148, 1990.

11. Colquhoun EQ, Hettiarachchi M, Ye JM, Richter EA, Hniat AJ, Rattigan S, and Clark MG. Vasopressin and angiotensin II stimulate oxygen uptake in the perfused rat hindlimb. *Life Sci* 43: 1747–1754, 1988.

12. Dora KA, Colquhoun EQ, Hettiarachchi M, Rattigan S, and Clark MG. The apparent absence of serotonin-mediated vascular thermogenesis in perfused rat hindlimb may result from vascular shunting. *Life Sci* 48: 1555–1564, 1991.

13. Dora KA, Rattigan S, Colquhoun EQ, and Clark MG. Aerobic muscle contraction impaired by serotonin-mediated vasoconstriction. *J Appl Physiol* 77: 277–284, 1994.

14. Fuchi T, Rosdahl H, Hickner RC, Ungerstedt U, and Henriksson J. Microdialysis of rat skeletal muscle and adipose tissue: dynamics of the interstitial glucose pool. *Acta Physiol Scand* 151: 249–260, 1994.

15. Grant RT and HP Wright. Anatomical basis for non-nutritive circulation in skeletal muscle exemplified by blood vessels of rat biceps femoris tendon. *J Anat* 106: 125–133, 1970.

16. Henriksson J. Microdialysis of skeletal muscle at rest. *Proc Nutr Soc* 58: 919–923, 1999.

17. Hettiarachchi M, Parsons KM, Richards SM, Dora KA, Rattigan S, Colquhoun EQ, and Clark MG. Vasoconstrictor-mediated release of lactate from the perfused rat hindlimb. *J Appl Physiol* 73: 2544–2551, 1992.

18. Hickner RC, Bone D, Ungerstedt U, Jorfeldt L, and Henriksson J. Muscle blood flow during intermittent exercise: comparison of the microdialysis ethanol technique and ^{133}Xe clearance. *Clin Sci* 86: 15–25, 1994.

19. Hickner RC, Ekelund U, Mellander S, Ungerstedt U, and Henriksson J. Muscle blood flow in cats: comparison of microdialysis ethanol technique with direct measurement. *J Appl Physiol* 79: 638–647, 1995.

20. Hickner RC, Ungerstedt U, and Henriksson J. Regulation of skeletal muscle blood flow during acute insulin-induced hypoglycemia in the rat. *Diabetes* 43: 1340–1344, 1994.

21. Hyman C, Rosell S, Rosén A, Sonnenschein RR, and Uvnäs B. Effects of alterations of total muscular blood flow on local tissue clearance of radio-iodide in the cat. *Acta Physiol Scand* 46: 358–366, 1959.

22. Jacob S, Hauer B, Becker R, Artzner S, Grauer P, Loblein K, Nielsen M, Renn W, Rett K, Wahl HG, Stumvoll M, and Haring HU. Lipolysis in skeletal muscle is rapidly regulated by low physiological doses of insulin. *Diabetologia* 42: 1171–1174, 1999.

23. Kerckhoffs DA, Arner P, and Bolinder J. Lipolysis and lactate production in human skeletal muscle and adipose tissue following glucose ingestion. *Clin Sci (Colch)* 94: 71–77, 1998.

24. Kuznetsova LV, Tomasek N, Sigurdsson GH, Banic A, Erni D, and Wheatley AM. Dissociation between volume blood flow and laser-Doppler signal from rat muscle during changes in vascular tone. *Am J Physiol Heart Circ Physiol* 274: H1248–H1254, 1998.

25. Newman JM, Dora KA, Rattigan S, Edwards SJ, Colquhoun EQ, and Clark MG. Norepinephrine and serotonin vasoconstriction in rat hindlimb control different vascular flow routes. *Am J Physiol Endocrinol Metab* 270: E689–E699, 1996.

26. Newman JM, Steen JT, and Clark MG. Vessels supplying septa and tendons as functional shunts in perfused rat hindlimb. *Microvasc Res* 54: 49–57, 1997.

27. Pappenheimer JR. Vasoconstrictor nerves and oxygen consumption in the isolated perfused hindlimb muscles of the dog. *J Physiol* 99: 182–200, 1941.

28. Radegran G, Pilegaard H, Nielsen JJ, and Bangsbo J. Microdialysis ethanol removal reflects probe recovery rather than local blood flow in skeletal muscle. *J Appl Physiol* 85: 751–757, 1998.

29. Rattigan S, Dora KA, Colquhoun EQ, and Clark MG. Serotonin-mediated acute insulin resistance in the perfused rat hindlimb but not in incubated muscle: a role for the vascular system. *Life Sci* 53: 1545–1555, 1993.

30. Rattigan S, Dora KA, Colquhoun EQ, and Clark MG. Inhibition of insulin-mediated glucose uptake in rat hindlimb by an α-adrenergic vascular effect. *Am J Physiol Endocrinol Metab* 268: E305–E311, 1995.

31. Rattigan S, Dora KA, Tong AC, and Clark MG. Perfused skeletal muscle contraction and metabolism improved by angiotensin II-mediated vasoconstriction. *Am J Physiol Endocrinol Metab* 271: E96–E103, 1996.

32. Renkin EM. Effects of blood flow on diffusion kinetics in isolated, perfused hindlegs of cats: a double circulation hypothesis. *Am J Physiol* 183: 125–136, 1955.

33. Rosdahl H, Lind L, Millgard J, Lithell H, Ungerstedt U, and Henriksson J. Effect of physiological hyperinsulinemia on blood flow and interstitial glucose concentration in human skeletal muscle and adipose tissue studied by microdialysis. *Diabetes* 47: 1296–1301, 1998.

34. Ruderman NB, Houghton CR, and Hems R. Evaluation of the isolated perfused rat hindquarter for the study of muscle metabolism. *Biochem J* 124: 639–651, 1971.

35. Shepherd AP and Burgar CG. A solid-state arteriovenous oxygen difference analyzer for flowing whole blood. *Am J Physiol Heart Circ Physiol* 232: H437–H440, 1977.

36. Stallknecht B, Donsmark M, Enevoldsen LH, Fluckey JD, and Galbo H. Estimation of rat muscle blood flow by microdialysis probes perfused with ethanol, [^{14}C]ethanol, and ^{3}H$_2$O. *J Appl Physiol* 86: 1054–1061, 1999.

37. Vincent MA, Rattigan S, Clark MG, Bernard SL, and Glenny RW. Spatial distribution of nutritive and nonnutritive vascular routes in perfused rat hindlimb muscle using microspheres. *Microvasc Res* 61: 111–121, 2001.

38. Wallgren F, Amberg G, Hickner RC, Ekelund U, Jorfeldt L, and Henriksson J. A mathematical model for measuring blood flow in skeletal muscle with the microdialysis ethanol technique. *J Appl Physiol* 79: 648–659, 1995.

Vasoconstrictor-mediated thermogenesis present in perfused skeletal muscle but absent from perfused heart

C.A. Di Maria, S. Rattigan, M.G. Clark*

Biochemistry, Medical School, University of Tasmania, GPO Box 252-58, Hobart 7001, Australia

Abstract

Resting muscle thermogenesis as controlled by vasocontrictors was compared in rat hindlimb and cardiac muscle. An α-adrenergic agonist combination of phenylephrine + atenolol increased oxygen uptake and perfusion pressure in the constant flow hindlimb and neither increase was blocked by 10 μM tetrodotoxin. The same adrenergic combination also increased oxygen uptake and perfusion pressure in the perfused heart but the former along with beating was completely blocked by tetrodotoxin. Vasoconstriction by phenylephrine occurs in the heart but is not linked to thermogenic' increases as in hindlimb, implying that all metabolic energy in heart is conserved for contractile activity. The findings highlight a fundamental difference between skeletal and cardiac muscle. © 2002 Elsevier Science Ltd. All rights reserved.

Keywords: Resting muscle thermogenesis; Vascular control of muscle metabolism; Vascular effects in heart; Na^+ channel

1. Introduction

Not all homeotherms possess functional brown adipose tissue and are instead reliant on thermogenesis from other tissues to combat the threat of cold or to compensate from over-eating. There is substantial evidence that skeletal muscle contributes to heat production through shivering but there is also some evidence that the muscle possesses non-shivering mechanisms (Jansky, 1995). This has been demonstrated in a number of species by infusing norepinephrine or related adrenergic agonists in vivo (Jansky, 1995). However, the mechanisms that could account for resting muscle thermogenesis are uncertain with proposed contributions from increases in total blood flow to muscle (Simonsen et al., 1999), mitochondrial proton leakage (Rolfe and Brand, 1996; Rolfe et al., 1999), mitochondrial uncoupling due to UCP-3 (Clapham et al., 2000) and Na^+ ion cycling (Tong et al., 1999).

*Corresponding author. Tel.: +61-3-6226-2672; fax: +61-3-6226-2703.

E-mail address: michael.clark@utas.edu.au (M.G. Clark).

Involvement of metabolic futile cycles is also a possibility (Newsholme and Crabtree, 1976) and there is evidence from malignant hyperpyrexia in mammals (MacLennan and Phillips, 1992) and heat-producing muscles in certain fish (Block, 1994) that Ca^{2+} cycling between sarcoplasmic reticulum and myoplasm is a pronounced thermogenic process. Attempts to study resting muscle thermogenesis in vivo have met with mixed success and thus many workers have instead used in vitro muscle preparations. But this too has proved problematic. Indeed, a number of workers have shown that perfused, but neither incubated nor perifused, hindlimb muscle responds to a variety of vasomodulators, including norepinephrine and various α-(but not β) adrenergic agonists, angiotensin II, and vasopressin by rapidly increasing the rate of oxygen consumption and lactate release (see review Clark et al., (1995), and references therein). Owing to the magnitude of the response in perfused muscle, which is often 50% or more over basal for oxygen uptake and lactate release, and the increased release of a number of other metabolites, including glycerol, fatty acids and breakdown products of nucleotides, this has been interpreted as an increase in

resting muscle thermogenesis (Jansky, 1995). Vasoconstriction appears to be essential for the thermogenic response on two grounds. Firstly, as indicated above, only perfused muscle preparations respond. Thus, an effect of the vasoconstrictors to directly stimulate oxygen uptake or lactate release when added to isolated incubated (therefore non-perfused) muscles does not occur (Dubois-Ferriere and Chinet, 1981; Hettiarachchi et al., 1992). Secondly, blockade of the pressor effect with various types of vasodilators also blocks the increases in metabolism (Colquhoun et al., 1990). More recent studies suggest that a major change in blood flow pattern within the muscle is a key component of the vasoconstrictor-mediated increase in metabolism. Thus, there is evidence for redistribution of flow to nutritive capillary networks (Newman et al., 1996) at the expense of flow from a non-nutritive, possibly connective tissue route (Newman et al., 1997).

Although the detailed mechanism for vasoconstrictor-mediated thermogenesis in resting muscle is still unknown, there is fragmentary evidence to suggest that cation cycling may be involved. Thus, the vasoconstrictor-mediated oxygen uptake in perfused rat hindlimb muscle can be blocked by membrane stabilizers such as propranolol (or quinidine) or by inhibition of the Na^+/K^+ ATPase without inhibition of the increase in perfusion pressure and thus, the redistribution of flow (Tong et al., 1997, 1998). In addition, in the perfused rat hindlimb, oxygen uptake without vasoconstriction can be stimulated by the Na^+ channel activator, veratridine, and this stimulation is inhibited by propranolol (or quinidine) or by inhibition of the Na^+/K^+ ATPase. Taken together, this suggests the involvement of Na^+ channels in the vascular thermogenesis of the resting muscle (Tong et al., 1998, 1999).

In the present study, the presence of vascular thermogenesis was investigated in perfused non-contracting cardiac muscle and compared to skeletal muscle. To do this, we have used doses of an α-adrenergic combination of phenylephrine and atenolol, sufficient to cause vasoconstriction in each system and tetrodotoxin (10 μM) to arrest beating in the heart. Tetrodotoxin has no effect on the vascular thermogenesis elicited by vasoconstrictors in the hindlimb muscles (Tong et al., 1999). Veratridine was used to demonstrate that, in both skeletal hindlimb muscles and cardiac muscle, the increased thermogenesis was due to the Na^+ channel opening.

2. Materials and methods

2.1. Animals

Male rats (180–230 g body weight) of the Hooded-Wistar strain, maintained ad libitum on a standard commercial laboratory chow (Gibson's Hobart, Australia) at 22°C in a 12 h light : 12 h dark cycle were used for these experiments. Rats were anaesthetized with pentobarbital sodium (7–8 mg/100 g body weight, intraperitoneally) before removal of their hearts for perfusion. All aspects of animal handling were in accordance with the recommendations of the Animal Welfare Committee of the National Health and Medical Research Council (in Australian code of practice for the care and use of animals for scientific purposes, 1990). Experimental procedures were approved by the Committee on the ethical aspects of research involving animals of the University of Tasmania.

2.2. Hindlimb perfusions

Hindlimbs were perfused in a constant flow non-recirculating mode, as described elsewhere (Colquhoun et al., 1988) using essentially the technique of Ruderman and colleagues (Ruderman et al., 1971). The perfusion medium was Krebs–Henseleit bicarbonate buffer containing (in mM) 118 NaCl, 4.8 KCl, 1.2 MgSO$_4$, 1.2 KH$_2$PO$_4$, 25 NaHCO$_3$, 2.5 CaCl$_2$, 5 glucose and 4% (w/v) bovine serum albumin. The medium was equilibrated with O$_2$/CO$_2$ (19 : 1), and the perfusion temperature was 37°C. Atenolol (0.3 mM) was present in the perfusion medium when phenylephrine was infused to prevent activation of β-adrenoceptors and at this dose, is without effect on basal or agonist-stimulated oxygen uptake (Tong et al., 1997). The flow rate was 14 ml min^{-1} (0.87 ml min^{-1} g wet wt^{-1}). Oxygen concentration in the venous perfusate was constantly measured at 37°C with a Clark-type O$_2$ electrode calibrated with air and O$_2$ gas. Arterial P_{O_2} was measured before and after each perfusion and oxygen uptake calculated from arterial–venous difference, as described previously, using the appropriate Bunsen coefficient (Dora et al., 1992). Perfusion pressure was continuously recorded with a pressure transducer fitted in the arterial line. When present, tetrodotoxin and veratridine were each infused at 10 μM. Phenylephrine was present at 1 μM. For the veratridine perfusions, 0.5 mM sodium nitroprusside (SNP) was included in the perfusion media to block any vasoconstriction due to the Na^+ channel opening in vascular smooth muscle and thus, any subsequent redistribution of flow that might occur.

2.3. Heart perfusions

Hearts were perfused in the Langendorff manner using a system based on that of Williamson (1964). The perfusion medium was Krebs–Henseleit bicarbonate buffer, as described above, which contained 0.05 mM EDTA, 5 mM pyruvate, and 5 mM glucose, and was equilibrated with O$_2$/CO$_2$ (19 : 1); the perfusion temperature was 37°C. The perfusion medium also

contained 0.3 mM atenolol when phenylephrine was infused. Each heart was perfused at constant flow $(6.79 \pm 0.12 \, \text{ml} \, \text{min}^{-1}$, equivalent to $8.94 \pm 0.25 \, \text{ml} \, \text{min}^{-1} \text{g}$ wet wt heart^{-1} (mean $\pm$ SE, $n = 18$)). Oxygen concentration in the venous perfusate was constantly measured at 37°C with an in-line Clark-type O_2 electrode calibrated with air and O_2 gas and uptake calculated, as described above. The cannulated heart was contained within a sealed chamber to prevent exchange of O_2–CO_2 between effluent perfusate and the atmosphere (chamber volume 10 ml) and in this system, drift in measurement was less than $2\% \, \text{h}^{-1}$ (Richards et al., 1993). Aortic pressure was continuously recorded with a CFP blood pressure monitor (Model 8138).

Contracting hearts were arrested by infusion into the perfusate line just prior to the heart of either tetrodotoxin (TTX) or KCl to give a final concentration of 10 μM and 40 mM, respectively. KCl was used in place of TTX to arrest the heart for veratridine infusion experiments as TTX is an inhibitor of veratridine-mediated oxygen uptake in perfused hindlimb (Tong et al., 1999) and likely to be so in heart. As indicated, phenylephrine or veratridine solutions (in isotonic saline) were infused to give final concentrations of 50 and 10 μM, respectively. The total infusion rate of agents did not exceed 1 : 50 of the perfusate flow rate.

2.4. Statistics

Statistical testing was performed using the Sigma Stat™ statistical program (Jandel Software Corp.) and significant differences were recognized at $P < 0.05$.

3. Results

3.1. Perfused hindlimb

Fig. 1 shows a typical trace of oxygen uptake and perfusion pressure obtained during 1 μM phenylephrine infusion with and without 10 μM tetrodotoxin. Mean values with standard errors for a total of five experiments are shown in Fig. 2. Phenylephrine in the presence of the β-adrenergic antagonist, 0.3 mM atenolol, significantly increased both the oxygen uptake and perfusion pressure. Mean basal values (before phenylephrine) for oxygen uptake and perfusion pressure were $31.5 \pm 1.0 \, \mu\text{mol} \, \text{h}^{-1} \text{g}^{-1}$ and 40 ± 5 mm Hg, respectively, and these increased to $39.1 \pm 1.4 \, \mu\text{mol} \, \text{h}^{-1} \text{g}^{-1}$ $(P < 0.001)$ and 53 ± 5 mm Hg $(P < 0.001)$, when phenylephrine was infused. Infusion of 10 μM tetrodotoxin for 10 min before and during phenylephrine had no effect on the magnitude of the changes in oxygen uptake or pressure due to phenylephrine

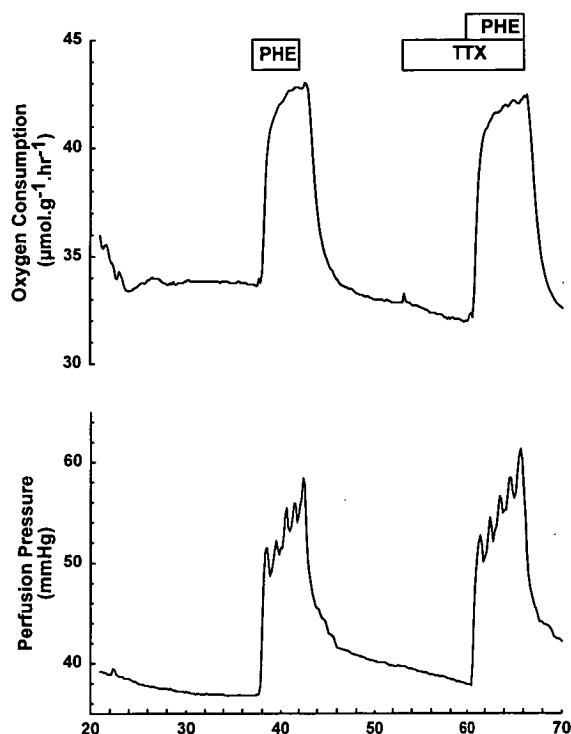Fig. 3 shows the effects of veratridine on oxygen uptake and perfusion pressure in the presence of 0.5 mM

Fig. 1. Time course for the effect of phenylephrine (PHE, 1 μM) on oxygen uptake and perfusion pressure by the perfused rat hindlimb with and without 10 μM tetrodotoxin (TTX). The perfusion buffer contained 0.3 mM atenolol and perfusions were conducted at constant flow. A representative trace is shown.

sodium nitroprusside (SNP). 10 μM veratridine significantly increased oxygen uptake from 26.1 ± 0.4 to $38.1 \pm 0.9 \, \mu\text{mol} \, \text{h}^{-1} \text{g}^{-1}$ $(P < 0.001)$ representing an increase over basal of approx. 45%. Perfusion pressure was only marginally increased by veratridine from 41.3 ± 1.7 to 43.4 ± 2.3 mm Hg, but this was not significant $(P > 0.05)$.

3.2. Perfused heart

Hearts were allowed to equilibrate for 20–30 min until steady state levels of oxygen uptake and perfusion pressure were obtained. Preliminary experiments were conducted to determine a dose of the α-adrenergic agonist combination of phenylephrine + 0.3 mM atenolol that would reproducibly increase both oxygen uptake and perfusion pressure at constant flow. These preliminary experiments showed that the heart was considerably less sensitive to phenylephrine and a dose of 50 μM was considered optimal.

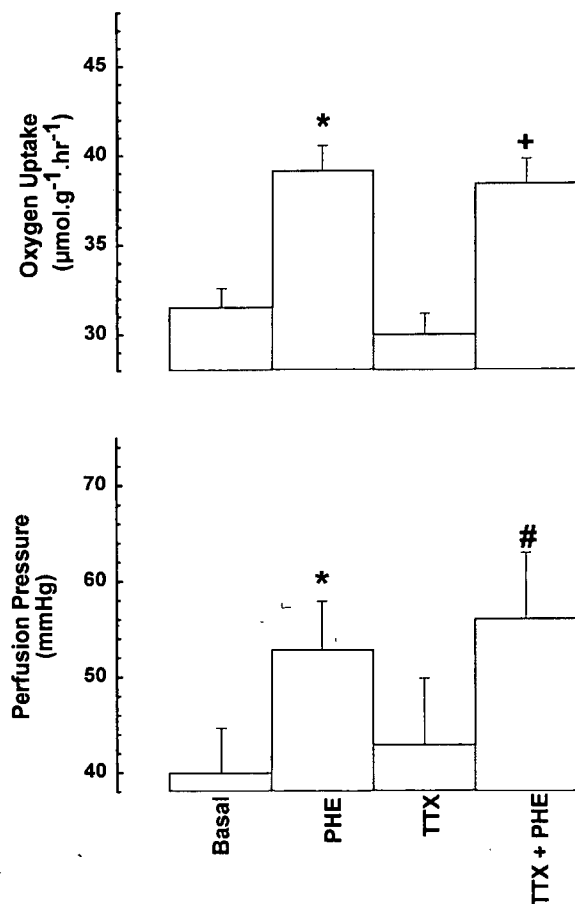Fig. 4 shows a typical trace of oxygen uptake and perfusion pressure obtained during a 7–10 min infusion

Fig. 2. Effects of phenylephrine (1 µM), tetrodotoxin (10 µM) and a combination of the two on oxygen uptake and perfusion pressure of the constant-flow perfused rat hindlimb. Other details were as for Fig. 1. Values are means ± SE for n = 5; *, significantly different from basal; #, significantly different from TTX treatment tested by repeated one-way analysis of variance and pair-wise comparisons using the Student–Newman–Kuels test.

Fig. 3. Effects of veratridine (Vera, 10 µM) in the presence of 0.5 mM sodium nitroprusside (SNP) on oxygen uptake and perfusion pressure of the constant-flow perfused rat hindlimb. Values are means ± SE for n = 5; ***, significantly different from basal.

of 50 µM phenylephrine + 0.3 mM atenolol, while the heart was contracting. After 15–20 min from the cessation of phenylephrine infusion, when oxygen and pressure values had returned to pre-infusion levels, infusion of TTX was commenced. Contraction rapidly declined within 2 min after TTX infusion and no contraction was observed for the remainder of the experiment (data not shown). When oxygen uptake and perfusion pressure had again stabilized, infusion of phenylephrine was re-commenced at the same rate as prior to arrest. For some of the hearts, there was a transient stimulation of oxygen uptake coinciding with the commencement of phenylephrine infusion, but this was transient and overall, there was no sustained increase in oxygen uptake (Fig. 4) despite a marked
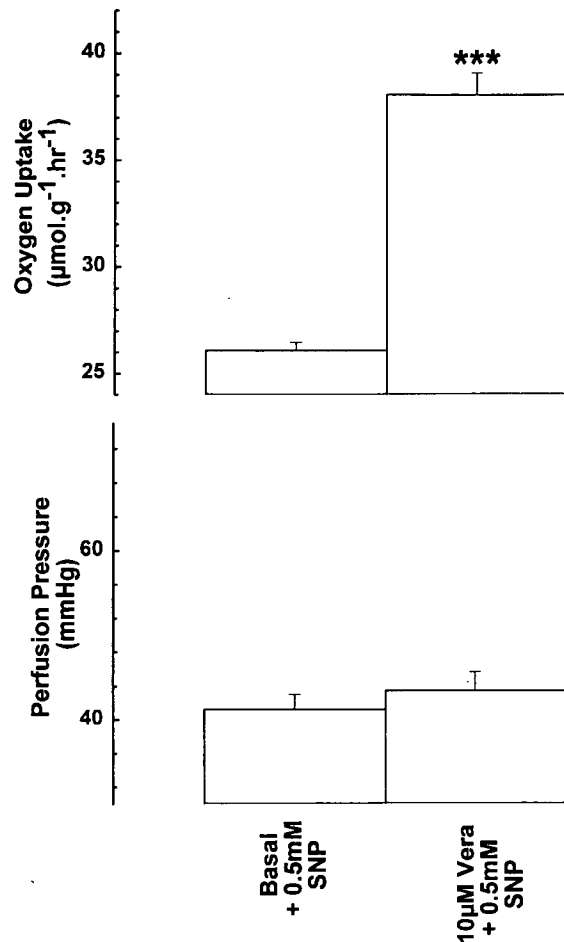
increase in perfusion pressure (Fig. 5). Atenolol (0.3 mM) alone did not affect basal oxygen uptake or perfusion pressure (compare Figs. 5 and 7).

Fig. 5 shows the mean values ± SE (from 10 experiments) for oxygen uptake and perfusion pressure, recorded just prior to the first phenylephrine infusion (Basal) and TTX infusion, and at the end of both phenylephrine infusions, as conducted in the protocol of Fig. 4. Repeated one-way analysis of variance and pair-wise comparisons using the Student–Newman–Kuels test demonstrated that phenylephrine caused a significant ($P < 0.05$) increase in oxygen uptake (70.4%) when infused in contracting hearts, but no change in TTX-arrested hearts. However, perfusion pressure was significantly ($P < 0.05$) increased by phenylephrine in
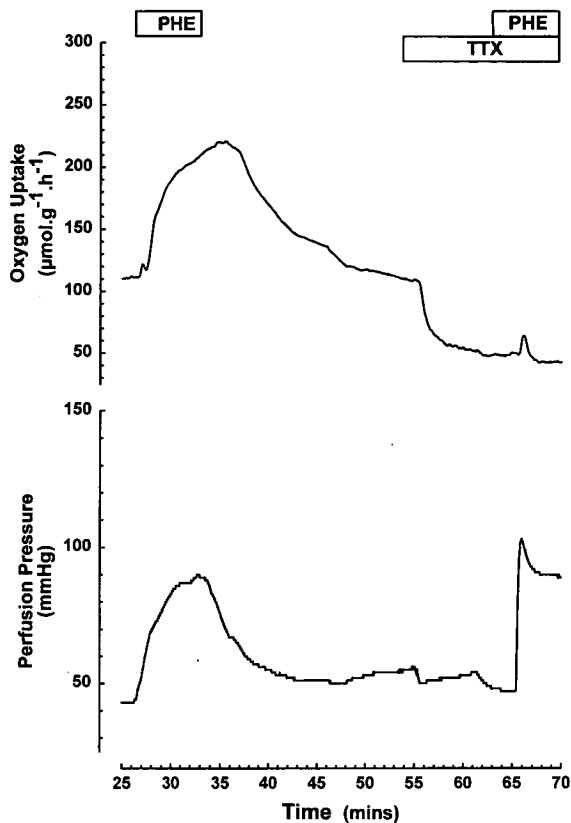
Fig. 4. Time course for the effect phenylephrine (50 μM) on oxygen uptake and perfusion pressure by the perfused rat heart with and without 10 μM tetrodotoxin. The perfusion buffer contained 0.3 mM atenolol and perfusions were conducted at constant flow. A representative trace is shown; means of all experiments are shown in Fig. 5.
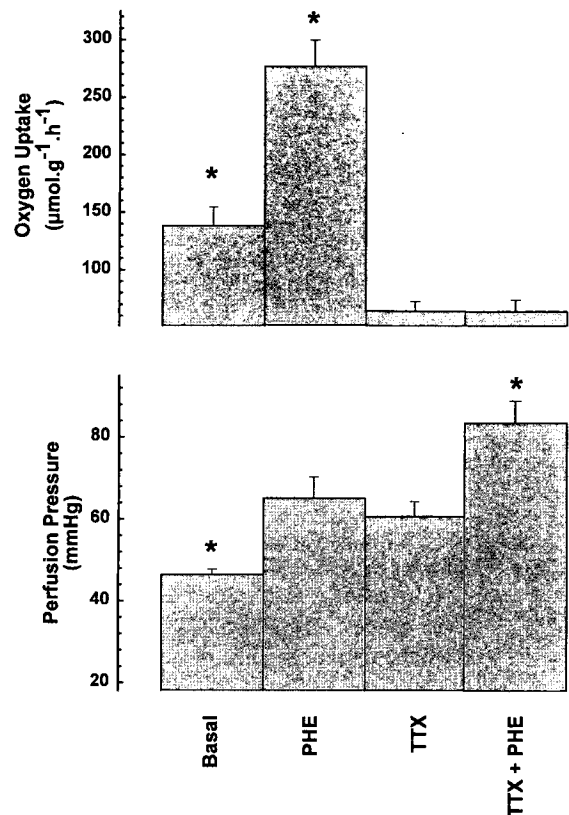

Fig. 5. Effects of phenylephrine (50 μM), tetrodotoxin (10 μM) and a combination of the two, on oxygen uptake and perfusion pressure of the constant-flow perfused rat heart. Other details were as for Fig. 4. Values are means ± SE for $n = 8$; *, significantly different to TTX treatment.

both contracting (32.7%) and TTX-arrested (51.4%) hearts. TTX-arrest of contracting hearts resulted in a significant ($P < 0.05$) decrease in oxygen uptake (52.5%) but no significant change in perfusion pressure.

Fig. 6 shows a typical trace of oxygen uptake and perfusion pressure obtained during veratridine experiments. Hearts were allowed to equilibrate for 20–30 min until steady state levels of oxygen uptake and perfusion pressure were obtained. Infusion of 40 mM KCl was then commenced to arrest contraction. Contraction ceased within 2 min and no contraction was observed for the remainder of the KCl infusion (data not shown). Shortly after commencing KCl infusion, there were initial transient changes in oxygen uptake and perfusion pressure (Fig. 6). After 15 min, when oxygen uptake and perfusion pressure had stabilized, veratridine (10 μM) infusion was commenced. Oxygen uptake was stimulated by veratridine after a delay of approximately 3 min (Fig. 6). This delay was similar to that seen with the perfused hindlimb (Tong et al., 1998).

Fig. 7 shows the mean ± SE values (from eight experiments) of oxygen uptake and perfusion pressure, determined just prior to KCl (Basal), veratridine infusions, and after 10 min of veratridine plus KCl infusion. Repeated one-way analysis of variance and pair-wise comparisons using the Student–Newman–Kuels test demonstrated that KCl arrest caused a significant ($P < 0.05$) decrease (32.7%) in oxygen uptake and increase (165%) in perfusion pressure, while veratridine infusion resulted in a significant ($P < 0.05$) increase (55.6%) in arrested-heart oxygen uptake and a further small rise (12.8%) in perfusion pressure.

4. Discussion

The main finding emerging from this study is that vasoconstrictor-mediated thermogenesis is absent from heart. Thus, the constant-flow perfused heart, when arrested, did not respond to the α-adrenergic agonist
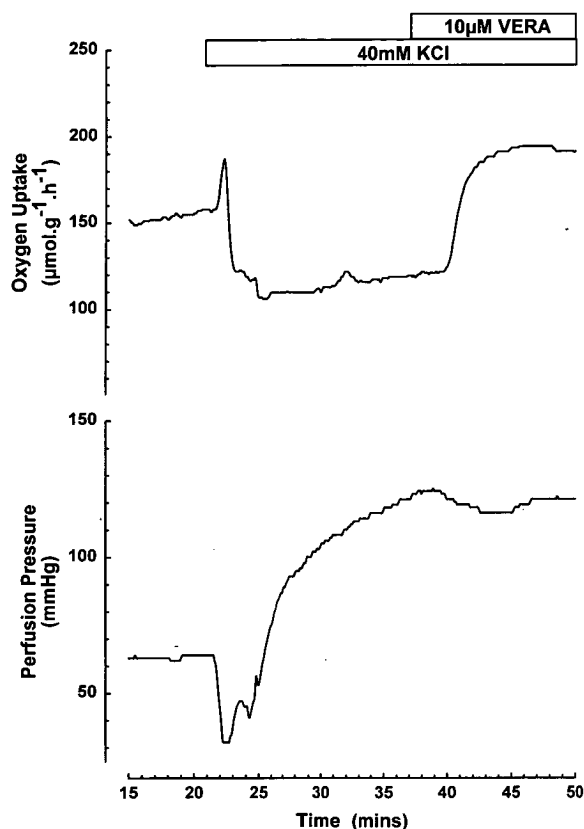
Fig. 6. Time course for the effect of veratridine (Vera, 10 μM) on oxygen uptake and perfusion pressure of the KCl (40 mM)-arrested rat heart. A representative trace is shown; means of all experiments are shown in Fig. 7.

Fig. 7. Effects of veratridine (10 μM), KCl (40 mM) and a combination of the two on oxygen uptake and perfusion pressure of the constant-flow perfused rat heart. Values are means ± SE for $n = 8$; *, significantly different from KCl treatment.

combination of phenylephrine + atenolol in terms of increased oxygen uptake, despite a rise in perfusion pressure. This contrasts with the constant-flow perfused hindlimb which, at rest, showed a marked increase in oxygen uptake with pressure rise, in response to the same α-adrenergic agonist combination (Fig. 1). The finding is also in contrast to the result when phenylephrine was applied to the beating heart. Since, under these conditions, there was both an increase in pressure and oxygen uptake, it would seem likely that energy expenditure by the heart is closely coupled to supporting myocyte contractility. Thus, the increase in oxygen consumption by phenylephrine during beating is the result of the well-established α-adrenergic inotropic effect of this and other catecholamines (Aass et al., 1983; Benfey, 1982; Schumann et al., 1974).

The absence of a vasoconstrictor-mediated thermogenesis in heart, may reflect the absence of either a flow redistribution process, or a specific thermogenic mechanism that responds to flow redistribution. There is
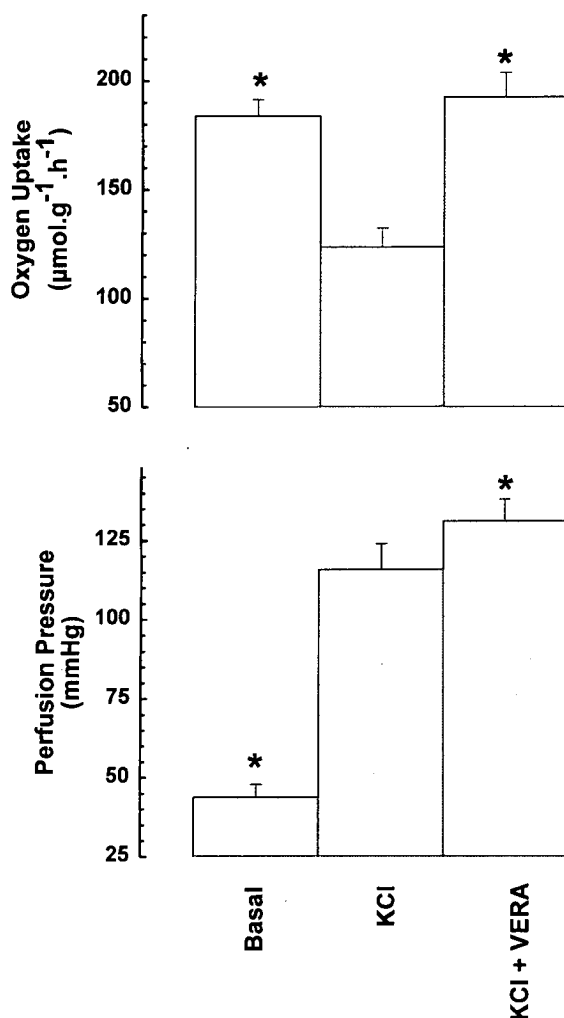
compelling evidence for two vascular routes in skeletal muscle, both from older (Barlow et al., 1961; Grant and Wright, 1970; Pappenheimer, 1941) and more recent studies (Clark et al., 1995). Perfusion flow can thus be distributed between a nutritive route which is in intimate contact with the muscle fibres, or a non-nutritive route which has poor delivery of nutrients and which may be located in nearby connective tissues. Implications are that, for skeletal muscle at rest, blood flow is heterogeneous with a considerable proportion of the total flow entering muscle not actually in contact with muscle fibres for its passage through the tissue. Absence of a thermogenic response to the vasoconstrictor,

phenylephrine, by the heart, may reflect homogeneous flow in this tissue and the absence of a non-nutritive route. It is also possible that heart lacks the signalling system that we have previously proposed for the skeletal muscle where the re-direction of flow, mediated by the vasoconstrictors, activates a thermogenic mechanism in the striated muscle cells (Clark et al., 1995).

Comparison of heart and skeletal muscle in terms of putative thermogenic mechanism involving Na^+ cycling revealed no major difference. Both the tissues responded positively to the sodium channel opener, veratridine (10 µM), although beating of the heart had to be prevented by high K^+ and some constriction of the myocardial vasculature resulted.

In a previous publication (Tong et al., 1998), we have described the similarities between vasoconstrictor-mediated increases in metabolism and those produced by veratridine in the perfused hindlimb. Veratridine, like norepinephrine, increased oxygen uptake and lactate release. Each was blocked by low Na^+ medium (Tong et al., 1998), by the membrane-stabilizer, ($\pm$)-propranolol (Tong et al., 1998) or by the Na^+/K^+ ATPase inhibitor, ouabain (Tong et al., 1999). Veratridine-mediated increases in metabolism are not associated with changes in perfusion pressure, are unaffected by agents such as sodium nitroprusside (Tong et al., 1998), and therefore unlikely to involve redistribution of flow between non-nutritive and nutritive routes.

We have previously reported that vasoconstrictor-mediated increases in metabolism were insensitive to tetrodotoxin (5–50 µM), but those of veratridine were completely abolished at 1 µM (Tong et al., 1999). With the added knowledge that tetrodotoxin at these doses completely prevents beating of the heart and opportunity presented itself, where we could investigate the presence or otherwise of the tetrodotoxin-insensitive vascular thermogenesis in the arrested heart. In the present study, it is clear that the response to veratridine (in terms of increased oxygen uptake) is present even in the arrested heart, suggesting that the mechanism is present. However, it cannot be entirely ruled out that the lack of response to phenylephrine in TTX-exposed hearts reflects the absence of the specific tetrodotoxin-insensitive process that exists in the skeletal muscle.

In summary, the heart differs from skeletal muscle in its response to the α-adrenergic agonist, phenylephrine. In skeletal muscle, vasoconstriction is associated with an increase in oxygen uptake. For the arrested heart, there is no response. This is likely to be the result of the absence of heterogeneity of flow, or differences in the expression of early mechanisms linking vasoconstriction to Na^+ movement. Down-stream processes appear to be similar as veratridine stimulates oxygen uptake in both heart and skeletal muscle.

References

Aass, H., Skomedal, T., Osnes, J.B., 1983. Demonstration of an alpha adrenoceptor-mediated inotropic effect of norepinephrine in rabbit papillary muscle. J. Pharmacol. Exp. Ther. 226, 572–578.

Barlow, T.E., Haigh, A.L., Walder, D.N., 1961. Evidence for two vascular pathways in skeletal muscle. Clin. Sci. 20, 367–385.

Benfey, B.G., 1982. Function of myocardial alpha-adrenoceptors. Life Sci. 31, 101–112.

Block, B.A., 1994. Thermogenesis in muscle. Annu. Rev. Physiol. 56, 535–577.

Clapham, J.C., Arch, J.R., Chapman, H., Haynes, A., Lister, C., Moore, G.B., Piercy, V., Carter, S.A., Lehner, I., Smith, S.A., Beeley, L.J., Godden, R.J., Herrity, N., Skehel, M., Changani, K.K., Hockings, P.D., Reid, D.G., Squires, S.M., Hatcher, J., Trail, B., Latcham, J., Rastan, S., Harper, A.J., Cadenas, S., Buckingham, J.A., Brand, M.D., Abuin, A., 2000. Mice overexpressing human uncoupling protein-3 in skeletal muscle are hyperphagic and lean. Nature 406, 415–418.

Clark, M.G., Colquhoun, E.Q., Rattigan, S., Dora, K.A., Eldershaw, T.P., Hall, J.L., Ye, J., 1995. Vascular and endocrine control of muscle metabolism. Am. J. Physiol. 268, E797–E812.

Colquhoun, E.Q., Hettiarachchi, M., Ye, J.M., Rattigan, S., Clark, M.G., 1990. Inhibition by vasodilators of noradrenaline and vasoconstrictor-mediated, but not skeletal muscle contraction-induced oxygen uptake in the perfused rat hindlimb; implications for non-shivering thermogenesis in muscle tissue. Gen. Pharmacol. 21, 141–148.

Colquhoun, E.Q., Hettiarachchi, M., Ye, J.M., Richter, E.A., Hniat, A.J., Rattigan, S., Clark, M.G., 1988. Vasopressin and angiotensin II stimulate oxygen uptake in the perfused rat hindlimb. Life Sci. 43, 1747–1754.

Dora, K.A., Richards, S.M., Rattigan, S., Colquhoun, E.Q., Clark, M.G., 1992. Serotonin and norepinephrine vasoconstriction in rat hindlimb have different oxygen requirements. Am. J. Physiol. 262, H698–H703.

Dubois-Ferriere, R., Chinet, A.E., 1981. Contribution of skeletal muscle to the regulatory non-shivering thermogenesis in small mammals. Pflugers Arch. 390, 224–229.

Grant, R.T., Wright, H.P., 1970. Anatomical basis for non-nutritive circulation in skeletal muscle exemplified by blood vessels of rat biceps femoris tendon. J. Anat. 106, 125–133.

Hettiarachchi, M., Parsons, K.M., Richards, S.M., Dora, K.M., Rattigan, S., Colquhoun, E.Q., Clark, M.G., 1992. Vasoconstrictor-mediated release of lactate from the perfused rat hindlimb. J. Appl. Physiol. 73, 2544–2551.

Jansky, L., 1995. Humoral thermogenesis and its role in maintaining energy balance. Physiol. Rev. 75, 237–259.

MacLennan, D.H., Phillips, M.S., 1992. Malignant hyperthermia. Science 256, 789–794.

Newman, J.M., Dora, K.A., Rattigan, S., Edwards, S.J., Colquhoun, E.Q., Clark, M.G., 1996. Norepinephrine and serotonin vasoconstriction in rat hindlimb control different vascular flow routes. Am. J. Physiol. 270, E689–E699.

Newman, J.M., Steen, J.T., Clark, M.G., 1997. Vessels supplying septa and tendons as functional shunts in perfused rat hindlimb. Microvasc. Res. 54, 49–57.

Newsholme, E.A., Crabtree, B., 1976. Substrate cycles in metabolic regulation and in heat generation. Biochem. Soc. Symp. 41, 61–109.

Pappenheimer, J.R., 1941. Vasoconstrictor nerves and oxygen consumption in the isolated perfused hindlimb muscles of the dog. J. Physiol. 99, 182–200.

Richards, S.M., Rattigan, S., Colquhoun, E.Q., Clark, M.G., 1993. [32P]phosphate autoradiography as an indicator of regional myocardial oxygen consumption? J. Mol. Cell Cardiol. 25, 289–302.

Rolfe, D.F., Brand, M.D., 1996. Contribution of mitochondrial proton leak to skeletal muscle respiration and to standard metabolic rate. Am. J. Physiol. 271, C1380–C1389.

Rolfe, D.F., Newman, J.M., Buckingham, J.A., Clark, M.G., Brand, M.D., 1999. Contribution of mitochondrial proton leak to respiration rate in working skeletal muscle and liver and to SMR. Am. J. Physiol. 276, C692–C699.

Ruderman, N.B., Houghton, C.R., Hems, R., 1971. Evaluation of the isolated perfused rat hindquarter for the study of muscle metabolism. Biochem. J. 124, 639–651.

Schumann, H.J., Endoh, M., Wagner, J., 1974. Positive inotropic effects of phenylephrine in the isolated rabbit papillary muscle mediated both by alpha- and beta-adrenoceptors. Arch. Pharmacol. 284, 133–148.

Simonsen, L., Stefl, B., Christensen, N.J., Bulow, J., 1999. Thermogenic response to adrenaline during restricted blood flow in the forearm. Acta Physiol. Scand. 166, 31–38.

Tong, A.C., Rattigan, S., Dora, K.A., Clark, M.G., 1997. Vasoconstrictor-mediated increase in muscle resting thermogenesis is inhibited by membrane-stabilizing agents. Can. J. Physiol. Pharmacol. 75, 763–771.

Tong, A.C., Rattigan, S., Clark, M.G., 1998. Similarities between vasoconstrictor- and veratridine-stimulated metabolism in perfused rat hind limb. Can. J. Physiol. Pharmacol. 76, 125–132.

Tong, A.C., Di Maria, C.A., Rattigan, S., Clark, M.G., 1999. Na^+ channel and Na^+–K^+ ATPase involvement in norepinephrine- and veratridine-stimulated metabolism in perfused rat hind limb. Can. J. Physiol. Pharmacol. 77, 350–357.

Williamson, J.R., 1964. Metabolic effects of epinephrine in the isolated, perfused rat heart. 1. Dissociation of the glycogenolytic from the metabolic stimulatory effect. J. Biol. Chem. 239, 2721–2729.